Development of Dendritic Functionalized Mesoporous Silica as Reusable Catalyst for Organic Synthesis

Thesis submitted to
Cochin University of Science and Technology
in partial fulfilment of the requirements
for the award of the degree of
Doctor of Philosophy
in
Chemistry
Under the Faculty of Science

by

Jisha K. A.

Department of Applied Chemistry
Cochin University of Science and Technology
Kochi – 22

June 2017

Development of Dendritic Functionalized Mesoporous Silica as Reusable Catalyst for Organic Synthesis

Ph.D. Thesis under the Faculty of Science

By

Jisha K. A.
Research Fellow
Department of Applied Chemistry
Cochin University of Science and Technology
Kochi, India 682022
Email: jishapolymer@gmail.com

Supervising Guide

Dr. Prathapan S.
Associate Professor
Department of Applied Chemistry
Cochin University of Science and Technology
Kochi, India 682022
Email: prathapans@gmail.com

Doctoral Committee Member

Dr. K. Sreekumar
Professor
Department of Applied Chemistry
Cochin University of Science and Technology
Kochi, India 682022
Email: drsreekumar@gmail.com

Department of Applied Chemistry
Cochin University of Science and Technology
Kochi, India 682022

June 2017

DEPARTMENT OF APPLIED CHEMISTRY
COCHIN UNIVERSITY OF SCIENCE AND TECHNOLOGY
KOCHI - 682022, INDIA

Dr. Prathapan S.	Ph: 0484-2575804
Associate Professor	E-mail: prathapans@gmail.com

Date: 22/06/2017

Certificate

This is to certify that the thesis entitled **"Development of Dendritic Functionalized Mesoporous Silica as Reusable Catalyst for Organic Synthesis"** is an authentic record of research work carried out by **Mrs. Jisha K. A.**, under my supervision in partial fulfilment of the requirements for the award of the degree of Doctor of Philosophy in Chemistry under the faculty of Science of Cochin University of Science and Technology, and further that no part thereof has been presented before for the award of any other degree. All the relevant corrections and modifications suggested by the audience and recommended by the doctoral committee of the candidate during the presynopsis seminar have been incorporated in the thesis.

Dr. Prathapan S.
(Supervising Guide)

Declaration

I hereby declare that the work embodied in the thesis entitled **"Development of Dendritic Functionalized Mesoporous Silica as Reusable Catalyst for Organic Synthesis"** is based on original research work done by me under the supervision of **Dr. Prathapan S.**, Associate Professor, Department of Applied Chemistry, Cochin University of Science and Technology, Cochin-22, and the same has not been submitted elsewhere for the award of any other degree.

Kochi-22 **Jisha K. A.**
22/06/2017

"No place in this world is, as safe as mother's lap,
and nobody in this world is, as loving as mother."

Dedicated to my Mother

*(For her prayers, endless love,
encouragement and enduring support)*

Acknowledgement

The completion of my research and subsequent thesis has been a long journey. I have not travelled in vacuum in this journey. This thesis has been kept on track and been seen through to completion with the support and encouragement of numerous people including my supervising guides, my family, my friends, and various institutions. At the end of my thesis I would like to thank all those people who made this thesis possible and an unforgettable experience for me.

First and above all, I praise **God**, the almighty for providing me this opportunity and granting me the capability to proceed successfully. I pay my obeisance to **God**, the almighty to have bestowed upon me good health, courage, inspiration, zeal, great mother and the light throughout my personal life and education life.

At this moment of accomplishment, first of all people, I would like to thank my Ph. D supervising guide Dr. Prathapan S. (Associate professor, Department of Applied Chemistry, CUSAT) for supporting me during the past six years. It is my supreme honor to have worked as a student in his research community. My sincere gratitude is reserved for him for his invaluable insights, guidance and suggestions. I really appreciate his willingness to meet me at short notice every time and going through several drafts of my thesis. I remain amazed that despite his busy schedule, he was able to go through the final draft of my thesis and meet me in short time with comments and suggestions on almost every page. I am also very grateful to him for his scientific advice and knowledge and many insightful discussions and suggestions about my research and personal life. His laughing face and boosting words always encouraged me to go more confidently with my research work.

I express my utmost gratitude and reverence to Dr. K. Sreekumar (Professor, Department of Applied Chemistry, CUSAT), research adviser and doctoral committee member, for his guidance and all the useful discussions and brainstorming sessions, especially during the difficult conceptual development stage. His deep insights helped me at various stages of my research. His expertise, invaluable guidance, constant encouragement, affectionate attitude, understanding, patience and healthy criticism added considerably to my experience. He has given me the full freedom to

pursue various experiments in the lab without any objection. He ploughed through several preliminary versions of my text, making critical suggestions and posing challenging questions. I also remain indebted for his understanding and support during the times when I was really down and depressed due to personal problems. Without his continued inspiration, it would not have been possible to complete this work. He has inspired me to become an independent researcher and helped me realize the power of critical reasoning.

Dr. K. Girish Kumar, HOD, Department of Applied Chemistry deserves special mention at this point. His motivation and his constructive criticism have always boosted my confidence. He gave me best platform and provided opportunities in this department.

My honest thanks go to Dr. N. Manoj and Dr. M. R. Prathapachandra Kurup, former heads, Department of Applied Chemistry, CUSAT for providing me the opportunity to accomplish my research work in this department.

Faculty members of this Department have been very kind enough to extend their help at various phases of this research, whenever I approached them, and I do hereby acknowledge Dr. S. Sugunan, Dr. K. K. Muhammed Yusuff, Dr. P. V. Mohanan, Dr. Sabura Begum and Dr. P. A. Unnikrishnan. I would like to thank all members of the non teaching staff for their never ending help and support during this research.

I would like to acknowledge all the teachers who taught me since my childhood, I would not have been here without their guidance, blessing and support. My special thanks to Mrs. Roshni and Mrs. Jyothy (teachers, U C College, Aluva) for being another role model for me. Without their personal support, I could not have gone beyond graduate level. I feel privileged to be their student once, a feeling that every student of their will second.

I would also like to thank some people from early days of my research tenure. I thank them individually, Dr. Rajesh, Dr. Mangala, Dr. Kannan, Dr. Anoop, Dr. Mahesh, Dr. Priya and Dr. Elizabeth at this juncture. No words of gratitude are enough to acknowledge my labmates. I am indebted to Dr. Smitha, real motivator, Dr. Jibi, my financial helper, Mrs. Sinija, distinguished senior colleague,

▌▌▌ Preface ▌▌▌

The most important problem in catalysis is the cost related to the catalyst efficiency and the recovery of the catalyst from the reaction mixture for both economical and environmental reasons. Selectivity is another important aspect related to efficiency: chemoselectivity, regioselectivity, stereoselectivity, enantioselectivity, and diastereoselectivity, and these selectivity factors are always optimum with homogeneous catalysts. Most often, however, these catalysts cannot be removed from reaction media, because separation is too difficult due to their small size. Dendrimer catalysis has appeared since the early 1990s as an interesting possibility to explore, because homogeneous catalysts could be bound to the periphery or interior of dendrimers, providing homogeneous catalysts for a tailored, well-controlled definition of the molecular environment of the catalytic site and solubility. However, these catalysts cannot be removed from reaction media and in general, not reusable. Heterogenization of dendrimeric catalyst on solid support is a possible solution to overcome these twin deficiencies.

Heterogeneous catalytic reactions typically occur through the adsorption of reactants on the surface of the catalyst, followed by cleavage or recombination of the chemical bonds of the reactants on the catalyst surface. Therefore, the catalytic activity, selectivity, and shelf-life of heterogeneous catalysts strongly depend on the surface structure of the support materials. Hence, to successfully develop efficient heterogeneous catalysts, the rational choice of the support material and the use of the right synthetic strategy for placing the active catalytic groups on the support material are vital. Among many materials that are used as support material for heterogeneous catalysts, mesoporous silica materials are appealing because of their inherent physical robustness, high surface area, tunable monodisperse nanometer pores and suitable structural features to serve as hosts for a variety of catalytic groups. The versatility of functionalization techniques for mesoporous materials along with ability to readily separate the products upon reaction completion allow for continuous innovation in the catalysis field.

Major portion of the present work revolves around mesoporous silica supported dendritic Brønsted acid and base catalysts, with an aim to deliberately avoid metal based catalyst and to highlight the importance of metal free catalysis. The employment of mesoporous silica as solid support which

enables easy recovery of catalyst from the reaction mixture and reusability of the catalyst without loss of its activity is the major objective.

The thesis is divided into seven chapters. The **Chapter 1** gives an introduction to dendrimers and various methods used for dendrimer synthesis. It also includes disadvantages of dendrimeric catalysis in homogeneous phase and explains the need for heterogenization of dendrimers. It gives brief description about the importance of mesoporous silica as support for heterogenization of dendrimers. Various analytical methods used for the characterization of the synthesized systems are also described.

Chapter 2 is mainly focused on the synthesis of dendritic sulfonic acid and carboxylic acid functionalized mesoporous silica. Characterization techniques include elemental analysis, FTIR, SEM-EDAX analysis, Low angle XRD, Surface area analysis, solid state ^{13}C NMR, Raman spectroscopy and TG-DTG studies.

In **Chapter 3**, catalytic application of sulfonic acid terminated mesoporous silica for Biginelli Reaction and trisubstituted imidazole synthesis under solvent free condition is discussed. Various factors which control the reactions are studied and plausible mechanisms for both reactions are discussed.

Carboxylic acid functionalized mesoporous silica as effective reusable organo acidic catalyst for Ullmann type coupling reaction is given in **Chapter 4.** The experimental parameters are optimized, scope of the substrate, reusability of the catalyst and mechanism are studied.

Chapter 5 deals with the synthesis and characterization of dendritic amine functionalized mesoporous silica. Catalytic application of this synthesized system in Paal-Knorr reaction is described. The experimental parameters are optimized, scope of the substrate, reusability of the catalyst and mechanism are studied.

Chapter 6 discusses a detailed study on Henry reaction using dendritic amine functionalized mesoporous silica and L-proline modified mesoporous silica. Both nitroalkenes and β-nitroalkanols are synthesized using these catalytic systems. The experimental parameters are optimized, scope of the substrate, reusability of the catalyst and mechanisms are studied for both the products.

Chapter 7 consolidates the research findings and conclusions drawn from the earlier chapters.

▐▐▐ Contents ▐▐▐

Chapter 3
Sulfonic Acid Functionalized Mesoporous Silica: Effective Organo Acidic Catalyst for Biginelli Reaction and Trisubstituted Imidazole Synthesis under Solvent Free Condition

Chapter 4

Carboxylic Acid Functionalized Mesoporous Silica as Effective Reusable Organo Acidic Catalyst for Ullmann Type Coupling Reaction

Chapter 5

Dendritic Amine on Mesoporous Silica: First Organo Base Catalyst for Paal-Knorr Reaction under Solvent Free Condition; A Green Approach

Chapter 6
Dendritic Amine Functionalized Mesoporous Silica:
Detailed Study on Henry Reaction

List of Abbreviations

BAPA	bis(3-aminopropyl)amine
DCC	N,N'-Dicyclohexylcarbodiimide
DCM	Dichloromethane
DHPM	Dihydropyrimidinones
DIEA	*N,N*-Diisopropylethylamine
DMF	Dimethylformamide
DMSO	Dimethyl sulfoxide
EAA	Ethyl Acetoacetate
HOBt	2-Hydroxybenzotriazole
MeOH	Methanol
m. p.	Melting Point
MS	Mesoporous Silica
NaF	Sodium fluoride
NH_4OAc	Ammonium Acetate
NMP	N-Methyl-2-pyrrolidone
PAMAM	Poly(amidoamine) dendrimers
P123	Copolymer of ethylene oxide and propylene oxide
PPI	Poly(propyleneimine)
TEOS	Tetraethyl Orthosilicate
TFA	Trifluroacetic Acid
THF	Tetrahydrofuran
TLC	Thin Layer Chromatography
TMS	Tetramethylsilane
TMOS	Tetramethyl Orthosilicate
TOF	Turnover Frequency
rt	Room Temperature

Chapter 1

INTRODUCTION

This chapter gives a brief description of dendrimers and methods of their synthesis. Need for organocatalysts and modification of dendrimers on solid support are discussed here. The role of mesoporous silica as support, its synthesis and functionalization are explained in this chapter. High surface area, tunable pore size and narrow pore size distribution make mesoporous silica effective support for dendrimers. Recent literature on organic reactions catalyzed by mesoporous silica supported dendrimers and dendrimers as organocatalysts are also reviewed in this Chapter.

1.1 Introduction

A powerful tool to enhance the sustainability of chemical processes is undoubtedly catalysis. After the advent of the concept of catalysis, numerous catalysts were developed, which include, several ligands, metal catalysts, polymers, supported catalysts, organocatalysts etc.[1, 2] The importance of polymers has expanded over the last few decades resulting in the development of various classes of polymers. Based on the diverse set of applications ranging from catalytic field to medical devices, polymers can be synthesized with specific chemical, physical and medicinal properties. As the fourth major class of polymer architecture, coming after traditional types, which include linear, cross-linked and branched architectures, dendritic polymers became a very hot topic from 1980s.[3-7] Dendritic polymers are highly branched polymeric structure with complex secondary architecture and well defined spatial location of functional groups.[8-12] Mainly, they consist of four subclasses: (1) dendrimers, (2) hyperbranched polymers, (3) dendrigraft polymers, and (4) dendronized polymers (Figure 1.1).
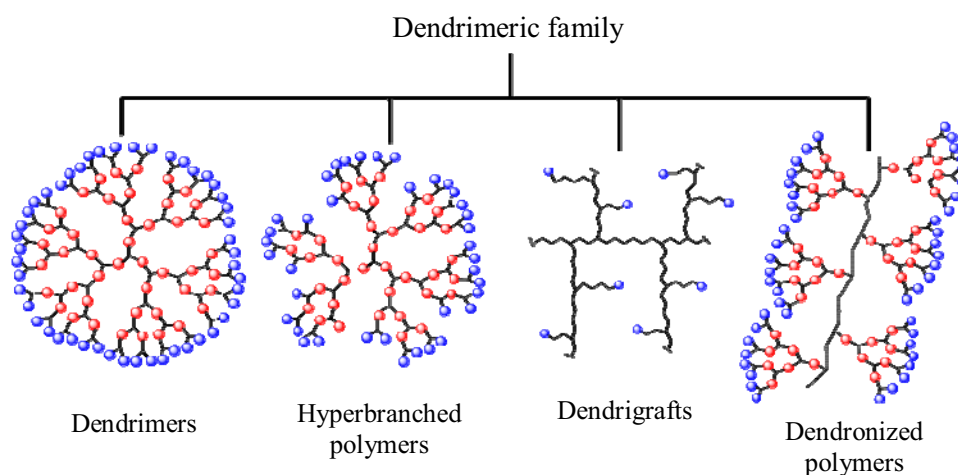
Figure 1.1 Classification of dendrimeric species

Among these important classes, dendrimers have wide application in different areas like biological field, catalysis, drug delivery, etc.[13] The term ''dendrimer'' is derived from the Greek 'dendra' means tree and 'meros' means parts and describes graphically the structure of this new class of macromolecules which have highly branched, three-dimensional features that resemble the architecture of a tree (Figure 1.2). The monomer units are assembled in a controlled step-growth polymerization process and are organized in layered "generations".[14] The branched structure of dendrimers affords a globular, three-dimensional macromolecular shape and generally imparts a set of properties including high solubility, low viscosity, adhesivity, and glass-transition temperature which differ from the corresponding linear analog.[15-20] As a consequence of the macromolecular structure and resulting properties, dendrimers are being evaluated in systems ranging from chemical catalysis to clinical therapies.[21-29]
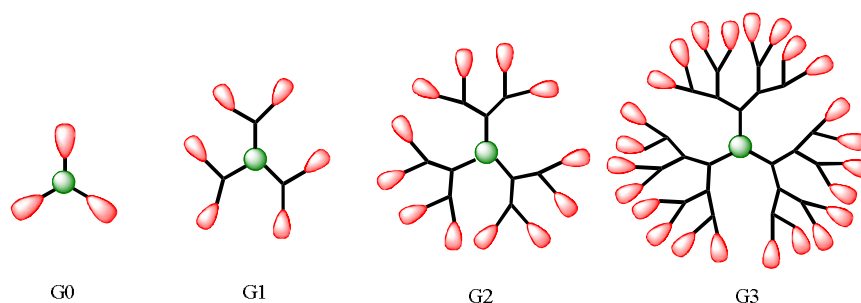
G0   G1   G2   G3

Figure 1.2 Typical architecture of G0, G1, G2 and G3 dendrimers

Dendrimers consist of three basic components: core, interior, and surface (Figure 1.3).[30] Core represents the centre part of dendrimers and it mainly affects the geometry of dendrimers. Interior means the space between the last outer branching point and the centre. In dendrimers, the surface consists of a varying number of peripheral functional groups.
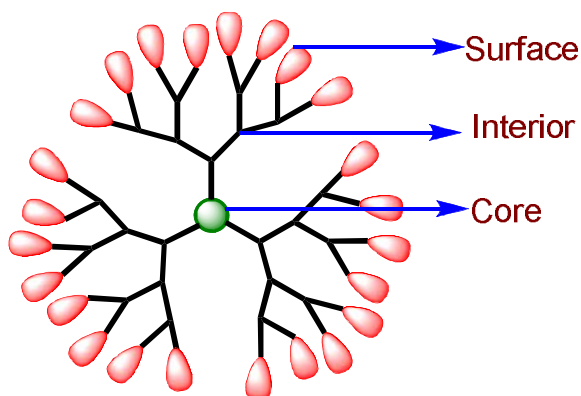
Figure 1.3 Structure of dendrimer

1.2   Synthesis of dendrimer

Dendrimers are generally prepared using either a divergent method or a convergent one. In the divergent method, dendrimer grows outwards from a multifunctional core molecule. The core molecule reacts with monomer molecules containing one reactive and two (or, more) dormant groups giving the first generation dendrimer. The new periphery of the molecule is activated for reactions with more monomers. The process is repeated for several generations and a dendrimer is built layer after layer (Figure 1.4).[31]
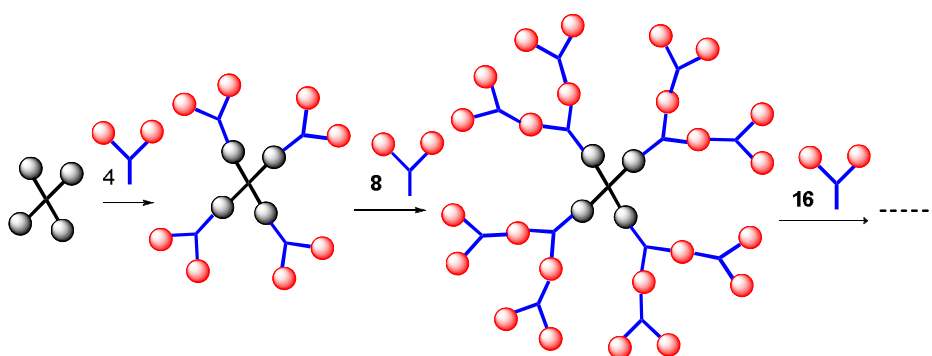
Figure 1.4 Synthesis of dendrimer by divergent method

The divergent approach is successful for the production of large quantities of dendrimers. Problems occur from side reactions and incomplete reactions of the end groups that lead to structure defects. To prevent side reactions and to force reactions to completion, large excess of reagents is required. It causes some difficulties in the purification of the final product.

In the convergent growth approach, dendrimer construction begins at what will eventually become the outer surface shell of the ideally branched macromolecule and proceeds inward, by a step-addition of branching monomers, followed by the final attachment of each branched dendritic sub-unit (or dendron) to a polyfunctional core (Figure 1.5).[32]
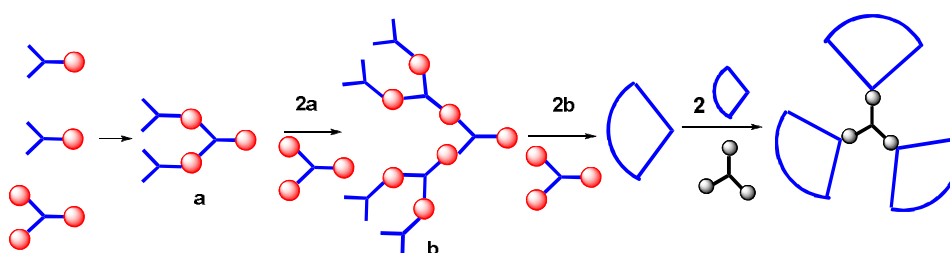
Figure 1.5 Synthesis of dendrimer by convergent method

The convergent growth method has several advantages. It is relatively easy to purify the desired product and the occurrence of defects in the final structure is minimized. It becomes possible to introduce subtle engineering into the dendritic structure by precise placement of functional groups at the periphery of the macromolecule. The convergent approach does not allow the formation of higher generations because steric problems occur in the reactions of the dendrons and the core molecule.

The most recent fundamental breakthrough in the practice of dendrimer synthesis has come with the concept and implications of 'double exponential' growth.[33] A schematic representation of double exponential and mixed growth is shown in Figure 1.6. This approach allows the preparation of monomers for both convergent and divergent growth from a single starting material. These two products are reacted together to give an orthogonally protected trimer, which may be used to repeat the growth process again.
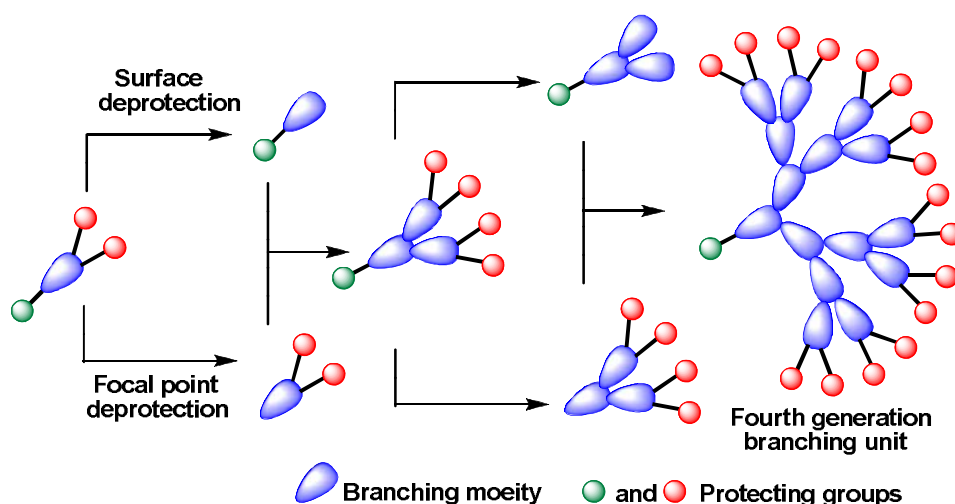
Figure 1.6 Double exponential synthesis method of dendrimer

Tomalia, *et al.*[34] published the synthesis and characterization of a novel class of poly(amidoamine) (PAMAM) dendrimer. They synthesized the PAMAM using divergent method in which Michael addition of a molecule of ammonia (the dendritic core) to three molecules of methyl acrylate, followed by amidation of the esters by an excess of ethylene diamine. The exhaustive Michael addition-amidation reaction sequence was

then repeated in a reiterative fashion to achieve an almost monodisperse dendritic structure with a molecular weight of over 25,000 Da. The structure of PAMAM dendrimer is shown in Figure 1.7.
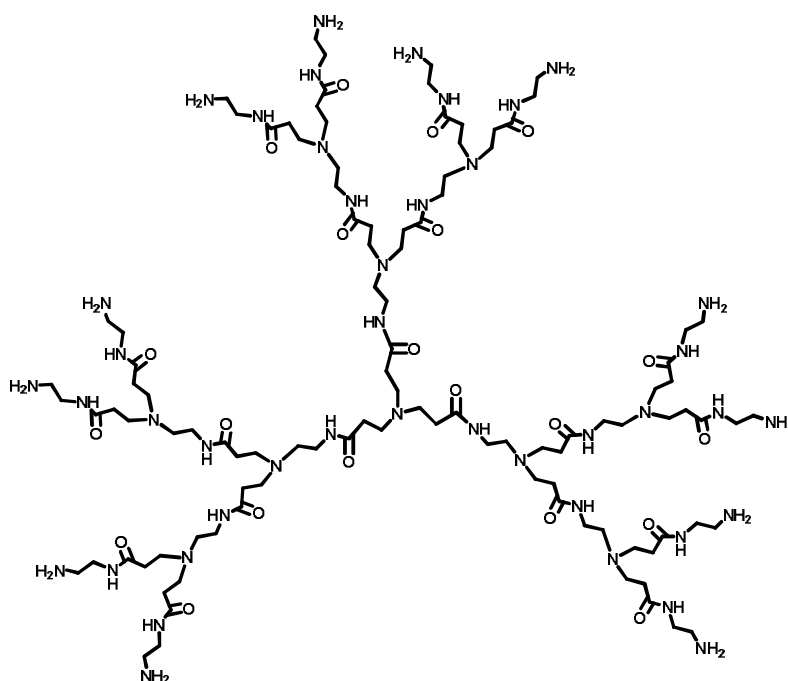
Figure 1.7 Structure of PAMAM dendrimer

Dendrimers became a hot topic in science after the discovery of PAMAM dendrimer and a multitude of dendrimers have been synthesized ranging from poly(propylene imine) (1),[35-37] dendritic polymers composed of glycerol and succinic acid (2),[38] polysilane containing SO_3Na end groups (3),[39] polysilane containing SH end groups (4)[39(d)] etc are shown in Figure 1.8.
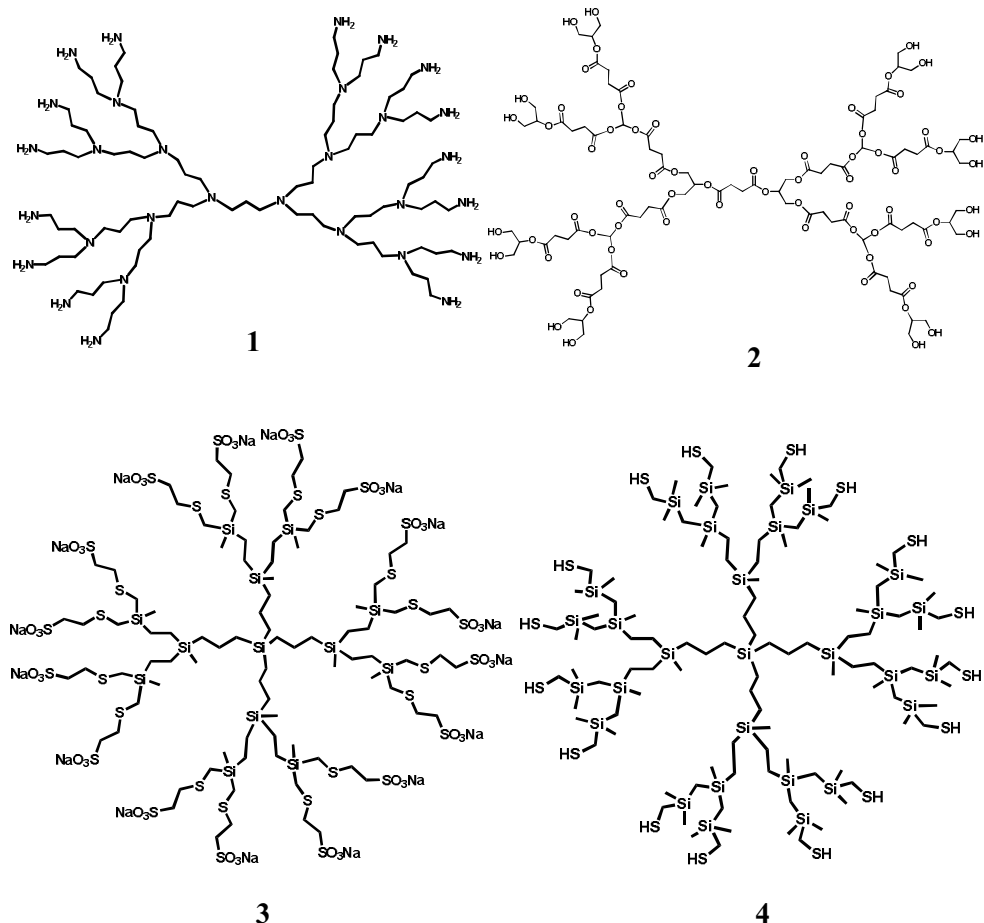
Figure 1.8 Structure of different dendrimers

Due to the high degree of branching in dendrimer, the number of functionalities at the surface increases fast relative to the overall size of the molecule. Therefore, important differences exist between the overall shape of low and high generation dendrimers. The latter can be thought of as spheres with closely situated surface functionalities that isolate the dendritic interior, whereas the low generation structures are nonspherical open structures. Thus, by increasing the generation of a dendrimer, a differentiation will gradually arise between the structure's interior and the exterior, and thereby the overall

properties become different from what is obtainable for small molecules. Nondendritic polymers possess the same ability to isolate parts of their structure, but these micro environments are, due to a less controlled synthesis, poorly defined. Hence, dendrimers constitute, in a unique way, structures which can be precisely designed for a desired function, and these properties have opened application areas such as material science, biology and medicine for applications such as synthesis, catalysis, chromatographic separation, and drug and vaccine development.[40]

1.3   Application of dendrimers in catalysis

For the exploration of catalytic applications, the choice of dendrimer platform generally reflects commercial availability or the ease of synthetic access. The development of synthetic routes that are environmentally friendly and industrially compatible represents an important step towards the successful application of dendrimers in catalysis.[41] Based on the activity and selectivity of the dendritic catalyst, they are classified in to three types. (a) core-functionalized, (b) periphery functionalized, and (c) focal point-functionalized (Figure 1.9).
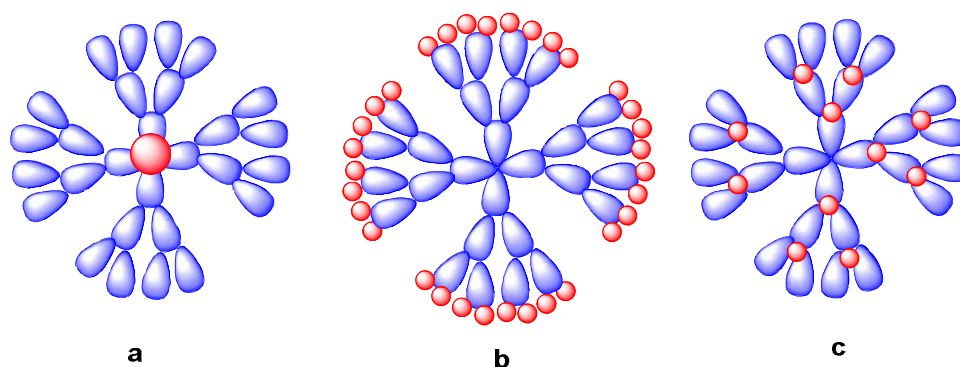
Figure 1.9 Location of catalytic entities in dendrimeric molecule (a) core, (b) periphery, (c) focal point

1.3.1 Core functionalized dendrimers

In this case, the catalyst could especially benefit from site isolation created by the environment of the dendritic structure. Site isolation effects in dendrimers can be beneficial for other functionalities. For reactions that are deactivated by excess ligand or in cases that a bimetallic deactivation mechanism is operative, core-functionalized systems can specifically prevent such deactivation pathways. Core-functionalized dendritic catalysts may benefit from the local environment created by the dendrimers which differs from the bulk solution.[42]

1.3.2 Periphery functionalized dendrimers

They have their catalytic sites located at the surface of the dendrimer support, and these active sites are therefore directly available to the substrate, which is in contrast to core functionalized systems in which the substrate enters the dendrimer prior to reaction. The high accessibility allows reaction rates that are comparable with homogeneous systems. On the other hand, the periphery functionalized systems contain multiple reaction sites, which result in extremely high local catalyst concentration.[43]

1.3.3 Focal point-functionalized (on a dendritic wedge) systems

Here, catalytic active sites are observed in the building blocks of dendrimers. Main advantages of this type of catalysts are: concentration of catalytically active site is enhanced when generation of dendrimers is increased and it is easily available for reactants than core functionalized dendrimers.[44-46]

1.4   Heterogenization of dendrimers on solid support

In principle, dendrimer is one of the most promising candidates which can meet the needs for an ideal catalyst such as persistent and controllable nanoscale dimensions, chemically reactive surface, favourable configurations in which all the active sites would always be exposed towards the reaction mixture so that they are easily accessible to migrating reactants. But dendrimer synthesis is a complicated procedure via convergent or divergent method. For getting 100 % loading of functional groups, excess reagents are used. This makes the problem in purification of each generation of dendrimers. Another problem is the regeneration of dendrimeric catalyst from reaction mixture and reusability in catalysis. To solve this problem, the possible solution is the heterogenization of dendrimers on a solid support.

A suitable support used in general is based on these properties: 1) inertness in reactions, 2) hardness and compressive strength, 3) stability and ease of regeneration, 4) high surface area, 5) porosity, and 6) low cost.[47] The heterogeneous catalysts are much more complex than their homogeneous counterparts, and many additional parameters such as type of support, spacer length and flexibility, surface coverage degree, surface area and porosity have to be optimized to achieve an acceptable catalytic performance.[48-49] A series of solid matrixes such as inorganic oxides, silica, modified silica, alumina, zeolites and clays have been adopted as supporting materials.[50] The use of inorganic solids can demonstrate certain advantages over other types of supports. In general, the rigid framework can prevent the aggregation of active catalysts which sometimes leads to the formation of inactive multinuclear species. The chemical and thermal stabilities of the inorganic supports are

also superior, rendering them compatible with a broad range of reagents and relatively harsh reaction conditions. Compared with organic polymeric supports, inorganic solids are generally superior in their mechanical properties, which make them less prone to attrition caused by stirring and solvent attack. One negative aspect of an inorganic solid-immobilized catalyst is the extreme difficulty in the characterization of the catalytic species, apart from common problems suffered by heterogenized catalysts.[51-57]

The ideal supported catalyst should thus satisfy many requirements in order to combine both the advantages of homogeneous and heterogeneous catalysis.[58] Heterogeneous catalytic reactions typically occur through the adsorption of reactants on the surface of the catalyst, followed by cleavage or recombination of the chemical bonds of the reactants on the catalyst surface.[59] Therefore, the catalytic activity, selectivity, and shelf-life of heterogeneous catalyst strongly depend on the surface structure of the support materials. Hence, to successfully develop efficient heterogeneous catalysts, the rational choice of the support material and the use of right synthetic strategy for placing the active catalytic groups on the support material are vital.[60]

1.5 Mesoporous silica

Mesoporous silica have well-defined pore sizes of about 2.0-50 nm and possess extremely high surface area and narrow pore size distribution. The first mesoporous silica material was reported as early as 1971, where, a material described as low-bulk density silica was obtained by hydrolyzing and condensing tetraethoxysilane in the presence of cationic surfactants.[61] This result did not gain much attention at the time it was published because the porosity and structural properties were not reported. Until 1992, the

Chemistry community did not realize the potential of this field, until scientists in Mobil Corporation laboratories published a series of reports on ordered mesoporous materials (M 41S) with pore sizes ranging from 1.5-10 nm.[62-66] The variant called MCM-41 with surface area 1000 m^2g^{-1} and pore volumes up to 1 cm^3/g, has been comprehensively studied and widely applied in many fields such as drug delivery, biosensors and catalysis.[67-70] The morphological transformations that led to converting bulk MCM-41 mesoporous silica to functionalized mesoporous silica nanospheres (MSNs) represented a step forward towards increasing control of kinetics in catalytic reactions occurring in functionalized MSN.[71, 72] The first report of utilizing mesoporous silica as catalysts in polymer synthesis was initiated by Aida's group in Japan.[73] The authors reported crystalline nanofibers of linear polyethylene with an ultra high molecular weight (6,200,000) and a diameter of 30 to 50 nanometers, formed by the polymerization of ethylene with mesoporous silica fibres–supported titanocene, with methylaluminoxane as a cocatalyst. Small-angle X-ray scattering analysis indicated that the polyethylene fibres consisted predominantly of extended-chain crystals. Another article in JACS highlighted the potential utility of the honeycomb-like porous framework as an extruder for nanofabrication of polymeric materials.[74]

Mesoporous silica materials may be divided into two main groups according to their internal arrangement of channels. The first group which shows a channel-like pore system was the first to be discovered and has been in the centre of research for a long time. This pore system exists in e.g. MCM-41, MCM-48 and SBA-15.[75] In MCM-41 and SBA-15 the pores are one dimensional channels which are arranged parallel to each other in a hexagonal fashion.[76] MCM-48 has a more complicated structure where the one

dimensional channels are branched in a three dimensional system. The channels have a uniform inner diameter. The second group includes materials like SBA-1, SBA-2, SBA-16 and KIT-5.[77] These materials have larger cages connected via smaller openings and channels in a three dimensional system. Periodic mesoporous silica have a high specific surface area >1000 m^2/g and also a high specific pore volume > 0.5 cm^3/g. The materials are thermally robust and relatively inert to chemical environments.[78-80]

1.6   Advantages of mesoporous silica

The systematic use of immobilization of organic functional groups has increased in the past three decades, mainly on silica, because this support offers pronounced advantages over other organic/inorganic supports as listed below.[81-84]

a)   Immobilization on silica results in a great variety of silylating agents, allowing pendant functional groups in the inorganic framework.

b)   Attachment is easier on silica surface than on organic polymeric supports, which have a high number of cross-linking bonds, requiring hours to reach equilibrium for surface activation.

c)   Silica gel is the most popular substrate for surface studies, because, it is the first commercially available high specific surface area substrate with constant composition, enabling easy analysis and interpretation of results.

d)   Silica gel has high mass exchange characteristics and no swelling.

e)   Silica support has great resistance to organic solvents.

f)   Silica has very high thermal resistance

g)   Easily available precursors and simple synthetic procedure

1.7   Synthesis of mesoporous silica

The first mesoporous silica synthesized with non-ionic triblock polymers were reported in 1998 by Stucky, *et al.*[77] These materials were named SBA-*X* (Santa Barbara Amorphous) where *X* is a number corresponding to a specific pore structure and surfactant, e.g. SBA-15 has hexagonally ordered cylindrical pores synthesized with P123 as surfactant while SBA-16 has spherical pores arranged in a body centred cubic structure and is synthesized with F127. SBA-15 is the most extensively studied mesoporous silica. Other families of mesoporous silica like MSU, KIT, FDU and AMS were also reported.[78, 85-87] Main ingredients needed for the silica synthesis are silica precursor and structure directing agents in the presence of acidic or basic medium. Mainly, two chemical reactions occur during the formation of mesoporous silica such as hydrolysis and condensation (Scheme 1.1). In aqueous solution, the alkoxides are hydrolysed and undergo polymerisation to form a silica network. Both steps can be controlled by varying the pH and adding salts to the aqueous solutions.[88-93]
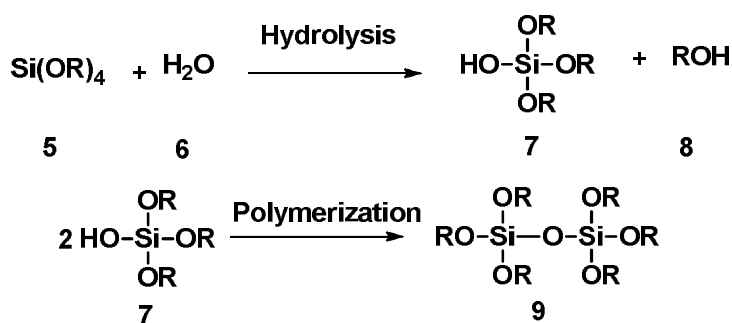
Scheme 1.1 Formation of mesoporous silica framework

Several types of silica precursors can be used for mesoporous silica. The most common are alkoxides, especially, tetramethyl orthosilicate (TMOS) or tetraethyl orthosilicate (TEOS). Other alkoxides with longer alkyl chains can also be used. An alternative, cheaper, silica precursor that can also be used is sodium silicate or combinations of this and alkoxides.[88-90] In the present work, TEOS has been used as the silica source. Different types of surfactants are used for the synthesis of mesoporous silica such as cationic, anionic and noninonic surfactants.

1.7.1 Removal of surfactants

The final step of the synthesis is the removal of surfactants. This is most often done by calcination, but there are alternatives such as chemical removal of the template or decomposition by microwave. Regardless of which method is used, the aim is always to completely remove the surfactants in a way that is as cheap and time effective as possible.[91]

1.7.1.1 Calcination

Calcination is the most common way to remove the surfactants from mesoporous silica. Calcination is performed in air, the material is heated to 550 °C and this temperature is held for 5-6 h before the material is cooled down to room temperature.[92-94] Shrinkage of hexagonal structures is a drawback here.

1.7.1.2 Chemical removal

An alternative route to the removal of the surfactants is to oxidize the P123. By using this alternative route, there is no shrinkage in the hexagonal structure as it is upon calcination and it is possible to functionalize the material in multiple steps. For this purpose, chemicals such as ethanol, hydrogen peroxide, sulfuric acid or ammonium perchlorate can be used.[95-97]

1.7.1.3 Microwave digestion

The fastest method to remove the template from mesoporous silica is to use microwave digestion. When mesoporous silica is mixed with HNO_3 and H_2O_2 or alternatively ethanol and hexane and exposed to microwave radiation for 2 min, the surfactants are completely removed. These samples also contain higher silanol concentration compared to calcinated samples. Moreover, there is no shrinkage of the framework with this method which yields higher surface area, larger pore size and pore volume compared to calcination.[98-104]

1.8 Factors affecting the synthesis of mesoporous silica

The synthesis of ordered mesoporous silica is controlled with a wide range of synthesis variables, which are dependent on the specific wet chemistry of the system studied. The mesoporous silica has been synthesized with mechanisms including relative kinetics and interactions between inorganic and organic components. Main variables like changing the silica source like fused silica, colloidal silica, tetraethyl orthosilicate, surfactants (eg: hexadecylamine, cetyltrimethyammonium bromide and P123) or reaction conditions such as solvent, temperature, aging time, reactant mole ratio, pH of the medium affecting the surface area, pore dimensions and structure of mesoporous silica. At the same time, these changes also affect the thermal, hydrothermal and mechanical stability of the materials.[80-83]

1.9 Structure of mesoporous silica surface

The surface of mesoporous silica consists of silanol groups (Si-OH) and less reactive siloxane groups (Si-O-Si). Silanol groups are formed on the surface by two main processes. First, such groups are formed in the course of silica synthesis, e.g. during the condensation polymerization of

Si(OH)$_4$ (Scheme 1.2).[105] Here, the supersaturated solution of the acid becomes converted into its polymeric form, which then changes into spherical colloidal particles containing Si-OH groups on the surface. Upon drying, the hydrogel yields xerogel, the final product, which retains some or all of the silanol groups on its surface. Secondly, surface OH groups can form as a result of rehydroxylation of dehydroxylated silica when it is treated with water or aqueous solutions. The surface silicon atoms tend to have a complete tetrahedral configuration, and in an aqueous medium their free valence becomes saturated with hydroxyl groups.
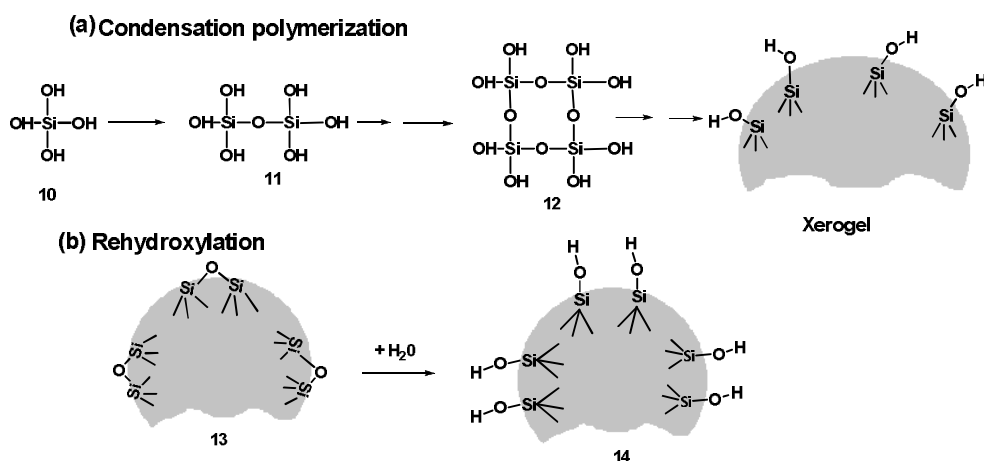
Scheme 1.2 Formation of silanol groups on the silica surface

Silica surface contains mainly three types of hydroxyl groups. They are free, isolated hydroxyl groups, geminal and vicinal hydroxyl groups (Figure 1.10). The silanol groups could be isolated (free silanol groups), where the surface silicon atom has three bonds into the bulk structure and the fourth to OH group. The vicinal or bridged silanols, where two isolated silanol groups attached to two different silicon atoms are bridged by hydrogen bond. A third type of silanols called geminal silanols consist of

two hydroxyl groups attached to one silicon atom. The geminal silanols are close enough to have H-bond whereas free silanols are too far separated.[105]
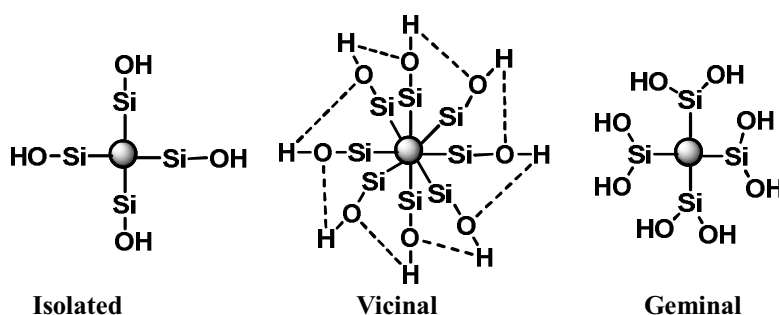
Figure 1.10 Different types of silanol groups on silica surface

1.10 Methods for heterogenization of catalysts

Regarding catalyst heterogenization, there are almost three approaches that have been described in the literature (Figure 1.11).[49] They are 1) formation of covalent bonds (covalent approach), 2) adsorption by ion pair formation, and 3) entrapment.
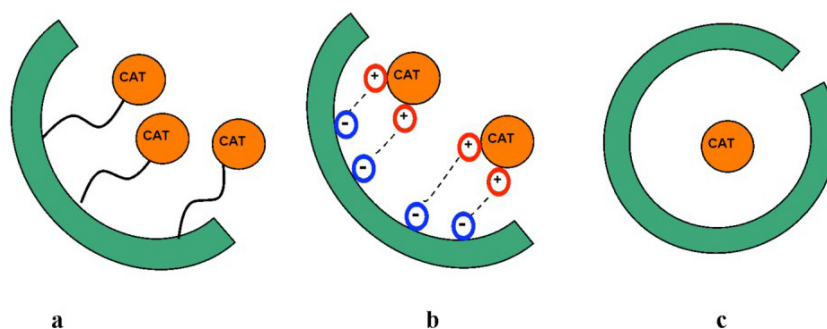
Figure 1.11 Anchoring methodologies: a) covalent binding, b) adsorption, c) entrapment[49]

The covalent approach is the most popular and versatile one.[48] It can be achieved by copolymerization of the modified catalyst with an appropriate monomer or more commonly by grafting the catalyst onto a polymeric

support that was synthesized in advance. Due to the stable covalent bond, the problem of catalyst leaching is generally low. The adsorption by *van der Waals* interactions and hydrogen bonding, as well as ion-formation by electrostatic interaction are also useful approaches for catalyst immobilization, because they avoid the chemical modification of the catalysts. However, the stability of the adsorbed or electrostatically bound catalyst strongly depends on several factors such as ionic strength of the medium and the solvent.[106] The encapsulation and entrapment of catalysts is the last example for the immobilization approach. It requires a porous support with pore sizes that are small enough to prevent catalyst leaching. There are two methods for this approach: The catalyst is built-up inside the preformed support like a "ship-in-a-bottle" or the support is synthesized around the catalyst. The advantage in this approach is that the catalyst does not have to be modified, but the resulting catalysts often suffer from diffusion problems.[107]

1.11 Functionalization of mesoporous silica via covalent approach

Functionalization of mesoporous silica materials with organic groups has attracted considerable research interest in the past few years.[108] In particular, ordered mesoporous materials such as SBA-15 are ideal candidates for functionalization due to their higher hydrothermal stability, desired morphology, adjustable pore sizes (2-30 nm), and thick walls that can be easily functionalized using silanol chemistry.[109-111] SBA-15 has been functionalized with various organic functional groups, including amines, thiols, carboxylic acid, sulfonic acid, and vinyl group. Two basic processes may be applied (Figure 1.12).[112-114] In the post-synthesis modification (grafting or coating), the preformed mesoporous silica is reacted with an appropriate organosilane. In the direct synthesis, co-condensation of the primary building blocks, namely, a silica

precursor (e.g., a tetraalkoxysilane) and an organosilane, is carried out in the presence of a suitable surfactant. In either case, further transformation may be necessary to create the required surface functional group.[115-123]
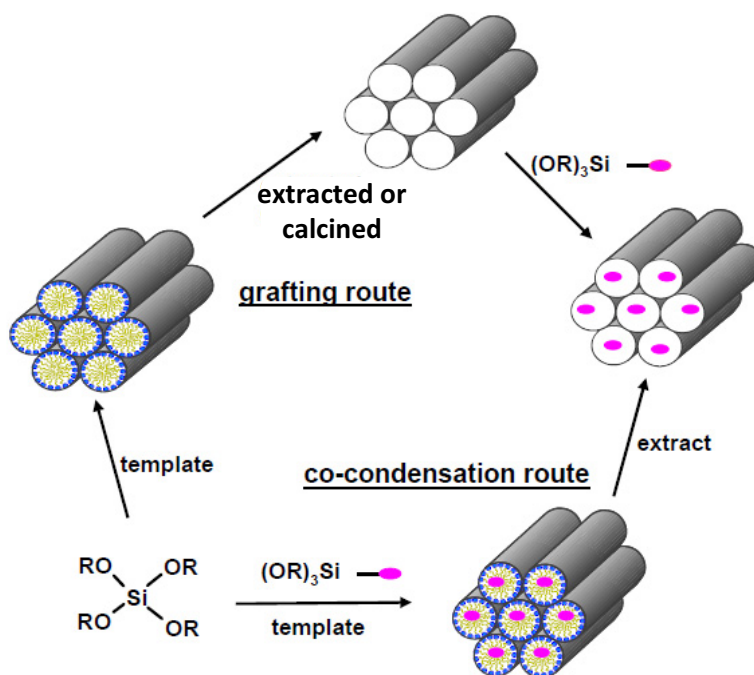
Figure 1.12 Functionalization of mesoporous silica by grafting and co-condensation method[112]

1.12 Heterogenization of dendrimers

Heterogenization of dendrimers on mesoporous silica has the following advantages:

1) The possibility of using excess of reagents to ensure the completion of reactions

2) Facility in the purification process after each generation

3) Desired products can be isolated easily by simple filtration and removed from the support material

4) High thermal and chemical stability of catalytically active site on supported dendrimer

5) Toxic or obnoxious low molecular weight compounds can be made odourless and less toxic when they are attached to solid polymer supports

6) Automation of repetitive synthesis steps is possible, which results in reproducibility and higher yields compared to manual laboratory work

7) Substrate is coupled to a chemically inert insoluble polymer by a covalent bond. This bond must remain stable during the whole chemical process

8) The high surface area and pore diameter of mesoporous silica make them capable of high loading

9) Simple filtration makes the removal of catalyst from the reaction mixture

10) Catalytically active sites are easily accessible to the reactants

11) Due to the covalent binding of dendrimers on mesoporous silica, reuse of catalyst does not destruct the structure of catalyst

12) Due to the chemical inertness of mesoporous silica, it should not interfere or harm the reaction media in catalysis and synthesis of dendrimers on it

13) Since there is high concentration of silanol groups on the surface of silica, it can be easily replaced by dendritic units

14) Mesoporous silica should be nontoxic and cheap to produce and dispose off

Because of these advantages, dendrimer on mesoporous silica have great demand in the field of catalysis. Strong mesoporous silica support and large amount of surface functionalities on dendrimers enable them to overcome the major problems faced in heterogeneous catalysis.

1.13 Supported dendrimer catalysis

The development of well-defined catalysts that facilitate fast and selective chemical transformations which can be separated from the product is still an important challenge. The catalytic species become more stable and show more selectivity when they are attached to the solid support. The most important advantage in using a supported catalyst is the simplification of product work-up, separation and isolation of products. In the case of supported catalyst, for separation and isolation of products, simple filtration is sufficient. In this section, brief description of mesoporous silica supported dendrimer catalysts and organocatalysis by dendrimers are presented.

Rosario and coworkers[124] synthesized the super paramagnetic nanoparticle MNP (Fe_2O_3/polymer) supported dendritic catalyst based on a bulky electron-rich phosphine Pd(II) complex (Figure 1.13). The catalytic activity of the MNP-Pd supported catalyst was investigated in a copper-free Sonogashira C–C cross-coupling reaction between halo arenes and phenylacetylene compounds. Quantitative yields were obtained within one hour with iodobenzene and bromobenzene derivatives in methanol. In contrast, in aqueous conditions, a conversion over 80 % was observed up to ten cycles with values of palladium leaching similar to those observed in methanol medium.
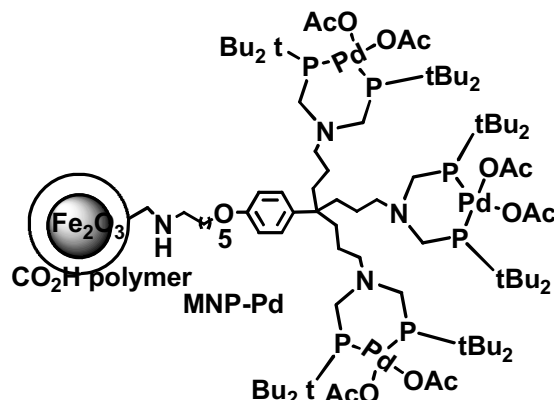
Figure 1.13 Core shell Fe$_2$O$_3$ /polymer supported diphosphino palladium complex

A new and rational method for the synthesis of Fe$_3$O$_4$@SiO$_2$@SiO$_2$(CH)$_3$Cl based magnetic nanoparticles with amino cobalt phthalocyanine tags (ACoPc-MNPs) was described by Zolfigol, *et al.*[125] It was evaluated as a reusable catalyst for the one-pot synthesis of tetrahydrobenzopyran derivatives (Scheme 1.3 and Figure 1.14). They have shown that the advantages of the present method are (a) easy and simple work-up, (b) short reaction times, (c) mild reaction conditions, (d) room temperature of the reaction, (e) excellent yields, and (f) ease of separation of the catalyst using an external magnet. Moreover, the catalyst used was easily recovered by applying an external magnetic field and reused without any noticeable loss of activity at least 4 times.
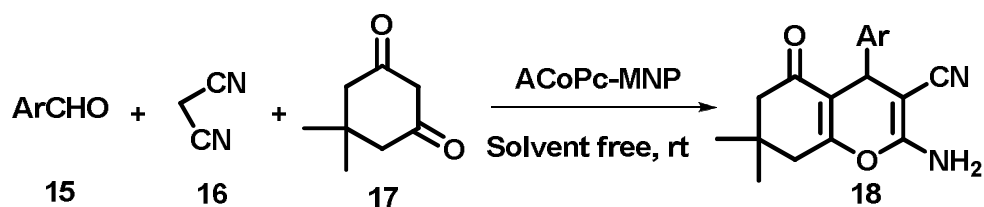
Scheme 1.3 ACoPc-MNP catalyzed synthesis of tetrahydrobenzopyran derivatives
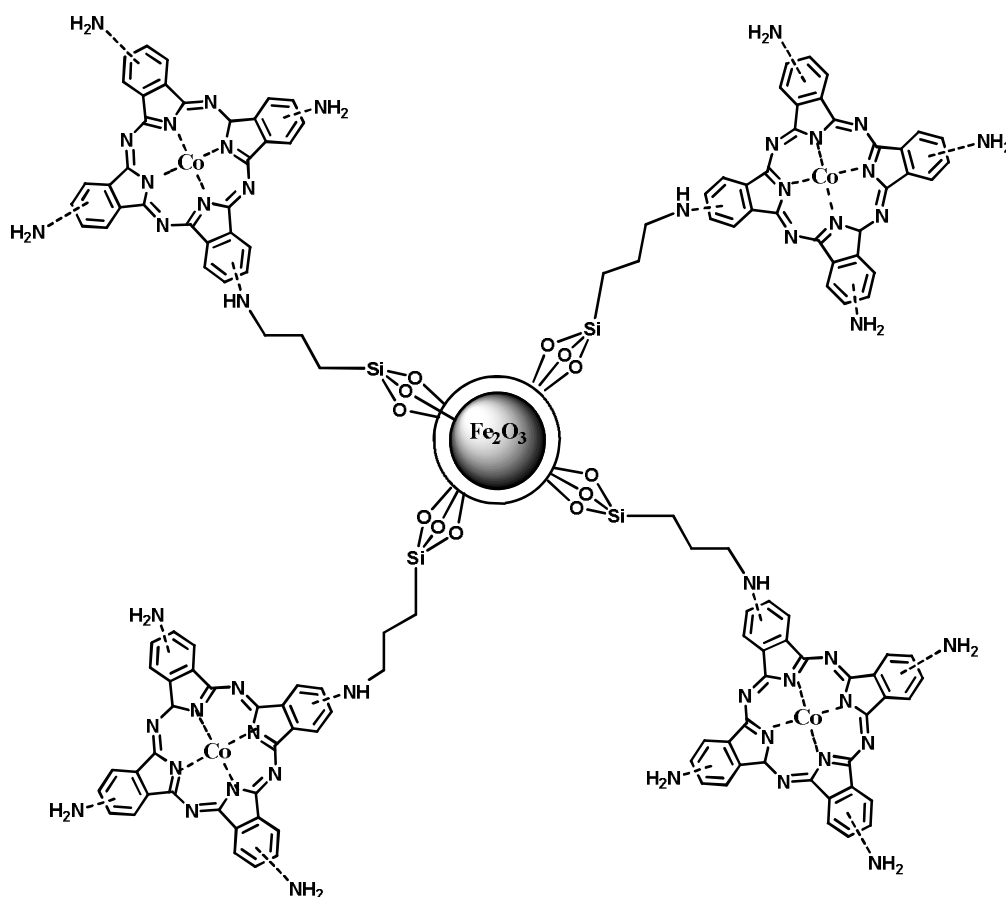
Figure 1.14 Structure of ACoPc-MNP[125]

Hongfang, *et al.*[126] reported the incorporation of PAMAM dendrimer on SBA-15 through post-synthesis method (Scheme 1.4). Highly dispersed Pt NPs were successfully encapsulated in the channels of PAMAM-SBA-15 support and used it for electron transfer reactions such as (i) the typical reduction reaction between $Fe(CN)_6^{3-}$ and $S_2O_2^{2-}$ at 40 °C and (ii) reduction of *p*-nitrophenol by $NaBH_4$ at 25 °C. After the catalytic reaction, the supported Pt catalyst was reusable after centrifugal separation and washing with water.

They have recycled the above reactions five times using Pt-G4-SBA15 catalyst under similar reaction conditions.
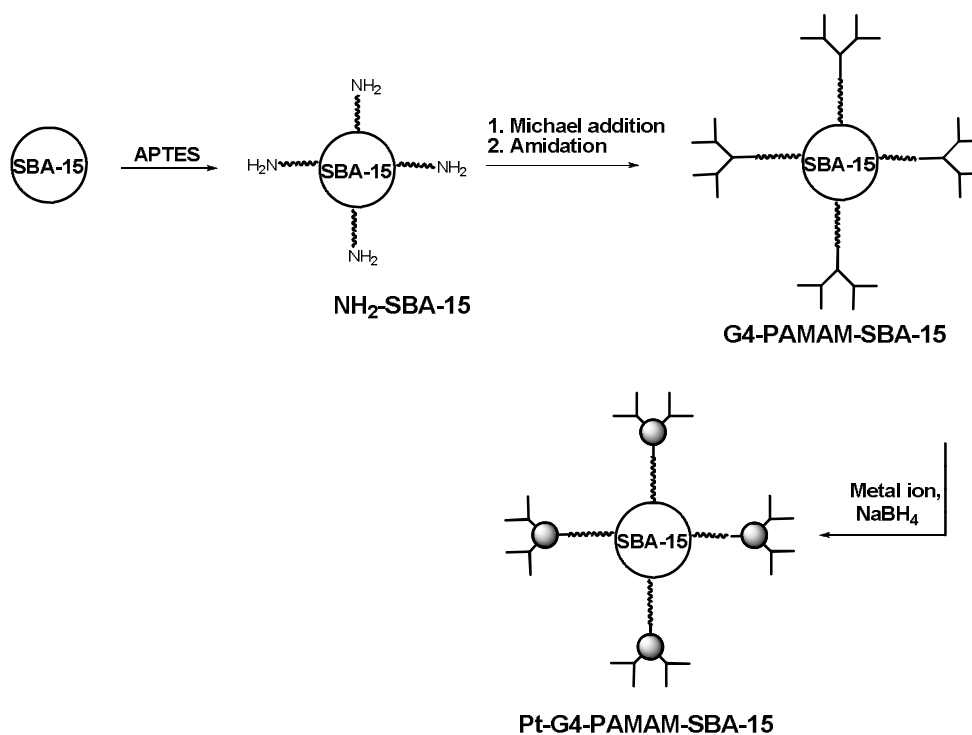
Scheme 1.4 Procedure for the synthesis of Pt NPs catalyst in G4-SBA-15.

A periodic mesoporous silica-supported recyclable Rhodium-complexed dendrimer catalyst for hydroformylation of olefins was reported by Reynhardt, *et al.*[127] (Figure 1.15). The G(0) materials were found to be excellent recyclable catalysts for olefin hydroformylation than G1 due to the lower levels of Rhodium in G1 because of steric hindrance (Figure 1.16). A turnover frequency (TOF) as high as 1800 h^{-1} was obtained for the hydroformylation of 1-octene at 70 °C.
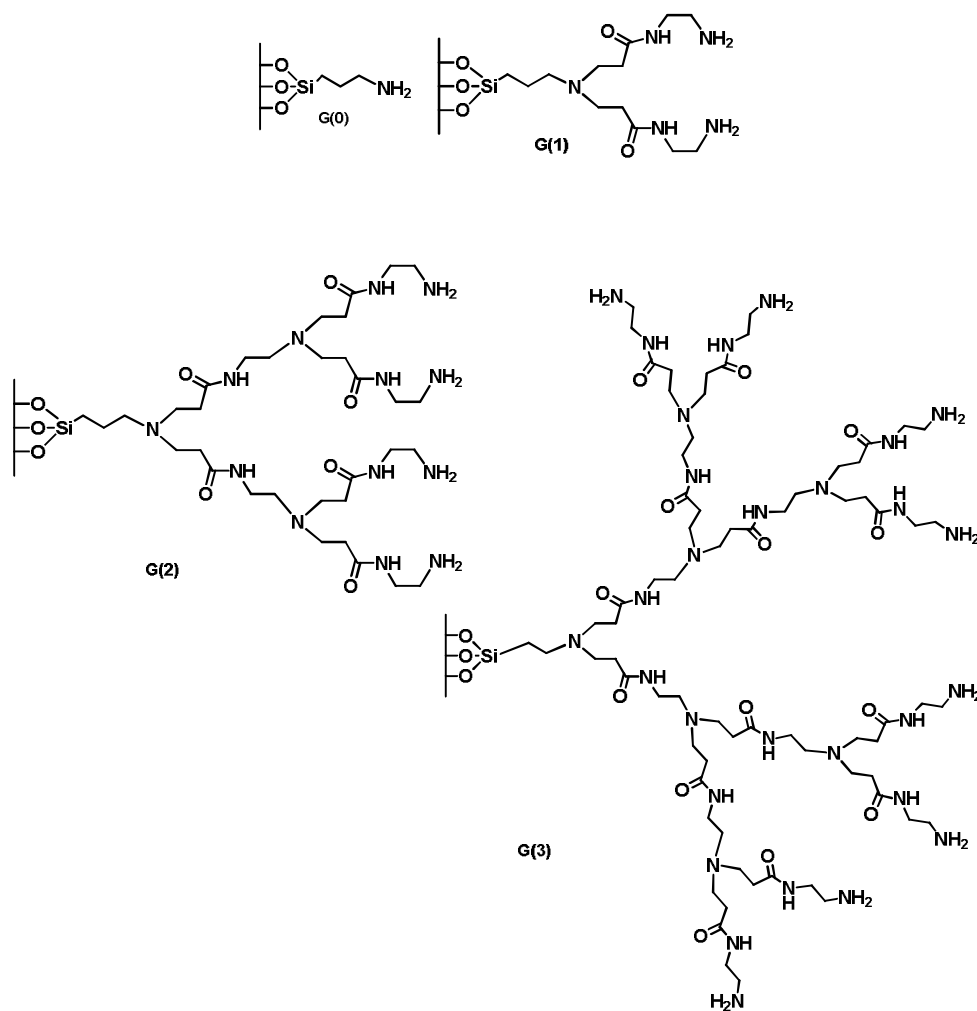
Figure 1.15 Structures of G0, G1, G2 and G3
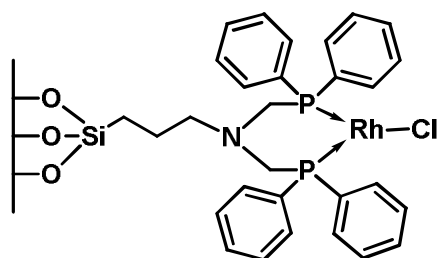
Figure 1.16 Structure of Rh-G0

A new kind of silica-supported third-generation dendrimers capped by 1,4-diaza-bicyclo[2.2.2]octane (DABCO) group stabilized palladium(0) nanoparticles was introduced by Xu and coworkers[128] (Scheme 1.5). The resulting silica-supported dendrimer-stabilized palladium(0) nanoparticles with a particle size of 10-20 nm were prepared in situ by treatment with $PdCl_2$ and hydrazine in ethanol at 60 °C for 24 h.
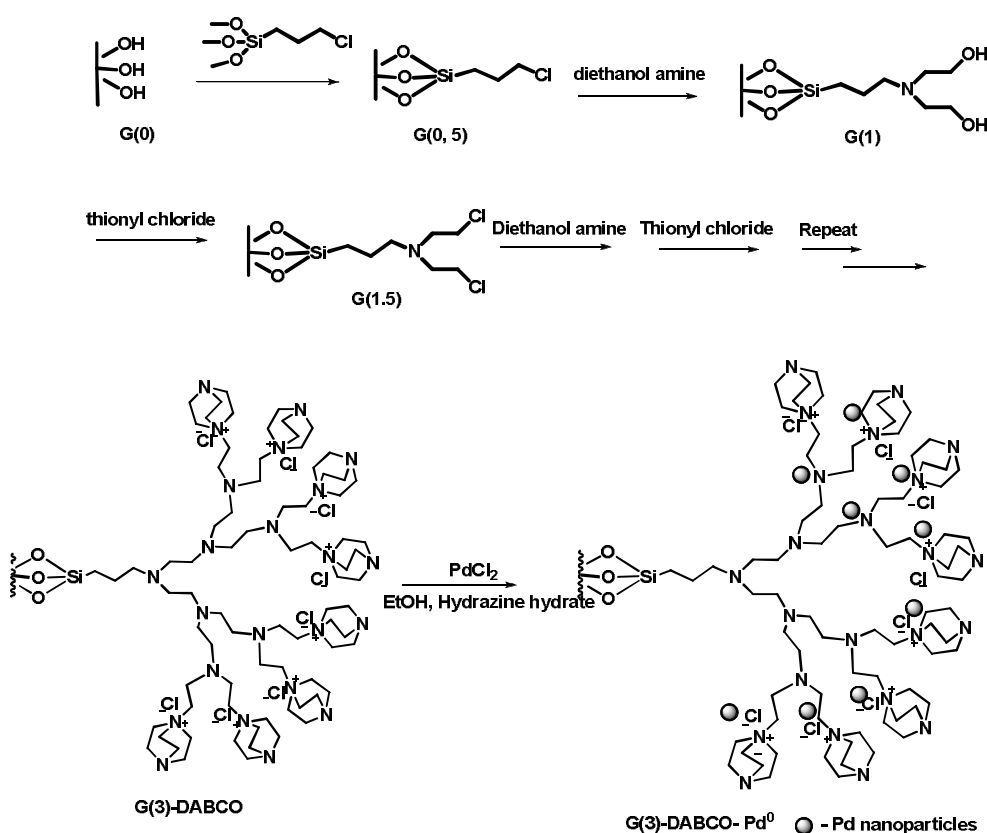
Scheme 1.5 Preparation of SiO_2-DEA-DABCO-pd^0 dendrimer

The authors have used it in the Suzuki–Miyaura and Mizoroki–Heck reactions, in which the dendrimer acted as a stabilizer for preventing the

nanoparticles from agglomeration, as a recycling vehicle, as well as a ligand in catalysis (Scheme 1.6 and 1.7). This novel catalyst exhibited high activity and stability for the coupling reactions. The advantages of this procedure are simple operation, short reaction time, need of only trace amount of catalyst, good to excellent yield and environmental friendliness. Furthermore, it could be easily recovered and reused up to five times without any apparent loss of activity.
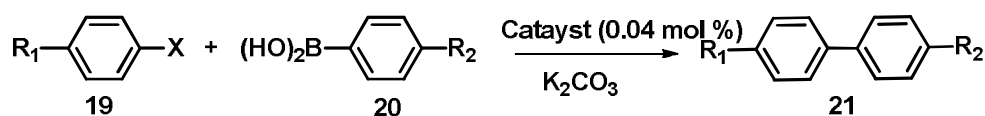
Scheme 1.6 Suzuki–Miyaura reaction
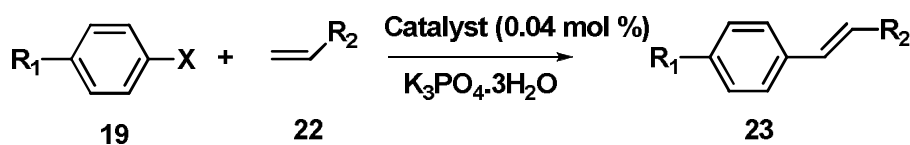
Scheme 1.7 Mizoroki–Heck reaction

Yijun and coworkers[129] have prepared a novel nanoscale catalyst system composed of nanosized Pd catalysts immobilized on $Fe_3O_4@SiO_2$–Gn–PAMAM (n = 1-4) (Scheme 1.8). The Pd particles are homogeneously dispersed on the surface of the $Fe_3O_4@SiO_2$–Gn–PAMAM (n = 1-4). The silica in the system may physically protect the Fe_3O_4 core apart from corruption in the reaction environments and the surface functional groups may contact PAMAM tightly. Thus, the silica is the key to the high stability of the system. These characteristics of the system leads to the high catalytic activity for hydrogenation of allyl alcohol and the rate of the reaction can also be controlled by changing the generation of PAMAM. The TOF values of the $Fe_3O_4@SiO_2$-Gn-PAMAM-Pd(0) (n = 1-4) catalyst are several times

higher than that of the corresponding catalyst prepared in the channel of mesoporous SBA-15, due to the absence of mass-transfer limitations and the lower amounts of Pd on the catalysts. The conversion of allyl alcohol using the catalysts is almost 100 % and the selectivity to the hydrogenated product of 1-propanol is about 89 % when the reaction reached completion. The composite of $Fe_3O_4@SiO_2$- G0-PAMAM-Pd(0) has the highest activity among them, with a TOF value 2.6 times the $Fe_3O_4@SiO_2$-G4-PAMAM-Pd(0). The activity of the catalyst was decreased with the increase of the generation. Possibly, the higher generation the PAMAM is, the harder the substrates find it to pass through the catalyst surface to interact on the active sites.
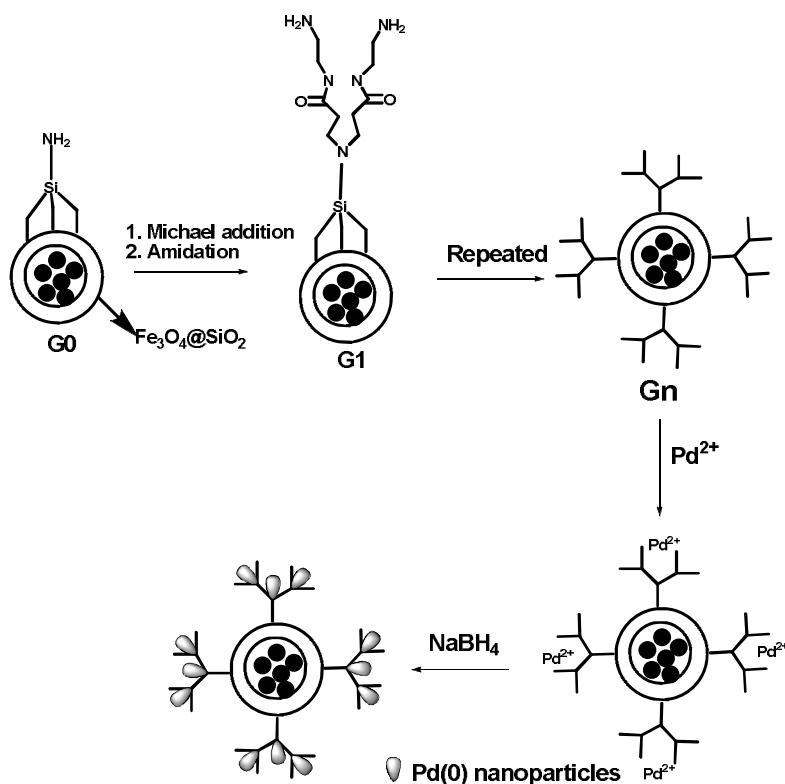
Scheme 1.8 Synthesis of $Fe_3O_4@SiO_2$–Gn–PAMAM

1.14 Dendrimer as organocatalyst

Organocatalysis is the part of catalysis that uses a compound composed of carbon, hydrogen, oxygen or sulfur, or other non-metal elements as catalyst, but that is not an enzyme. In contrast to metallic or organometallic catalysis, which uses in most cases, transition metal complexes (or lanthanides) as catalysts, the absence of metal in organocatalysis is an undeniable advantage when considering the principles of ''green chemistry''. Furthermore, it is cheaper and safer, since the products cannot be poisoned by the leaching of an eventually toxic metal.[131, 132] The first discovery of an organocatalytic reaction can be attributed to Justus von Liebig, who accidentally found in 1859 that, water, which was saturated with cyanide gas, upon addition of small amounts of an aldehyde, resulted in the formation of the crystalline oxalamide (Scheme 1.9).[131] Acetaldehyde was the first discovered pure "organocatalyst" that acted similarly to "enzymes." Almost five decades later, the German physical chemist; Georg Bredig published the first asymmetric C-C-bond forming reaction where the chiral mandelic acid was formed from benzaldehyde and hydrogen cyanide in the presence of an alkaloid like quinine (Scheme 1.10).[132] Most investigators have focused on tethering a single functional group on the surface, often in order to immobilize an existing homogeneous catalyst.

$$(CN)_2 \xrightarrow[\text{rt, CH}_3\text{CHO(aq)}]{\text{H}_2\text{O}}$$

24

25
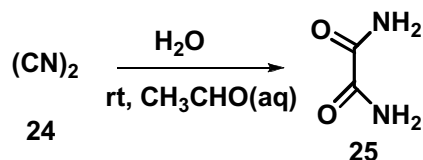
Scheme 1.9 Justus von Liebig's oxamide synthesis
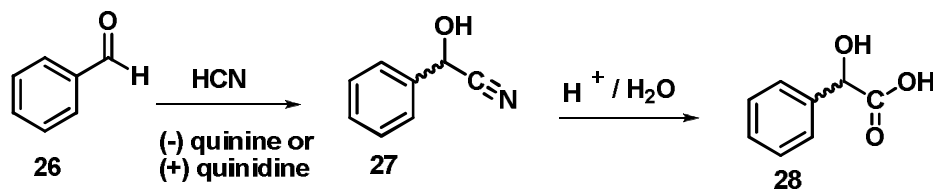
Scheme 1.10 Bredig's enantioselective mandelonitrile synthesis

Now-a-days, dramatic increase in the activity in the field of organocatalysis has occurred especially using supported organocatalysts because, it almost satisfies the rules of green chemistry. Main drawbacks of organocatalysts are poor reusability and use of high amount of catalysts. When the dendritic structures are considered, their surface contain higher amount of functional groups. Dendrimers with inorganic supports can overcome the present problems associated with organocatalysis. Dendrimers can be removed by nanofiltration or simple filtration. Only few works were reported on dendritic organocatalyst with or without support.

Davis, *et al.*[133] reported dendrimers containing an encapsulated tertiary amine which were prepared by coupling tris(2-aminoethyl) amine with dendritic branches derived from L-lysine (Figure 1.17). These dendrimers were used as catalysts in the Henry (nitroaldol) reaction between 4-nitrobenzaldehyde and nitroethane, and their catalytic performance was compared with that of triethylamine (Scheme 1.11). Attachment of the dendritic shell alters the rate of reaction and influences the *syn:anti* ratio of products. The presence of hydrogen bond interactions could also explain the relative difference in reactivity and selectivity between G1(N) and G2(N). Catalyst G1(N) has a small and potentially selective array of hydrogen bond donors capable of selecting a specific product. Catalyst G2(N) possesses many more hydrogen bond donors capable of interacting with the product in

a less selective way (i.e., interactions within the dendritic branches rather than at the core), perhaps leading to the lack of *syn:anti* selectivity. These multiple hydrogen bonding groups could speed up the reaction, however, by generating a favourable polar microenvironment.
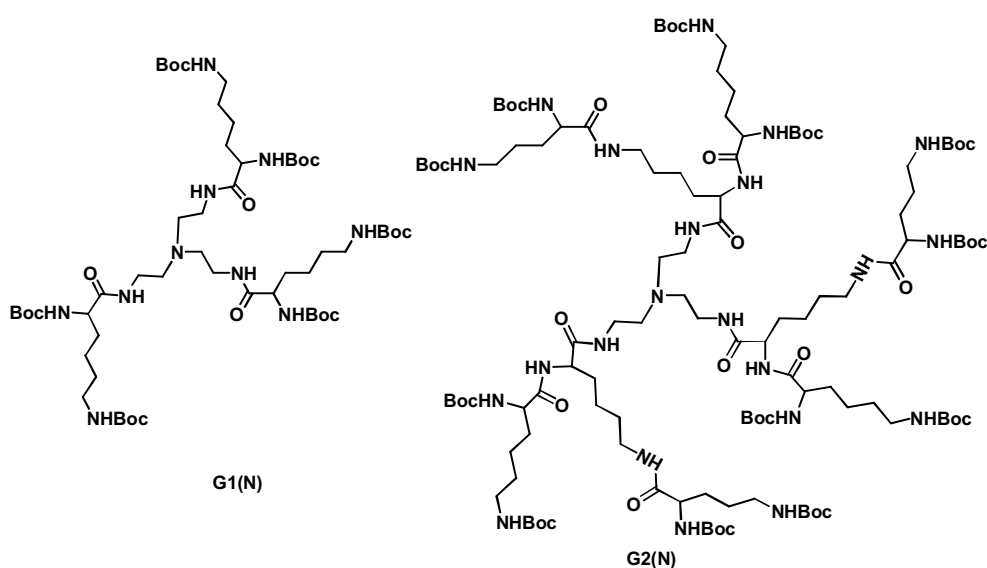
Figure 1.17 Structure of G1(N) and G2(N)
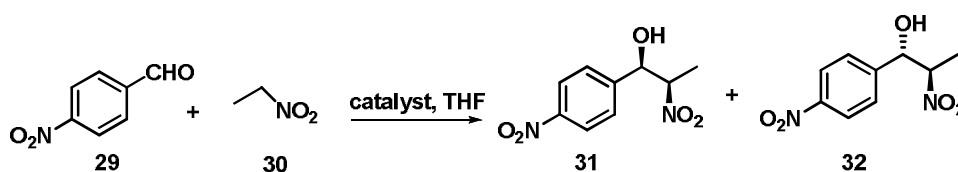
Scheme 1.11 Henry (nitroaldol) reaction

Rajesh, *et al*. [134] synthesized the G0 and G1 of PAMAM and checked their catalytic activity for Knoevenagel condensation (Figure 1.18 and Scheme 1.12). They found that 100 % conversion within 2 minutes was obtained for G1 as catalyst. This showed that when generation increased, amino capacity was also increased, this made the G1 a powerful base catalyst for this reaction. The same trend was also seen in the case of ring opening of various epoxides

using G1 (Scheme 1.13). Result showed that 70 % yield was obtained for the reaction between cyclohexene oxide and aniline in the presence of G1.
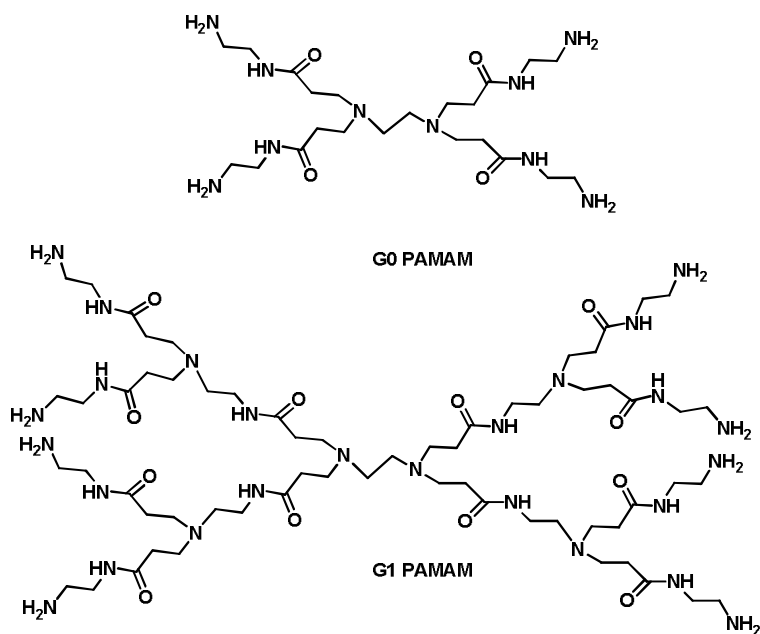
Figure 1.18 Structure of G0 and G1 PAMAM dendrimer
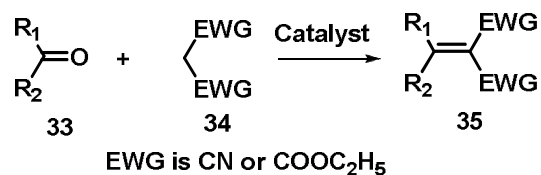
Scheme 1.12 Knoevenagel condensation
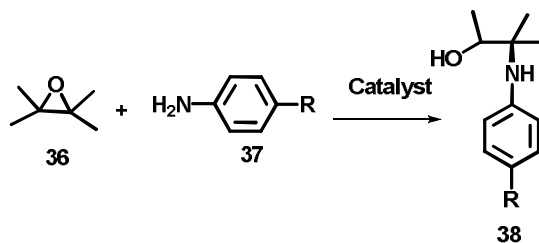
Scheme 1.13 Ring opening of epoxides

Kehat, *et al.*[135] synthesized polymer supported dendrons with terminal proline moieties and used to catalyze the aldol reaction (Figure 1.19).
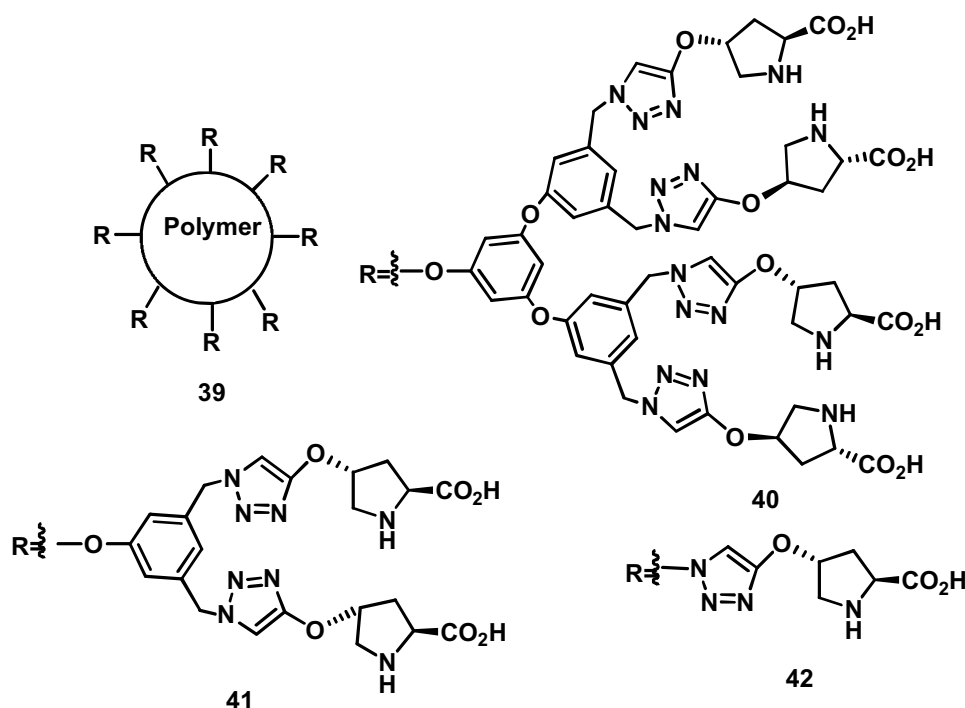
Figure 1.19 Structure of polymer supported dendrons with terminal proline moieties

The catalytic tests showed that both conversion and selectivity increased when the generation was increased. The results showed that yield of the aldol adduct when the reaction was catalyzed by the zeroth, first, and second generation dendrons were 42 %, 73 %, and 100 %, respectively, and the corresponding enantiomeric excess were 27 %, 68 %, and 68 %. For both parameters, this illustrated a positive dendritic effect.

Many supported dendrimers were used as organocatlysts for Knoevenagel condensation (Figure 1.20). Kapoor, *et al.*[136] reported the second generation PAMAM dendrons which were grown within the

channels of mesoporous silica functionalized with amines. These materials were used for catalyzing the Knoevenagel condensation of benzaldehyde with malononitrile. It was found that the reaction rate increased with increasing density of the tertiary aminopropyl groups. Similarly, Poly(styrene)-supported PAMAM dendrimers were used as catalysts for the Knoevenagel condensation of several substituted benzaldehydes with various activated methylene compounds.[137] The reactions proceeded rapidly (a few minutes) at moderate temperature with 100 % selectivity, and in nearly quantitative yields. The third generation G3 was found to be the most efficient. Recycling and reuse were performed at least ten times with the same efficiency. PAMAM dendrimers entrapped inside poly(p-xylene) nanotubes were also reported as heterogenous organocatalysts for the Knoevenagel condensation of malonodinitrile with benzaldehyde, and reused one more time with the same efficiency.[138]
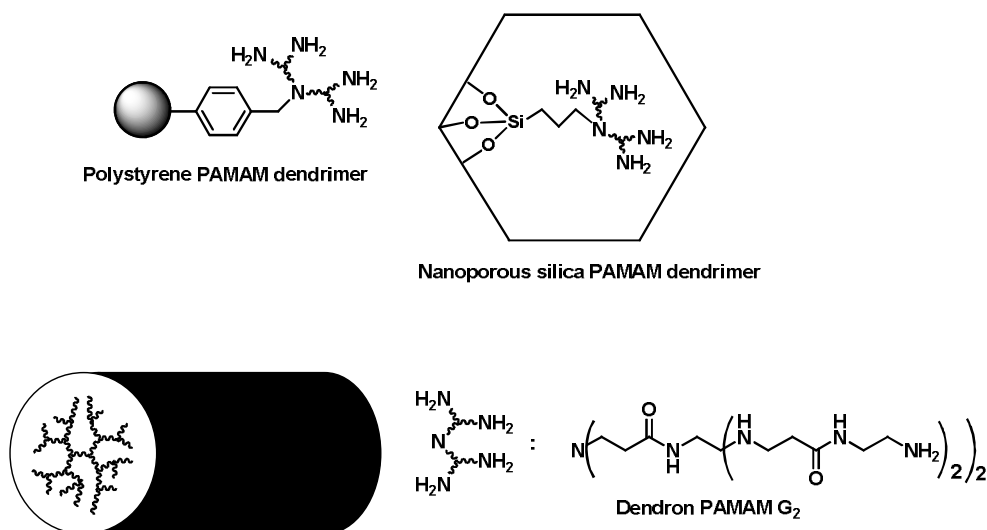
Figure 1.20 Structure of heterogeneous organo dendrimeric structures for
Knoevenagel condensation

1.15 Relevance of the present work

On an industrial scale, homogeneous catalysts are often expensive, involving troublesome workup, thus reducing their scope. Metal catalysts are toxic and expensive and are not easy to handle, difficult to separate and have limited reuse potential. In organocatalyzed reactions, the major drawback is the use of high amount of catalyst. A great challenge is to reduce the quantity of organocatalysts and exploit them with higher efficiency, i.e, in a more economical way. Such problems can be solved only by using the catalyst with high surface functionalities with heterogeneous nature. Dendrimeric catalyst is one such solution to introduce high amount of catalytically active sites. In such cases, major aim is the replacement of metal catalyst and introduces new catalyst systems in terms of green chemistry rules. Most of the works discussed in the field of dendrimer catalysis are based on dendritic metal catalysts.

In the present work, an attempt has been made to integrate the advantages of mesoporous silica as support and the synthesis of dendritic catalyst functions on it by stepwise growth technique. This may be the first report where dendritic systems with end groups of Brønsted acid functionalities like sulfonic acid and carboxylic acid groups have been used for catalysis. In addition to this, an attempt has been made to synthesize dendrimers with amino groups other than PAMAM and PPI. We have taken the challenge to synthesize this architecture on mesoporous silica support.

The main objectives of the research described in this thesis are:

1) To develop and characterize dendritic sulfonic acid and carboxylic acid functionalized mesoporous silica

2) To check the catalytic activity of dendritic sulfonic acid functionalized mesoporous silica for Biginelli reaction and trisubstituted imidazole synthesis

3) To test the activity of carboxylic acid functionalized mesoporous silica as effective reusable organo acidic catalyst for Ullmann type coupling reaction

4) To synthesize and characterize dendritic amine functionalized mesoporous silica and explore its catalytic application in Paal-Knorr reaction

5) Detailed study on Henry reaction using dendritic amine functionalized mesoporous silica and L-proline modified mesoporous silica.

1.16 Characterization methods

IR spectra were recorded with samples as KBr pellets using JASCO 4100 FTIR spectrometer in the range of 400-4000 cm^{-1}. The spectra were recorded at ambient temperature by making pressed pellets of the compounds.

The solution ^{1}H and ^{13}C NMR spectra were recorded using a Bruker Avance 400 MHz spectrometer using CDCl$_3$ or DMSO-d6 as solvent and TMS as internal standard (SAIF, CUSAT).

^{13}C cross-polarized magic angle-spinning (CP-MAS) NMR spectra were recorded on a Bruker 300 MHz instrument and obtained from (AIRF), IIT, Delhi and IISc, Bangalore.

GC analysis was carried out on a 1200 L Single Quadruple, Varian Gas Chromatograph model.

Thermogravimetric analysis was performed using a Perkin Elmer, Diamond TG/DTA system at a heating rate of 10 °C min^{-1} under an atmosphere of nitrogen using an aluminium pan from 40 °C to 730 °C (SAIF-STIC, CUSAT).

The surface characterization was carried out using the JEOL Model Scanning Electron Micrograph with an attached energy dispersive X-ray detector. Scanning was done at the 1-20 μm range and images were taken at a magnification of 15-20 kV. Data were obtained using INCA software. The standardization of the data analysis is an integral part of the SEM-EDAX instrument employed (SAIF, CUSAT).

Powder XRD patterns of all samples were collected using Rigaku (D. Max. C) X-ray diffractometer having CuKα (λ= 1.5405A^o) radiation (Dept. of Physics, CUSAT).

Adsorption and desorption isotherms for nitrogen were obtained at 77K using a micromeritics Tristar 3000 Surface area analyser. The specific surface area values were obtained using Brunauer-Emmett-Teller (BET) equation. The pore size distribution data were obtained using Barrett-Joyner-Halenda (BJH) method.

CHNS was performed at SAIF-STIC, CUSAT.

TLC was done on silica coated alumina plates (Merck, 60F 254). Melting points were determined in open capillary tubes on a Büchi Melting Point B-540 apparatus and are uncorrected.

The enatiomeric purity of the isolated products were determined by HPLC on a Chiralpak I-3 column eluted with a mixture of hexane/iPrOH

(9:1) at a flow rate of 0.5 mL min^{-1} and detected at 254 nm using Shimadzu HPLC model SPD 20A

Raman spectrum was recorded using advanced digital Laser Raman Microspectrometer with three lasers (785 nm) with the use of motorized neutral density filters at NCESS, Trivandrum. The spectral range of the equipment was from 50-4000 cm^{-1} shift from the Laser line, accomplished with an edge filter. The Raman scattered light was dispersed with a grating and was having dual grating 1200 l/ mm and 2400 l/ mm. The detection was done by a Peltier cooled CCD detector with 576 x 384 pixels, with spectral resolution of 1 cm^{-1}.

References

[1]   J. A. Gladysz, *Chem. Re*v., 2002, **102**, 3215.

[2]   D. Cole-Hamilton, R. P. Toose, *Catalyst Separation, Recovery and Recycling*, Springer: Heidelberg, Germany, 2006.

[3]   A. W. Bosman, H. M. Janssen, E. W. Meijer, *Chem. Rev.,*1999, **99**, 1665.

[4]   D. A. Tomalia, H. M. Brothers II, L. T. Piehler, Y. Hsu, *Polym. Mater. Sci. Eng.,* 1995, **73**, 75.

[5]   D. A. Tomalia, *Macromolecular Symposium*, 1996, **101**, 243.

[6]   P. R. Dvornic, D. A. Tomalia, *Science Spectra*, 1996, **5**, 36.

[7]   (a) A. K. Naj, *Persistent Inventor Markets a Molecule in the Wall Street Journal*: *New York*, **1996**. (b) F. Zeng, S. C. Zimmerman, *Chem. Rev.,* 1997, **97**, 1681.

[8]   C. J. Hawker, M. Piotti, *Speciality Monomers and Polymers,* ACS Symposium Series, American Chemical Society, Washington, DC, 2000, **755**, 107.

[9]   C. J. Hawker, J. M. J. Fréchet, *Step-Growth Polymers for High Performance Materials,* ACS Symposium Series, American Chemical Society, Washington, DC 1996, **624**, 132.

[10] F. Vogtle, G. Richardt, N. Werner, *Dendrimer Chemistry*, Wiley-VCH: Weinheim, 2009

[11] S. Campagna, P. Ceroni, F. Puntoriero, *Designing Dendrimers*, John Wiley & Sons: Hoboken, 2012.

[12] U. Boas, J. B. Christensen, P. M. H. Heegaard, *Dendrimers in Medicine and Biotechnology: New Molecular Tools*, Royal Society of Chemistry: UK, 2006.

[13] J. M. J. Frechet, D. A. Tomalia, *Dendrimers and other Dendritic Polymers*, John Wiley & Sons: UK, 2001.

[14] T. D. McCarthy, P. Karellas, S. A. Henderson, M. Giannis, D. F. O. Keefe, G. Heery, J. R. A. Paull, B. R. Matthews, G. Holan, *Mol. Pharm.,* 2005, **2**, 312.

[15] M. Fischer, F. Vogtle, *Angew. Chem., Int. Ed.,* 1999, **38**, 884.

[16] G. R. Newkome, C. N. Moorefield, F. Vogtle, *Dendritic Molecules: Concepts, Synthesis, Perspectives*, VCH, New York, 1996.

[17] D. A. Tomalia, A. M. Naylor, W. A. Goddard, *Angew. Chem., Int. Ed. Engl.,* 1990, **29**, 138.

[18] S. Gestermann, R. Hesse, B. Widndisch, F. Vogtle, *Dendritic Architectures*, Wiley-VCH, Weinheim, 2000.

[19] O. A. Mathews, A. N. Shipway, J. F. Stoddart, *Prog. Polym. Sci.*, 1998, **23**, 1.

[20] F. Zeng, S. C. Zimmerman, *Chem. Rev.,* 1997*,* **97**, 1681.

[21] G. R. Newkome, C. N. Moorefield, J. N. Keith, G. R. Baker, G. H. Escamilla, *Angew. Chem., Int. Ed.*, 1994*,* **33**, 666.

[22] F. Vogtle, S. Gestermann, R. Hesse, H. Schwierz, H. Windisch, *Prog. Polym. Sci.,* 2000*,* **25**, 987.

[23] R. F. Service, *Science,* 1995*,* **267**, 458.

[24] C. J. Hawker, J. M. J. Frechet. *J. Am. Chem. Soc.,* 1990*,***112**, 7638.

[25] S. M. Grayson, J. M. J. Frechet, C*hem. Rev.,* 2001*,* **101**, 3819.

[26] J. M. J. Frechet, *Science,* 1994*,* **263**, 1710.

[27]   D. A. Tomalia, H. Baker, J. Dewald, M. Hall, G. Kallos, S. Martin, J. Roeck, J. Ryder, P. Smith, *Macromolecules,* 1986*,* **19**, 2466.

[28]   J. Issberner, R. Moors, F. Vögtle, *Angew. Chem., Int. Ed. Engl.,* 1994, **33**, 2413.

[29]   W. Buhleier, F. V. Wehner, F. Vogtle, *Synthesis,* 1987*,* 155.

[30]   S. Tripathy, M. K. Das, *J. App. Pharm. Sci.,* 2013, **3**, 142.

[31]   C. J. Hawker, J. M. J. Frechet, Y. Jiang, A. E. Philippides, *In: Proceedings of the IUPAC International Symposium on Molecular Design of Functional Polymers*. US Patent, 1991.5041516, 1989, 19.

[32]   B. Klajnert, M. Bryszewska, *Acta Biochim. Pol.*, 2001, **48**,199.

[33]   C. Yiyun, X. Zhenhua, M. Minglu, X. Tonguen*, J. Pharma. Sci.,* 2008, **97**, 123.

[34]   D. A. Tomalia, J. R. Dewald, M. R. Hall, S. J. Martin, P. B. Smith*, Preprints of the 1st SPSJ International Polymer Conference*, Society of Polymer Science, Kyoto, Japan, 1984, 65.

[35]   B. Berg EMM, E. W. Meijer, *Angew Chem., Int. Ed. Engl.*, 1993, **32**, 308.

[36]   S. W. Krska, D. Seyferth, *J. Am. Chem. Soc.,* 1998, **120**, 3604.

[37]   H. Ihre, O. L. P. de Jesus, J. M. J. Frechet, *J. Am. Chem. Soc.,* 2001, **123**, 590.

[38]   N. R. Luman, T. Kim, M. W. Grinstaff, *Pure Appl. Chem.,* 2004, **76**, 1375.

[39]   (a) L. Xue, D. Wang, Z. Yang, Y. Liang, J. Zhang, S. Feng, *Eur. Polym. J.,* 2013, **49**, 1050. (b) F. Deubel, V. Bretzler, R. Holzner, T. Helbich, O. Nuyken, B. Rieger, R. Jordan, *Macromol. Rapid Commun.,* 2013, **34**, 1020. (c) M. A. Cole, C. N. J. Bowman, *J. Polym. Sci., Polym. Chem.*, 2013, **51**, 1749. (d) P. Ortega, R. Gómez, F. Javier, *Tetrahedron Lett.,* 2015, **56**, 5299.

[40]   J. I. Paez, M. Martinelli, V. Brunetti, M. C. Strumia, *Polymers,* 2012, **4**, 355.

[41]   D. Wang, D. Astruc, *Coord. Chem. Rev.,* 2013, **257,** 2317.

[42]   R. D. Adams, F. A. Cotton, *Catalysis by Di- and Polynuclear Metal Cluster Complexes*, Wiley-VCH Inc.: NewYork, 1998.

[43]   R. Heerbeek, P. C. J. Kamer, P. W. N. M. van Leeuwen, N. H. J. Reek, *Chem. Rev.,* 2002**, 102***,* 3717.

[44] M. E. Broussard, B. Juma, S. G. Train, W. J. Peng, S. A. Laneman, G. G. Stanley, *Science,* 1993, **260,** 1784.

[45] S. Hecht, J. M. J. Frechet, *Angew. Chem. Int. Ed. Engl.,* 2001, **40**, 74.

[46] C. B. Gorman, J. C. Smith, *Acc. Chem. Res.,* 2001, **34**, 60.

[47] C. N. Satterfield, *Heterogeneous Catalysis in Industrial Practice*, McGrew-Hill, Inc., Singapore, 1991, 2.

[48] (a) C. E. Song, S. G. Lee, *Chem. Rev.,* 2002, **102**, 3495. (b) J. M. Fraile, J. I. Garc, J. A. Mayoral, *Chem. Rev.,* 2009, **109**, 360.

[49] P. Hodge, *Chem. Soc. Rev.,* 1997, **26**, 417.

[50] (a) J. O. Metzger, *Angew Chem. Int. Ed.,* 1998, **37**, 2975. (b) M. S. Singh, S. Chowdhury, *RSC Adv.,* 2012, **2**, 4547. (c) R. S. Varma, *Green Chem.*, 1999, **1**, 43. (d) R. S. Varma, *Pure Appl. Chem.*, 2001, **73**, 193. (e) M. H. Sarvari, H. Sharghi, *Tetrahedron*, 2005, **61**, 10903. (f) K. Wilson, J. H. Clark, *Pure Appl. Chem.*, 2000, **72**, 1313. (g) A. Loupy, *Top. Curr. Chem.*, 1999, **206**, 153.

[51] J. H. Clark, *The Chemistry of Waste Minimization*, Blackie, London, 1995.

[52] P. Anastas, J. C. Warner, *Green Chemistry: Theory and Practice*, Oxford University Press, Oxford, 1998.

[53] P. Tundo, P. Anastas, *Green Chemistry: Challenging Perspectives*, Oxford University Press, Oxford, 2000.

[54] R. A. Sheldon, H. Van Bekkum, *Fine Chemicals through Heterogeneous Catalysis*, Wiley-VCH, Weinheim, 2001.

[55] C. G. Brundtland, *Our Common Future, The World Commission on Environmental Development,* Oxford University Press, Oxford, 1987.

[56] B. Pugin, *J. Mol. Catal. A: Chem.*, 1996, **107**, 273.

[57] (a) H. Fan, Y. M. Li, A. S. C. Chan., *Chem. Rev.*, 2002, **102**, 3385. (b) F. Svec, J. M. J. Frechet, *Chem. Mater.*, 1995, **7**, 707.

[58] Y. Wan, D. Zhao, *Chem. Rev.,* 2007, **107**, 2821.

[59] M. M. Heravi, B. Baghernejad, H. A. Oskooie, *Catal. Lett.,* 2009, **130**, 547.

[60] D. Barreca, M. P. Copley, A. E. Graham, J. D. Holmes, M. A. Morris, R. Seraglia, T. R. Spalding, E. Tondello, *Appl. Catal., A: Gen.,* 2006, **304**, 14.

[61] C. T. Kresge, M. E. Leonowicz, W. J. Roth, J. C. Vartuli, J. S. Beck, *Nature*, 1992, **359**, 710.

[62] P. Yang, D. Zhao, D. I. Margolese, B. F. Chmelka, G. D. Stucky, *Nature,* 1998*, ***396,** 152.

[63] F. Jiao, P. G. Bruce, *Angew. Chem. Int. Ed.,* 2004*, ***43**, 5958.

[64] S. Jun, S. H. Joo, R. Ryoo, M. Kruk, M. Jaroniec, Z. Liu, T. Ohsuna, O. Terasaki, *J. Am. Chem. Soc.,* 2000*, ***122**, 10712.

[65] R. Ryoo, S. H. Joo, M. Kruk, M. Jaroniec, *Adv. Mater.*, 2001, **13**, 677.

[66] J. S. Beck, J. C. Vartuli, W. J. Roth, M. E. Leonowicz, C. T. Kresge, K. D. Schmitt, C. T. Chu, D. H. Olson, E. W. Sheppard, C. T. McCullen, J. B. Higgins, J. L. Schlenker, *J. Am. Chem. Soc.,*1992, **114**, 10834.

[67] H. T. Chen, S. Huh, J. W. Wiench, M. Pruski, V. S. Y. Lin*, J. Am. Chem. Soc.,* 2005, **127**, 13305.

[68] D. R. Radu, C. Y. Lai, J. W. Wiench, M. Pruski, V. S. Y. Lin, *J. Am. Chem. Soc.,* 2004, **126**, 1640.

[69] S. Huh, H. T. Chen, J. W. Wiench, M. Pruski, V. S. Y. Lin, *Angew. Chem. Int. Ed.,* 2005, **44**, 1826.

[70] C. Y. Lai, W. Chia-Wen, R. Radu Daniela, G. Trewyn Brian, S. Y. Lin Victor, *Stud. Surf. Sci. Catal.,* 2008, **170B**, 1827.

[71] C. Y. Lai, B. G. Trewyn, D. M. Jeftinija, K. Jeftinija, S. Xu, S. Jeftinija, V. S. Y. Lin, *J. Am. Chem. Soc.,* 2003, **125**, 4451.

[72] Slowing II, B. G. Trewyn, S. Giri, V. S. Y. Lin*, Adv. Funct. Mater.,* 2007, **17**, 1225.

[73] T. Aida, K. Kageyama, J. I. Tamazawa, *Science*, 1999, **285**, 2113.

[74] D. R. Radu, C. Y. Lai, Jeftinija, E. W. Rowe, S. Jeftinija, V. S. Y. Lin, *J. Am. Chem. Soc.,* 2004, **126**, 13216.

[75] T. J. Barton, L. M. Bull, W. G. Klemperer, D. A. Loy, B. McEnaney, M. Misono, P. A. Monson, G. Pez, G. W. Scherer, J. C. Vartuli, O. M. Yaghi, *Chem. Mater.,* 1999, **11**, 2633.

[76] C. Yu, Y. Yu, D. Zhao, *Chem. Commun.,* 2000, 575.

[77] D. Zhao, J. Feng, Q. Huo, N. Melosh, G. H. Fredrickson, B. F. Chmelka, G. D. Stucky, *Science*, 1998, **279**, 548.

[78] R. Ryoo, J. M. Kim, C. H. Ko, C. H. Shin, *J. Phys. Chem.*, 1996, **100**, 17718.

[79] S. Che, A. E. Garcia-Bennett, T. Yokoi, K. Sakamoto, H. Kunieda, O. Terasaki, T. Tatsumi, *Nature Materials*, 2003, **2**, 801.

[80] G. Hernandez, R. Rodrıguez, *J. Non-Cryst. Solids.,* 1999*,* **246**, 209.

[81] I. P. Alimarin, V. I. Fadeeva, G. V. Kudryavtsev, I. M. Loskutova, T. I. Tikhomirova, *Talanta,* 1987*,* **34***,* 103*.*

[82] L. N. H. Arakaki, L. M. Nunes, J. A. Simoni, C. Airoldi, *J. Colloid Interface Sci.*, 2000, **228,** 46.

[83] A. R. Sarkar, P. K. Dutta, M. Sarkar, *Talanta,* 1996*,* **43**, 1857.

[84] V. I. Lygin, *Kinet. Catal.*, 1994, **35**, 480.

[85] S. A. Bagshaw, E. Prouzet, T. J. Pinnavaia, *Science*, 1995, **269**, 1242.

[86] C. Yu, Y. Yu, D. Zhao, *Chem. Commun.*, 2000, 575.

[87] F. Kleitz, D. Liu, G. M. Anilkumar, I. S. Park, L. A. Solovyov, A. N. Shmakov, R. Ryoo, *J. Phys. Chem. B.,* 2003, **107**, 14296.

[88] J. M. Kim, G. D. Stucky, *Chem. Comm.*, 2000, 1159.

[89] P. F. Fulvio, S. Pikus, M. Jaroniec, *J. Colloid Interface Sci.*, 2005, **287**, 717.

[90] J. Liu, Q. Yang, X. S. Zhao, L. Zhang, *Microporous Mesoporous Mater.*, 2007, **106**, 62.

[91] C. J. Brinker, *J. Non Cryst. Solids.*, 1988, **100**, 31.

[92] L. L. Hench, J. K. West, *Chem. Rev.*, 1990, **90**, 33.

[93] D. Margolese, J. A. Melero, S. C. Christiansen, B. F. Chmelka, G. D. Stucky, *Chem. Mater.*, 2000, **12**, 2448.

[94] R. J. P. Corriu, A. Mehdi, C. Reye, C. Thieuleux, A. Frenkel, A. Gibaud, *New J. Chem.*, 2004, **28**, 156.

[95] F. Berube, S. Kaliaguine, *Microporous Mesoporous Mater.*, 2008, **115**, 469.

[96] B. Tian, X. Liu, C. Yu, F. Gao, Q. Luo, S. Xie, B. Tu, D. Zhao, *Chem. Comm.*, 2002, 1186.

[97] Y. K. Bae, O. H. Han, *Microporous Mesoporous Mater.*, 2007, **106**, 304.

[98] R. van Grieken, G. Calleja, G. D. Stucky, J. A. Melero, R. A. Garcia, J. Iglesias, *Langmuir*, 2003, **19**, 3966.

[99] C. Yang, B. Zibrowius, W. Schmidt, F. Schuth, *Chem. Mater.*, 2003, **15**, 3739.

[100] C. Yang, B. Zibrowius, W. Schmidt, F. Schuth, *Chem. Mater.*, 2004, **16**, 2918.

[101] H. Cai, D. Zhao, *Microporous Mesoporous Mater.*, 2009, **118**, 513.

[102] Q. Yang, J. Liu, J. Yang, L. Zhang, Z. Feng, J. Zhang, C. Li, *Microporous Mesoporous Mater.*, 2005, **77**, 257.

[103] L. M. Yang, Y. J. Wang, G. S. Luo, Y. Y. Dai, *Microporous Mesoporous Mater.*, 2005, **81**, 107.

[104] T. Lai, Y. Shu, Y. Lin, W. Chen, C. Wang, *Mater Lett.*, 2009, **63**, 1693.

[105] L. T. Zhuravlev, *Colloids Surf. A,* 2000*,* **173**, 1.

[106] H. Yang, L. Zhang, W. Su, Q. Yang, C. Li, *J. Catal.,* 2007, **248**, 204.

[107] (a) I. F. J. Vankelecom, D. Tas, R. F. Parton, V. Van de Vyver, P. A. Jacobs, *Angew. Chem. Int. Ed.,* 1996, **35,** 1346. (b) R. F. Parton, I. F. J. Vankelecom, D. Tas, K. B. M. Janssen, P. P. Knops-Gerrits, P. A. Jacobs, *J. Mol. Catal. A: Chem.,* 1996, **113,** 283.

[108] Y. Zhu, H. Li, Q. Zheng, J. Xu, X. Li, *Langmuir*, 2012, **28**, 7843.

[109] J. K. Clark, D. J. Macquarrie, S. J. Tavener, *Dalton Trans.,* 2006, 4297.

[110] K. Moller, T. Bein, R. X. Fisher, *Chem. Mater.,* 1999, **11**, 665.

[111] A. P. Wight, M. E. Davis, *Chem. Rev.,* 2002, **102**, 3589.

[112] M. Hartmann, *Chem. Mater.,* 2005, **17**, 4577.

[113] Y. Wan, D. Y. Zhao, *Chem. Rev.*, 2007, **107**, 2821.

[114] C. S. Chen, C. C. Chen, C. T. Chen, Kao, *Chem. Commun.,* 2011, 2288.

[115] F. Cucinotta, F. Carniato, G. Paul, S. Bracco, C. Bisio, S. Caldarelli, L. Marchese, *Chem. Mater.*, 2011, **23**, 2803.

[116] D. Y. Zhao, Q. S. Huo, J. L. Feng, B. F. Chmelka, G. D. Stucky, *J. Am. Chem. Soc.,* 1998, **120**, 6024.

[117] D. H. Chen, Z. Li, Y. Wan, X. J. Tu, Y. F. Shi, Z. X. Chen, W. Shen, C. Z. Yu, B. Tu, D. Y. Zhao, *J. Mater. Chem.*, 2006, **16**, 1511.

[118] A. S. M. Chong, X. S. Zhao, *J. Phys. Chem. B.*, 2003, **107**, 12650.

[119] X. G. Wang, K. S. K. Lin, C. C. Chan Jerry, S. F. Cheng, *Chem. Commun.*, 2004, 2762.

[120] J. Liu, X. Feng, G. E. Fryxell, L. Q. Wang, A. Y. Kim, M. Gong, *Adv. Mater.*, 1998, **10**, 161.

[121] N. Liu, R. A. Assink, C. Brinker, *Chem. Commun.*, 2003, 370.

[122] Y. S. Kim, X. F. Guo, G. Kim, *Chem. Commun.*, 2009, 4296.

[123] Y. Q. Wang, B. Zibrowius, C. M. Yang, B. Spliethoff, F. Schüth, *Chem. Commun.*, 2004, 46.

[124] D. Rosario-Amorin, M. Gaboyard, C. S. N. Rodolphe, K. Heuze, *Dalton Trans.*, 2011, **40**, 44.

[125] M. A. Zolfigol, M. Safaiee, N. Bahrami-Nejada, *New J. Chem.,* 2016, **40**, 5071.

[126] L. Hongfang, J. Lü, Z. Zheng, R. Cao, *J. Colloid Interface Sci.,* 2011, **353**, 149.

[127] J. P. K. Reynhardt, Y. Yang, A. Sayari, H. Alper, *Chem. Mater.,* 2004, **16***,* 4095.

[128] Y. Xu, Z. Zhang, J. Zheng, Q. Du, Y. Li, *Appl. Organometal. Chem.,* 2013, **27**, 13.

[129] J. Yijun, J. Jiang, Q. Gao1, M. Ruan, H. Yu, L. Qi, *Nanotechnology*, 2008, **19**, 075714.

[130] (a) A. Molnar, B. Rac, *Curr. Org. Chem.*, 2006, **10**, 1697. (b) M. B. Gawande, P. S. Branco, R. S. Varma, *Chem. Soc. Rev.*, 2013, **42**, 3371.

[131] Liebigs, H. Pracejus, *Ann. Chem.* 1960, **634**, 9.

[132] G. Bredig, P. S. Fiske, *Biochem. Z.,* 1913, **46,** 7.

[133] A. V. Davis, M. Driffield, D. K. Smith, *Org. Lett.,* 2001, **3**, 3075.

[134] G. Rajesh Krishnan, K. Sreekumar, Catalysis by Polymer Supported Dendrimers, Their Metal Complexes and Nano Particle Conjugates, Ph. D thesis, 2008, Cochin University of Science and Technology, Cochin, India.

[135] T. Kehat, M. Portnoy, *Chem. Commun*., 2007, 2823.

[136] M. P. Kapoor, Y. Kasama, T. Yokoyama, M. Yanagi, S. Inagaki, N. Hironobu, L. R. Juneja, *J. Mater. Chem*., 2006, **16**, 4714.

[137] G. R. Krishnan, K. Sreekumar, *Eur. J. Org. Chem*., 2008, 4763.

[138] J. P. Lindner, C. Roben, A. Studer, M. Stasiak, R. Ronge, A. Greiner, H. J. Wendorff, *Angew. Chem. Int. Ed.,* 2009, **48**, 8874.

.....ౠ.....

Chapter 2

SYNTHESIS AND CHARACTERIZATION OF DENDRITIC ACID FUNCTIONALIZED MESOPOROUS SILICA

Supported organocatalyst has great demand in catalysis because it satisfies the rules of green chemistry. In the present instance, dendritic sulfonic acid functionalized and dendritic carboxylic acid functionalized mesoporous silica were synthesized. Three generations of both dendritic acids were successfully synthesized and characterized using various techniques.

2.1 Introduction

Catalysis was recognized first by Baron J. J. Berzelius in 1835 and was necessary for most chemical processes.[1] However, it remained a challenging problem due to the difficulties of catalyst recovery and reuse for economical and ecological reasons.[2] The field of catalysis in industry as well as in academia is mainly dominated by heterogeneous and metal catalysts with the newly launched area of organocatalysis.[3, 4] Main advantages of organocatalysis, are metal free catalytic centre, cheaper and safer, the products cannot be poisoned by leaching of an eventually toxic metal.[5, 6] A disadvantage is that, some organocatalysts are needed in stoichiometric amounts. Furthermore, the workup procedure for the separation of the organocatalyst from the product is often tedious. A possible solution for these problems is the immobilization of an organocatalyst on an insoluble support, which allows simple separation, recovery and recycling of the catalyst, and better reactivity of the catalyst due to both the high local concentration of the catalyst on the support and cooperative catalytic effects. These features can help to reduce the amount of catalyst needed.[7]

Brønsted and Lewis acids are the most important and common catalysts in organic synthesis. However, the use of soluble acids or corrosive mineral acids is linked with a great number of environmental and economical harms.[8] Indeed, large amount of catalysts are needed, and some tedious work-up steps are needed when Lewis acids are utilized. Moreover, usually, more than stoichiometric amount of these acids is required, and a large quantity of anions (especially chloride) is released in aqueous medium. The separation from the reaction mixture is very difficult and some related problems should

be taken into account, such as the need of neutralization, the impossibility of the catalyst reuse and the reactor corrosion. It would be very useful to have solid acids that could be separated by filtration and reused.[9]

Novel nano structured support materials can be used in the preparation of heterogeneous catalysts to maximize the surface area of the active phase.[10-12] Among nano structured supports, mesoporous silica materials show their unique advantages over others, because of the tunable pore size, high surface area and large pore volume.[13-16] To enhance the functionality of mesoporous silica materials, considerable efforts have been made to expand the framework compositions. The hybridization of inorganic and organic species on molecular to mesoscopic scales is a powerful tool for developing functional materials, because, their cooperative and synergistic effects, as well as the compatibility of different functionalities, can be introduced in the design of such materials.[17] In particular, dendritic mesoporous silica were found to be applicable to overcome the problem faced by organocatalyst.[18]

2.1.1 Silica supported organo acidic catalysts

Organic sulfonic acids exhibit an acid strength comparable to those of sulfuric acid or other strong acids frequently used in organic synthesis.[19] Sulfonic acid functionalized mesoporous silica materials have attracted much research attention because of their potential applications as solid acid catalysts. The synthesis and catalytic activities of the mesoporous silica containing propylsulfonic acid group have been reported by different research groups recently.[20] Strong acid catalyst consisting of silica containing alkanesulfonic acid groups was prepared by Ford, *et al*.[21] Subsequently, other

groups have introduced variations in the preparation of this type of MCM-41-SO$_3$H materials.[22-24] Analogous to alkanesulfonic acids, arenesulfonic acids covalently anchored to mesoporous silica have also been prepared.[21] They can be obtained by sulfonation of phenyl groups linked to silica frameworks of MCM-41 or SBA-15. There are many acid catalyzed reactions, including some large-scale industrial processes, that can be promoted using polystyrene bearing sulfonic acid groups.[25] With respect to polymeric arenesulfonic acids, the obvious advantage of MCM-41-SO$_3$H, is the large surface area of these materials compared to crosslinked polystyrene; this factor being reflected in a higher catalytic activity as a result of the easier accessibility of substrates to the acid sites.[26-33] The high catalytic activity of these materials can be attributed to their high surface area and the high accessibility of the acid centers to the reactants.[24, 34-37] Anchoring sulfonic acid groups with different acid strength onto mesoporous materials might increase the potential catalytic applications. Previous studies show that phenylsulfonic acid group have stronger acid strength than propylsulfonic acid group.[38] Therefore, it is interesting to synthesize and investigate the catalytic properties of mesoporous silica materials containing phenylsulfonic acid group.

Silica gel supported L-pyrrolidine-2-carboxylic acid-4-hydrogen sulfate has been developed by Arash and coworkers.[39] They used it as green catalyst for the synthesis of 3,4-dihydropyrimidin-2-(1*H*)-ones and thiones (Scheme 2.1). Compared with classical Biginelli reaction conditions, this new method has the advantages of high yields and simple workup procedures.
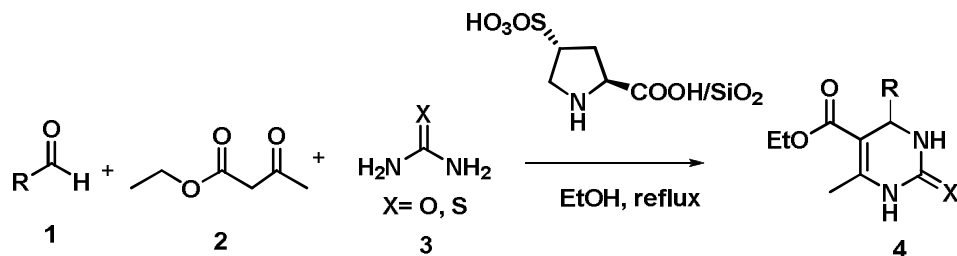
Scheme 2.1 Silica gel supported L-pyrrolidine-2-carboxylic acid-4-hydrogen sulfate catalyzed Biginelli reaction

Akbar, *et al.*[40] synthesized the organosulfonic acid functionalized silica-coated magnetic nanoparticle catalysts (Fe_3O_4@SiO_2@Et-PhSO$_3$H) (**5**) and (Fe_3O_4@SiO_2@Me&Et-PhSO$_3$H)(**6**) (Figure 2.1) and their hydrophobicity and acidity were investigated, and tested for the three-component Biginelli reaction of benzaldehyde, ethyl acetoacetate, and urea under solvent-free condition.
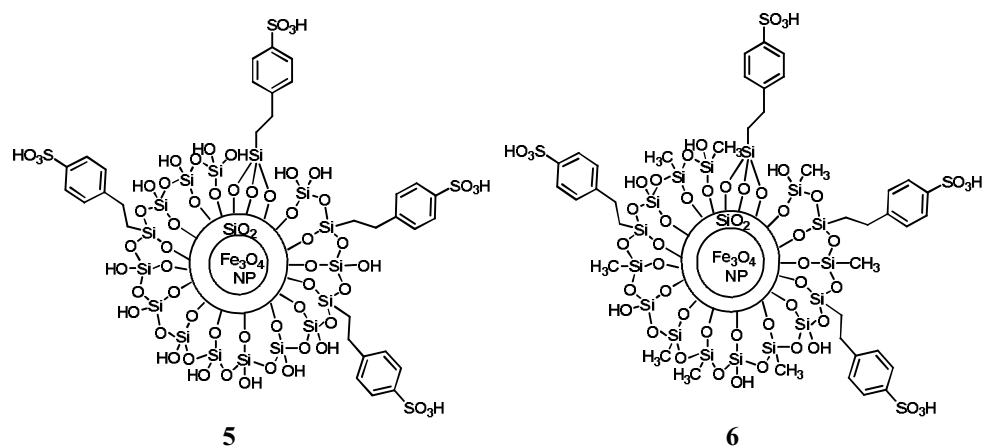
Figure 2.1 Structure of catalyst 5 and 6

This result showed that catalyst **5** had greater catalytic activity towards Biginelli reaction. This may be due to the hydrophobic nature of their surface framework and shielding effect of the methyl groups bound to

this surface for sulfonic acid centres. They found that the catalyst was easily separated by an external magnet and the recovered catalyst was reused in four cycles without significant loss of activity.

Zolfigol, *et al.*[41] reported that silica-functionalized sulfonic acid (SFSA) efficiently catalyzed one-pot multi-component condensation of enolizable ketones or alkyl acetoacetates with aryl aldehydes, acetonitrile and acetyl chloride to afford the corresponding *β*-acetamido ketone or ester derivatives in high to excellent yields and in relatively short reaction times. (Scheme 2.2). The promising points for the application of the solid-supported catalysts in the reaction are; efficiency, generality, high yields, relatively short reaction times, mild conditions, cleaner reaction profile and simplicity.
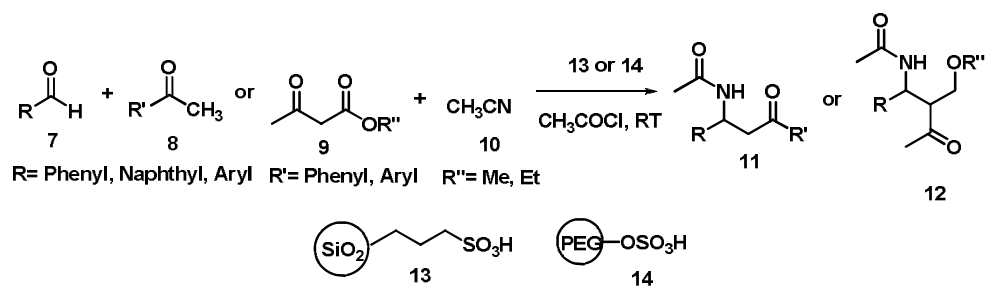
Scheme 2.2 Synthesis of *β*-acetamido ketone or ester

In a similar manner, glutathione molecules have been immobilized on magnetic nanoferrites via their thiol groups and the resulting catalyst nano-FGT have been used for the efficient synthesis of a wide variety of aryl, alkyl, and heterocyclic amines[42-44] (Scheme 2.3). Such organocatalytic approach enables facile conversion of functionalized amines selectively into the corresponding pyrroles without affecting several sensitive functional groups.
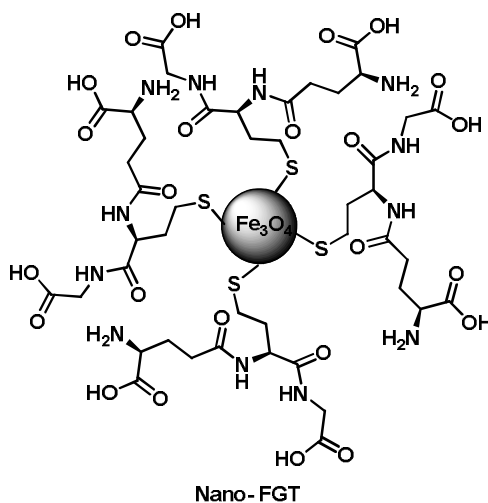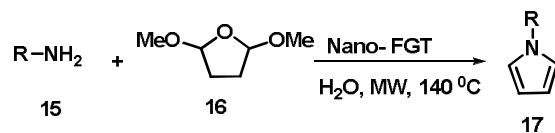
Scheme 2.3 Nano FGT catalyzed Paal Knorr reaction

2.2   Objective of the present work

Main drawbacks of organocatalyst are the high stoichiometric amount of catalyst required for organic synthesis and non reusability of the catalyst. Attachment of catalytically active site on solid supports is a possible solution to overcome this. Here, the concept of supported dendrimers arises. In this chapter, the synthesis of dendritic sulfonic acid functionalized mesoporous silica and dendritic carboxylic acid functionalized mesoporous silica by stepwise growth technique is reported.

2.3   Results and discussion

2.3.1 Synthesis of mesoporous silica

Mesoporous silica with high surface area and ordered uniform pore diameter was synthesized successfully using tetraethyl orthosilcate (TEOS)

as the silica source and Pluronic 123 as surfactant in the presence of 2 M HCl (Scheme 2.4). Removal of surfactant was done by calcination at 550 °C for 6 h and this has led to the formation of highly ordered mesoporous silica (**MS**).[45-47]
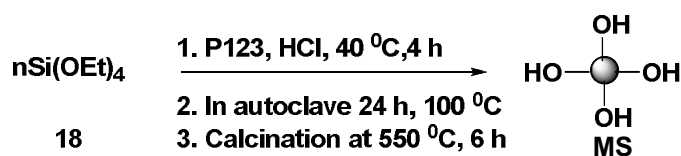
Scheme 2.4 Synthesis of mesoporous silica

2.3.1.1 Synthesis of chlorine functionalized mesoporous silica (CMS)

Chlorine functionalized mesoporous silica was synthesized using two methods (1) Co-condensation method and (2) Graft method. Here 3-chloropropyltrimethoxysilane was used as chlorinating agent for both methods. In co-condensation, TEOS and 3-chloropropyltrimethoxysilane was condensed in the presence of P123, NaF and 2 M HCl in a single step and surfactant was removed by Soxhlet extraction using ethanol for 24 h (Scheme 2.5).[48] The final sample was denoted as **CMS 1**. In graft method, first mesoporous silica (MS) was synthesized and it was further functionalized with 3-chloropropyltrimethoxysilane in dry toluene at 100 °C for 24 h. The sample obtained was denoted as **CMS 2** (Scheme 2.6).[49]
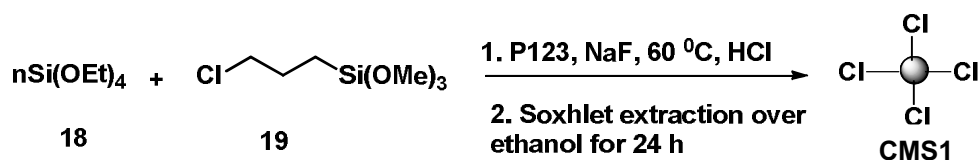
Scheme 2.5 Synthesis of **CMS 1**
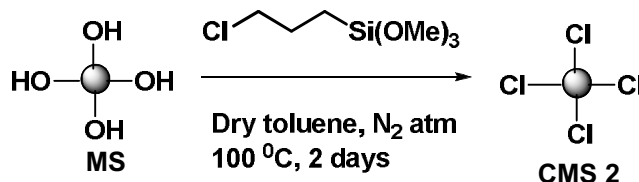
Scheme 2.6 Synthesis of **CMS 2**

2.3.2 Characterization of mesoporous silica (MS) and CMS

2.3.2.1 IR spectral studies

To verify the presence of organic functional groups present in the **MS** sample, FTIR spectroscopy was used. The characteristic peaks of silica were observed at 1100-1000 cm^{-1} corresponding to the intense silicon-oxygen covalent bond vibrations and the symmetric stretching vibrations of Si-O-Si appear at 800 cm^{-1}. The bands obtained around 3400-3500 cm^{-1} and 1630 cm^{-1} were associated with stretching vibration of unreacted Si-OH group and adsorbed H$_2$O. The results indicate that the surface groups in the mesoporous silica materials are heavily loaded with Si-OH groups (Figure 2.2).[50]
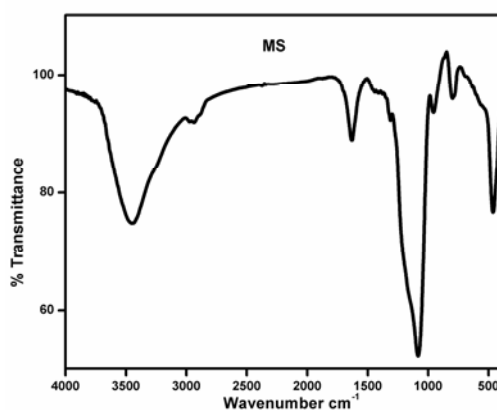
Figure 2.2 IR spectrum of mesoporous silica (**MS**)
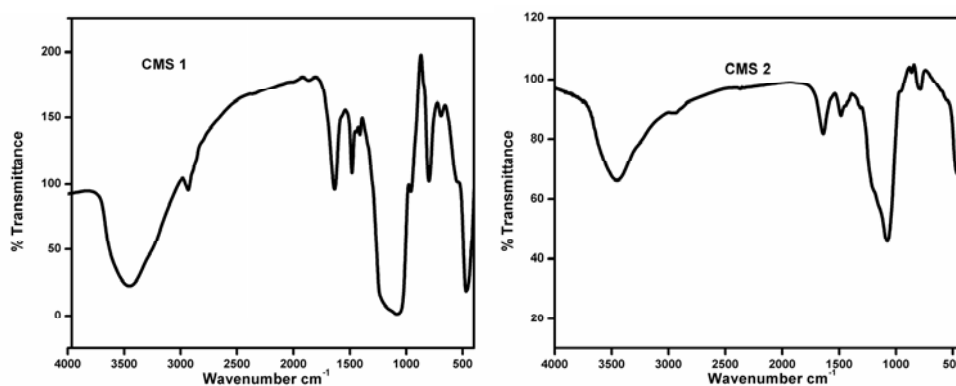
Figure 2.3 IR spectra of **CMS 1** and **CMS 2**

Almost identical IR spectrum was obtained for **CMS 1** and **CMS 2** (Figure 2.3). In addition to the characteristic vibration peaks of silica framework, new band at 2951 cm^{-1} was observed indicating the symmetric stretching vibration of CH$_2$ in both the spectra. When compared to **MS**, band observed at 700 cm^{-1} shows the characteristic vibration of C-Cl bond. This confirmed the introduction of chlorine fragments on mesoporous silica surface.[51]

2.3.2.2 SEM- EDAX Analysis

SEM micrographs and EDAX spectrum of **MS** is shown in Figure 2.4. From the scanning electron micrographs, it was found that, **MS** has almost spherical geometry. Mass % of C, O and Si present in the **MS** obtained from the EDAX analysis is presented in the Table 2.1.
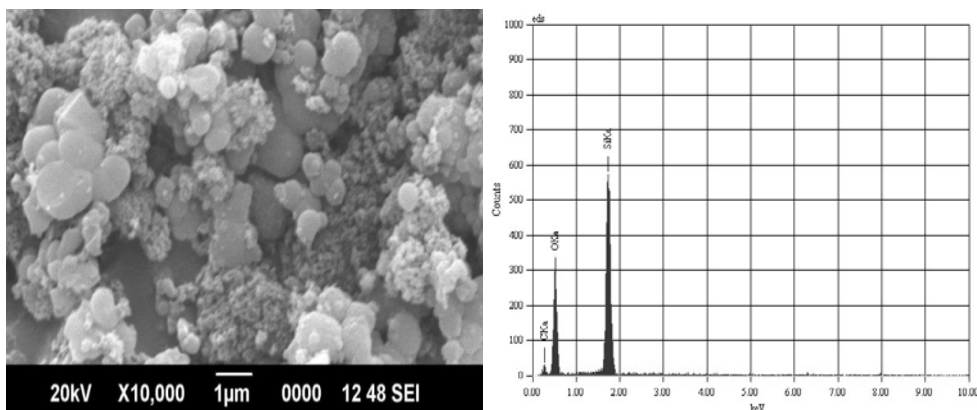
Figure 2.4 SEM and EDAX spectrum of **MS**

Table 2.1 Elemental composition of **MS**

Element	Mass %
C	7.86
O	37.1
Si	55.04

Presence of chlorine in **CMS 1** and **CMS 2** was confirmed by EDAX analysis. The result showed that mass % of chlorine was high for **CMS 1** than **CMS 2**. 6.3 mass % of chlorine was found for **CMS 1** (Figure 2.5 and Table 2.2). This was also confirmed by Volhard's method. From the titration method, chlorine capacity was found to be 3.2 mmols g^{-1} for **CMS 1** and for **CMS 2**, it was 2.8 mmols g^{-1}. SEM micrograph of **CMS 1** is shown in the Figure 2.6. From the scanning electron micrographs, it was found that, spherical nature of mesoporous silica was maintained after the condensation of TEOS and chlorine fragment in a single step.
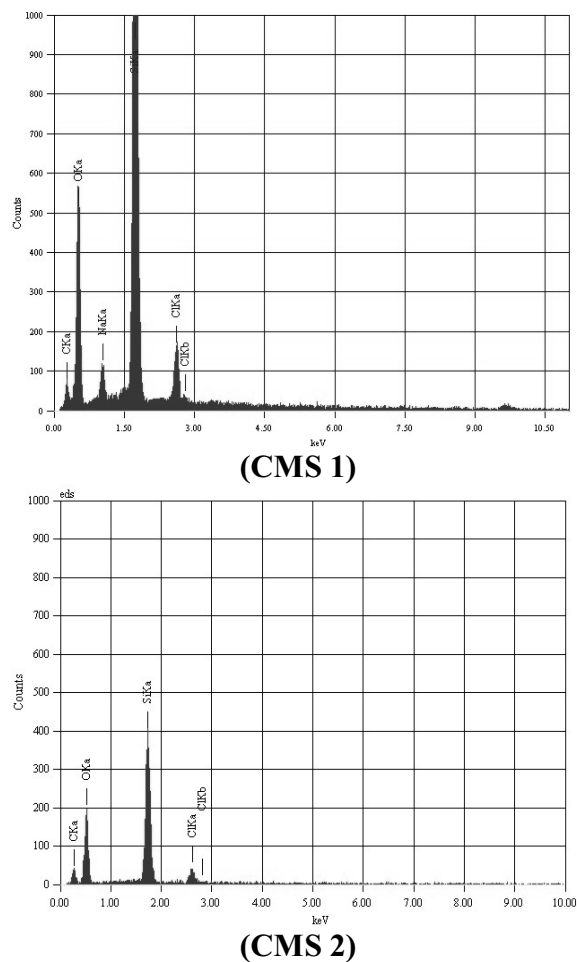
(CMS 1)

(CMS 2)

Figure 2.5 EDAX spectra of **CMS 1** and **CMS 2**

Table 2.2 Elemental composition of **CMS 1** and **CMS 2**

Element	Mass % (CMS 1)	Mass % (CMS 2)
C	5.3	15.5
O	19.4	31.1
Si	66.4	47.8
Cl	6.3	5.5
Na	2.4	--
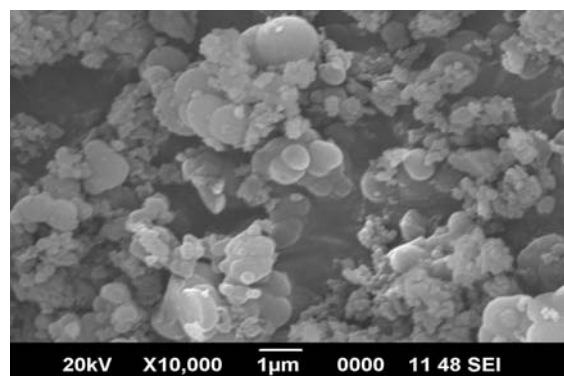
Figure 2.6 SEM of **CMS 1**

2.3.2.3 Low angle XRD analysis

The powder X-ray patterns of the solid **MS** confirm the typical mesoporous structure (Figure 2.7). The XRD shows four low-angle reflection peaks at 0.4, 0.8, 1.5 and 1.7° separately, which can be indexed to the (100), (110), (200) and (210) diffractions, characteristic of the 2D hexagonal symmetry suggesting perfect long-range order in this material.[52] XRD pattern of **CMS 1** sample is similar to that of **MS** sample and having a strong broad reflection at 0.8, 1.5 and 1.7°. This confirmed that hexagonal symmetry of mesopores of **CMS 1** was obtained by the co-condensation method.[53]
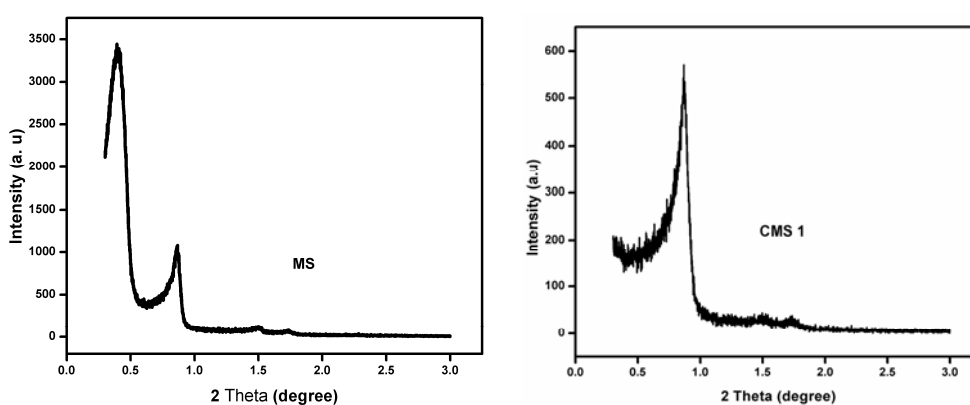
Figure 2.7 Low angle XRD of **MS** and **CMS 1**

2.3.2.4 Surface area analysis

The surface area of **MS, CMS 1** and **CMS 2** were determined using BET method and the pore size by BJH method (isotherms with hysteresis). The results are shown in Figure 2.8. The nitrogen adsorption/desorption isotherms of **MS, CMS 1** and **CMS 2** show type IV isotherm with H1 hysteresis loop with a sharp step up in a narrow range of relative pressure (P/P_0=0.6-0.9) arising from the capillary condensation of nitrogen in the mesopores which proves the mesoporous nature of the synthesized silica support.
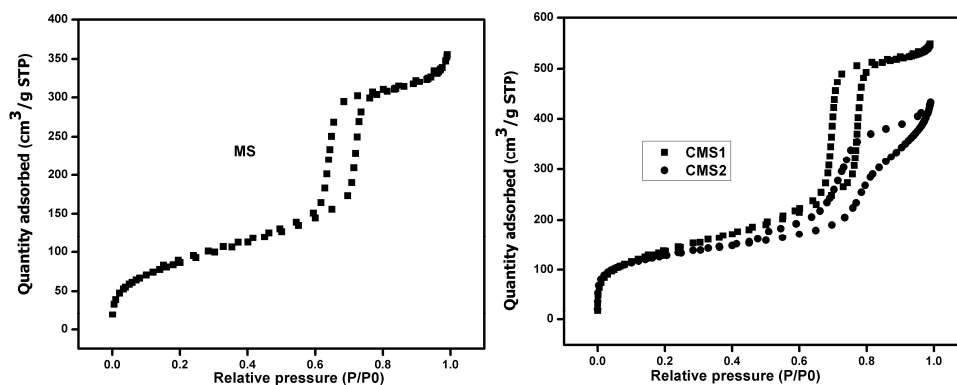
Figure 2.8 BET isotherm of **MS, CMS 1** and **CMS 2**

Table 2.3 Surface properties of **MS**, **CMS 1** and **CMS 2**

Sample	Surface area (m²/g)	Pore volume (cm³/g)	Average pore diameter (nm)
MS	586	0.9	10.2
CMS 1	516	0.86	9.87
CMS 2	470	0.75	8.47

The specific surface area, pore volume and pore diameter of the samples are summarized in the Table 2.3. It is clear that **MS** sample shows surface area of 586 m²/g with pore diameter 10.2 nm, whereas, a moderate

decrease was observed for sample **CMS 2**. In the case of **CMS 2**, position of capillary condensation was shifted to low pressure values, suggesting decrease in the pore diameter, pore volume and specific surface area when compared to **MS**. The overall shape of isotherm of **MS, CMS 1** and **CMS 2** remained unchanged. This confirmed successful introduction of chlorine fragment using grafting method. Among **CMS 1** and **CMS 2, CMS 1** shows high specific surface area, pore volume and pore diameter. This confirmed the successful formation of mesoporous structure on **CMS 1** by the co-condensation method.

2.3.2.5 TG-DTG Analysis

The thermal stability of the silica samples was established by TG-DTG analysis. The thermogravimetric analysis of **MS** and **CMS 1** was performed under nitrogen atmosphere (Figure 2.9). In **MS** sample, no appreciable weight loss was observed. This means that **MS** is highly thermally stable up to 730 °C. In the case of **CMS 1**, TG curve showed nearly 17 % of weight loss between 300-400 °C. It was assigned to cleavage of organic and chlorine fragments on the surface of silica.
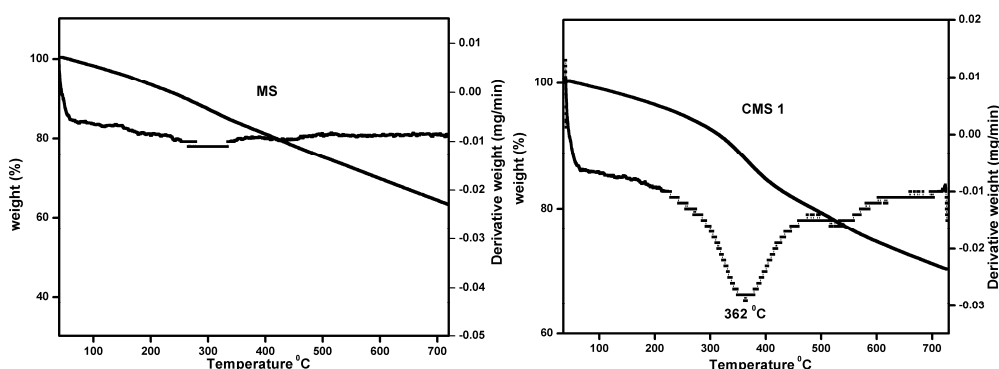
Figure 2.9 TG-DTG curves of **MS** and **CMS 1**

2.3.2.6 CP MAS ^{13}C NMR spectrum of CMS 1

^{13}C CP-MAS NMR spectra are used to confirm the presence of organic functionalization on the silica surface. **CMS 1** (Figure 2.10) shows three main peaks at 49, 28 and 24 ppm corresponding to the three carbons originating from 3-chloropropyltrimethoxysilane group. Peak at 66 ppm corresponds to the unreacted methoxy group present on silica surface. The small peaks (66-76 ppm) are credited to the presence of surfactant P123.
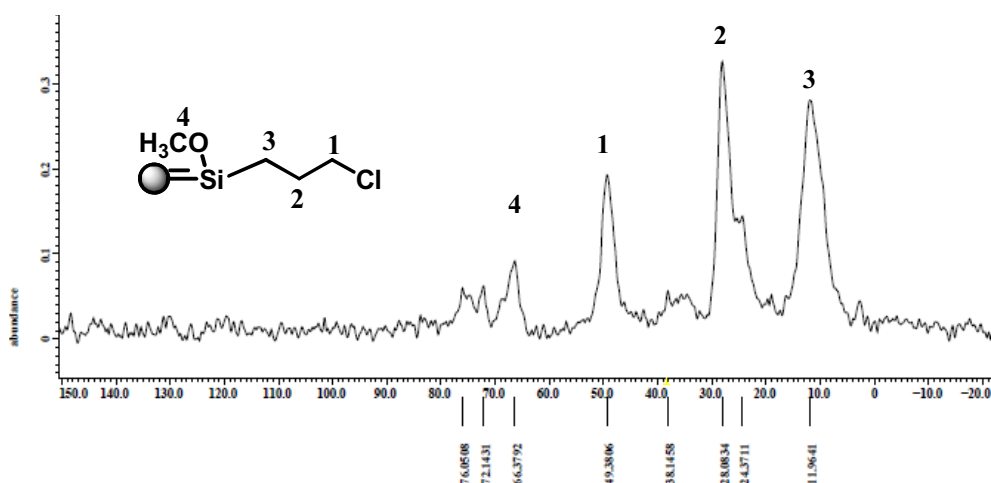
Figure 2.10 Solid state CP MAS ^{13}C NMR spectrum of **CMS 1**

2.3.3 Dendrimer synthesis on CMS 1

Due to the high chlorine capacity, surface area and pore diameter, **CMS 1** was selected for the dendrimeric growth on mesoporous silica surface. **CMS 1** was reacted with 1,3,5-triazine-2,4,6-trithiol trisodium salt solution in DMF at 50 °C for 24 h. After the reaction, white solid was filtered and washed with DMF, DCM and water. The resulting sample was

denoted as **A1**. **A1** was reacted with trimesoyl chloride in the presence of THF and triethylamine at 50 °C for 2 days. The sample obtained was denoted as **A2**. The overall reaction sequence is given in Scheme 2.7. The above mentioned procedure was repeated alternatively, **A3, A4, A5** and **A6** were obtained (Scheme 2.7). Structure of **A6** is shown in the Figure 2.11.

Scheme 2.7 Dendrimeric growth on **CMS 1**
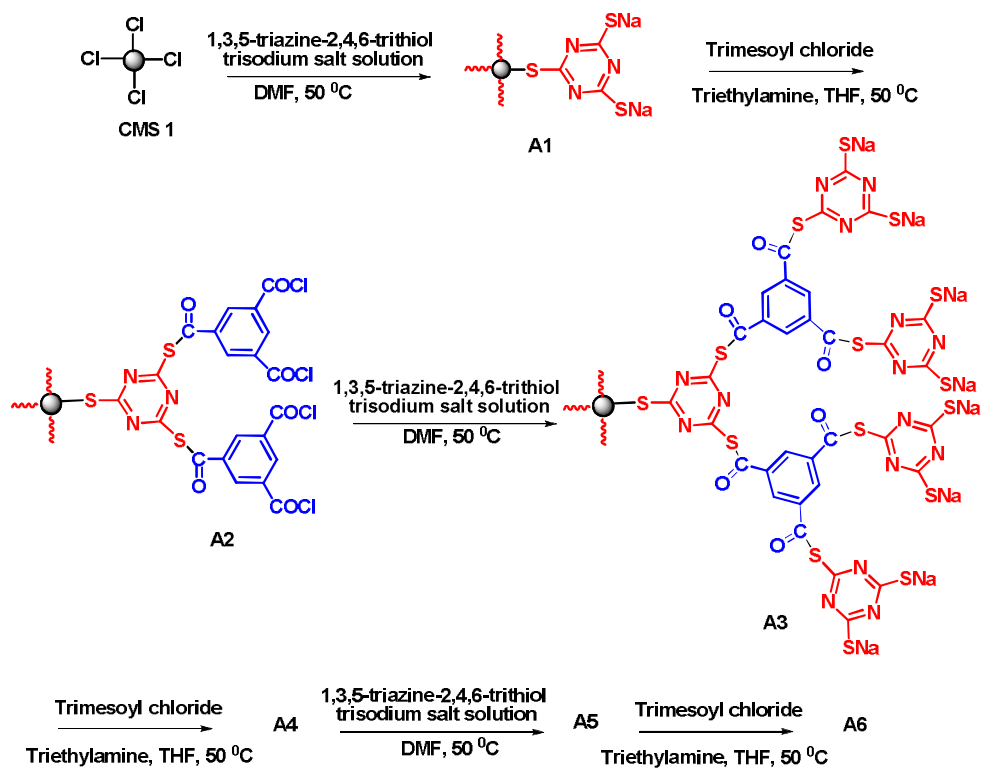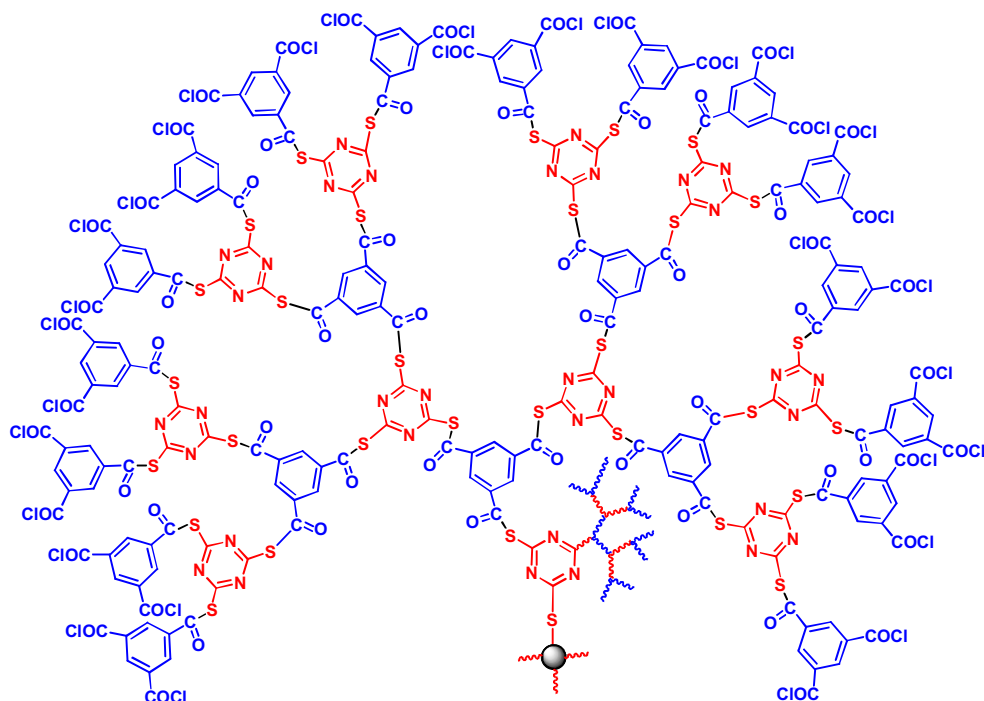
Figure 2.11 Structure of **A6**

2.3.3.1 Characterization of A1, A2, A3, A4 and A6

To confirm the dendritic growth on **CMS 1**, EDAX analysis of **A1, A2, A3, A4, A5** and **A6** was performed. EDAX spectrum and elemental composition of the samples are shown in the following Figures 2.12, 2.13, 2.14 and Tables 2.4, 2.5, 2.6. From the Table 2.4, 7.17 mass % of Na was present in the **A1** sample and this was absent in **A2** and also 3.22 mass % of chlorine was found. This confirmed the complete conversion of **A1** to **A2**. Similar trend was also observed in the case of **A3, A4, A5** and **A6**. From this analysis, it clearly supported the successful growth of dendrimeric structure on **CMS 1**.

(A1)

(A2)
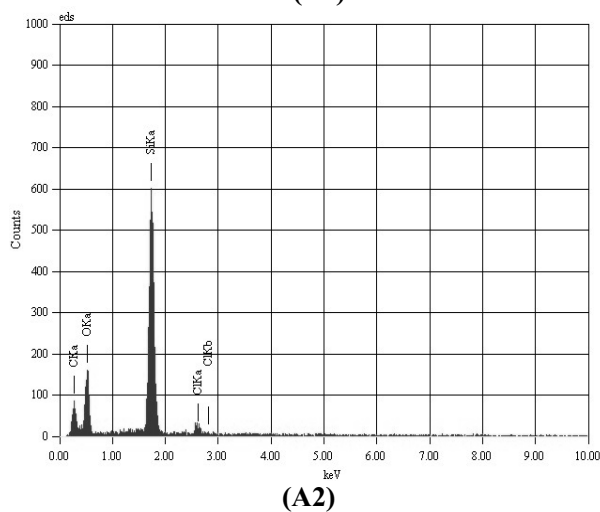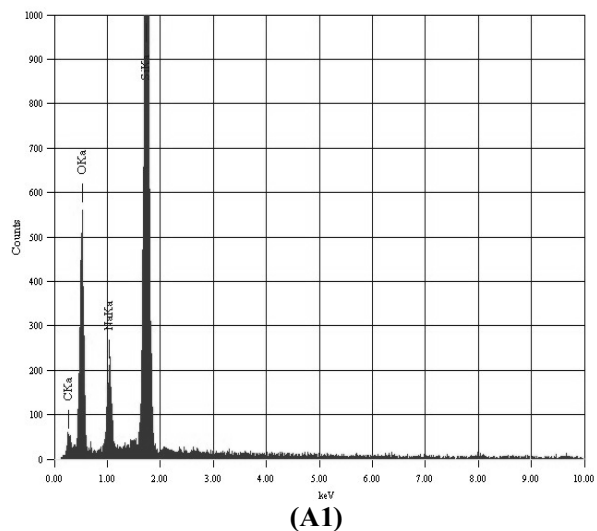
Figure 2.12 EDAX spectra of **A1** and **A2**

Table 2.4 Elemental composition of **A1** and **A2**

Element	Mass % (A1)	Mass % (A2)
C	5.8	22.0
O	26.3	19.3
Si	60.3	55.3
Na	7.1	--
Cl	--	3.2
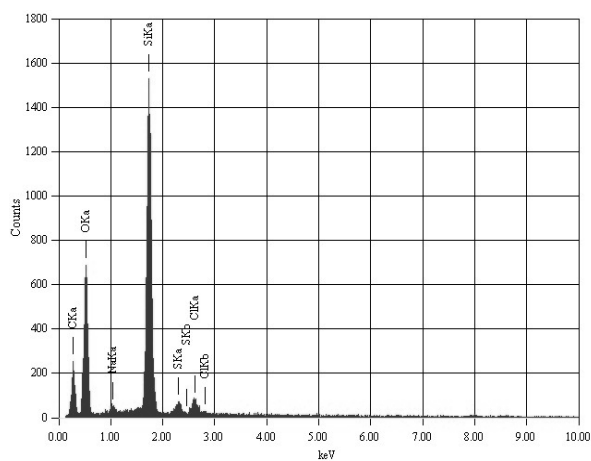
(A3)
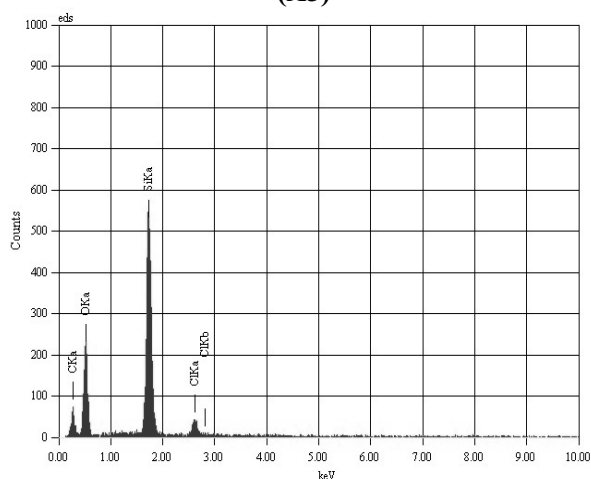
(A4)

Figure 2.13 EDAX spectra of **A3** and **A4**

Table 2.5 Elemental composition of **A3** and **A4**

Element	Mass % (A3)	Mass % (A4)
C	22.7	18.8
O	25.6	27
Si	45.5	49
Na	1.1	--
Cl	2.7	5.1
S	2.2	--
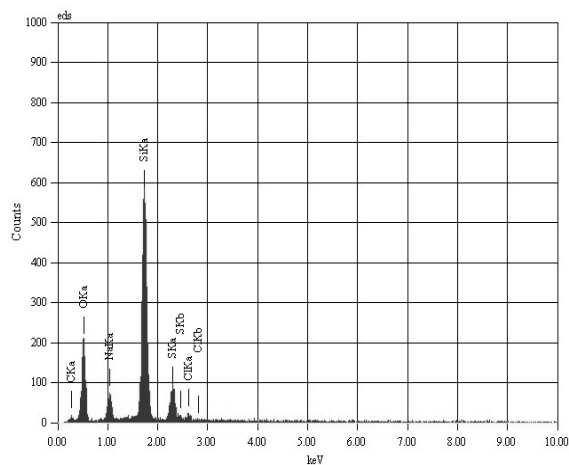
(A5)
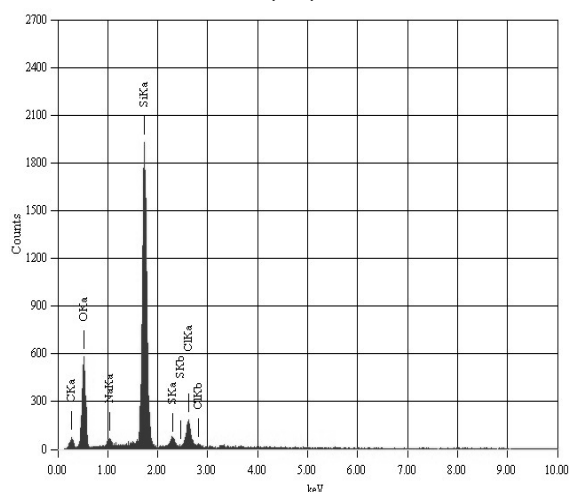
(A6)

Figure 2.14 EDAX spectra of **A5** and **A6**

Table 2.6 Elemental composition of **A5** and **A6**

Element	Mass % (A5)	Mass % (A6)
C	3.4	6.2
O	23.0	22.1
Si	53.2	59.8
Na	5.6	1.4
Cl	2.4	7.7
S	11.5	2.5

2.3.4 Synthesis of dendritic sulfonic acid on mesoporous silica

The sample **A1** was collected and acidified with 0.5 N HCl for 24 h at room temperature. The reaction mixture was filtered and washed with water until the disappearance of chlorine and dried to get **SH1**. **SH1** was oxidized with H_2O_2 in the presence of methanol and one drop of H_2SO_4 at room temperature for 6 h.
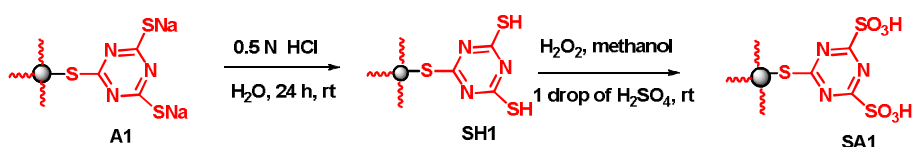
Scheme 2.8 Synthesis of **SA1**
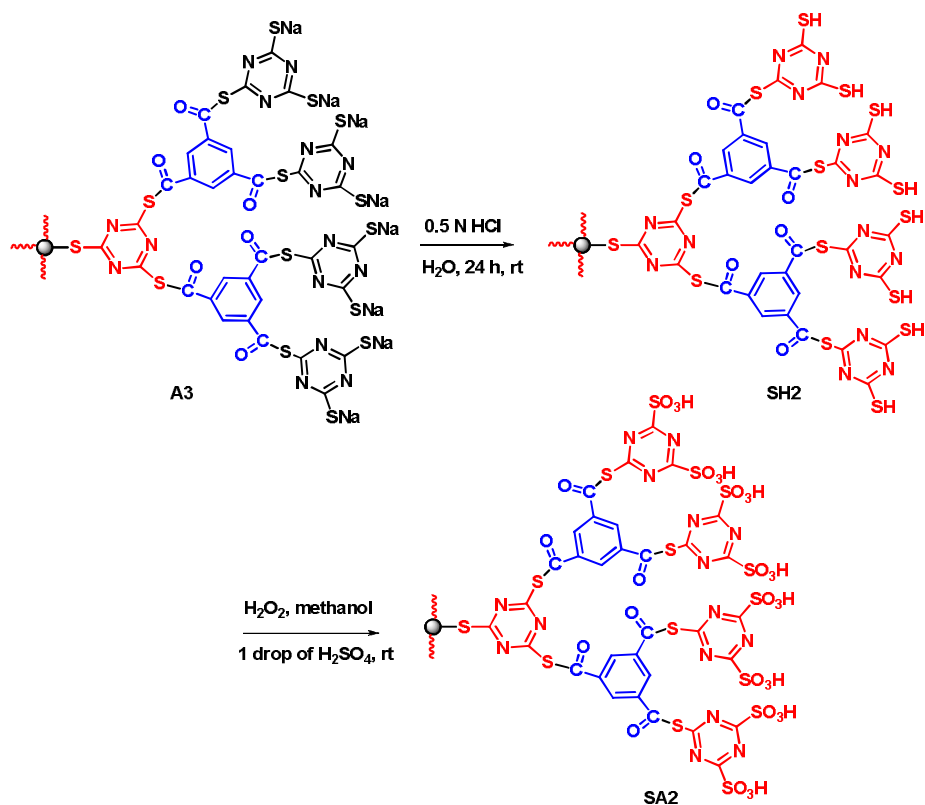
Scheme 2.9 Synthesis of **SA2**

The solid was filtered off and washed with methanol and water and dried. The sample obtained was denoted as **SA1**. Similarly, the samples **A3** and **A5** on acidification followed by oxidation, the samples **SA2** and **SA3** are obtained. The reaction sequence is given in Scheme 2.8 and 2.9. The structure of **SA3** is given in the Figure 2.15.
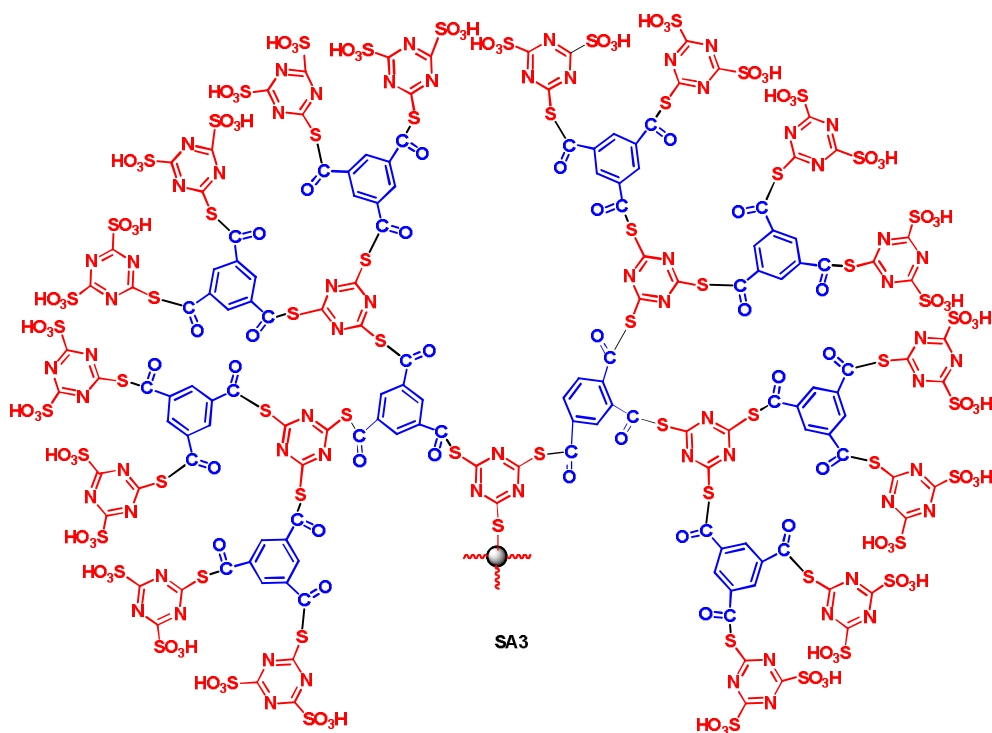
Figure 2.15 Structure of **SA3**

Due to the presence of large amount of SO_3H groups on the surface of mesoporous silica, acid capacity of **SA1, SA2** and **SA3** was estimated using acid-base titration method. Results are given in Table 2.7. It clearly shows that acidity was increased from **SA1** to **SA3**.

Table 2.7 Acid capacity of **SA1-3** samples

Sample	Acidity (mmol/gm)
SA1	3.8
SA2	6.8
SA3	10.2

2.3.5 Characterization of dendritic sulfonic acid on mesoporous silica
2.3.5.1 IR spectra

The immobilization of functional groups on silica framework was examined by IR spectroscopy in every step. The IR spectra of all **SH** samples are given in the Figure 2.16. A new band at nearly 2340-2370 cm^{-1} corresponding to the stretching vibration of SH bond was obtained. In **SH2** and **SH3**, compared with **SH1**, strong band at 1700-1735 cm^{-1} due to stretching vibration of C=O group were obtained. This shows the successful growth of dendritic structure.
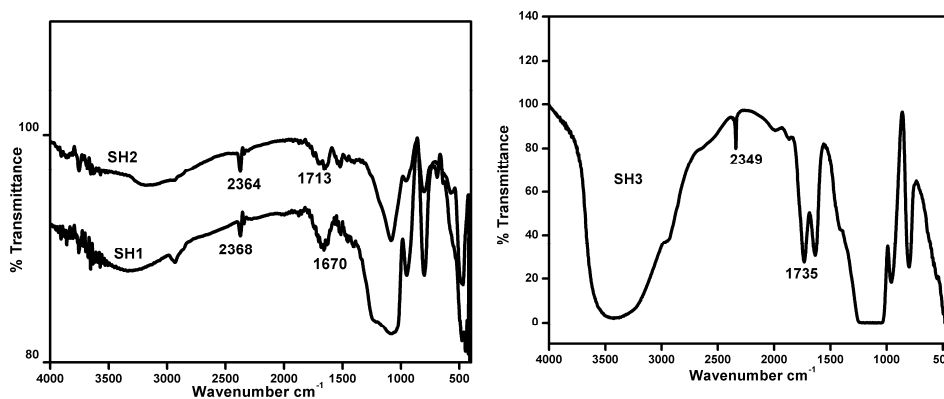
Figure 2.16 IR spectra of **SH1-3** samples

Evidence for oxidation of SH groups on the surface was observed in the IR spectra shown in Figure 2.17. Peak at nearly 2300 cm^{-1} was completely disappeared and is the strong indication of complete oxidation of

SH group to SO_3H group. It can be seen that the strong vibration bands exist at 1370 and 1454 cm^{-1} corresponding to asymmetric stretching of SO_2 moieties. The differences in the peaks in the region of 3500-2800 cm^{-1} of **SH** and **SA** samples are clearly visible. This gives the information on the formation of the sulfonic acid groups. The differences are mainly due to the S-OH stretching mode occurring in the frequency region of 3100-2900 cm^{-1} in addition to the Si-OH group at 3500 cm^{-1}. There is no change in the symmetric stretching vibration of C=O group at 1700-1735 cm^{-1} and basic peaks of mesoporous silica framework in **SA2** and **SA3** samples. This strongly supported that mesoporous silica frame work and dendritic structures were not destructed after the oxidation of **SH** samples with H_2O_2.
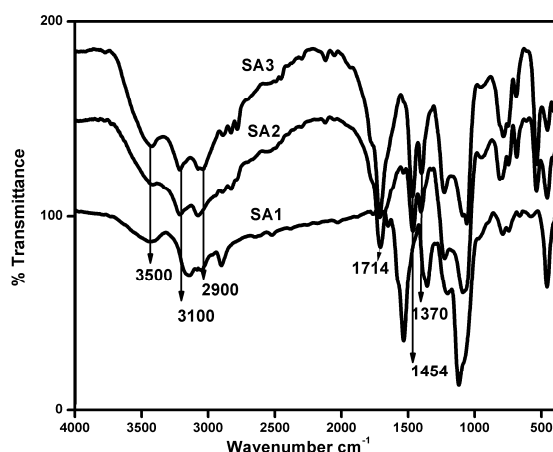
Figure 2.17 IR spectra of **SA1-3** samples

2.3.5.2 Raman spectra

The nature of sulfur species formed over the mesoporous silica framework was further explored using Raman spectroscopy. Prior to the thiol oxidation step, **SH3** showed a strong peak at 2380 cm^{-1} characteristic of the thiol group of **SH3**. After H_2O_2 oxidation, the SH groups disappeared

with the subsequent formation of new bands at 1700 and 748 cm^{-1}, which are attributed to the symmetric and asymmetric vibrational modes of SO$_3$ (Figure 2.18). The presence of other sharp peaks shows the presence of anchored organic groups arising from the organic linker. All these results confirm the integrity of the sulfonic acid groups within the silica support.[54-58]
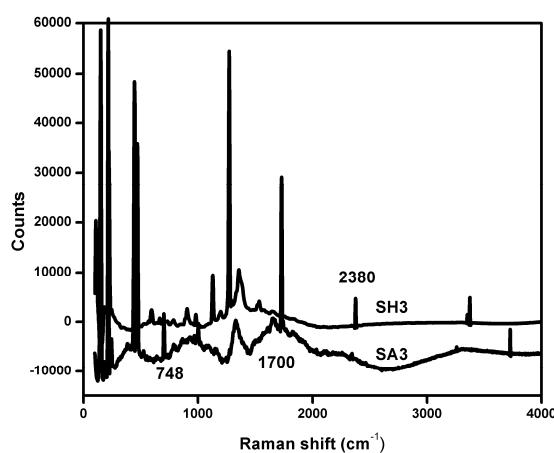
Figure 2.18 Raman spectra of **SH3** and **SA3**

2.3.5.3 Surface area analysis

N$_2$ adsorption/desorption isotherms of **SA1, SA2** and **SA3** are shown in Figure 2.19. The isotherms of **SA1** and **SA2** samples are classified as type IV adsorption with H1 hysteresis which is the characteristic of mesoporous silica materials. Pore size distribution of **SA1-3** samples (Table 2.8) was estimated by employing the BJH method, which indicated the existence of uniform large mesopores. The surface area was decreased after each generation and sharpness of adsorption branches was indicative of narrow mesopore size distribution. The position of capillary condensation was shifted to lower pressure values suggesting a reduction in the mesopore size, because, the capillary condensation is an increasing function of the pore

diameter. Moreover, the **SA1-3** samples showed decreased specific surface area, pore volume and pore diameter. There was no change in the shape of the isotherm for **SA1** and **SA2**. In the case of **SA3**, the shape of the isotherm was almost flat. This may be due to the pore filling by dendritic groups on mesoporous silica, which destruct the mesoscale ordering of the support.
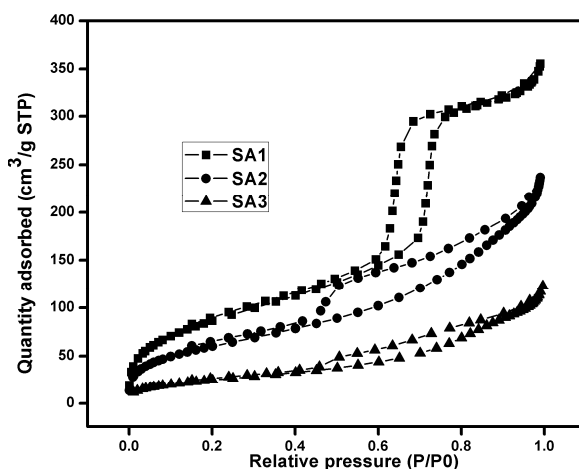
Figure 2.19 BET isotherms of **SA1-3** samples

Table 2.8 Surface properties of **SA1-3** samples

Sample	Surface area (m^2/g)	Pore volume (cm^3/g)	Pore diameter (nm)
SA1	347	0.64	5.4
SA2	289	0.54	3.6
SA3	78	0.29	2.1

2.3.5.4 Low angle XRD

XRD patterns acquired for the three SA samples are shown in Figure 2.20. **SA1** sample with a *d*100 reflection at 0.9° indicated ordered hexagonal mesopore structure. It is interesting to note that the XRD pattern of **SA2** showed little intensity in the low angle region, but no shift in the

peak position was observed. In the case of **SA3**, the peaks have disappeared. These results imply that the mesopore structure was destroyed due to the dendritic growth. The presence of dendritic groups has reduced the contrast between scattering by the walls and the channels. Random placement of functional groups may be an additional factor leading to disappearance of peaks of **SA3**.
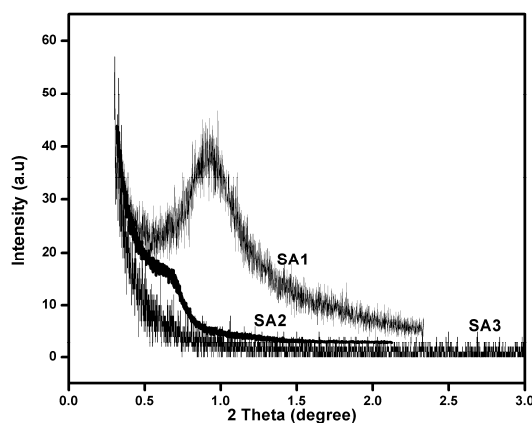
Figure 2.20 Low angle XRD of **SA1-3** samples

2.3.5.5 TG-DTG Analysis

Thermal stability and degree of dendritic functionalization of **SA** samples were studied using TG-DTG analysis and the results are presented in the Figures 2.21 and 2.22. In **SA2**, weight loss below 100 °C was due to the removal of adsorbed water molecules. In all **SA1-3** samples, weight loss at nearly 200-250 °C was due to the removal of SO_2 molecules. In **SA2** and **SA3** samples, another weight loss was observed between 350-550 °C corresponding to the decomposition of dendritic fragment.
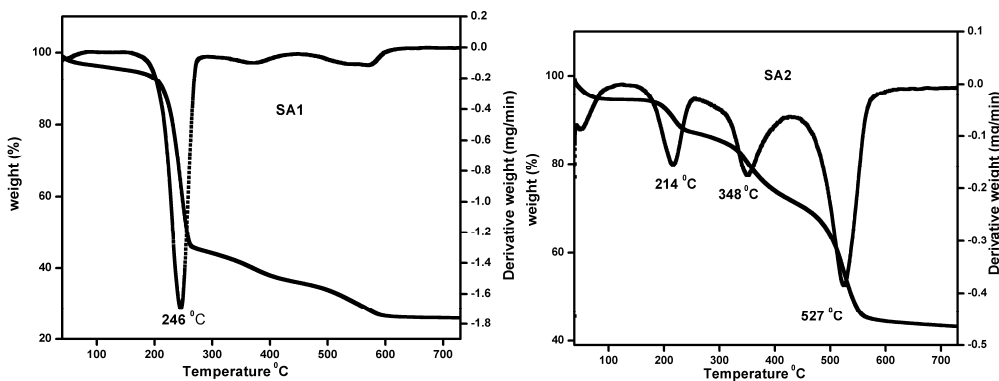
Figure 2.21 TG-DTG Curves of **SA1** and **SA2**
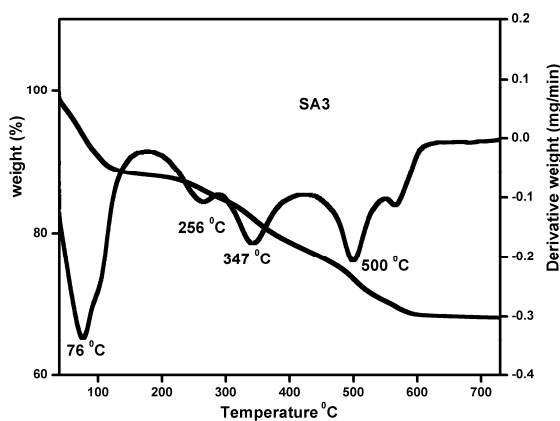
Figure 2.22 TG-DTG Curves of **SA3**

2.3.5.6 CP MAS ^{13}C NMR spectrum

The incorporation of dendritic functional groups on mesoporous silica was further confirmed by solid state CP-MAS ^{13}C NMR spectrum. The solid state ^{13}C CP-MAS NMR spectrum of **SA3** is shown in the Figure 2.23. A sharp new peak at 171 ppm corresponds to C=O group of dendritic part. The other three main peaks at 135, 132 and 131 ppm are corresponding to the three different carbons from aromatic ring and triazine ring. Peaks at 70, 36 and 30 ppm correspond to the propyl chain. These results strongly support the successful formation of dendrimeric structure on **CMS 1**.
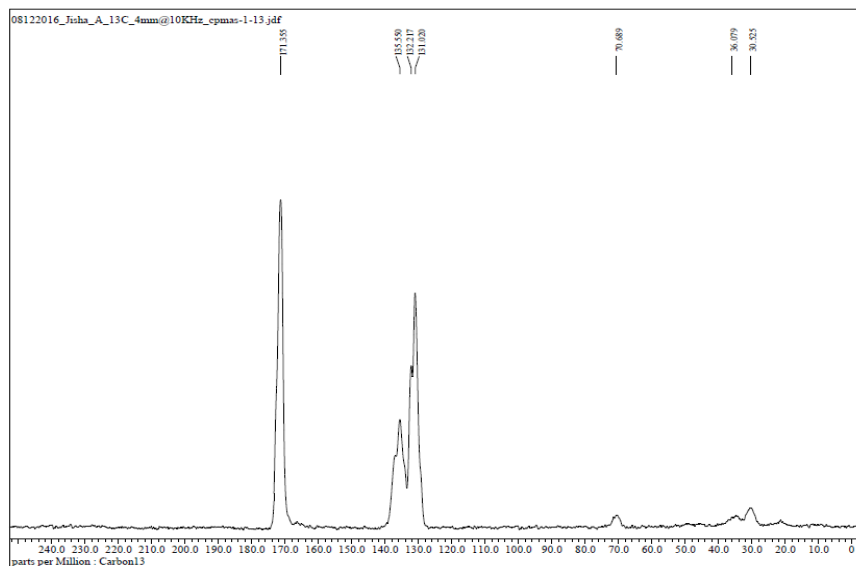
Figure 2.23 Solid state[13]C CP-MAS NMR spectrum of **SA3**

2.3.5.7 SEM Analysis

Scanning electron micrograph of **SA3** shows irregular agglomerates of different shapes (Figure 2.24). The loss of spherical nature was due to the crushing of the SA3 due to prolonged stirring or may be due to the umbrella effect (to stretch to maximum extent) on silica surface.
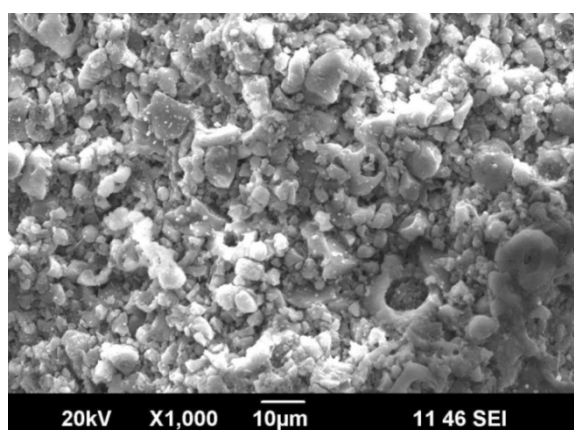
Figure 2.24 SEM image of **SA3**

2.3.6 Synthesis of dendritic carboxylic acid on mesoporous silica

Due to the importance of supported Brønsted acids, especially carboxylic acid groups, dendrtitic carboxylic acid was synthesized on **CMS 1**. The samples **A2, A4** and **A6** were obtained. **A2** sample underwent base hydrolysis followed by acidification with dil. HCl.
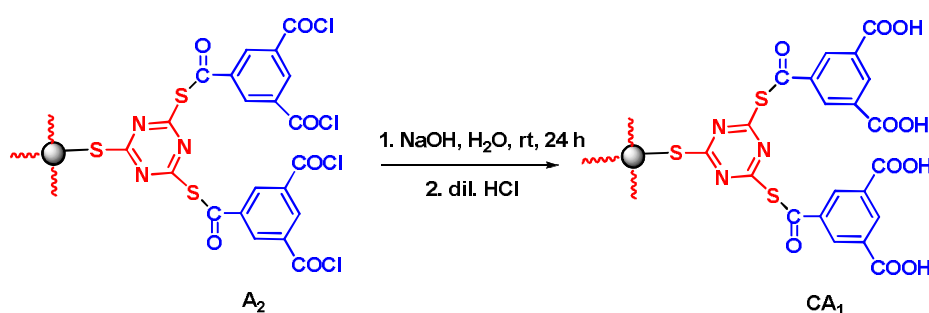
Scheme 2.10 Synthesis of **CA1**
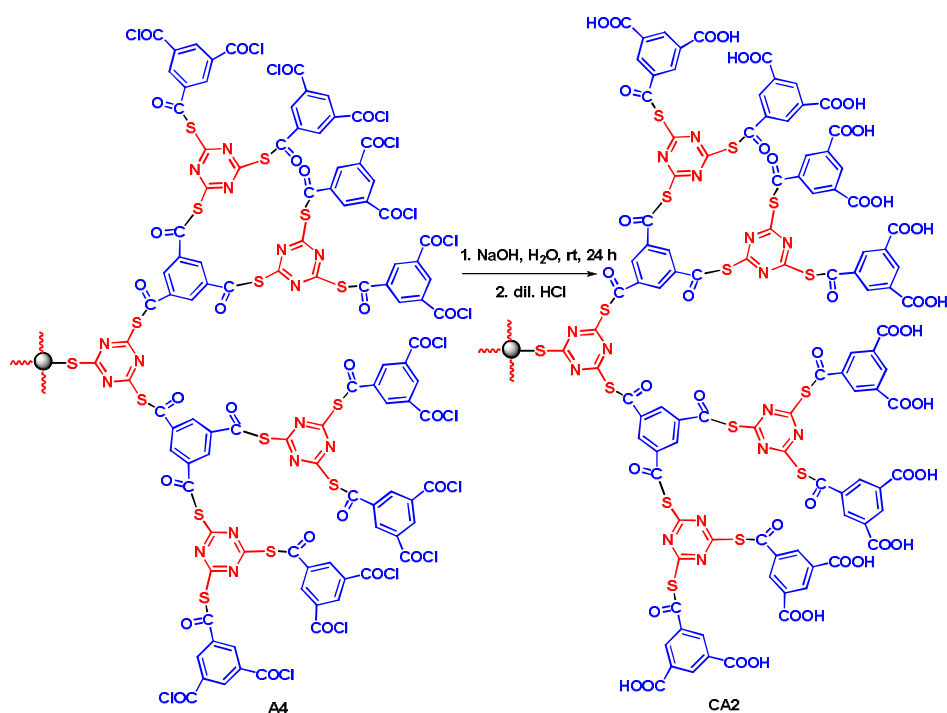
Scheme 2.11 Synthesis of **CA2**

The obtained white powder was dried and denoted as **CA1** (Scheme 2.10). Same procedure was repeated for **A4** and **A6** samples and final solid powder was represented as **CA2** and **CA3** respectively. The overall reaction sequence is given in the Scheme 2.11. The structure of third generation of **CA3** sample is shown in the Figure 2.25.

CA3
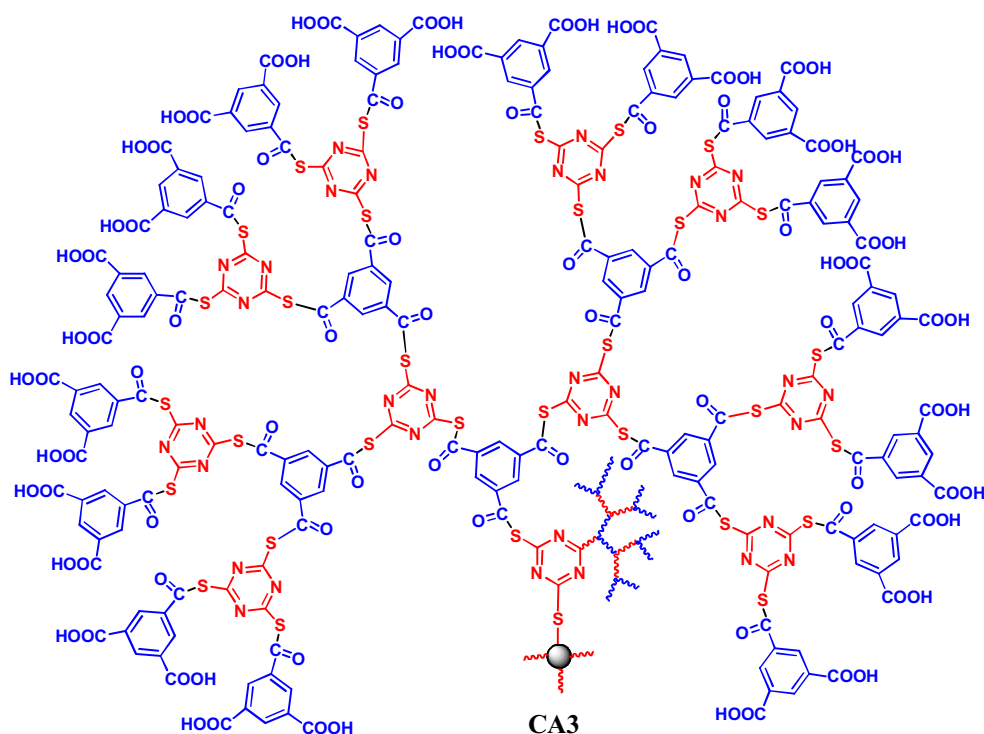
Figure 2.25 Structure of **CA3**

Since the terminal groups of **CA1, CA2** and **CA3** are carboxylic acid groups, acid capacity was estimated by acid-base titration method and results are summarized in Table 2.9. Acidity was increased from **CA1** to **CA3** and high acidity was exhibited by **CA3**. This means that on going to higher generation, number of carboxylic acid groups also increased as reflected in this result.

Table 2.9 Acid capacity of **CA1-3** samples

Sample	Acidity (mmol /gm)
CA1	4.2
CA2	7.7
CA3	12.8

CHNS analysis was carried out to quantify the organic functionalities on **SA3** and **CA3** and results are summarized in Table 2.10. Compared with **SA3, CA3** has high C, H, N and S content which confirmed the effective functionalization of dendritic groups on **CMS 1**

Table 2.10 CHNS analysis of **SA3** and **CA3**

Sample	C	H	N	S
SA3	9.76	2.24	0.26	1.85
CA3	10.72	2.42	0.41	1.89

2.3.7 Characterization of dendritic carboxylic acid on mesoporous silica

2.3.7.1 IR spectral studies

IR spectra of **A2, A4, A6, CA1, CA2** and **CA3** are given in the Figure 2.26. A strong absorption band at 1712-1734 cm^{-1} in **A2**, **A4** and **A6** is due to the C=O stretching frequency of S-CO group and peaks at nearly 680 cm^{-1} indicating the C-Cl stretching frequency confirmed the perfect grafting of dendritic groups. In the case of **CA1, CA2** and **CA3** samples, new peaks at 1756 cm^{-1} correspond to the C=O of COOH group. When compared with **A** samples, broadening of peaks at 3500-3000 cm^{-1} may be due to the OH stretching frequency of COOH groups. These results revealed the effective framework.
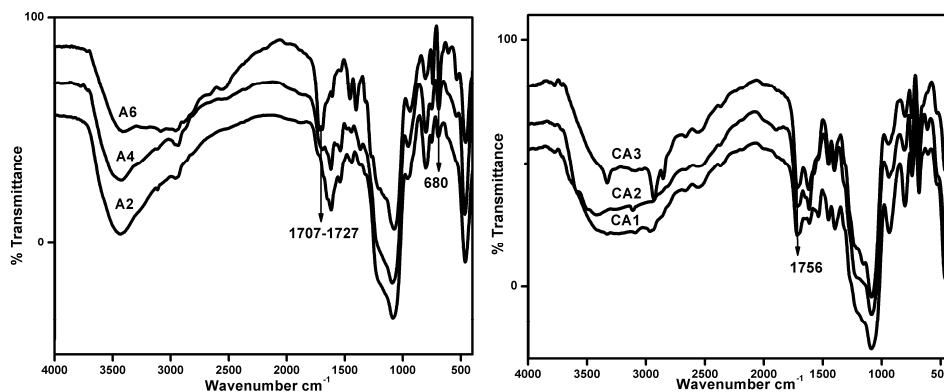
Figure 2.26 IR spectra of **A** samples and **CA1-3** samples

2.3.7.2 Surface area analysis

BET plots of the **CA1-3** samples are given in the Figure 2.27 and surface properties are given in the Table 2.11. Results showed a typical type IV isotherm and corresponding hysteresis loop, confirming the nature of mesoporous materials.
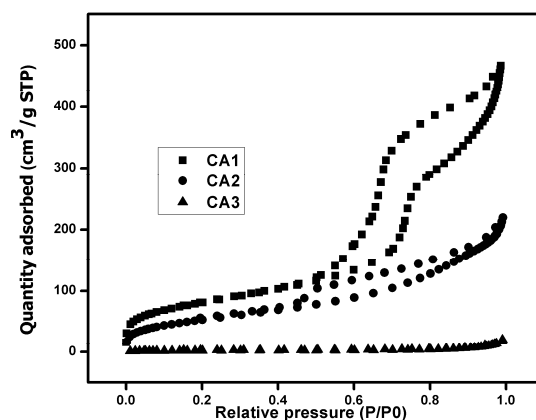
Figure 2.27 BET isotherms of **CA1-3** samples

Surface area, pore diameter and pore volume decreased after each generation and overall shape of the adsorption/desorption isotherms remained unchanged for **CA1** and **CA2**. But for **CA3**, the isotherm was flat, the mesopore structure

was destroyed. The prominent steps of capillary condensation in primary mesopores were evident, indicating that ordering of mesoporous silica was not affected by the dendritic functionalization upto the second generation. But for **CA3** there was no mesoscale ordering. This may be due to the pore filling with dendritic growth.

Tale 2.11 Surface properties of **CA1-3** samples

Material	Surface area (m^2/g)	Pore volume (cm^3/g)	Pore diameter (nm)
CA1	282	0.57	4.3
CA2	173	0.33	3.0
CA3	7	0.03	0.9

2.3.7.3 Low angle XRD

Powder XRD analysis was carried out to study the structural ordering of **CA** samples. The diffraction patterns of **CA1** and **CA2** are given in the Figure 2.28. **CA1** showed low angle diffraction at 1.2° with low intensity.
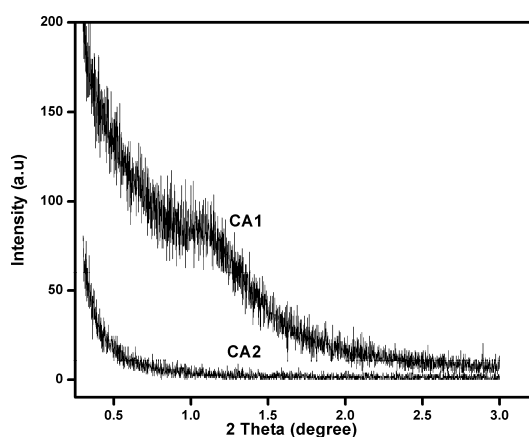
Figure 2.28 Low angle XRD of **CA1** and **CA2**

This is characteristic of mesoporous silica materials, but this was absent in **CA2**. For **CA3**, in the low angle region, there were no diffraction peaks. It may be due to the destruction of ordered nature of mesoporous silica. This is mainly due to the pore filling of mesoporous silica with dendritic functionalities and confirmed that the ordered nature of the mesoporous silica support was partially preserved after dendritic growth up to the second generation.

2.3.7.4 TG-TDG analysis

Thermal stability and degree of dendritic functionalization of **CA1-3** samples were studied using TG-DTG analysis and results are given in Figure 2.29 and 2.30.
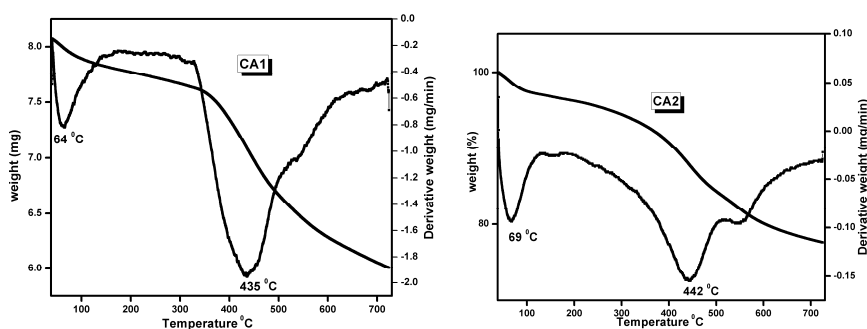
Figure 2.29 TG-DTG of **CA1** and **CA2**
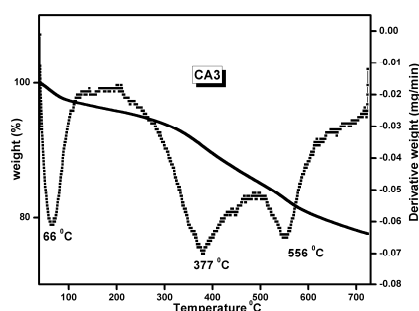
Figure 2.30 TG-DTG of **CA3**

For the samples, weight loss below 100 °C was due to the removal of adsorbed water molecules. Another weight loss of 18 %, 14 % and 20 % were observed between 350-450 °C corresponding to the decomposition of dendritic structure liberating CO_2. In the case of **CA2** and **CA3**, one more weight loss was observed at 556 °C which was corresponding to the decomposition of dendritic fragment.

2.3.7.5 CP MAS ^{13}C NMR spectrum

Solid state CP MAS ^{13}C NMR spectrum of **CA3** sample is shown in the Figure 2.31. The peaks below 200 ppm were similar to the peaks obtained in the case of **SA3**. The additional peaks at 235 and 230 ppm are corresponding to the carbon of carboxylic acid. This gives the strong evidence of formation of dendritic carboxylic acid on mesoporous silica.
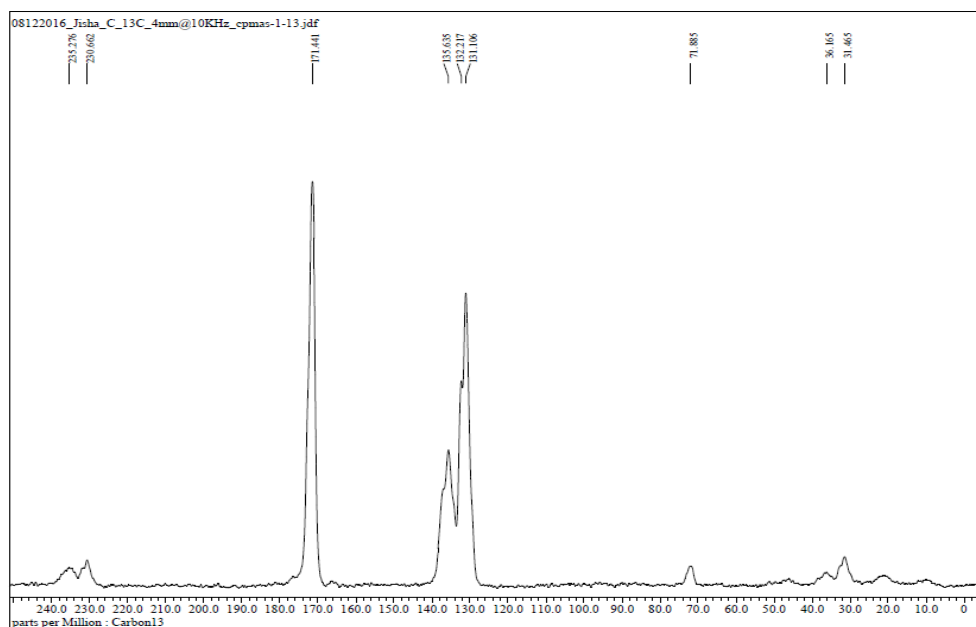
Figure 2.31 Solid state ^{13}C CP-MAS NMR spectrum of **CA3**

2.3.7.6 SEM Analysis

The morphological change on the surface of the mesoporous silica after dendritic growth was examined by SEM analysis. SEM image of **CA3** sample is shown in Figure 2.32. The micrographs revealed that the spherical surface of the starting mesoporous silica got disrupted and became crushed into powder, which, then aggregated into small units.
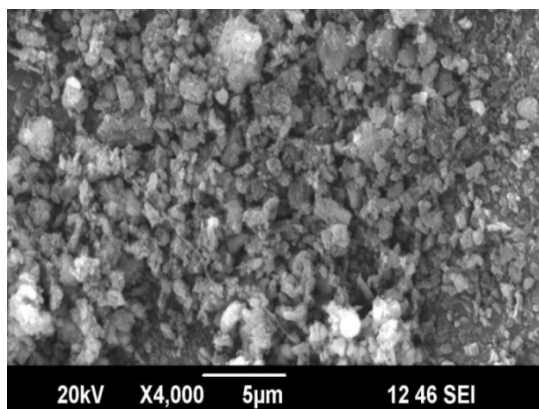
Figure 2.32 SEM image of **CA3**

2.4 Conclusion

In conclusion, chlorine functionalized mesoporous silica was synthesized by two methods viz. co-condensation method and grafting method and well characterized by various techniques. The results showed that **CMS 1** has high surface area, pore diameter and high chlorine capacity. **CMS 1** was selected for the synthesis of dendritic functionalized mesoporous silica. Here two types of Brønsted acid functionalized silica were synthesized. Three generations of dendritic carboxylic acid and dendritic sulfonic acid functionalized mesoporous

silica were synthesized by stepwise growth technique. All characterization methods strongly supported the successful formation of both dendritic functionalities on silica framework and mesoporous nature of silica was retained after functionalization. Amount of acidic functionalities on both dendritic functionalized silica was found to be high and highest for third generation **SA3** and **CA3** respectively.

2.5 Experimental
2.5.1 Materials

All the solvents were purified according to standard procedures. All reagents used in the preparation and modification of silica were used as received. Tetraethyl orthosilicate, 3-chloropropyltrimethoxysilane, Pluronic P123 and 1,3,5-triazine-2,4,6-trithiol trisodium salt solution were received from Aldrich.

2.5.2 Synthesis of mesoporous silica

Mesoporous silica (**MS**) was synthesized using the triblock copolymer Pluronic P123 as template under acid condition. Typically, a Pluronic P123 template (6.4 g) was dissolved with stirring in a solution of 2 M HCl (150 mL) at 40 °C, and tetraethyl orthosilicate (TEOS) (13.6 g) was added. The resulting mixture was stirred at 40 °C for 20 h, and aged at 100 °C for 24 h under static condition in autoclave. The recovered solid was extensively washed with deionized water and dried at 100 °C for 12 h. The surfactant template was removed by calcination in air at 550 °C for 6 h. Yield: 10 g, White powder; IR (cm^{-1}): 3500-3400, 1630, 1100-1000, 800.

2.5.3 Synthesis of chlorine functionalized mesoporous silica

2.5.3.1 Co-condensation method

Triblock copolymer ($EO_{20}PO_{70}EO_{20}$) Pluronic P123 (8.0 g) was dissolved in an aqueous solution of HCl (pH=1.5) (80 mL). The resulting clear solution was added to a mixture of 3-chloropropyltrimethoxysilane (1.78 g) and tetraethyl orthosilicate (13.6 g). The mixture was vigorously stirred for 3 h at room temperature until a transparent solution appeared. The flask containing solution was transferred to a hot oil bath at 60 °C and NaF (76.0 mg) was immediately added to induce the polycondensation. A white precipitate appeared within a few minutes and the resulting suspension was further stirred for 2 days at 60 °C. The resulting white powder was filtered off, washed with water and the surfactant was selectively removed by Soxhlet extraction with ethanol for 24 h. After drying at 120 °C overnight under vacuum, **CMS 1** was obtained as white powder. Yield: 10.5 g, White powder; IR (cm^{-1}): 2930, 1100-1000, 700.

2.5.3.2 Grafting method

Mesoporous silica (**MS**) (6 g) was suspended in dry toluene (150 mL), and 3-chloropropyltrimethoxysilane (6 mL) was added under stirring. The mixture obtained was stirred at 100 °C for 2 days. The solid was obtained after washing with toluene and with ethanol intensively to eliminate the physically adsorbed reactants and toluene. The sample after being vacuum-dried at 100 °C for 6 h was labelled **CMS 2**. Yield: 5.5 g, White powder; IR (cm^{-1}): 2930, 1100-1000, 700.

2.5.4 Preparation of dendritic functionalities on CMS 1

To a solution of 1,3,5-triazine-2,4,6-trithiol trisodium salt solution (10 mL) in DMF (45 mL) was added **CMS 1** (10 g) and stirred for 24 h at 50 °C. The resulting reaction mixture was filtered and washed with DMF, DCM and water. The solid powder was dried at 100 °C under vacuum and represented as **A1**. Yield: 9.7 g, White powder. IR (cm^{-1}): 3500, 2950, 1450, 1100.

A1 (9 g) was added to the solution of trimesoyl chloride (3 g) in THF (50 mL) and triethylamine (45 mL) and refluxed for 2 days. The solid was recovered from the reaction mixture by filtration and washed sequentially with THF, DCM and water. The white powder was dried at 100 °C under vacuum. The sample was denoted as **A2.** Yield: 8.8 g, White powder. The above mentioned procedure was repeated alternatively to get **A3, A4, A5** and **A6**. Yield: 7.5 g, (**A3**, White powder); 7.2 g, (**A4**, Pale yellow powder); 6.5 g, (**A5**, Pale yellow powder); 6.2 g (**A6**, Pale yellow powder).

2.5.5 Synthesis of trimesoyl chloride

Trimesic acid (3 g) was refluxed with thionyl chloride (5 mL) in DCM (30 mL) for 2 h. After the reaction, excess thionyl chloride and other volatiles were removed under vacuum. The residue obtained was directly used for further reactions. Yield: 100 %, Yellow powder.

2.5.6 Preparation of dendritic sulfonic acid functionalized mesoporous silica

A1, A3 and **A5** (4 g each) was treated with 0.5 N HCl (20 mL) and water (20 mL) at room temperature for 24 h. The solid was collected by filtration and washed with water until no trace of chlorine was present and

dried. The resulting sample was denoted as **SH1, SH2,** and **SH3**. The dried samples (3 g each) were oxidized to corresponding sulfonic acid by treatment with 30 % aq. H_2O_2 (30 mL) for 6 h under stirring at 30 °C in methanol (10 mL) and few drops of concentrated sulfuric acid. The reaction mixture was filtered and washed with water and dried at 100 °C under vacuum. The samples obtained were represented as **SA1, SA2** and **SA3**

SH1: Yield; 3.8 g, White powder, IR (cm^{-1}): 2368, 1670, 1100, 495.

SH2: Yield; 3.7 g, White powder, IR (cm^{-1}): 2364, 1713, 1100, 495.

SH3: Yield; 3.4 g, Light yellow powder, IR (cm^{-1}): 2349, 1735, 1680, 1100, 495.

SA1: Yield; 2.7 g, White powder, IR (cm^{-1}): 3500, 3100-2900, 1370, 1100, 495.

SA2: Yield; 2.7g, White powder, IR (cm^{-1}): 3500, 3100-2900, 1714, 1454, 1370, 1100, 495.

SA3: Yield; 2.4 g, Light yellow powder, C (9.76 %), H (2.24 %), N (0.26 %), S (1.85 %); IR (cm^{-1}): 3500, 3100-2900, 1714, 1454, 1370, 1100, 495; Solid State ^{13}C NMR (100 MHz); 171, 135, 132, 131, 70, 36, 30.

2.5.7 Preparation of dendritic carboxylic acid functionalized mesoporous silica

A2, A4 and **A6** (4 g each) were reacted with NaOH (0.24 g) in water (30 mL) for 24 h at room temperature. The reaction mixture was acidified with dilute HCl and the solid separated was collected by filtration and washed well with water and dried at 100 °C under vacuum.

CA1; Yield; 3.7 g, White powder, IR (cm^{-1}): 3500-2900, 1756, 1450, 1380, 1100, 960, 800, 495.

CA2; Yield; 3.7 g, Light yellow powder, IR (cm^{-1}): 3500-2900, 1756, 1450, 1380, 1100-1000, 960, 800, 495.

CA2; Yield; 3.8 g, Light yellow powder, C (10.72 %), H (2.42 %), N (0.41 %), S (1.89 %); IR (cm^{-1}): 3500-2900, 1756, 1450, 1380, 1100-1000, 960, 800, 495; Solid State ^{13}C NMR (100 MHz); 235, 230, 171, 135, 132, 131, 70, 36, 30.

2.5.8 Estimation of chlorine capacity

Chlorine capacity was determined by the modified Volhard's method.[59] The chlorine functionalized mesoporous silica (250 mg) was heated with pyridine (2.5 mL) for 1 h at 100 °C. The suspension was diluted with acetic acid: water (1: 1) (25 mL). The halide was displaced by the addition of conc. HNO_3 (5 mL) and precipitated with a measured excess of standard $AgNO_3$ (0.1 N) solution. AgCl that was formed was coated with toluene, and the excess $AgNO_3$ was back titrated with standard NH_4SCN solution, using ferric alum [$FeNH_4$ (SO_4).$12H_2O$] as indicator. A red color due to the formation of $Fe(SCN)_3$ indicated that an excess of SCN was present and that the end-point was reached.

2.5.9 Estimation of acid capacity

The acid capacity was determined by acid-base titration method. Typically, 200 mg of the sample was suspended in 30 mL of 0.1 M NaOH solution and stirred at room temperature for 24 h. The filtrate was titrated with HCl solution (0.1 M).

References

[1]   A. Herrmann, B. Cornils, *Applied Homogeneous Catalysis with Organometallic Compounds*, Wiley, Weinheim, 1996. (b) D. Astruc, *Organometallic Chemistry and Catalysis*, Springer, Berlin, 2007.

[2]   D. Wang, C. Deraedt, J. Ruiz, D. Astruc, *Acc. Chem. Res*., 2015, **48**, 1871.

[3]   N. End, K. U. Schoning, *in Top. Curr. Chem.,* A. Kirschning, Springer Berlin / Heidelberg, 2004, 241.

[4]   S. Bertelsen, K. A. Jorgensen, *Chem. Soc. Rev.,* 2009, **38**, 2178.

[5]   G. Bredig, P. S. Fiske, *Biochem. Z.,* 1913, **46**, 7.

[6]   H. Pracejus, *Liebigs Ann. Chem.,* 1960, **634**, 9.

[7]   (a) A. Dahan, M. Portnoy, *J. Polym. Sci., Part A: Polym., Chem.,* 2005, **43**, 235. (b) A. Mansour, T. Kehat, M. Portnoy, *Org. Biomol. Chem.,* 2008, **6**, 3382. (c) T. Kehat, M. Portnoy, *Chem. Commun.,* 2007, **46**, 2823. (d) R. Breinbauer, E. N. Jacobsen, *Angew. Chem. Int. Ed.,* 2000, **39**, 3604.

[8]   M. B. Smith, J. March, *March's Advanced Organic Chemistry: Reactions, Mechanisms, and Structure*, John Wiley and Sons, New York, **2000**.

[9]   K. Wilson, J. H. Clark, *Pure Appl. Chem*., 2000, **72,** 1313.

[10]   X. L. Fang, Z. H. Liu, M. F. Hsieh, M. Chen, P. X. Liu, C. Chen, N. F. Zheng, *ACS Nano.*, 2012, **6**, 4434.

[11]   Z. Ma, S. Dai, *ACS Catal.,* 2011, **1**, 805.

[12]   Z. K. Sun, B. Sun, M. H. Qiao, J. Wei, Q. Yue, C. Wang, Y. H. Deng, S. Kaliaguine, D. Y. Zhao, *J. Am. Chem. Soc.,* 2012, **134**, 17653.

[13]   G. Lu, S. Z. Li, Z. Guo, O. K. Farha, B. G. Hauser, X. Y. Qi, Y. Wang, X. Wang, S. Y. Han, X. G. Liu, J. S. DuChene, H. Zhang, Q. C. Zhang, X. D. Chen, J. Ma, S. C. J. Loo, W. D. Wei, Y. H. Yang, J. T. Hupp, F. W. Huo*, Nat. Chem.,* 2012, **4**, 310.

[14]   Q. L. Zhu, J. Li, Q. Xu, *J. Am. Chem. Soc.,* 2013, **135**, 10210.

[15]   U. Diaz, D. Brunel, A. Corma, *Chem. Soc. Rev.,* 2013, **42**, 4083.

[16] W. Li, Q. Yue, Y. H. Deng, D. Y. Zhao, *Adv. Mater*., 2013, **25**, 5129.

[17] A. B. Descalzo, R. Martıinez-Manez, F. Sancenon, K. Hoffmann, K. Rurack, *Angew. Chem. Int. Ed.*, 2006, **45**, 5924.

[18] Y. J. Yu, J. L. Xing, J. L, Pang, S. H. Jiang, K. F. Lam, T. Q. Yang, Q. S. Xue, K. Zhang, P. Wu, *ACS Appl. Mater. Interfaces,* 2014, **6**, 22655.

[19] F. L. James, W. H. Bryan, *J. Org. Chem*., 1958, **23**, 1225.

[20] (a) M. H. Lim, C. F. Blanford, A. Stein, *Chem. Mater.,* 1998*,* **10**, 467. (b) Q. H. Yang, J. Liu, J. Yang, M. P. Kapoor, S. Inagaki, C. Li, *J. Catal*., 2004, **228**, 265. (c) W. M. Van Rhjin, D. E. De Vos, B. F. Sels, W. D. Bossaert, P. A. Jacobs, *Chem. Commun*., 1998, 317. (d) X. D. Yuan, H. I. Lee, J. W. Kim, J. E. Yie, J. M. Kim, *Chem. Lett.*, 2003, **32**, 650.

[21] W. T. Ford, R. D. Badley, *J. Org. Chem.,* 1989, **54**, 5437.

[22] V. Dufaud, M. E. Davis, *J. Am. Chem. Soc*., 2003, **125**, 9403

[23] W. Van Rhijn, D. De Vos, W. Bossaert, J. Bullen, B. Wouters, P. Grobet, P. Jacobs, *Stud. Surf. Sci. Catal*., 1998, **117**, 183.

[24] W. M. Van Rhijn, D. E. De Vos, B. F. Sels, W. D. Bossaert, P. A. Jacobs, *Chem. Commun.,* 1998, 317.

[25] S. L. Bafna, V. M. Bhale, *J. Phys. Chem*., 1959, **63**, 1971.

[26] A. Corm, H. Garcìa, *Adv. Synth. Catal*., 2006, **348**, 1391.

[27] K. Shimizu, E. Hayashi, Y. Hatamachi, T. Kodama, Y. Kitayama, *Tetrahedron Lett.,* 2004*,* **45**, 5135.

[28] B. Das, K. Venkateswarlu, H. Holla, M. Krishnaiah, *J. Mol. Catal. A: Chem.,* 2006, **253,** 107.

[29] R. Gupta, S. Paul A. Loupy, *J. Mol. Catal. A: Chem.,* 2006*,* **266**, 50.

[30] B. Das, K. Suneel, K. Venkateswarlu, B. Ravikanth, *Chem. Pharm. Bull.,* 2008*,* **56**, 366.

[31] B. Das, B. S. Kanth, K. R. Reddy, A. S. Kumar, *J. Heterocycl Chem.,* 2008*,* **45**, 1499.

[32] B. Das, K. Venkateswarlu, M. Krishnaiah, H. Holla, *Tetrahedron Lett.,* 2006*,* **47**, 8693.

[33] B. Karimi, M. Khalkhali, *J. Mol. Catal. A: Chem.,* 2007*,* **271**, 75.

[34] M. H. Lim, C. F. Blanford, A. Stein, *Chem. Mater.*, 1998, **10**, 467.

[35] D. Margolese, J. A. Melero, S. C. Christiansen, B. F. Chmelka, G. D. Stucky, *Chem. Mater.,* 2000, **12**, 2448.

[36] X. D. Yuan, H. I. Lee, J. W. Kim, J. E. Yie, J. M. Kim*, Chem. Lett.*, 2003, **32**, 650.

[37] W. D. Bossaert, D. E. De Vos, W. M. Van Rhijn, J. Bullen, P. J. Grobet, P. A. Jacobs, *J. Catal.*, 1999*,* **182**, 156.

[38] J. Yang, Q. Yang, G. Wang, Z. Feng, J. Liu, *J. Mol. Catal. A: Chem.,* 2006, **256**, 122.

[39] G. C. Arash, P. Zamani, *Chin. Chem. Lett.*, 2013, **24**, 804.

[40] M. Akbar, B. Movassagh, B. Karimi, *In Proceedings of the 17th Int. Electron. Conf. Synth. Org. Chem.*, 2013, **17**.

[41] M. A. Zolfigol, A. Khazaeia*,* A. Zareb, M. Mokhlesia, T. H. Zadehb, A. H. F. Derakhshan-Panaha, A. R. M. Hassan Keypoura, A. A. Dehghani-Firouzabadid, M. Merajoddinb, *J. Chem. Sci.,* 2012, **124**, 501.

[42] V. Polshettiwar, B. Baruwati, R. S. Varma, *Chem Commun*., 2009, 1837.

[43] V. Polshettiwar, R. S. Varma, *Tetrahedron,* 2010, **66**, 1091.

[44] R. S. Varma, *Green Chem*., 2014, **16**, 2027.

[45] D. Zhao, J. Feng, Q. Huo, *Science*, 1998, **279,** 548.

[46] (a) R. K. Iler, *The Chemistry of Silica: Solubility, Polymerization, Colloid and Surface Properties, and Biochemistry*, Wiley-Interscience, New York, 1979. (b) A .V. Kiselev, *Surface Chemical Compounds and Their Role in Adsorption Phenomena*, Moscow State University Press, Moscow, 1957.

[47] L. T. Zhura, *Colloids Surf. A: Physicochem. Eng. Aspects,* 2000, **173**, 1.

[48] M. Makowska-Janusik, A. Kassiba, N. Errien, A. Mehdi*, J. Inorg. Organomet. Polym.,* 2010, **20**, 761.

[49] M. Laskowska, L. Laskowski, K. Dzilinski, *Current Topics in Biophysics*, 2012, **35**, 11.

[50] J. Chen, Q. Li, R. Xu, F. Xiao, *Angew. Chem. Int. Edn.*, 1996, **34**, 2694.

[51] W. Liu, J. Liu, X. Yang, K. Wang, Q. Wang, M. Yang, L. Li, X. Jianguo, *Nanotechnology*, 2013, **24**, 415501.

[52] Q. Cai, Z. S. Luo, W. Q. Pang, Y. W. Fan, X. H. Chen, F. Cui, *Chem. Mater.*, 2001, **13**, 258.

[53] B. Rac, A. Molnar, P. Forgoa, M. Mohaib, I. Bertoti, *J. Mol. Catal. A: Chem.,* 2006, **244**, 46.

[54] N. B. Colthup, L. H. Daly, S. E. Wiberly, *Introduction to Infrared and Raman Spectroscopy*, Academic Press, New York, 1964.

[55] K. Wilson, A. F. Lee, D. J. Macquarrie, J. H. Clark, *Appl. Catal. A: Gen.*, 2002, **228**, 127.

[56] M. Ristova, L. Pejov, M. Zugic, B. Soptrajanov, *J. Mol. Struct.,* 1999, **482**, 647.

[57] M. Chidambaram, C. Venkatesan, A. P. Singh, *Appl. Catal. A Gen.*, 2006, **310**, 79.

[58] S. Shylesh, P. Samuel, Srilakshmi, R. Parischa, A. P. Singh, *J. Mol. Catal. A: Chem.,* 2007, **274**, 153.

[59] B. Yan, A. W. Czarnik, *Optimization of Solid-Phase Combinatorial Synthesis*, Marcel Dekker: New York, 2002.

.....ೞ೧ೱ.....

SULFONIC ACID FUNCTIONALIZED MESOPOROUS SILICA: EFFECTIVE ORGANO ACIDIC CATALYST FOR BIGINELLI REACTION AND TRISUBSTITUTED IMIDAZOLE SYNTHESIS UNDER SOLVENT FREE CONDITION

A simple, highly efficient and ecofrendily approach for the preparation of dihydropyrimidinones via Biginelli reaction and trisubstituted imidazole synthesis is discussed in this chapter. Sulfonic acid functionalized dendrimers on mesoporous silica (SA1-3) were effectively used as organo acidic catalysts for the synthesis of these two compounds. SA3 showed high catalytic activity towards both reactions due to the high amount of sulfonic acid groups on the surface of mesoporous silica. The main advantages of this catalyst for these reactions are: cleaner reaction profile, high reaction rates and excellent yields, simple experimental and work-up procedures, no side reaction, solvent free condition, recyclable and environmentally benign nature of the catalyst and use of metal free catalyst.

3.1 Introduction

In recent years, the use of solid-supported catalysts has gained considerable attention both in industrial and academic research due to their unique properties such as enhanced reactivity as well as selectivity, efficiency, straightforward work-up, and the eco-friendly reaction conditions.[1] Solid acids based on micelle template silica and other mesoporous high surface area support materials have started to play a significant role in fine chemical synthesis processes. A wide range of important organic reactions can be efficiently catalyzed by these materials. The catalyst can be designed to provide different types of acidity as well as high degrees of reaction selectivity. Main advantages of solid acids are the high turnover numbers and their easy separation from the organic components.[2, 3] One useful example of silica supported catalyst is silica-functionalized sulfonic acid in which the reactive centres are highly mobile similar to that of homogeneous catalysts.[4-9] This has been used as an efficient acidic catalyst for some organic transformations such as acetalization of carbonyl compounds,[10] thioacetalization of carbonyl compounds,[11] synthesis of benzimidazoles,[12] preparation of 3,4-dihydropyryimidinones,[13] synthesis of 1,4-dihydropyridines,[14] bromination of carbonyl compounds,[15] and bromination of phenols, alkoxyarenes and anilines.[16]

However, all reported works include single functionalization with sulfonic acid on mesoporous silica. But studies revealed that no reports were found in the case of sulfonic acid terminated supported or non-supported dendrimers as organo catalyst for organic transformations. The synthesis of sulfonic acid terminated dendrimers on mesoporous silica and their use as catalyst for multicomponent reactions is reported.

3.1.1 Multicomponent reactions

Multicomponent reactions have drawn great interest enjoying an outstanding status in modern organic synthesis and medicinal chemistry, because, they are one pot processes bringing together three or more components and show high atom economy and high selectivity.[17] They have great involvement in convergent synthesis of complex and important organic molecules from simple and readily available starting materials, and have emerged as a powerful device for drug discovery.[18] Speed, diversity, efficiency, and environmental amiability are some of the key features of this class of reactions.[19-24] In this chapter, a detailed study of two multicomponent reactions, Biginelli reaction and trisubstituted imidazole synthesis is presented.

3.1.2 Biginelli reaction

Dihydropyrimidinones (DHMPs) and their derivatives constitute one important class of compounds which exhibit pharmacological activities such as calcium channel blockers, anti-inflammatory, antitumor, α-adreno receptor antagonist, antihypertensive agents, antibacterial, antioxidative, anti-HIV and antiviral activity.[25, 26] Biologically active dihydropyrimidinone derivatives such as Monastrol (**A**), (R)-SQ 32926 (**B**) and (+)-SNAP-7941(**C**) are lead compounds possessing outstanding antitumor, antihypertensive and melanin-concentrating hormone receptor antagonism activities, respectively (Figure 3.1).[27]
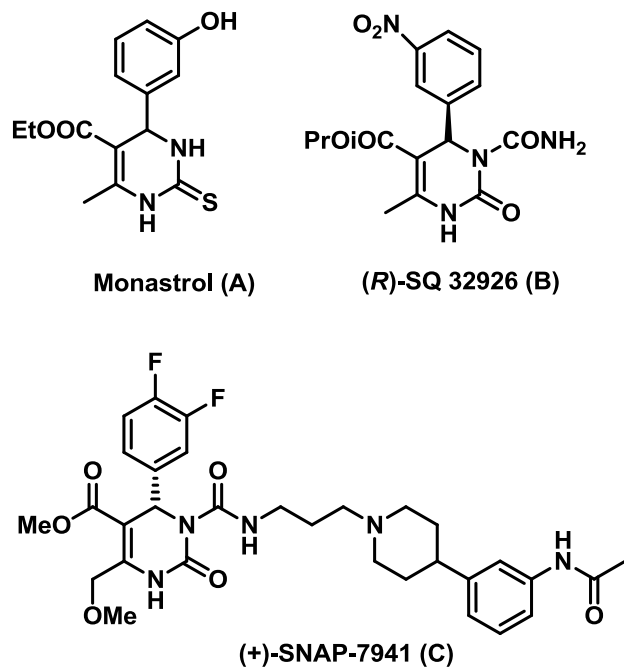
Figure 3.1 Structure of biologically active dihydropyrimidinone
derivatives

In 1893, Biginelli first introduced these biologically potent
DHPMs.[28] He apparently did this reaction in a multicomponent way, by the
cyclocondensation of aldehyde, ethyl acetoacetate and urea in the presence
of HCl under reflux condition in the presence of ethanol. But, only very low
yield of 20-60 % was obtained and nearly 24-36 h was needed for the
completion of the reaction (Scheme 3.1).
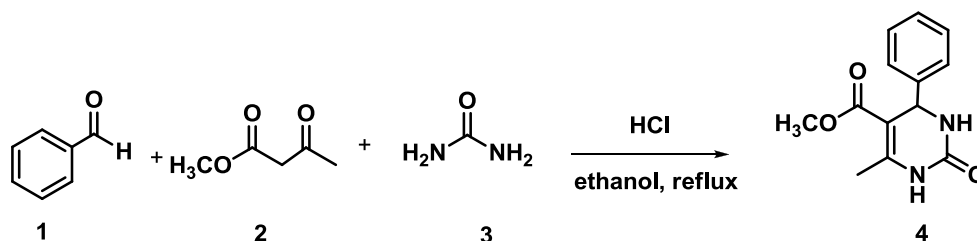
Scheme 3.1 Classical synthesis of Biginelli product

Recently, several types of homogeneous[29] and heterogeneous[30] catalysts were introduced by scientists. Lewis acids such as $SbCl_3$,[31] CaF_2,[32] Fe_3O_4/ SMPA,[33] $Cu(OTf)_2$,[34] ZnI_2 and $ZrCl_4/ZrOCl_2$[35] are commonly used catalysts for the Biginelli reaction. Many ionic liquids ($[Et_3NSO_3H]HSO_4$,[36] $[Hmim]HSO_4$,[37] $[cmmim][BF_4]$,[38] etc and sulfonic acid functionalized Brønsted acidic ionic liquids,[39] metal-organic complexes,[40, 41] and bismuth salts[42] were used as catalysts and high yields of DHPMs were obtained. However, most of these methods required use of toxic solvents, high temperature, expensive or highly acidic catalysts. They were also impaired by the requirement of a large amount of catalyst, difficulty in recycling the catalyst and prolonged reaction times, side reactions, difficulty to separate the products etc. Hence, the development of gentle methods using catalysts derived from renewable resources for the synthesis of DHPMs still remain a great challenge for organic chemists. In recent years, microwave irradiation,[43] ultrasound,[44] ionic liquids,[45] solvent-less protocols, and supported reagents[46] have appeared to be effective techniques. However, they faced the problems of use of toxic and expensive transition metals, sealed reaction vessels and difficulty in reusing the catalysts. Thus, development of new, efficient, simple and convenient protocols that lead to substituted DHPMs in high purity is of considerable interest.

Very recently, silica-modified magnetite-polyoxometalates functionalized with sulfamic acid groups were synthesized by Azarifar and coworkers (Scheme 3.2).[47] This heterogeneous nano catalyst was explored to present high catalytic performance for the synthesis of 3,4-dihydropyrimidinones under mild reaction conditions. With this catalyst, 85 % yield was obtained for the reaction between benzaldehyde, ethyl acetoacetate and urea within

30 min at 100 °C. They reported that this catalyst could be easily separated by an external magnet. Recyclability and high stability of the catalyst combined with low reaction times and excellent yields make the reported protocol very useful and attractive for the synthesis of 3,4-dihydropyrimidinones.
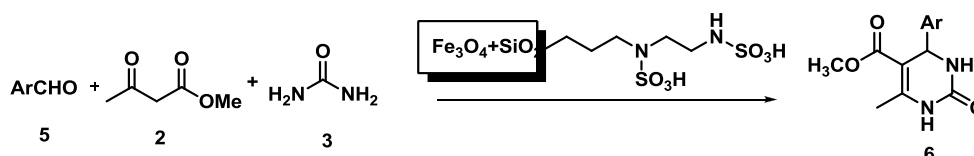
Scheme 3.2 Synthesis of dihydropyrimidinones using silica- magnetite-polyoxometalates with sulfamic acid

Tabrizian, *et al.*[48] effectively evaluated amine-functionalized titania for the synthesis of 3,4-dihydopyrimidin-2(1*H*)-ones through a one-pot three component condensation reaction of various aldehydes, β-dicarbonyl compounds and urea (or thiourea) at 100 °C under solvent-free condition with good to excellent yields (Scheme 3.3). The catalyst can be recovered easily by simple filtration and reused for eight consecutive runs without significant decrease of its catalytic efficiency.
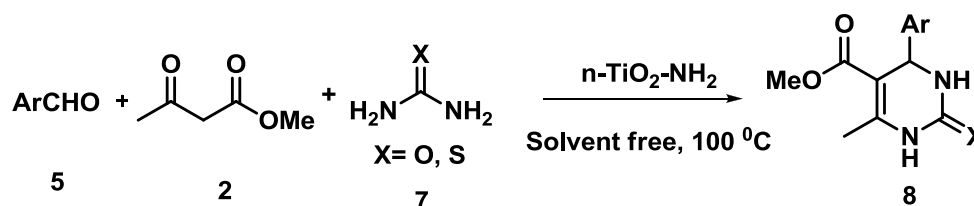
Scheme 3.3 Synthesis of dihydropyrimidinones using n-TiO$_2$-NH$_2$

Similarly, Hosseini, *et al.*[49] introduced zirconia sulfuric acid (ZrSA) as a highly powerful heterogeneous solid acid catalyst for the one-pot synthesis of 3,4-dihydropyrimidin-2(1*H*)-ones under solvent-free conditions (Scheme 3.4).

They found that 15 mol % of ZrSA gave 99 % yield for benzaldehyde, methyl acetoacetate and urea under solvent free condition at 90 °C. They reported high catalytic activity, short reaction time, mild reaction conditions, excellent yields, reusable nature and simple work-up as the advantages of the catalyst.

Scheme 3.4 Synthesis of dihydropyrimidinones using ZrSA
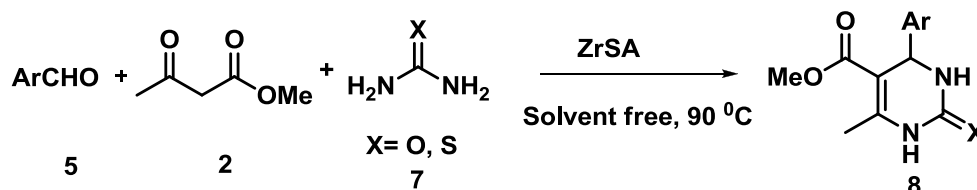
3.1.3 Trisubstituted imidazole synthesis

Imidazole is a planar 5-membered ring and is amphoteric: it can have the role of both an acid and as a base. The acidic proton is located on N-1. The basic site is N-3, protonation gives the imidazolium cation, which is symmetrical. The compound is classified as aromatic due to the presence of a sextet of π-electrons, consisting of a pair of electrons from N-1 and one from each of the remaining four atoms of the ring.[50] Imidazole nucleus is a fertile source of biologically important molecules. Compounds containing the imidazole group have many pharmacological properties and are important in biochemical processes. They are well known as inhibitors of P38MAP kinase, and act as fungicides, herbicides, anti-inflammatory agents, antithrombotic agents, plant-growth regulators, and therapeutic agents. They are also used in photography as photosensitive compounds. Some substituted triarylimidazoles are selective antagonists of the glucagon receptor and inhibitors of IL-1 biosynthesis.[51]

Trisubstituted imidazole derivatives are well known to be proton pump inhibitory, antiinflammatory, antiparasitic, fungicidal, plant-growth regulators, and therapeutic agents.[52-56] Owing to the wide series of pharmacological and biological applications, synthesis of imidazoles has become an important goal in recent years. In 1882, Radziszewski[57] and Robinson[58] reported the first synthesis of highly substituted imidazoles from 1,2-dicarbonyl compound, different aldehydes, and ammonia (Scheme 3.5).
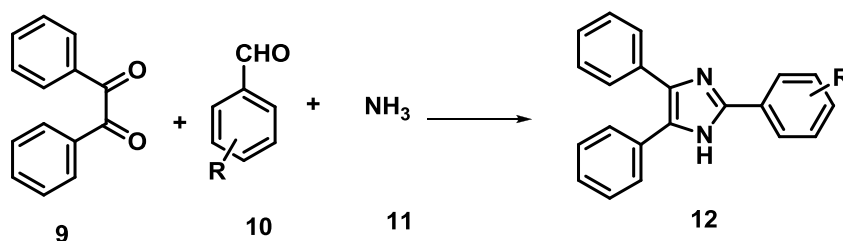
Scheme 3.5 Conventional synthesis of trisubstituted imidazole

The conventional imidazole synthesis is more difficult, produces poor yield, and requires corrosive reagents. In the last decade, numerous methods have been developed for the synthesis of trisubstituted imidazoles using various catalytic systems including ionic liquids,[59-64] metal salts,[65-68] inorganic or organic matrices-supported catalysts,[69-77] N-halo reagents etc.[78-83] Recently, ChCl.2ZnCl$_2$,[84] Choline chloride and oxalic acid,[85] Kieselguhr supported [Fe(NO$_3$)$_3$],[86] dimethylurea/citric acid,[87] nano aluminium nitride,[8] and Wang-OSO$_3$H[89] under microwave or ultrasonic irradiation, solvent-free or classical conditions were used for the synthesis of imidazole derivatives.

Most of these methods are associated with limitations such as heating at high temperature (180-200 °C), longer reaction time (8-24 h), use of toxic solvents, corrosive reagents and the necessity of neutralization of the strong

acid media.[90] Thus, to overcome these drawbacks, highly efficient and flexible protocols for the synthesis of 2,4,5-trisubstituted imidazoles are still required, as there is scope for further improvements towards mild reaction conditions, development of simple work-ups, cheap reagents, convenient procedures and higher yields of products.

Very recently, Naeimi and coworkers[91] successfully synthesized the ionophore silica coated magnetite nanoparticles (Figure 3.2) and effectively used them as a recyclable heterogeneous catalyst for the one-pot synthesis of 2,4,5-trisubstituted imidazoles.
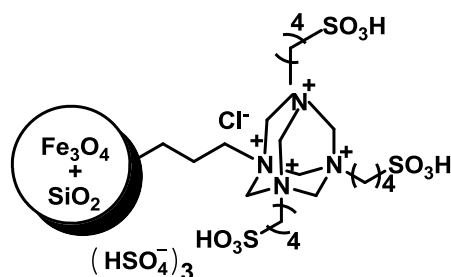
Figure 3.2 Structure of $Fe_3O_4@SiO_2 \cdot HM \cdot SO_3H$

The catalyst was recovered using external magnet and used for six runs without loss of its activity. In this synthesis, only 1 mmol loading of ionic liquid on 1 g of $Fe_3O_4@SiO_2$ was sufficient to achieve high catalytic activity.

An efficient and reusable nano catalyst, $Cu/GA/Fe_3O_4@SiO_2$, was described by Shaabani and coworkers.[92] They evaluated its catalytic application in the synthesis of imidazole derivatives in ethanol and under solvent-free conditions. The results show that the nano catalyst is effective, recoverable and stable under the reaction conditions (Scheme 3.6).
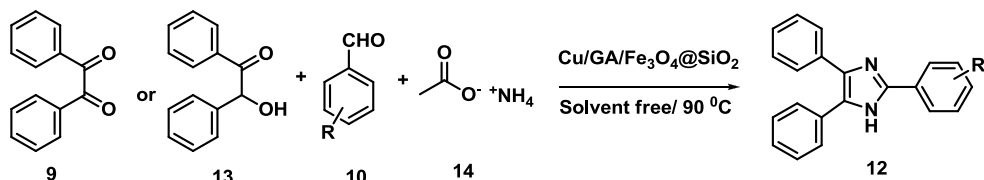
Scheme 3.6 Synthesis of trisubstituted imidazole using Cu/GA/Fe$_3$O$_4$@SiO$_2$

Tungstophosphoric acid supported on core-shell polystyrene-silica microspheres was synthesized and characterized by Gorsd, *et al.*[93] The acidic characteristics of the solids were evaluated by potentiometric titration, showing that they exhibited strong acid sites. Due to its acidic nature, it was used as catalyst for the synthesis of trisubstituted imidazole. High yield was obtained in the solvent-free synthesis of 2,4,5-triphenyl-1*H*-imidazole and other eight trisubstituted imidazoles, without formation of by-products resulting from competitive reactions or decomposition products.

An extremely efficient method has been developed by Esmaeilpour, *et al.*[94] for the synthesis of biologically active three and tetrasubstituted imidazoles via condensation of benzil with various aromatic aldehydes, a primary amine and ammonium acetate using Fe$_3$O$_4$@SiO$_2$-imid-PMAn as a recyclable nano catalyst under solvent-free conditions and microwave irradiation. The main advantages of this method are cleaner reaction profiles, high reaction rates and excellent yields, simple experimental and work-up procedures and no side reactions (Scheme 3.7).
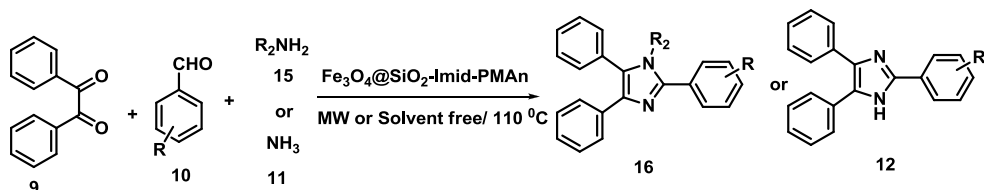
Scheme 3.7 Synthesis of trisubstituted imidazole using Fe$_3$O$_4$@SiO$_2$-imid-PMAn

3.2 Objective of the present work

Overview of relevant literature revealed that not many reports are available on the use of dendritic catalysts for multicomponent reactions especially for Biginelli reaction and trisubstituted imidazole synthesis. Similarly, no reports are available on the use of sulfonic acid terminated dendritic structures as homogeneous and heterogeneous catalyst. Here, the synthesis of sulfonic acid functionalized dendritic moiety on mesoporous silica surface by step wise growth technique is reported. Due to the presence of large amount of sulfonic acid functionality, it can be effectively used as heterogeneous organo catalyst for functional group transformations. In this chapter, the catalytic activity of sulfonic acid groups on mesoporous silica has been explored as heterogeneous organo catalyst for Biginelli reaction and for the synthesis of trisubstituted imidazoles.

3.3 Results and discussion

3.3.1 Synthesis of sulfonic acid terminated dendrimers on mesoporous silica

The synthetic procedure and detailed characterization of sulfonic acid terminated dendrimers on mesoporous silica were described in Chapter 2 and the structure of **SA1**, **SA2** and **SA3** are shown in Figure 3.3. The acid group capacity of **SA1**, **SA2** and **SA3** were found to be 3.8, 6.8 and 10.2 mmol per gram respectively. The characterization techniques like BET surface area analysis, IR spectra, TG-DTG analysis, Raman spectra, low angle XRD, SEM analysis and solid state ^{13}C NMR spectrum strongly confirmed the growth of dendrimers on mesoporous silica.
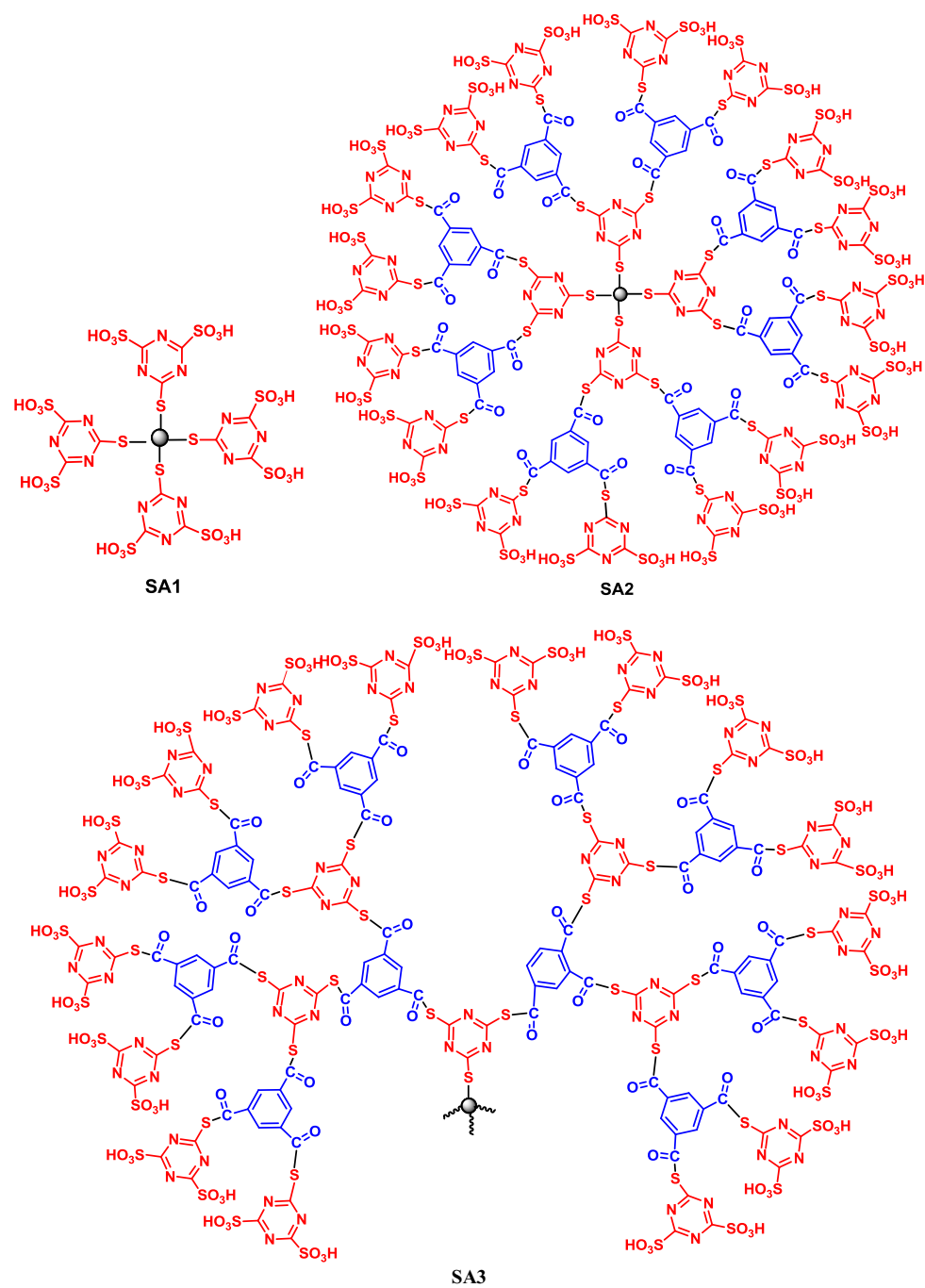
Figure 3.3 Structure of **SA1**, **SA2** and **SA3**

3.3.2 Catalytic performance
3.3.2.1 Biginelli reaction
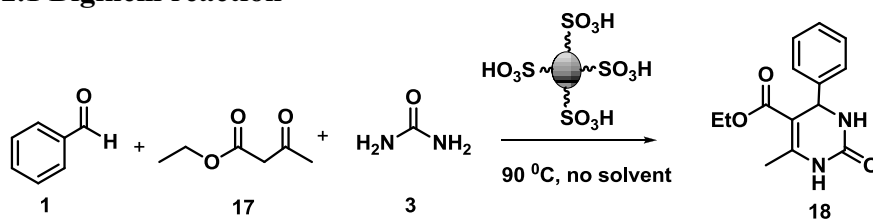
Scheme 3.8 Synthesis of dihydropyrimidinones

The Biginelli condensation of benzaldehyde, ethyl acetoacetate (EAA) and urea was investigated without any catalyst (Table 3.1, entry 1). But no product was obtained. This means that a catalyst was necessary for this reaction. So the reaction between benzaldehyde, ethyl acetoacetate and urea was repeated in the presence of 3.06 mol % of **SA3** under solvent free condition at 90 °C (Scheme 3.8 and Table 3.1, entry 4). After 2 h, dihydropyrimidinone was obtained in 84 % yield. This result indicated that the present catalyst was active towards this reaction. The reaction conditions such as catalyst generation, amount of catalyst, different solvents and temperature were optimized. The effect of different generations of the catalyst (**SA1**, **SA2** and **SA3**) was examined. It was found that the yield of the desired product 3,4-dihydropyrimidin-2-one increased with the generation of the catalyst employed. Among the three catalysts, highest yield was obtained with third generation catalyst **SA3** (Table 3.1, entry 4).

Table 3.1 Effect of different generation of catalysts

Entry	Catalysts	Yield (%)[a, b]
1	No Catalyst	-
2	**SA1**	70
3	**SA2**	81
4	**SA3**	84

[a]benzaldehyde (1 mmol), EAA (1 mmol), urea (1mmol), catalyst (0.003 g), 90 °C, no solvent, 2 h, [b]isolated yield.

In order to evaluate the appropriate catalyst loading, the model reaction was performed using 2.04 to 6.12 mol % of **SA3** at 90 °C without solvent (Table 3.2). It was found that 5.10 mol % of the catalyst afforded the maximum yield in 2 h. Higher percentages of the catalyst loading (6.12 mol %) showed no substantial improvement in the yields.

Table 3.2 Optimization of the amount of catalyst

Amount of catalyst SA3 (g)	Amount of catalyst SA3 (mol %)	Yield (%)[a, b]
0.002	2.04	80
0.003	3.06	84
0.004	4.08	90
0.005	**5.10**	**95**
0.006	**6.12**	**95**

[a]benzaldehyde (1 mmol), EAA (1 mmol), urea (1 mmol), 90 °C, no solvent, 2 h, [b]isolated yield.

Various solvents such as methanol, tetrahydrofuran, toluene, dichloromethane, acetonitrile, water and solvent free condition were screened for Biginelli reaction at 50 °C. It was found that solvent free condition was the most effective for the generation of the desired product (Table 3.3).

Table 3.3 Optimization of solvent on the reaction

Entry	Solvent	Yield (%)[a, b]
1	Methanol	70
2	Tetrahydrofuran	52
3	Toluene	58
4	Dichloromethane	72
5	Acetonitrile	61
6	Water	65
7	**No solvent**	**79**

[a]benzaldehyde (1 mmol), EAA (1 mmol), urea (1 mmol), SA3 (5.10 mol %), 50 °C, 2 h, [b]isolated yield.

Next, the effect of temperature was evaluated for the model reaction. It was observed that the reaction did not proceed at room temperature. By elevating the reaction temperature from 50 °C to 90 °C, the yield of desired product increased considerably. Same yield was obtained for both 90 °C and 110 °C reactions (Table 3.4). So, 90 °C was selected as optimal reaction temperature.

Table 3.4 Effect of temperature on the reaction
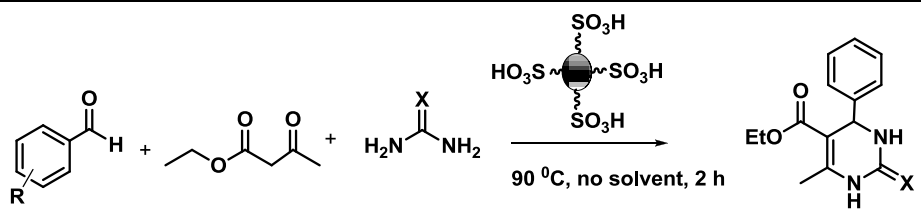
Entry	Temperature, °C	Yield (%)[a, b]
1	Room temperature	-
2	50	79
3	70	84
4	**90**	**95**
5	**110**	**95**

[a]benzaldehyde (1 mmol), EAA (1 mmol), urea (1 mmol), SA3 (5.10 mol %), no solvent, 2 h, [b]isolated yield.

With the optimized reaction conditions in hand, the generality of the procedure for the Biginelli reaction was investigated with various aldehydes and urea/thiourea and a set of substituted DHPMs were obtained in high to excellent yields at appropriate times under solvent-free condition (Table 3.5). Aromatic aldehydes bearing both electron-donating and electron withdrawing groups readily underwent the transformation, giving good yields of corresponding Biginelli compounds. Meta and para derivatives of nitrobenzaldehyde and para derivative of bromobenzaldehyde and chlorobenzaldehyde successfully produced the desired products in excellent yields indicating that the position of the substituents had no significant effect on the yield.

Since thiopyrimidinones are important pharmacophores with regard to biological activity, synthesis of 3,4- dihydropyrimidin-2-(1*H*)-thiones using thiourea instead of urea was also tried (Table 3.5 Entries 10, 11). Result showed that the above mentioned optimized conditions were successful for the synthesis of the 3,4-dihydropyrimidin-2-(1*H*)-thiones in good yield. The structure of all synthesized products are given in the Table 3.6.

Table 3.5 Biginelli reaction with different substrates

Entry	R	X	Product	Yield (%)[a, b]
1	H	O	**3a**	95
2	4-nitro	O	**3b**	89
3	3-nitro	O	**3c**	90
4	4-bromo	O	**3d**	91
5	4-methyl	O	**3e**	89
6	4-chloro	O	**3f**	84
7	4-hydroxy	O	**3g**	86
8	4-N-(CH$_3$)$_2$	O	**3h**	85
9	4-methoxy	O	**3i**	94
10	H	S	**3j**	91
11	4-methoxy	S	**3k**	85

[a]aldehyde (1 mmol), EAA (1 mmol), urea/thiourea (1 mmol), SA3 (5.10 mol %), 90 °C, no solvent, 2 h, [b]isolated yield.

Table 3.6 Structure of synthesized Biginelli products

(3a) (3b) (3c) (3d)

(3e) (3f) (3g) (3h)

(3i) (3j) (3k)
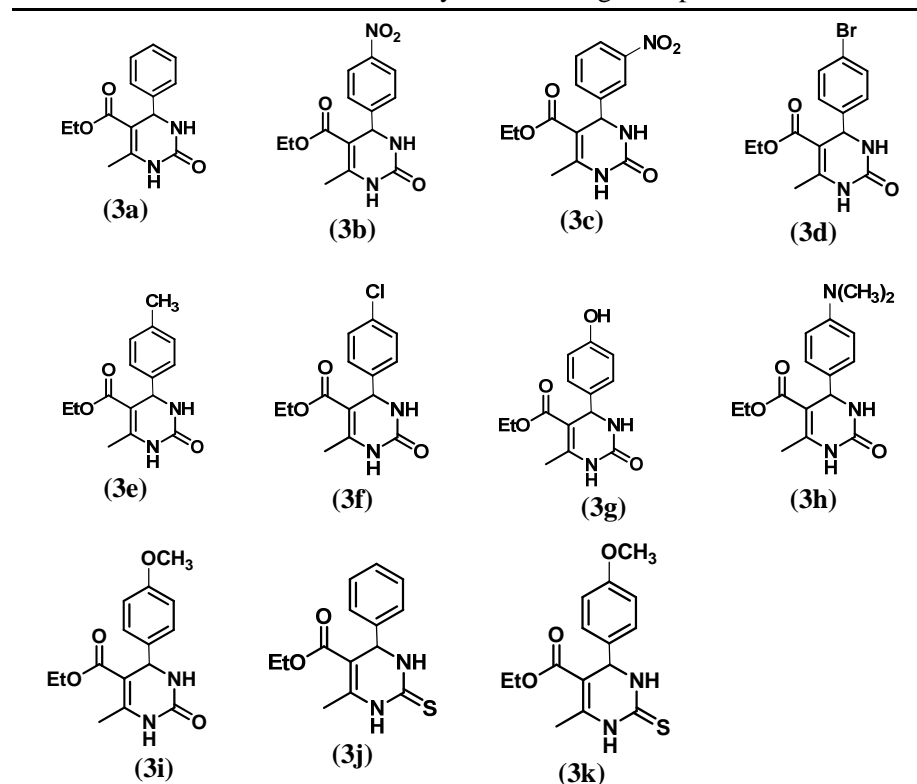
3.3.2.1.2 Proposed mechanism for Biginelli reaction

Proposed mechanism showed that the aldehyde and ethyl acetoacetate undergo aldol condensation to form intermediate **19** followed by the elimination of water molecule to form the intermediate 21. The nucleophilic addition of NH_2 of urea /thiourea to intermediate 21 followed by cyclization-dehydration to form 3,4- dihydropyrimidin-2(1*H*)-ones **18** (Scheme 3.9).[94b]
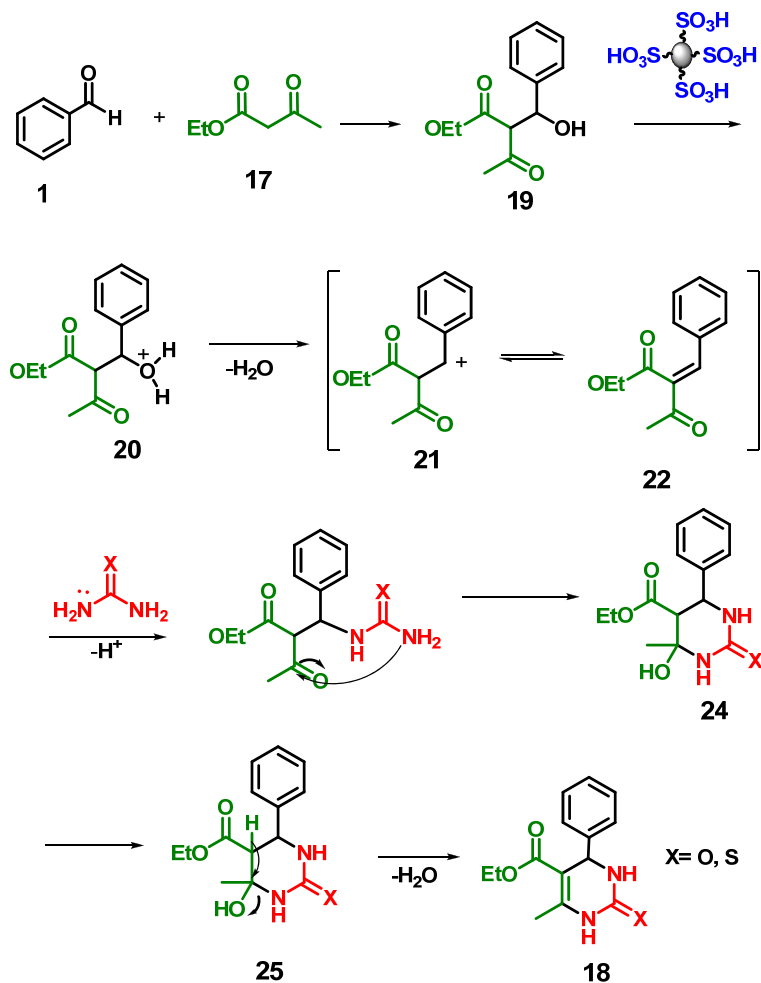
Scheme 3.9 Proposed mechanism for the formation of dihydropyrimidinones

3.3.2.2 Trisubstituted imidazole synthesis

After the success of sulfonic acid terminated mesoporous silica in the preparation of 3, 4-dihydropyrimidin-2-(1*H*)-ones, it was decided to explore the catalytic activity of sulfonic acid terminated mesoporous silica in the preparation of trisubstituted imadazole derivatives. Generally, the synthetic

procedure involves stirring the mixture of aldehyde, benzil, ammonium acetate and catalyst for 2 h at 70 °C (Scheme 3.10). The investigation was initiated with the reaction of benzaldehyde (1 mmol), benzil (1 mmol) and ammonium acetate (2 mmol) in the presence of 3.06 mol % of **SA3** under solvent free condition. Progress of the reaction was monitored by TLC. After the completion of the reaction, hot ethanol was added and the catalyst was removed by filtration. The filtrate was dried to give the crude product. For further purification, it was recrystallized from ethanol to afford the pure product. 83 % yield was obtained after 2 h. This means that the present catalyst showed good catalytic activity towards this reaction.
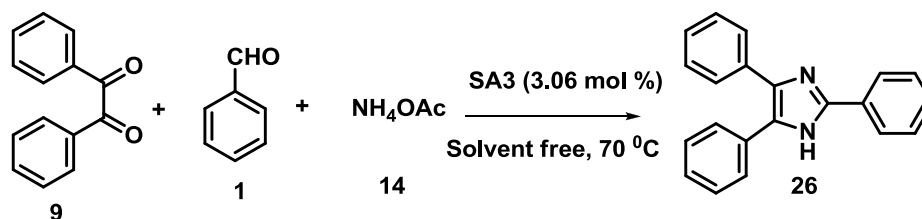
Scheme 3.10 Synthesis of trisubstituted imidazole

To optimize the reaction conditions, the reaction in the absence of any catalyst and also different generations of the catalyst was studied. The reaction did not occur in the absence of any catalyst (Table 3.7, Entry 1). This indicates the necessity of a catalyst for this reaction. On going to higher generations from **SA1** to **SA3**, reaction yield was increased. Data presented in Table 3.7 clearly indicated that **SA3** gave highest yield. This is due to the presence of higher amounts of sulfonic acid groups on **SA3** which make it strong acidic catalyst towards this reaction.

Table 3.7 Effect of different generations of the catalyst

Entry	Catalyst	Yield (%)[a, b]
1	No Catalyst	-
2	**SA1**	54
3	**SA2**	72
4	**SA3**	**83**

[a]benzaldehyde (1 mmol), benzil (1 mmol), ammonium acetate (2 mmol) and catalyst (0.003g), no solvent, 70 °C, 2 h, [b]isolated yield

The amount of catalyst was optimized and found that the yield was affected by the amount of **SA3** used. Yield of the product was low when low amount of catalyst was used. 5.10 mol % of **SA3** was found to be the most effective in stitching all the starting substrates to trisubstituted imidazole with high yields (Table 3.8) and higher amounts such as 6.12 mol % did not boost the yields.

Table 3.8 Effect of amount of catalyst

Amount of catalyst SA3 (g)	Amount of catalyst SA3 (mol %)	Yield (%)[a, b]
0.002	2.04	71
0.003	3.06	83
0.004	4.08	90
0.005	**5.10**	**96**
0.006	**6.12**	**96**

[a]benzaldehyde (1 mmol), benzil (1 mmol), ammonium acetate (2 mmol),70 °C, no solvent, 2 h, [b]isolated yield

To examine the influence of solvent, model reaction between benzil, benzaldehyde and ammonium acetate at 50 °C was performed in various solvents under identical conditions and results are summarized in Table 3.9. It was observed that solvent free condition was best suited for this reaction.

Table 3.9 Optimization of solvent on the reaction

Entry	Solvent	Yield (%)[a, b]
1	Methanol	78
2	THF	53
3	Toluene	50
4	DCM	62
5	Acetonitrile	64
6	Water	60
7	**No solvent**	**82**

[a]benzaldehyde (1 mmol), benzil (1 mmol), ammonium acetate (2 mmol), 50 °C, **SA3** (5.10 mol %), 2 h, [b]isolated yield

In order to check whether the temperature has any role on this reaction, the reaction was done at room temperature. But no product was obtained. When the temperature was increased from room temperature to 70 °C, yield was increased but further increase in temperature showed no change in the percentage conversion (Table 3.10).

Table 3.10 Effect of temperature on the reaction
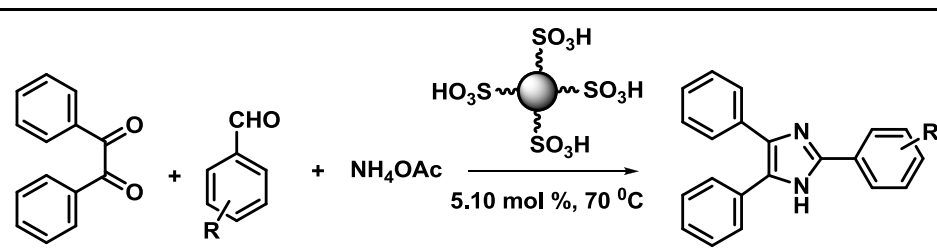
Entry	Temperature, °C	Yield (%)[a, b]
1	Room temperature	-
2	50	82
3	**70**	**96**
4	**90**	**96**

[a]benzaldehyde (1 mmol), benzil (1 mmol), ammonium acetate (2 mmol), no solvent, **SA3** (5.10 mol %), 2 h, [b]isolated yield

To establish the catalytic efficiency, the optimized reaction condition was applied to a number of aldehydes. This is summarized in Table 3.11. It was observed that, the corresponding trisubstituted imidazoles were obtained in all the cases in excellent yields. Results showed that the process tolerated both

electron donating and electron withdrawing substituent on the aldehyde. Table 3.11 clearly confirmed that sulfonic acid functionalized mesoporous silica was an effective catalyst for the synthesis of triarylimidazoles, under mild reaction conditions. The structure of all the products is given in the Table 3.12.

Table 3.11 Synthesis of trisubstituted imidiazole using different substrates

Entry	Aldehyde	Product	Yield (%)[a, b]
1	benzaldehyde	**3a'**	96
2	2-nitrobenzaldehyde	**3b'**	91
3	3-nitrobenzaldehyde	**3c'**	88
4	4-nitrobenzaldehyde	**3d'**	92
5	4-chlorobenzaldehyde	**3e'**	94
6	4-hydroxybenzaldehyde	**3f'**	90
7	4-methoxybenzaldehyde	**3g'**	88
8	3,4-dimethoxybenzaldehyde	**3h'**	92
9	4-methylbenzaldehyde	**3i'**	93
10	4-bromobenzaldehyde	**3j'**	87
11	3-bromobenzaldehyde	**3k'**	84
12	salicylaldehyde	**3l'**	92

[a]benzaldehyde (1 mmol), benzil (1 mmol), ammonium acetate (2 mmol), no solvent, **SA3** (5.10 mol %), 70 °C, 2 h, [b]isolated yield

Table 3.12 Structure of synthesized trisubstituted imidazoles

(3a')	(3b')	(3c')	(3d')
(3e')	(3f')	(3g')	(3h')
(3i')	(3j')	(3k')	(3l')
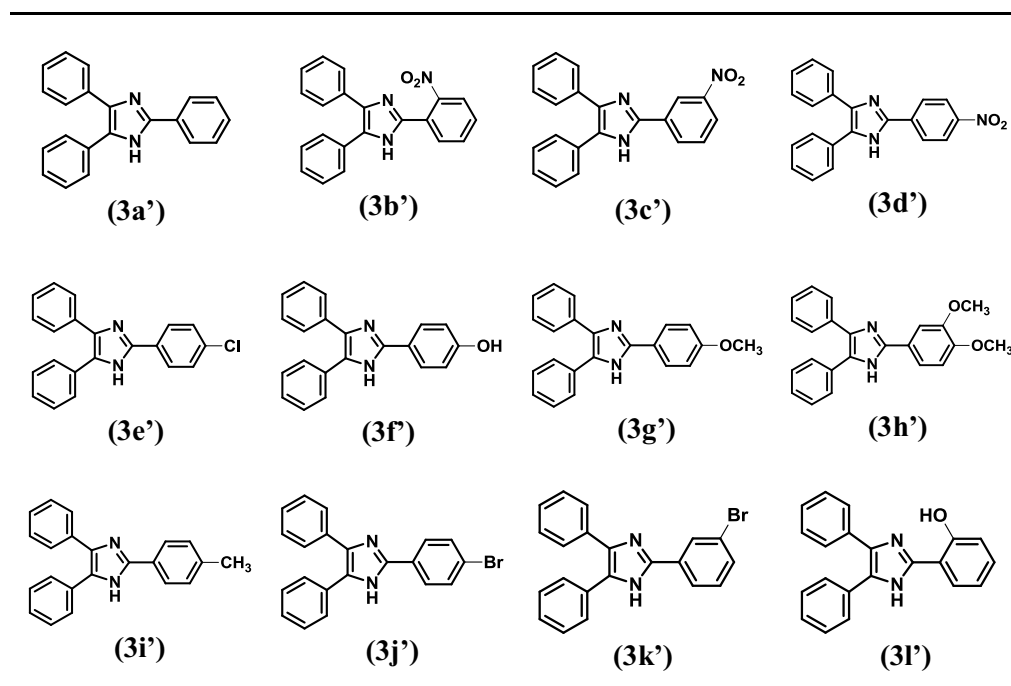
3.3.2.2.1 Mechanism for the formation of trisubstituted imidazoles

Proposed mechanism for the formation of trisubstituted imidazole is shown in Scheme 3.11. Aldehyde was activated in the presence of catalyst to form the intermediate **19**. It undergoes nucleophilic addition of NH_3 formed from the dissociation of ammonium acetate to form the diamine intermediate **30**. This intermediate condenses with benzil to form the intermediate **32** followed by dehydration and rearranges to the trisubstituted imidazoles **26** by a [1,5] hydrogen shift.
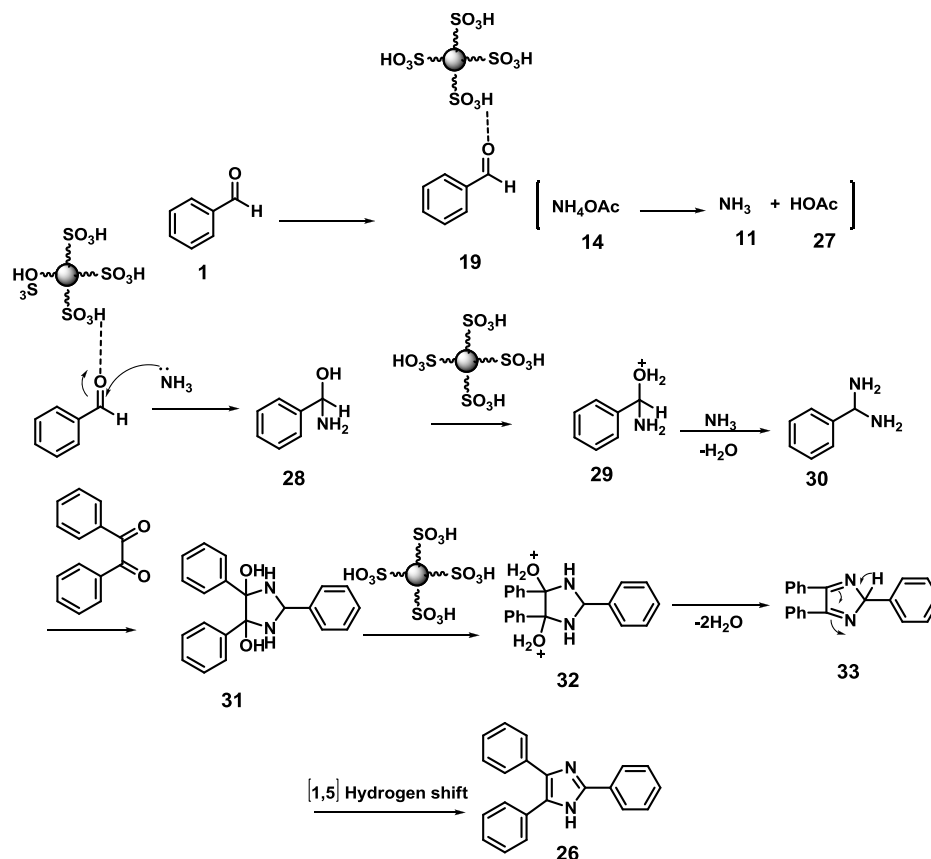
Scheme 3.11 Proposed mechanism for the formation of trisubstituted imidazole

3.3.2.3 Reusability of the catalyst (SA3)

The reusable capacity of **SA3** in the Biginelli reaction and trisubstituted imidazole synthesis was tested using the same procedures. The catalyst was easily recovered from the reaction mixture by using hot ethanol, washed with ethanol, methanol, dichloromethane, water and finally dried at 120 °C for 2 h prior to the next run. During the reusable experiment, with fresh reactants, under the same reaction conditions, no considerable change in the activity of the catalyst was observed for at least 4 consecutive runs which

clearly demonstrated the stability of the catalyst under these conditions in the reactions.

Table 3.13 Reusability studies of the catalyst in Biginelli reaction and in the synthesis of trisubstituted imidazoles

No. of cycles	Biginelli Reaction (Yield %)[a, b]	Trisubstituted imidazoles (Yield %)[c, d]
1	95	96
2	95	94
3	93	92
4	92	90

[a] benzaldehyde (1 mmol), EAA (1 mmol), urea (1 mmol), **SA3** (5.10 mol %), 90 °C, solvent free condition, 2 h, [b] isolated yield, [c] benzaldehyde (1 mmol), benzil (1 mmol), ammonium acetate (2 mmol), **SA3** (5.10 mol %), 70 °C, solvent free condition, 2 h, [d] isolated yield

From the Table 3.13, it clearly showed that sulfonic acid functionalized mesoporous silica (**SA3**) can be used as effective heterogeneous acid catalyst for Biginelli reaction and for the synthesis of trisubstituted imidazoles under solvent free condition up to four cycles.

3.4 Conclusion

Sulfonic acid functionalized dendritic moiety on mesoporous silica was synthesized and characterized by various physicochemical techniques. Catalytic activity was tested for two multicomponent reactions, Biginelli reaction and trisubstituted imidazole synthesis. Three generations of the dendrimers such as **SA1**, **SA2** and **SA3** were found to be very effective catalysts for both reactions. Due to the high amount of sulfonic acid groups on **SA3**, it was found to be an efficient organo catalyst for these reactions. In Biginelli reaction, 5.10 mol % of the catalyst gave 84-95% yield under solvent free condition at 90 °C. In the case of trisubstituted imidazole

synthesis also, **SA3** was the best catalyst. 84-96 % yield was obtained using 5.10 mol % of **SA3** under solvent free condition at 70 °C. The catalyst could be efficiently recycled and reused up to fourth run with negligible loss of efficiency for both the reactions. Main advantages of these reactions using **SA3** as catalysts are: easy work up procedure, no side products, simple purification procedure, solvent free condition, use of metal free catalyst etc. The excellent catalytic performance, thermal stability and separation of the catalyst by simple filtration make it a good heterogeneous system and useful alternative to other heterogeneous catalysts.

3.5   Experimental

3.5.1 Materials

All reagents were purchased from the local chemical suppliers and were used as received. All the solvents were purified according to the standard procedures.

3.5.2 Synthesis of sulfonic acid functionalized dendritic mesoporous silica
Same as given in Chapter 2

3.5.3 General procedure for the Biginelli reaction

A solution of the aldehyde (1 mmol), ethyl acetoacetate (1 mmol), urea (1 mmol), and **SA3** (5.10 mol %) was heated at 90 °C for 2 h in a single-neck flask under solvent free condition. Hot ethanol was added to the reaction mixture and filtered to remove the catalyst for reuse. The filtrate was poured onto crushed ice and stirring was continued for several minutes, and the solid product was filtered. The crude product was purified by recrystallization from ethanol.

3.5.4 General procedure for the synthesis of trisubstituted imidazoles

The mixture of benzil (1 mmol), aldehyde (1 mmol) and NH$_4$OAc (2 mmol) was stirred at 70 °C in the presence of **SA3** catalyst (5.10 mol %) in a single-neck flask under solvent free condition for 2 h. After the completion of the reaction, hot ethanol was added and filtered to remove the catalyst for reuse. After separation of the catalyst by filtration, the filtrate was poured into ice-water. The resulting solid was filtered, washed with water, dried, and recrystallized from ethanol to get the corresponding 2,4,5-triaryl-1*H*-imidazoles.

3.5.5 Reusability of the catalyst for Biginelli reaction

The reusability of the catalyst for subsequent catalytic cycles was examined using benzaldehyde, ethyl acetoacetate and urea as substrates. After the completion of the reaction, the solid catalyst was separated from the reaction mixture by washing the catalyst with hot ethanol and washed with methanol, dichloromethane and acetone. The catalyst was dried under vacuum at 120 °C for about 2 h. The dried solid catalyst was weighed and added to a fresh reaction mixture of benzaldehyde, ethyl acetoacetate and urea. The progress of the reaction was monitored by thin layer chromatography (TLC). The procedure was repeated for four reaction cycles.

### 3.5.6 Reusability of the catalyst for the synthesis of trisubstituted imidazoles

The reusability of the catalyst for subsequent catalytic cycles was examined using benzil, benzaldehyde and ammonium acetate as substrates.

After the completion of the reaction, the solid catalyst was separated from the reaction mixture by washing the catalyst with hot ethanol and washed with ethanol, dichloromethane and acetone. The catalyst was dried under vacuum at 120 °C for about 2 h. The dried solid catalyst was weighed and added to a fresh reaction mixture of benzil, benzaldehyde and ammonium acetate. The progress of the reaction was monitored by thin layer chromatography (TLC). The procedure was repeated for four reaction cycles.

3.5.7 Characterization of products

3.5.7.1 Dihydropyrimidinone derivatives (Table 3.5)

1) **5-(Ethoxycarbonyl)-6-methyl-4-phenyl-3,4-dihydropyrimidin-2(*1H*)-one**
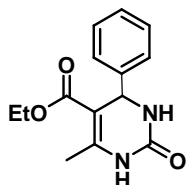
White solid, m. p. 204 °C (204-206 °C)[95], LC-MS (M$^+$) m/z 261; ^{1}H NMR (DMSO-d$_6$, 400 MHz) δ: 9.10 (s, 1H), 7.61 (s, 1H), 7.36-7.26 (m, 5H), 5.18 (s, 1H), 3.99 (q, *J* = 7.1 Hz, 2H), 2.26 (s, 3H), 1.10 (t, *J* = 7.1 Hz, 3H); ^{13}C NMR (DMSO-d$_6$, 100 MHz) δ: 165.8, 152.8, 148.4, 145.3, 128.5, 127.5, 126.7, 99.8, 59.5, 54.6, 18.3, 14.4.

2) **5-(Ethoxycarbonyl)-4-(4-nitrophenyl)-6-méthyl-3,4-dihydropyrimidin-2 (1*H*)-one**
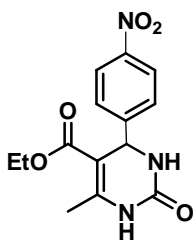
White solid, m. p. 211 °C (211-213 °C)[95], LC-MS (M$^+$) m/z 305; ^{1}H NMR (DMSO-d$_6$, 400 MHz) δ: 9.33 (s, 1H), 7.92 (s, 1H), 7.24 (d, *J* = 8.2 Hz, 2H), 7.21 (d, *J* = 8.2 Hz, 2H), 5.17 (s, 1H), 3.96 (q, *J* = 7.1 Hz, 2H), 2.25 (s, 3H), 0.9 (t, *J* = 7.1 Hz, 3H); ^{13}C NMR (DMSO-d$_6$, 100 MHz) δ: 166.6, 153.3, 153.1, 150.6, 148.0, 129.0, 125.1, 99.7, 61.0, 54.9, 19.1, 15.2.

### 3) 5-(Ethoxycarbonyl)-4-(3-nitrophenyl)-6-methyl-3,4-dihydropyrimidin-2(1*H*)-
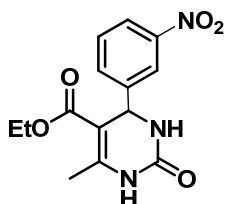
White solid, m. p. 230 °C (229-231 ºC)[96], LC-MS (M[+]) m/z 305; ^{1}H NMR (DMSO-d_6, 400 MHz) δ: 9.41 (s, 1H), 7.94 (s, 1H), 7.73-8.15 (m, 4H), 5.31 (s, 1H), 3.98 (q, *J* = 7.0 Hz, 2H), 2.26 (s, 3H), 1.12 (t, *J* = 7.0 Hz, 3H); ^{13}C NMR (DMSO-d_6, 100 MHz) δ: 165.6, 152.3, 149.9, 147.4, 133.5, 130.7, 122.9, 121.5, 98.8, 59.9, 54.0, 19.0, 18.4, 14.5.

4) 5-(Ethoxycarbonyl)-4-(4-bromophenyl)-6-méthyl-3,4-dihydropyrimidin-2(1*H*)-one
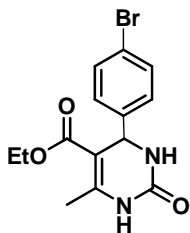
White solid, m. p. 210 °C (210-212 °C)[97], LC-MS (M+) m/z 339; ^{1}H NMR (DMSO-d_6, 400 MHz) δ: 9.28 (s, 1H), 7.82 (s, 1H), 7.56 (d, *J* = 8.2 Hz, 2H), 7.21 (d, *J* = 8.2 Hz, 2H), 5.15 (s, 1H), 3.98 (q, *J* = 7.0 Hz, 2H), 2.26 (s, 3H), 1.09 (t, *J* = 7.0 Hz, 3H); ^{13}C NMR (DMSO-d_6, 100 MHz) δ: 166.6, 153.1, 149.9, 145.3, 132.7, 129.7, 121.5, 99.9, 60.5, 54.6, 18.9, 15.2.

5) 5-(Ethoxycarbonyl -4-(4-methylphenyl)-6-méthyl 3,4-dihydropyrimidin-2(1*H*)-one
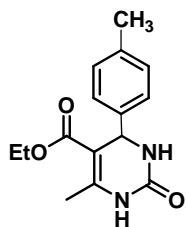
White solid, m. p. 215 °C (215-217 °C)[98], LCMS (M[+]) m/z 274; ^{1}H NMR (DMSO-d_6, 400 MHz) δ: 9.21 (s, 1H), 7.74 (s, 1H), 7.11-7.15 (m, 4H), 5.11 (s, 1H), 3.99 (q, *J* = 7.1 Hz, 2H), 2.26 (s, 3H), 2.24 (s, 3H), 1.10 (t, *J* = 7.1 Hz, 3H); ^{13}C NMR (DMSO-d_6, 100 MHz) δ: 165.8, 152.6, 148.6, 142.4, 136.8, 129.4, 126.6, 99.8, 59.6, 54.1, 21.1, 18.2, 14.5

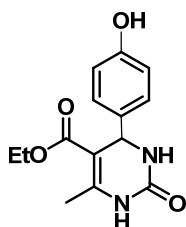6) **5-(Ethoxycarbonyl-4-(4-chlorophényl)-6-méthyl-3,4-dihydropyrimidin -2(1*H*)-one**
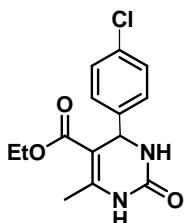
White solid, m. p. 215 °C (214-216 °C)[98a], LCMS (M$^+$) m/z 294; ^{1}H NMR (DMSO-d$_6$, 400 MHz) δ: 9.28 (s, 1H), 7.79 (s, 1H), 7.24-7.41 (m, 4H), 5.16 (s, 1H), 3.99 (q, *J* = 7.1 Hz, 2H), 2.26 (s, 3H), 1.08 (t, *J* = 7.1 Hz, 3H); ^{13}C NMR (DMSO-d$_6$, 100 MHz) δ: 166.4, 153.1, 149.9, 144.9, 132.9, 129.6, 129.4, 99.9, 60.5, 54.86, 18.9, 15.2.

7) **5-(Ethoxycarbonyl)-4-(4-hydroxyphenyl)-6-methyl-3,4-dihydropyrimidin-2(1*H*)-one**

White solid, m. p. 234 °C (234-236 °C)[95], LCMS (M$^+$) m/z 276; ^{1}H NMR (DMSO-d$_6$, 400 MHz) δ: 9.21 (s, 1H), 9.08 (s, 1H), 7.56 (s, 1H), 7.05 (d, *J* = 8.1 Hz, 2H), 6.70 (d, *J* = 8.1 Hz, 2H), 5.04 (s, 1H), 3.96 (q, *J* = 7.1 Hz, 2H), 2.24 (s, 3H), 1.02 (t, *J* = 7.1 Hz, 3H); ^{13}C NMR (DMSO-d$_6$, 100 MHz) δ: 165.7, 156.8, 152.7, 147.8, 135.8, 127.7, 115.2, 115.2, 100.2, 59.3, 53.9, 18.1, 14.4.

8) **5-(Ethoxycarbonyl)-4-(4-(dimethylamino)phényl)-6-methyl-3,4-dihydropyrimidin-2(1*H*)-one**
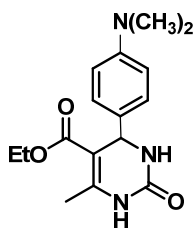
Orange solid, m. p. 255 °C (254-256 °C)[95], LCMS (M$^+$) m/z 303; ^{1}H NMR (DMSO-d$_6$, 400 MHz) δ: 9.14 (s, 1H), 7.64 (s, 1H), 7.14 (d, *J* = 8.6 Hz, 2H), 6.86 (d, *J* = 8.6 Hz, 2H), 5.05 (s, 1H), 3.98 (q, *J* = 7.1 Hz, 2H), 2.52 (s, 3H), 2.23 (s, 3H), 1.08 (t, *J* = 7.1 Hz, 3H); ^{13}C NMR (DMSO-d$_6$, 100 MHz) δ: 165.5, 152.4, 149.9, 147.6, 132.7, 126.9, 112.3, 99.9, 59.2, 53.3, 17.8, 14.2.

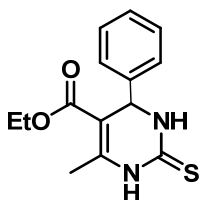## 9) 5-(Ethoxycarbonyl)-6-méthyl-4-(4-methoxylphenyl)-3,4-dihydropyrimidin-2(1*H*)-one
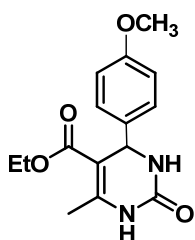
White solid m. p. 204 °C (204-205 °C)[99], LCMS (M$^+$) m/z 290; ^{1}H NMR (DMSO-d$_6$, 400 MHz) δ: 9.15 (s, 1H), 7.72 (s, 1H), 7.18 (d, *J* = 8.1 Hz, 2H), 6.86 (d, *J* = 8.1 Hz, 2H), 5.10 (s, 1H), 3.97 (q, *J* = 7.1 Hz, 2H), 3.74 (s, 3H), 2.25 (s, 3H), 1.12 (t, *J* = 7.1 Hz, 3H); ^{13}C NMR (DMSO-d$_6$, 100 MHz) δ: 166.2, 159.2, 152.9, 148.8, 137.8, 128.1, 114.5, 100.3, 59.9, 55.8, 54.1, 18.5, 14.9.

10) 5-(Ethoxycarbonyl)-6-methyl-4-phenyl-3,4-dihydropyrimidin-2(1*H*)-thione

White solid, m. p. 203 °C (202-204 °C)[100], LCMS (M$^+$) m/z 276; ^{1}H NMR (DMSO-d$_6$, 400 MHz) δ: 9.80 (s, 1H), 9.20 (s, 1H), 7.31-7.22 (m, 5H), 5.24 (s, 1H), 3.97 (q, *J* = 7.1 Hz, 2H), 2.24 (s, 3H), 1.12 (t, *J* = 7.1 Hz, 3H); ^{13}C NMR (DMSO-d$_6$, 100 MHz) δ: 174.2, 165.3, 144.4, 143.3, 128.2, 127.3, 126.5, 101.3, 59.5, 54.6, 17.4, 13.8.

11) 5-(Ethoxycarbonyl)-6-méthyl-4-(4-méthoxylphenyl)-3,4-dihydropyrimidin-2(1*H*)-thione
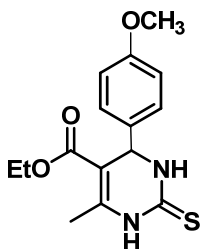
White solid, m. p. 155 °C (154-156 °C)[101], LCMS (M$^+$) m/z 307; ^{1}H NMR (DMSO-d$_6$, 400 MHz) δ: 9.79 (s, 1H), 9.26 (s, 1H), 7.16 (d, *J* = 8.5 Hz, 2H), 6.77 (d, *J* = 8.5 Hz, 2H), 5.21 (s, 1H), 3.98 (q, *J* = 7.1 Hz, 2H), 3.70 (s, 3H), 2.25 (s, 3H), 1.13 (t, *J* = 7.1 Hz, 3H); ^{13}C NMR (DMSO-d$_6$, 100 MHz) δ: 164.7, 158.3, 134.8, 131.1, 127.2, 113.6, 112.9, 101.3, 59.9, 54.4, 54.1, 16.9, 13.3.
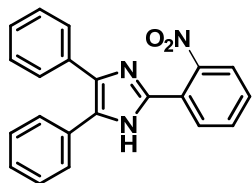
3.5.7.2 2,4,5-Trisubstituted imidazoles (Table 3.11)

1) 2,4,5-Triphenyl-*1H*-imidazole
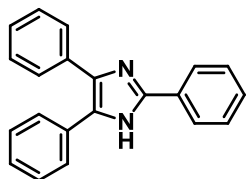
White solid, m. p. 266 °C (266-267 °C)[102], LCMS (M$^+$) m/z 296; ^{1}H NMR (DMSO-d$_6$, 400 MHz) δ: 12.7 (s, 1H), 8.1 (d, *J* = 7.8 Hz, 2H), 7.1-7.9 (m, 13H); ^{13}C NMR (DMSO-d$_6$, 100 MHz) δ: 146.2, 136.5, 135.5, 130.1, 130.4, 129.8, 128.7, 128.3, 127.1, 127.0, 125.2

2) 2-(2-Nitrophenyl)-4,5-diphenyl-1*H*-imidazole

White solid, m. p. 232 °C (231-232 °C)[102], LCMS (M$^+$) m/z 341; ^{1}H NMR (DMSO-d$_6$, 400 MHz) δ: 12.93 (s, 1H), 7.98-7.23 (m, 14H); ^{13}C NMR (DMSO-d$_6$, 100 MHz) δ: 151.4, 141.0, 134.4, 130.8, 128.5, 126.4, 125.0, 122.9, 122.1.

3) 2-(3-Nitrophenyl)-4,5-diphenyl-1*H*-imidazole
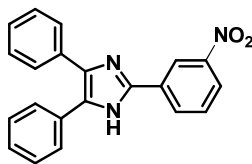
Yellow solid, m. p. >300 °C[102], LCMS (M$^+$) m/z 341; ^{1}H NMR (DMSO-d$_6$, 400 MHz) δ: 13.09 (s, 1H), 8.94 (s, 1H), 8.54 (d, *J* = 7.5 Hz, 1H), 8.22 (d, *J* = 7.8 Hz, 1H), 7.82 (d, *J* = 7.8 Hz, 1H), 7.54-7.31 (m, 10H); ^{13}C NMR (DMSO-d$_6$, 100 MHz) δ: 148.3, 143.3, 131.8, 131.1, 130.4, 128.6, 128.4, 127.1, 122.6, 119.4.

4) 2-(4-Nitrophenyl)-4,5-diphenyl-1*H*-imidazole
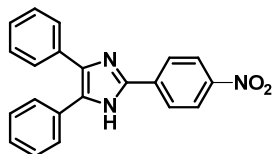
Orange solid, m. p. 200 °C (200-202 °C)[102], LCMS (M$^+$) m/z 341; ^{1}H NMR (DMSO-d$_6$, 400 MHz) δ: 11.7 (s, br.), 7.00- 8.52 (m, 14H); ^{13}C NMR (DMSO-d$_6$, 100 MHz) δ: 148.2, 147.8, 145.5, 137.4, 134.1, 131.9, 131.2, 130.7, 129.5, 128.2, 126.7, 126.1, 124.0.

5) 2-(4-Chlorophenyl)-4,5-diphenyl-1*H*-imidazole
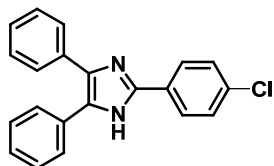
White solid, m. p. 263 °C (262-263 °C)[102], LCMS (M$^+$) m/z 330; ^{1}H NMR (DMSO-d$_6$, 400 MHz) δ: 12.75 (s, 1H), 8.10 (d, *J* =8.1 Hz, 2H), 7.55-7.23 (m, 12H); ^{13}C NMR (DMSO-d$_6$, 100 MHz) δ: 144.1, 137.8, 135.4, 132.4, 130.7, 129.8, 129.4, 128.6, 128.5, 128.4, 128.2, 127.8, 127.0, 126.8, 126.5.

6) 2-(4-Hydroxyphenyl)-4,5-diphenyl-1*H*-imidazole

White solid, m. p. 232 °C (231-232 °C)[102], LCMS (M$^+$) m/z 312; ^{1}H NMR (DMSO-d$_6$, 400 MHz) δ: 12.35 (s, 1H), 9.54 (s, 1H), 7.89 (d, *J* = 8.4 Hz, 2H), 7.53-7.21 (m, 10H), 6.87 (d, *J* = 8.4 Hz, 2H); ^{13}C NMR (DMSO-d$_6$, 100 MHz) δ: 157.6, 146.6, 127.1, 125.7, 124.3, 121.9, 114.7, 112.8, 98.5, 95.5.

7) 2-(4-Methoxyphenyl)-4,5-diphenyl-1*H*-imidazole
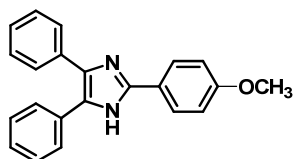
White solid, m. p. 220 °C (220-222 °C)[102], LCMS (M$^+$) m/z 326; ^{1}H NMR (DMSO-d$_6$, 400 MHz) δ: 12.51 (s, 1H), 8.02 (d, *J* = 8.1 Hz, 2H), 7.51-7.33 (m, 10H), 7.03 (d, *J* = 8.1 Hz, 2H), 3.81 (s, 3H); ^{13}C NMR (DMSO-d$_6$, 100 MHz) δ: 158.3, 145.0, 136.0, 134.6, 131.3, 121.4, 127.4, 126.0, 123.0, 113.8, 54.6.
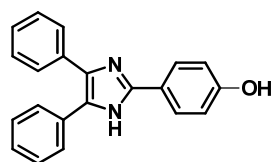
8) 2-(3,4-Dimethoxyphenyl)-4,5-diphenyl-1*H*-imidazole
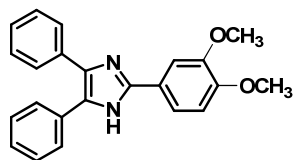
White solid, m. p. 214 °C (213-216 °C)[102], LCMS (M$^+$) m/z 356; ^{1}H NMR (DMSO-d$_6$, 400 MHz) δ: 12.51 (s, 1H), 7.65 (s, 1H), 7.4-7.55 (m, 6H), 7.36 (t, *J* = 7.2 Hz, 2H), 7.28 (t, *J* = 7.2 Hz, 2H), 7.20 (t, *J* = 7.8 Hz, 1H), 7.15 (d, *J* = 7.8 Hz, 1H), 3.78 (s, 3H), 3.75 (s, 3H); ^{13}C NMR (DMSO-d$_6$, 100 MHz) δ: 148.6, 147.0, 146.3, 137.2, 135.9, 131.7, 129.0,

128.8, 128.6, 128.0, 127.5, 126.8, 123.9, 117.0, 113.3, 112.5, 56.1, 55.8.

9) 2-(4-Methylphenyl)-4,5-diphenyl-1*H*-imidazole
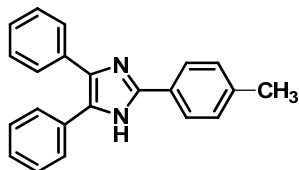
Colourless needle, m. p. 231 °C (231-232 °C)[102], LCMS (M$^+$) m/z 310; ^{1}H NMR (DMSO-d$_6$, 400 MHz) δ: 12.57 (s, 1H), 7.99 (d, *J* = 7.8 Hz, 2H), 7.55-2.21 (m, 12H), 2.33 (s, 3H); ^{13}C NMR (DMSO-d$_6$, 100 MHz) δ: 146.2, 138.9, 132.9, 129.6, 128.6, 127.8, 127.4, 127.1, 125.2, 21.3.

10) 2-(4-Bromophenyl)-4,5-diphenyl-1*H*-imidazole
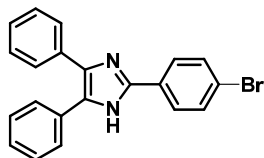
White solid, m. p. 250 °C (249-251 °C)[102], LCMS (M$^+$) m/z 374; ^{1}H NMR (DMSO-d$_6$, 400 MHz) δ: 12.02 (s, 1H), 7.44-7.40 (m, 4H), 7.37 (d, *J* = 7.8 Hz, 2H), 7.30-7.26 (m, 4H), 7.23-7.28 (m, 2H), 7.04-6.97 (d, *J* = 7.0 Hz, 2H); ^{13}C NMR (DMSO-d$_6$, 100 MHz) δ: 124, 126.6, 126.8, 128.5, 129.6, 130.3, 131.1, 131.4, 134.7, 137.8, 148.0, 145.6, 147.4.

11) 2-(3-Bromophenyl)-4,5-diphenyl-1*H*-imidazole
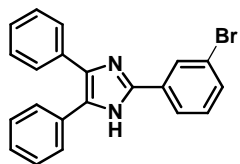
White solid, m. p. 120 °C(120-122 °C)[102], LCMS (M$^+$) m/z 374; ^{1}H NMR (DMSO-d$_6$, 400 MHz) δ: 9.40 (s, 1H), 7.78-7.26 (m, 14H); ^{13}C NMR (DMSO-d$_6$, 100 MHz) δ: 121.8, 125.6, 126.0, 126.7, 127.4, 127.7, 127.7, 128.1, 131.0.

12) 2-(2-Hydroxyphenyl)-4,5-diphenyl-1*H*-imidazole
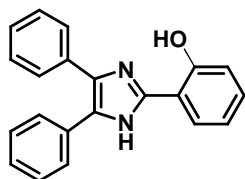
White solid, m. p. 202 °C (202-204 °C)[102], LCMS (M$^+$) m/z 312; ^{1}H NMR (DMSO-d$_6$, 400 MHz) δ: 13.01 (s, 1H), 12.94 (s, 1H), 8.06 (d, *J* = 7.2 Hz, 1H), 7.53-6.91 (m, 13H); ^{13}C NMR (DMSO-d$_6$, 100 MHz) δ: 146.0, 136.0, 130.1, 130.0, 129.0, 128.9, 128.4, 128.2, 127.6, 126.7, 125.6.

References

[1] M. A. Zolfigol, A. Khazaeia, A. Zare, M. Mokhlesi, T. H. Zadeh, A. Hasaninejad, F. D. Panah, A. M. Zare, H. Keypour, A. A. D. Firouzabadi, M. Merajoddin, *J. Chem. Sci.,* 2012, **124**, 501.

[2] J. H. Clark, *Acc. Chem. Res.*, 2002, **35**, 791.

[3] A. Habibi, E. Sheikhhosseini, M. Bigdeli, S. Balalaie, E. Farrokhi, *Int. J. Org. Chem.*, 2011, **1**, 143.

[4] N. C. Marziano, L. Ronchin, C. Tortato, S. Ronchin, A. Vavasori, *J. Mol. Catal. A: Chem.*, 2005, **235**, 26.

[5] A. K. Chakraborti, B. Singh, S. V. Chankeshwara, A. R. Patel, *J. Org. Chem.*, 2009, **4**, 5967.

[6] J. Zhou, F. Chen, Q. B. Wang, B. Zhang, L. Y. Zhang, A. Yusulf, *Chin. Chem. Lett.,* 2010, **21**, 922.

[7] B. Roy, B. Mukhopadhyay, *Tetrahedron Lett.*, 2007, **48**, 3783.

[8] B. Mukhopadhyay, *Tetrahedron Lett.*, 2006, **47**, 4337.

[9] (a) J. H. Clark, C. N. Rhodes, *Clean synthesis using porous inorganic solid catalysts and supported reagents,* 1st ed., UK: Royal Society of Chemistry, 2000. (b) P. Salehi, M. A. Zolfigol, F. Shirini, M. Baghbanzadeh, *Curr. Org. Chem.,* 2006, **10**, 2171. (c) A. Khalafi- Nezhad, A. Parhami, R. Bargebid, S. Molazade, A. Zare, H. Foroughi, *Mol. Divers.,* 2011, **15 ,** 373. (d) A. Zare, A. Hasaninejad, M. Shekouhy, A. R. Moosavi Zare, *Org. Prep. Proced. Int.,* 2008, **40**, 457.

[10] K. Shimizu, E. Hayashi, Y. Hatamachi, T. Kodama, Y. Kitayama, *Tetrahedron Lett.,* 2004, **45**, 5135.

[11] B. Karimi, M. Khalkhali, *J. Mol. Catal. A: Chem.,* 2007, **271**, 75.

[12] B. Das, B. S. Kanth, K. R. Reddy, A. S. Kumar, *J. Heterocycl. Chem.,* 2008, **45**, 1499.

[13] R. Gupta, S. Paul, A. Loupy, *J. Mol. Catal. A: Chem.,* 2006, **266**, 50.

[14] B. Das, K. Suneel, K. Venkateswarlu, B. Ravikanth, *Chem. Pharm. Bull.,* 2008, **56**, 366.

[15] B. Das, K. Venkateswarlu, H. Holla, M. Krishnaiah, *J. Mol. Catal. A: Chemical.,* 2006*,* **253**, 107.

[16] B. Das, K. Venkateswarlu, H. Holla, M. Krishnaiah, *Tetrahedron Lett.,* 2006, **47**, 8693.

[17] (a) D. M. D Souza, T. J. J. Mueller, *Chem. Soc. Rev.,* 2007, **36**, 1095. (b) A. Domling, *Chem. Rev.,* 2006, **106**, 17.

[18] X. Yu, X. Pan, J. Wu, *Tetrahedron*, 2011, **67**, 1145.

[19] A. Domling, I. Ugi, *Angew. Chem. Int. Ed.,* 2000*,* **39**, 3169.

[20] V. Nair, C. Rajesh, A. U. Vinod, S. Bindu, A. R. Sreekanth, J. S. Mathen, L. Balagopal, *Acc. Chem. Res.,* 2003, **36**, 899.

[21] J. Zhu, H. Bienayme, *Multicomponent Reactions*, Weinheim, Germany, Wiley-VCH, 2005.

[22] A. Hasaninejad, A. Zare, M. Shekouhy, J. A. Rad, *J. Comb. Chem.,* 2010, **12**, 844.

[23] M. A. Zolfigol, A. Khazaei, A. R. Moosavi-Zare, A. Zare, V. Khakyzadeh, *Appl. Catal. A: General,* 2011*,* **400**, 70.

[24] A. Khazaei, M. A. Zolfigol, A. R. Moosavi-Zare, A. Zare, A. Parhami, A. Khalafi-Nezhad, *Appl. Catal. A: General,* 2010*,* **386**, 179.

[25] (a) E. W. Hurst, R. Hull, *J. Med. Chem.*, 1961, **3**, 215. (b) M. Ashok, B. S. Holla, N. S. Kumari, *Eur. J. Med. Chem.,* 2007, **42**, 380. (c) S. S. Bahekar, D. B. Shinde, *Bioorg. Med. Chem. Lett.*, 2004, **14**, 1733.

[26] (a) C. O. Kappe, *Acc. Chem. Res.,* 2000, **33**, 879. (b) A. D. Patil, N. V. Kumar, W. C. Kokke, *J. Org. Chem.,*1995, **60**, 1182. (c) B. B. Snider, J. Chen, A. D. Patil, A. J. Freyer, *Tetrahedron Lett.*, 1996, **37**, 6977. (d) L. Heys, C. G. Moore, P. J. Murphy, *Chem. Soc. Rev.,* 2000, **29***,* 57.

[27] (a) J. P. Wan, Y. Lin, K. Hu, Y. Liu, *Beilstein J. Org. Chem.,* 2014, **10***,* 287. (b) T. U. Mayer, T. M. Kapoor, S. J. Haggarty, R. W. King, S. L. Schreiber, T. J. Mitchison, *Science,* 1999, **286***,* 971. (c) B. Schnell, U. T. Strauss, P. Verdino, K. Faber, C. O. Kappe, *Tetrahedron: Asymmetry,* 2000, **11***,* 1449. (d) B. Borowsky, M. M. Durkin, K. Ogozalek, M. R. Marzabadi, J. DeLeon, R. Heurich, H. Lichtblau, Z. Shaposhnik, I. Daniewska, T. P. Blackburn, T. A. Branchek, C. Gerald, P. J. Vaysse, C. Forray, *Nat. Med.,* 2002, **8***,* 825.

[28] P. Biginelli, *Gazz. Chim. Ital.,* 1893, **23**, 360.

[29] (a) C. O. Kappe, S. F. Falsone, *Synlett.*, 1998, 718. (b) B. C. Ranu, A. Hajra, U. Jana, *J. Org. Chem.*, 2000, **65**, 6270. (c) Y. Ma, C. Qian, L. Wang, M. Yang, *J. Org. Chem.*, 2000, **65**, 3864. (d) G. Sabitha, G. S. K. K. Reddy, C. S. Reddy, J. S. Yadav, *Synlett.,* 2003, 858. (e) D. S. Bose, R. K. Kumar, L. Fatima, *Synlett,* 2004, 279. (f) J. Lu, H. Ma, *Synlett*, 2000, 63. (g) E. H. Hu, D. R. Sidler, U. H. Dolling, *J. Org. Chem.*, 1998, **63**, 3454. (h) J. S. Yadav, B. V. S. Reddy, R. Srinivas, C. Venugopal, T. Ramalingam, *Synthesis*, 2001,**1341**, 5I.

[30] (a) J. S. Yadav, B. V. S. Reddy, P. Sridhar, J. S. S. Reddy, K. Nagaish, N. Lingaiah, P. S. Saiprasad, *Eur. J. Org. Chem.*, 2004, 552. (b) A. K. Mitra, K. Banerjee, *Synlett.*, 2003, 1509. (c) F. Bigi, S. Carloni, B. Frullanti, R. Maggi, G. Sartori, *Tetrahedron Lett.*, 1999, **40**, 3465. (d) V. R. Rani, N. Srinivas, M. R. Kishan, S. J. Kulkarni, K. V. Raghavan, *Green Chem.*, 2001, **3**, 305. (e) V. R. Choudhary, V. H. Tillu, V. S. Narkhede, H. B. Borate, R. D.Wakharkar, *Catal. Commun.*, 2003, **4**, 449.

[31] I. Cepanec, M. Litvic, M. Filipsn-Litvic, I. Grungold, *Tetrahedron*, 2007, **63**, 11822.

[32] S. Chitra, K. Pandiarajan, *Tetrahedron Lett.,* 2009, **50**, 2222.

[33] F. Zamani, S. M. Hosseini, S. Kianpour, *Solid State Sci.,* 2013, **26**, 139.

[34] K. K. Pasunooti, H. Chai, C. N. Jensen, C. N. B. K. Gorityala, S. Wang, X.W. Liu, *Tetrahedron Lett.,* 2011, **52**, 80.

[35] B. Liang, X. T. Wang, J. X. Wang, Z. Y. Du, *Tetrahedron,* 2007, **63**, 1981.

[36] J. C. Rodriguez-Domínguez, D. Bernardi, G. Kirsch, *Tetrahedron Lett.*, 2007, **48**, 5777.

[37] A. Zare, Z. Nasouri*, J. Mol. Liq*., 2016, **216**, 364.

[38] G. Garima, V. P. Srivastava, L. D. S. Yadav, *Tetrahedron Lett.*, 2010, **51**, 6438.

[39] A. N. Dadhania, V. K. Pate, D. K. Raval, *J. Chem. Sci.,* 2012, **124**, 921.

[40] R. Kore, R. Srivastava*, J. Mol. Catal. A.,* 2011, **345**, 117.

[41] P. Karthikeyan, S. A. Aswar, P. N. Muskawar, P. R. Bhagat, S. S. Kumar, *J. Organomet. Chem*., 2013, **723**, 154.

[42]   X. Zhang, X. Gu, Y. Gao, S. Nie, H. Lu, *Appl. Organometal. Chem.*, 2016, 1.

[43]   H. Khabazzadeh, K. Saidi, H. Sheibani, *Bioorg. Med. Chem. Lett.,* 2008, **18**, 278.

[44]   X. Zhang, Y. Li, C. Liu, J. Wang, *J. Mol. Catal. A: Chem.,* 2006, **253**, 207.

[45]   F. Dong, L. Jun, Z. Xinli, Y. Zhiwen, L. Zuliang, *J. Mol. Catal. A: Chem.,* 2007, **274**, 208.

[46]   G. H. Mahdavinia, H. Sepehrian, *Chin. Chem. Lett.*, 2008, **19**, 1435.

[47]   D. Azarifar, O. Badalkhani, Y. Abbasi, *J. Sulfur Chem.*, 2016, **37**, 656.

[48]   E. Tabrizian, A. Amoozadeh, T. Shamsi, *Reac. Kinet. Mech. Cat.,* 2016, **119**, 245.

[49]   M. M. Hosseini, E. Kolvari, N. Koukabi, M. Ziyaei, M. A. Zolfigo, *Catal. Lett.,* 2016, **146**, 1040.

[50]   R. Rambabu, J. Subbarao, P. Pavan Kumar, *IJPSR*, 2015, **6**, 1761.

[51]   B. Maleki, H. K. Shirvan, F. Taimazi, E. Akbarzadeh, *Int. J. Org. Chem.*, 2012, **2**, 93.

[52]   J. Sisko, *Org. Chem.*, 1998, **63**, 4529.

[53]   S. Maeda, M. Suzuki, T. Iwasaki, Matsumoto, K. Iwasawa, *Chem. Pharm. Bull.,*1984, **32**, 2536.

[54]   T. Maier, R. Schmierer, K. Bauer, H. Bieringer, H. Buerstell, B. Sachse, *US Patent*, 4820335, 1989.

[55]   R. Schmierer, H. Mildenberger, H. Buerstell, *German Patent,* 361464, 1987.

[56]   J. Heeres, L. J. J. Back, J. H. Mostmans, J. Vancutsem, *J. Med. Chem.,* 1979, **22**, 1003.

[57]   B. Radziszewski, *Chem. Ber.*, 1882, **15**, 1493.

[58]   H. H. Robinson, F. R. Japp, *Chem. Ber.,* 1882, **15**, 1268.

[59]   D. I. MaGee, M. Bahramnejad, M. Dabiri, *Tetrahedron Lett.,* 2013, **54,** 2591.

[60]   X. Deng, Z. Zhou, A. Zhang, G. Xie, *Res. Chem. Intermed.,* 2013, **39**, 1101.

[61]   C. Kurumurthy, G. S. Kumar, G. M. Reddy, P. Nagender, P. S. Rao, B. Narsaiah, *Res. Chem. Intermed.,* 2012, **38**, 359.

[62]   H. Zang, Q. Su, Y. Mo, B. W. Cheng, S. Jun, *Ultrason. Sonochem.,* 2010, **17**, 749.

[63]   A. R. Khosropour, *Can. J. Chem.,* 2008, **86**, 264.

[64]   M. Xia, Y. D. Lu, *J. Mol. Catal. A: Chem*., 2007, **265**, 205.

[65]   L.W. Wang, Y. H. Wang, H. Tian, Y. F. Yao, J. H. Shao, B. Liu*, J. Fluorine Chem.*, 2006, **127**, 1570.

[66]   C. Yu, M. Lei, W. Su, Y. Xie, *Synth. Commun*., 2007, **37**, 3301.

[67]   S. D. Sharma, P. Hazarika, D. Konwar, *Tetrahedron Lett.,* 2008, **49**, 2216.

[68]   G. V. M. Sharma, Y. Jyothi, P. S. Lakshmi, *Synth. Commun.,* 2006, **36**, 2991.

[69]   K. Ramesh, S. Narayana Murthy, K. Karnakar, Y. V. D. Nageswar, K. Vijayalakhshmi, *Tetrahedron Lett.,* 2012, **53**, 1126.

[70]   B. F. Mirjalili, A. Bamoniri, M. A. Mirhoseini*, Scientia Iranica C.*, 2013, **20**, 587.

[71]   B. Sadeghi, B. B. F. Mirjalili, M. M. Hashemi, *Tetrahedron Lett.,* 2008, **49**, 2575.

[72]   S. Kantevari, S. V. N. Vuppalapati, D. O. Biradar, L. Nagarapu, *J. Mol. Catal. A: Chem.*, 2007, **266**, 109.

[73]   A. R. Karimi, Z. Alimohammadi, J. Azizian, A. A. Mohammadi, M. R. Mohmmadizadeh, *Catal. Commun.*, 2006, **7**, 728.

[74]   A. Shaabani, A. Rahmati, *J. Mol. Catal. A: Chem*., 2006, **249**, 246.

[75]   M. M. Heravi, K. Bakhtiari, H. A. Oskooie, S. Taheri, *J. Mol. Catal. A: Chem.*, 2007, **263**, 279.

[76]   S. S. Pandit, S. K. Bhalerao, U. S. Aher, G. L. Adhav, V. U. Pandit, *J. Chem. Sci.*, 2011, **123**, 421.

[77]   L. Wang, C. Cai, *Monatsh. Chem*., 2009, **140**, 541.

[78]   S. Samai, G. C. Nandi, P. Singh, M. S. Singh*, Tetrahedron*, 2009, **65**, 10155.

[79]   S. N. Murthy, B. Madhav, Y. V. D. Nageswar, *Tetrahedron Lett.,* 2010, **51**, 5252.

[80]   H. Zheng, Q. Y. Shi, K. Du, Y. J. Mei, P. F. Zhang, *Catal. Lett.,* 2013, **143**, 118.

[81] P. V. Maske, S. J. Makhija, *Asian J. Biomed. Pharm. Sci.,* 2013, **20**, 63.

[82] S. F. Hojati, S. A. Nezhadhoseiny, Z. Beykzadeh, *Monatsh Chem.*, 2013**, 144**, 387.

[83] B. F. Mirjalilia, A. Bamonirib, N. Mohaghegh, *Curr. Chem. Lett.,* 2013, **2**, 35.

[84] A. Mobinikhaledi, A. K. Amiri, *Res. Chem. Intermed.*, 2015, **41**, 2063.

[85] M. Bakavoli, H. Eshghi, M. Rahimizadeh, M. R. Housaindokht, A. Mohammadi, H. Monhemi, *Res. Chem. Intermed.,* 2015, **41**, 3497.

[86]   X. Xu, Y. Li, *Res. Chem. Intermed.*, 2015, **41**, 4169.

[87] B. Bafti, H. Khabazzadeh, *J. Chem. Sci.,* 2014, **126**, 881.

[88] M. Hajjami, A. G. Choghamarani, Z. Yousofv, M. Norouzi, *J. Chem. Sci.*, 2015, **127**, 1221.

[89] A. V. Dhanunjaya Rao, R. Surasani, B. P. Vykunteswararao, T. Bhaskarkumar, B. Srikanth, N. R. Jogdand, D. Kalita, J. K. D. Lilakar, V. Siddaiah, P. D. Sanasi, A. Raghunadh, *Synth. Commun.,* 2016, **46**, 1519.

[90] T. D. Ananda Kumar, N. Yamini, C. V. S. Subrahmanyam, K. Satyanarayana, *Synth. Commun.,* 2014, **44**, 2256.

[91] H. Naeimi, D. Aghaseyedkarimi, *Dalton Trans.,* 2016, **45**, 1243.

[92] A. Shaabani, H. Sepahvand, S. E. Hooshmand, M. B. Boroujeni*, Appl. Organometal. Chem.,* 2016, **30**, 414.

[93] M. Gorsd, G. Sathicq, G. Romanelli, L. Pizzio, M. Blanco*, J. Mol. Catal. A: Chem.,* 2016, **420**, 294.

[94] (a) M. Esmaeilpour, J. Javidi, M. Zandia, *New J. Chem.,* 2015, **39**, 3388. (b) M. K. Raj, H. S. P. Rao, S. G. Manjunatha, R. Sridharan, S. Nambiar, J. Keshwan, J. Rappai, S. Bhagat, B. S. Shwetha, D. Hegde, U. Santhosh, *Tetrahedron Lett.*, 2011, **52**, 3605.

[95] W. Su, J. Li, Z. Zheng, Y. Shen, *Tetrahedron Lett.,* 2005, **45**,6037.

[96] A. S. Paraskar, G. K. Dzwkar, A. Sudalai, *Tetrahedron Lett.,* 2003, 3305.

[97] M. M. Herari, K. Bakhtiari, *Catal. Commun.,* 2006, **7**, 373.

[98] (a) M. Gohain, D. Prajapati, J. S. Sandhu, *Synlett.,* 2004*,* **2**, 235. b) S. Jayakumar; T. K. Sabeer, *J. Chem. Pharm. Res.*, 2011, **3**, 1089.

[99] S. B. Sapcal, K. F. Shelke, B. B. Shingate, M. S. Shingare, *Bull. Korean Chem. Soc.,* 2010, **31**, 351.

[100] R. J. Kalbasi, A. R. Massah, B. Daneshvarnejad, *Appl. Clay Sci.,* 2012, **55**, 1.

[101] B. Gangadasu, P. Narender, B. C. Raju, V. J. Rao, *Indian J. Chem.,* 2006, **45,** 1259.

[102] S. Samai, G. C. Nandi, P. Singh, M. S. Singh, *Tetrahedron*, 2009, **65**, 10155.

.....ೞಞ.....

Chapter 4

CARBOXYLIC ACID FUNCTIONALIZED MESOPOROUS SILICA AS EFFECTIVE REUSABLE ORGANO ACIDIC CATALYST FOR ULLMANN TYPE COUPLING REACTION

Contents

4.1   Introduction
4.2   Objective of the present work
4.3   Results and discussion
4.4   Conclusion
4.5   Experimental

Classical Ullmann coupling reaction and Ullmann type reactions are metal catalyzed reactions at high temperature. Due to the present interest in heterogeneous organocatalysis in the context of green chemistry, here an attempt has been made to perform the Ullmann type C-O and C-N coupling reaction using dendritic carboxylic acid anchored on mesoporous silica. Presence of large number of carboxylic acid groups on the surface of mesoporous silica makes it effective acidic catalyst for these reactions. The third generation dendritic catalyst CA3 showed high activity towards these reactions and could be recycled up to four runs without loss of its activity.

4.1 Introduction

Carbon-carbon (C-C) bond-forming reactions are fundamental in synthetic organic chemistry, because, they allow for the assembly of more complex molecular systems from simpler ones.[1] Recently, transition-metal catalyzed carbon-carbon and carbon-hetero atom bond forming reactions have received paramount attention because of their manifold industrial applications.[2-7] Accordingly, an extraordinarily diverse range of methods for creating C-C bonds and carbon-hetro atom bonds have been established over the last one hundred years or so and this provides the capacity to construct a remarkable array of chemical structures.[8] Amongst the most venerable of these methods is the Ullmann reaction and Ullmann type reaction.
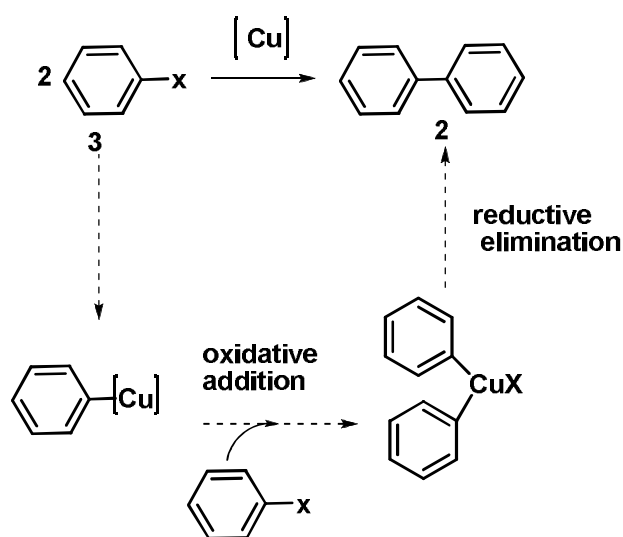
4.1.1 Classical Ullmann reaction and Ullmann type reaction

In 1901 Fritz Ullmann found that Cu compounds were able to catalyze the formation of biaryl through coupling of two molecules of aryl halides.[9] Formation of a new C–C bond between two aryls by the condensation of two molecules of aromatic halide in the presence of finely divided copper is known as classical Ullmann reaction (Scheme 4.1).[10] This is the first transition metal mediated coupling reaction for the formation of aryl-aryl bond. The reaction is most often been done on aryl iodides, but bromides and chlorides have also been used. Aryl bromides and chlorides do not usually react unless there is an electron withdrawing group like nitro, ester, etc. at ortho and/or para to the halogen atom.[11]
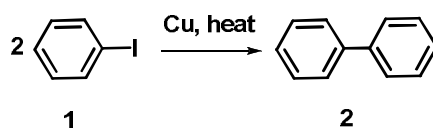

Scheme 4.1 Classical Ullmann reaction

The generally accepted mechanism for this reaction involves the formation of an organocuprate intermediate from a molecule of aryl halide, which then reacts with a second molecule through oxidative addition, furnishing the final product after reductive elimination (Scheme 4.2).[12, 13] The classical Ullmann reaction is limited to electron deficient aryl halides and requires harsh reaction conditions.

Scheme 4.2 Mechanism of Ullmann reaction

A few years after the discovery of the classical Ullmann reaction, the same methodology was applied by Ullmann to the synthesis of *N*-aryl amines and ethers, in 1903 and 1905 respectively,[14, 15] and in 1906 the first Cu catalyzed synthesis of aryl amides was reported by Irma Goldberg[16] (Scheme 4.3). Goldberg also reported the first catalytic arylation of amines in the same year. Almost 30 years later, in 1929, William Hurtley reported the coupling between *o*-bromobenzoic acid and *β*-dicarbonyls mediated by Cu bronze or $Cu(OAc)_2$.[17, 18]

Ullmann, 1903
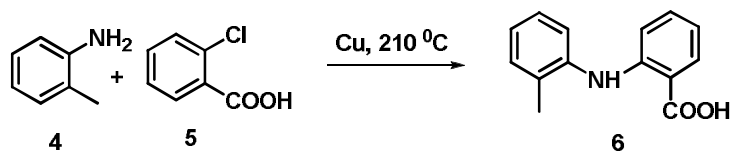
Ullmann, 1905
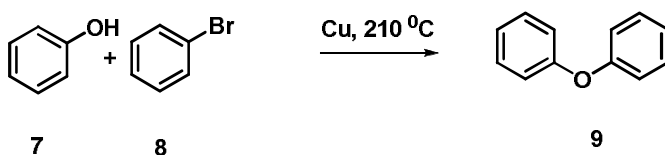
Goldberg, 1906
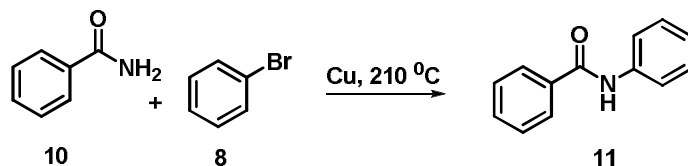
Haurtley, 1929
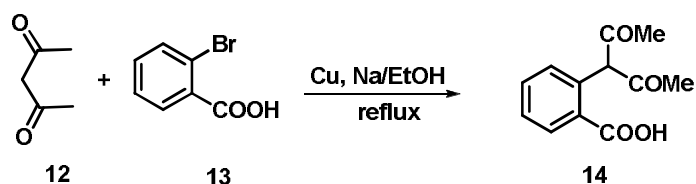
Scheme 4.3 Ullmann type coupling reactions

According to commonly accepted nomenclature, the term "Ullmann condensation reaction or Ullmann type coupling" refers to a copper-mediated reaction between an aryl halide and an amine, phenol or thiophenol to synthesize the corresponding aryl amine, ether or thioether compounds, respectively.[19] Since their discovery, Ullmann-type coupling reactions have become a typical method for preparing aryl amines, biaryl ethers, and *N*-aryl heterocycles that are important in the pharmaceutical and materials world.

4.1.2 Copper catalysts for Ullmann-type coupling reactions

Many different copper sources such as Cu(0), Cu(I) and Cu(II)) have been used to catalyze Ullmann-type reactions, and either salts and oxides seemed to work well for the arylation of several nucleophiles. This suggested that a common Cu species could be formed during the reaction from the different sources. Many works have therefore been carried out since the early 1960s in this direction, investigating the particular electrochemical behaviour of Cu sources. Since Cu(I) seemed to lead to slightly higher reaction rates, it was proposed by Weingarten in 1964 that Cu(I) species could have been the common intermediate. It was demonstrated, indeed, that Cu(II) species used as catalysts could be reduced to Cu(I) in the presence of coordinating solvent/nucleophiles, and that phenoxides and amines used as nucleophiles in the coupling could get oxidised as the redox counterpart.[20, 21]

After these reactions, several investigations were carried out on Ullmann type reaction using different reaction conditions in the presence of a variety of copper catalysts. But these Cu-mediated reactions required harsh conditions such as high temperature, strong bases, long reaction time, stoichiometric amounts of copper reagent, electron-poor aromatic substrates with very low response to product, polar solvents with high boiling point and very low yield. Moreover, problems related to the solubility of many Cu compounds were evident, hence excess amount of Cu source had often to be used. So these drawbacks had limited the applications of Ullmann reaction during these periods. But with the increasing understanding of the mechanism of the Ullmann reaction and development of novel ligands[22] (Figure 4.1) and modification of catalytic system with other metals like palladium, nickel, gold and application of the green technologies allowed

the Ullmann type reaction to be conducted under mild conditions with desirable yields with excellent functional group tolerance.[23-33] This facilitated the wide application of the Ullmann type reaction to the synthesis of heterocycles, drug-like molecules, natural products, pharmaceuticals, agrochemicals, molecules for material applications.[34]

O, O-Ligands
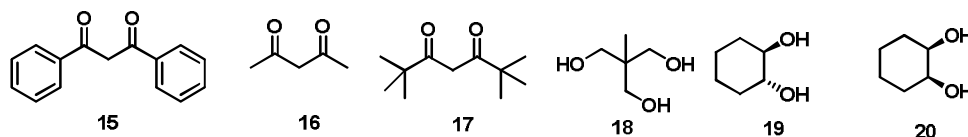
N, N Ligands
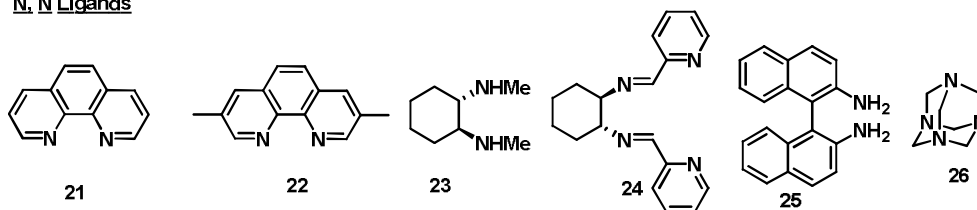
N, O Ligands
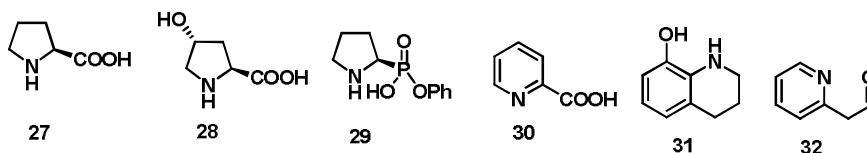
Figure 4.1 Ligands used for Ullmann reaction[22]

Large numbers of catalysts were reported using the concept of heterogeneous and green protocol in the presence of different metal salts. Some of the reported catalysts are: CuI/oxalic diamide,[35] CuI,[36] Zn(0), NiCl$_2$.6H$_2$O, and Ph$_3$P,[37] Cu-Schiff base on MCM-41,[38] Cu-TDPAT,[39] Ph-MCM-41 supported Pd-catalyst,[40] Ph–Al-MCM-41,[41] Pd catalyst on the phenyl-functionalized SBA-15,[42] ordered mesophorous carbon supported Pd-catalyst,[43]

porous MOF-supported palladium NPs,[44] graphene oxide supported palladium nanoparticle catalyst in ionic liquid-supercritical carbon dioxide system,[45] carbon spheres supported Pd NPs,[46] gold nanoparticles,[47] Pd NPs supported on ionic liquid derived nano-fibrillated mesoporous carbon Pd@IFMC,[48] and gold nanoparticle supported on a magnetic/s-graphene nanocomposite.[49] But all of them have a metal centre for catalytic activity.

4.2 Objective of the present work

From the literature review, it is found that many metal catalysts with different ligands under different reaction conditions were developed for Ullmann reaction and Ullmann type reactions. Different supported metal catalysts were developed which include mesoporous silica, metal organic frame work, nano fibres etc. All these works faced the problems such as toxicity of metal, cost of metal, leaching of metal, reusability of metal catalyst and harsh reaction conditions like high temperature, long reaction time, use of expensive ligands and strong base etc. The development of sustainable, environmentally benign, and cost-effective chemistry, "green" concept and techniques in Ullmann reactions and Ullmann type reactions is still in great demand. Due to the interest in the field of metal free catalysis, that is organocatalysis, the Ullmann type reactions catalyzed by metal free catalyst was considered. Literature survey showed that no metal free catalyst was reported for these reactions. In Chapter 2 the synthesis of dendritic carboxylic acid functionalized mesoporous silica was presented. Three generations of dendritic catalyst **CA1-3** showed high acidity. The acid loading was increased on going to higher generations.

4.3   Results and discussion

4.3.1 Synthesis of dendritic carboxylic acid on mesoporous silica

Detailed synthetic procedure for the synthesis of **CA1-3** samples was given in Chapter 2. Figure 4.2 and 4.3 show the structures of **CA1**, **CA2** and **CA3** samples.
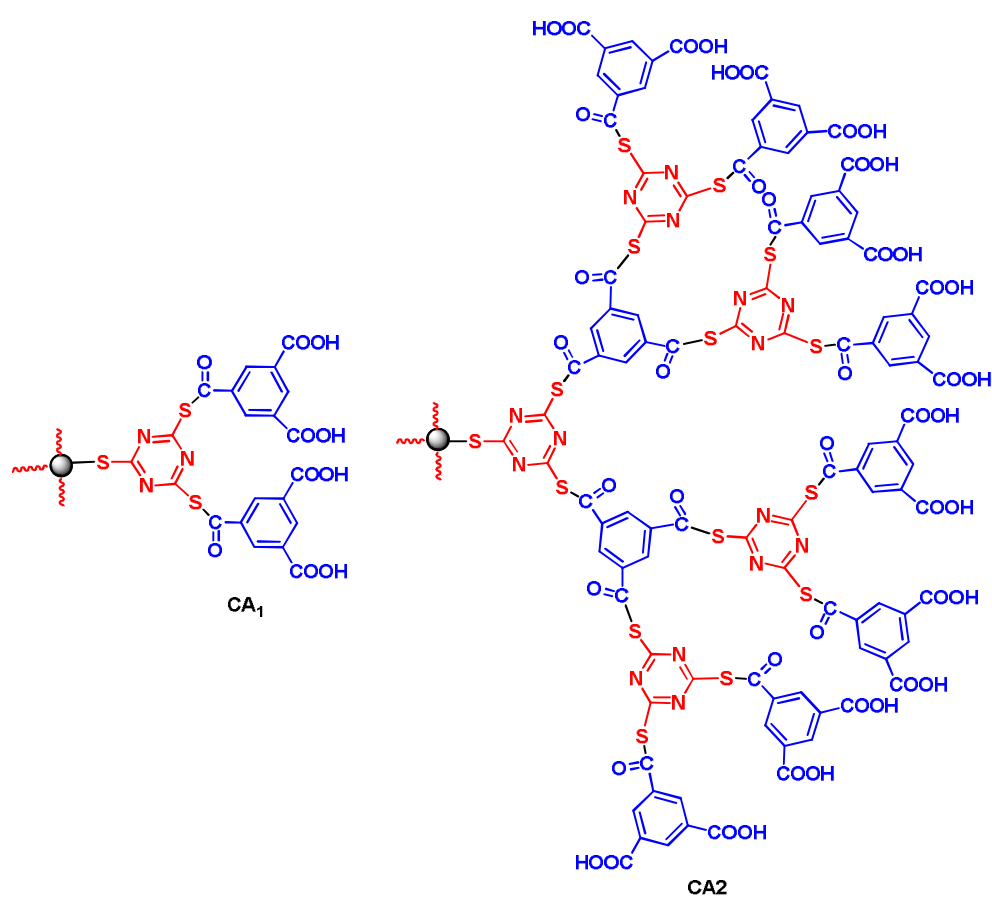

Figure 4.2 Structure of **CA1** and **CA2**
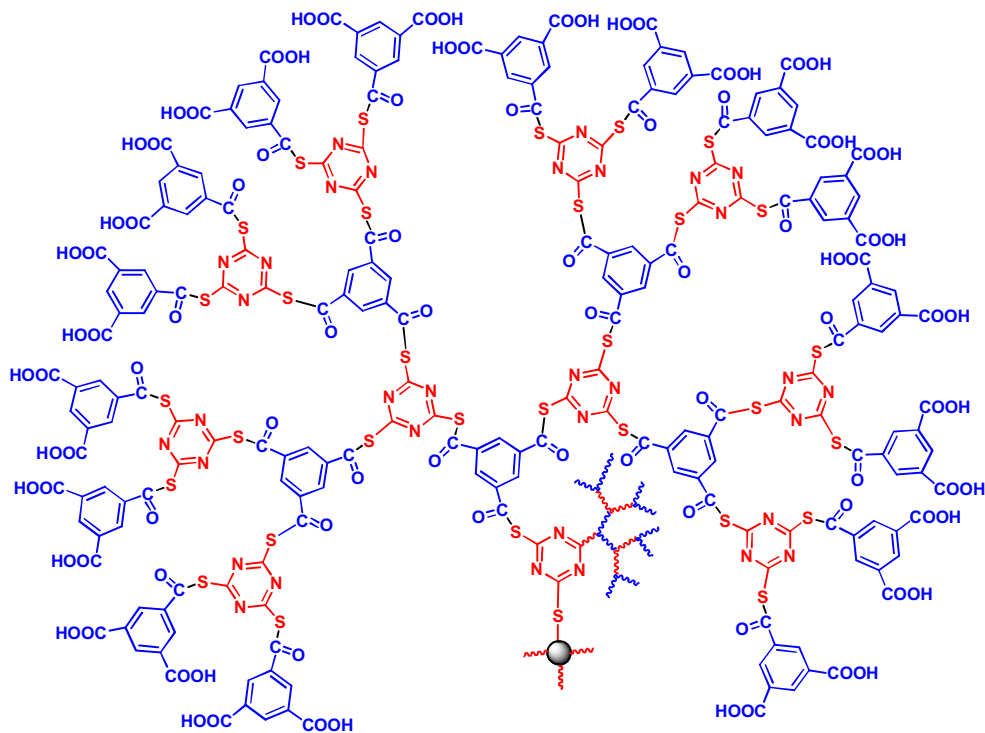
Figure 4.3 Structure of **CA3**

4.3.2 Catalytic application of dendritic carboxylic acid on mesoporous silica

4.3.2.1 Ullmann type coupling reaction

The reaction between 1 mmol each of 4-nitroiodobenzene and phenol was performed in the presence of 10.3 mol % of **CA3** and K_2CO_3 as base in the presence of DMSO at 110 °C (Scheme 4.4). It was found that in the presence of catalyst, 90 % yield was obtained after 8 h. This result showed that catalyst **CA3** was active towards this reaction. The reaction conditions like temperature, role of base, solvent, amount of catalyst and different generations of catalysts were optimized.
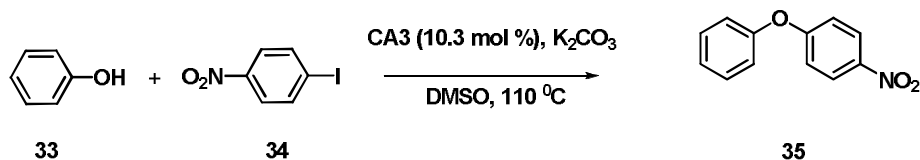
Scheme 4.4 Ullmann type coupling reaction catalyzed by **CA3**

4-Nitroiodobenzene was chosen as the arylating agent for O-arylation of phenol and this reaction was selected as a model reaction to optimize the reaction conditions. Initially, the different generation of catalysts was optimized and results are summarized in Table 4.1.

Table 4.1 Effect of different generation of catalysts

Entry	Catalysts	Yield (%)[a, b]
1	No Catalyst	No product
2	**CA1**	45
3	**CA2**	85
4	**CA3**	**90**

[a]phenol (1 mmol), 4-nitroiodobenzene (1 mmol), catalyst (0.008 g), K_2CO_3 (0.08 g), DMSO (2 mL), 90 °C, 8 h, [b]isolated yield

Results showed that no product was obtained without the catalyst; the yield was increased when different generations of the catalyst were used. 90 % yield was obtained for **CA3**. Optimization of amount of **CA3** revealed that as the amount of **CA3** was increased from 2.6 mol % to 10.3 mol %, the percentage conversion also increased and maximum conversion was obtained for 10.3 mol % and no further improvement in yield was observed with 12.9 mol % of **CA3**. 10.3 mol % of **CA3** was selected for further optimization studies (Table 4.2).

Table 4.2 Effect of amount of **CA3**

Entry	Amount of catalyst CA3 (g)	Amount of catalyst CA3 (mol %)	Yield (%)[a, b]
1	0.002	2.6	60
2	0.004	5.2	79
3	0.006	7.7	82
4	**0.008**	**10.3**	**90**
5	0.010	12.9	90

[a]phenol (1 mmol), 4-nitroiodobenzene (1 mmol), K_2CO_3 (0.08 g), DMSO (2 mL), 90 °C, 8 h, [b]isolated yield

In continuation, the role of solvent in deciding the outcome of coupling reactions was investigated. In order to find the best solvent for this reaction, different solvents such as protic and aprotic solvents and solvent free condition were tested at 50 °C (Table 4.3). In water, no product was obtained. Except DMF and DMSO, all other solvents and solvent free condition gave very low yield. DMF and DMSO gave almost comparable yield; but maximum yield was given by DMSO. DMSO was selected as the reaction medium for further studies.

Table 4.3 Optimization of solvents

Entry	Solvent	Yield (%)[a, b]
1	Methanol	14
2	Ethanol	18
3	Dioxane	22
4	Dichloromethane	15
5	Acetonitrile	13
6	Water	-
7	No solvent	5
8	DMF	29
9	**DMSO**	**34**
10	Toluene	10

[a]phenol (1 mmol), 4-nitroiodobenzene (1 mmol), K_2CO_3 (0.08 g), **CA3** (10.3 mol %), 50 °C, 8 h, [b]isolated yield

Effect of temperature on the reaction was also studied. Results given in the Table 4.4 showed that at room temperature, no product was obtained. When the temperature was increased, the yield was gradually increased and highest yield was obtained at 90 °C. But further increment in the temperature showed no difference in the reaction yield. So, 90 °C was chosen as the reaction temperature.

Table 4.4 Effect of temperature

Entry	Temperature, °C	Yield (%)[a, b]
1	Room temperature	-
2	50	34
3	60	56
4	70	75
5	**90**	**90**
6	**110**	**90**

[a]phenol (1 mmol), 4-nitroiodobenzene (1 mmol), K_2CO_3 (0.08 g), DMSO (2 mL), **CA3** (10.3 mol %), 8 h, [b]isolated yield

Another important factor is the role of base on product yield. Results are summarized in the Table 4.5. From the Table it is clear that without base, no product was obtained. In addition, the reaction did not take place in the presence of triethylamine as base. The reaction with other bases gave good yield. But K_2CO_3 and KOH gave better yield. K_2CO_3 was selected as the base for this reaction.

Table 4.5 Effect of different bases on the reaction

Entry	Bases	Yield (%)[a, b]
1	KOH	90
2	NaOH	85
3	**K_2CO_3**	**90**
4	Triethylamine	-
5	No base	-
6	Na_2CO_3	78

[a]phenol (1 mmol), 4-nitroiodobenzene (1 mmol), **CA3** (10.3 mol %), 90 °C, 8 h, [b]isolated yield

To compare the catalytic activity of metal salts with **CA3**, the reaction was done with different metal salts and the results are given in Table 4.6. All metal salts responded to this reaction, but highest yield was obtained for **CA3**. This means that **CA3** shows superior catalytic activity than given metal salts.

Table 4.6 Different metal salts on Ullmaan type coupling reaction

Entry	Metal salts	Yield (%)[a, b]
1	$CuSO_4$	54
2	$CuCl_2$	46
3	$Pd(OAc)_2$	34
4	$NiSO_4$	25
5	**CA3**	**90**

[a]phenol (1 mmol), 4-nitroiodobenzene (1 mmol), K_2CO_3 (0.08 g), DMSO (2 mL), **CA3** (10.3 mol %), 90 °C, 8 h, metal salts (0.10 g), [b]isolated yield
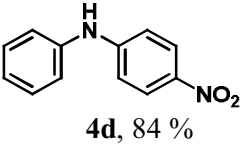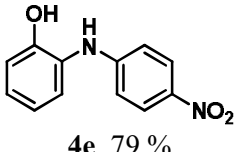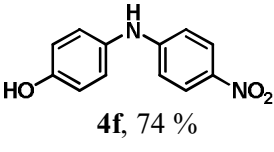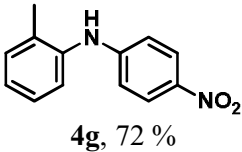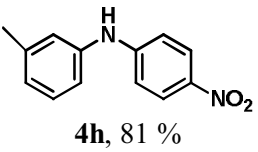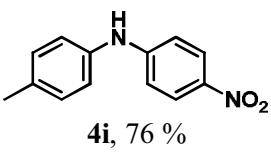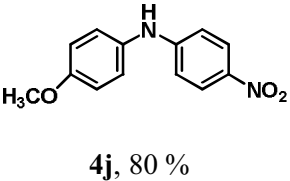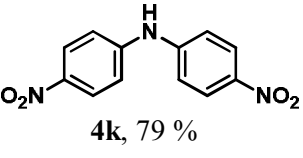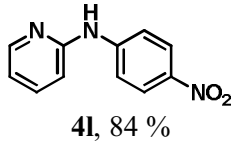
According to the above results, the optimized reaction conditions for C-O coupling reactions are 10.3 mol % of **CA3** in DMSO at 90 °C for 8 h in the presence of K_2CO_3. The generality of the C–O coupling reaction using **CA3** was investigated under the standard reaction conditions and the results are summarized in the Table 4.7. The synthesis of the C-O products was investigated with various phenol derivatives using 4-nitroiodobenzene and all of them gave good to excellent yields at appropriate times.

Table 4.7 Ullmann type C-O coupling reactions
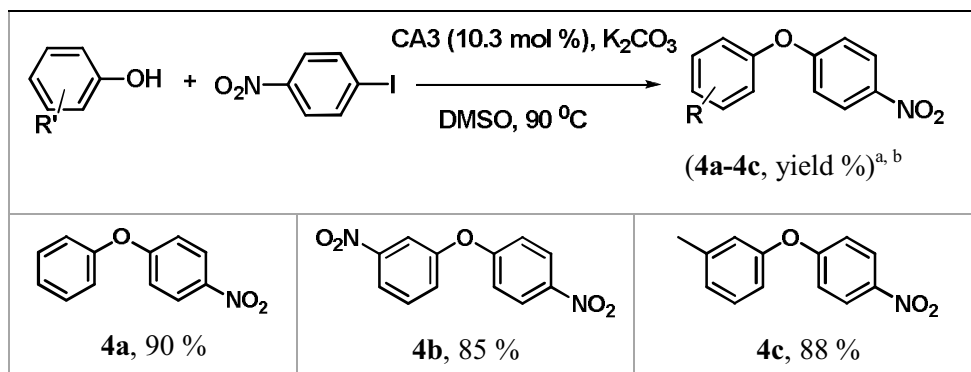
4a, 90 %   **4b**, 85 %   **4c**, 88 %

[a]phenol (1 mmol), 4-nitroiodobenzene (1 mmol), K_2CO_3 (0.08 g), DMSO (2 mL), 90 °C, 8 h, **CA3** (10.3 mol %), [b]isolated yield

The synthesis of C-N coupling products was attempted using the same optimized reaction conditions. Various aromatic amines and heterocyclic amines were selected for the coupling reaction with 4-nitroiodobenzene. Results are summarized in Table 4.8 which show that amine derivatives were successfully coupled with 4-nitroiodobenzene to obtain respective N-arylated products. In the case of reaction between 4-nitroiodobenzene and 2-aminophenol and 4-aminophenol, the catalyst selectively gave C-N coupling products instead of C-O coupling products with 79 % and 74 % yield respectively. It was also found that in the case of aromatic amines, electron withdrawing and electron donating substituent on the aromatic ring did not show much difference in the yield indicating that the nature of the substituent on aromatic ring had no significant effect on the yield. Heterocyclic amines also gave very good results for C-N coupling under the same reaction conditions.

Table 4.8 Ullmann type C-N coupling reactions

4d, 84 %	**4e**, 79 %	**4f**, 74 %
4g, 72 %	**4h**, 81 %	**4i**, 76 %
4j, 80 %	**4k**, 79 %	**4l**, 84 %

[a]amines (1 mmol), 4-nitroiodobenzene (1 mmol), K_2CO_3 (0.08 g), DMSO (2 mL), 90 °C, 8 h, **CA3** (10.3 mol %), [b]isolated yield

4.3.2.2 Mechanism for the formation of C-O and C-N coupling reactions

Since the original work of Ullmann and Goldberg, it has been known that various copper sources are effective in the C–C and C–X coupling reactions, ranging from Cu(I) to Cu(II) salts, and even including metallic copper. [9-16] It was generally agreed that, at a certain point of the reaction, the coordination of the nucleophile to the Cu atom was involved, activation of the aryl halide was the most troublesome aspect of the process. The actual

mechanism for the Ullmann reaction is not known with certainty, but there are a number of mechanisms proposed which include oxidative addition/reductive elimination,[50-52] single electron transfer mechanism,[53-54] mechanistic pathways involving sigma-bond metathesis[55-57] and π-complexation.[58-61] In the present catalytic system, because of the absence of any metal species on the **CA3**, a new pathway is proposed for the formation of C-O and C-N coupling products.
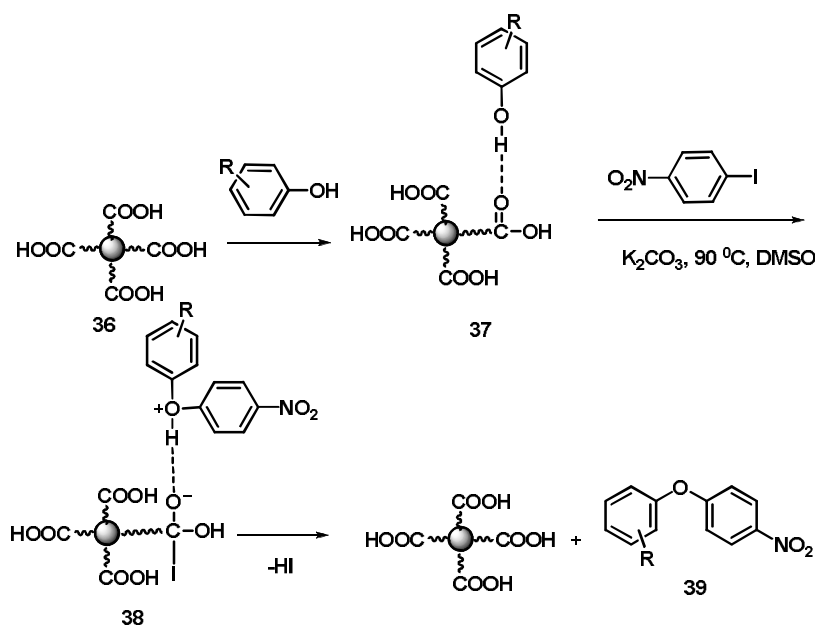
Scheme 4.5 Proposed mechanism for C-O coupling reaction

Scheme 4.5 shows the proposed mechanism for the formation of Ullmann type C-O coupling reaction. The intermediate **37** is formed by the hydrogen bonding interaction between phenol and C=O of the catalyst **CA3**. In the following steps electrophilic attack of carbocation to the oxygen atom of phenol and at the same time, nucleophilic attack of I⁻ to the C=O of catalyst occurs to form the intermediate **38**. This unstable species undergoes dissociation by the elimination of HI leading to the product **39**.

A similar mechanism was proposed for the formation of C-N products also and is shown in Scheme 4.6. Hydrogen bonded complex **40** was formed by the interaction of catalyst **CA3** and amine. In the next step, electrophilic attack of carbocation to the nitrogen atom of amine occurs and at the same time, nucleophilic attack of I⁻ to the C=O of catalyst takes place to form the intermediate **41**. This unstable species undergoes dissociation followed by the elimination of HI leading to the product **42**.
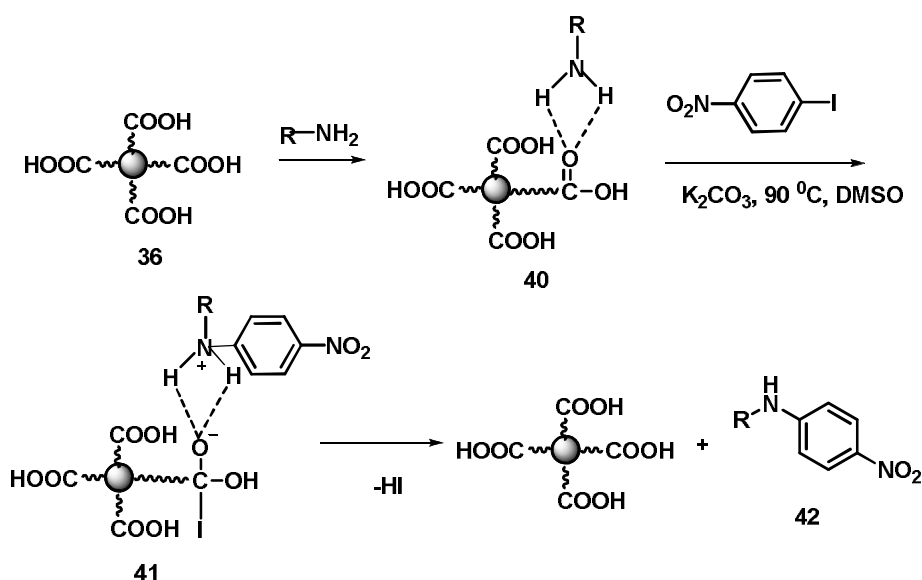
Scheme 4.6 Proposed mechanism for C-N coupling reaction

4.3.2.3 Reusability studies of C-O coupling and C-N coupling reaction

After the reaction, the catalyst was filtered from the reaction mixture and it was washed with DMSO and DCM to remove the complete removal of products from the catalyst surface. The catalyst was acidified with dil. HCl and washed well with water to remove any residual K_2CO_3 on the surface of the catalyst. The catalyst was dried at 120 °C under vacuum for

2 h and again used with fresh reactants using the same reaction conditions for both reactions. Results given in the Table 4.9 show that even after fourth cycle there was no appreciable change in the yield of the product.

Table 4.9 Reusability studies on C-O coupling and C-N coupling

No. of cycles	Yield (%)[a, b]	Yield (%)[c, d]
1	90	84
2	90	82
3	89	80
4	86	79

[a]phenol (1 mmol), 4-nitroiodobenzene (1 mmol), K_2CO_3 (0.08 g), DMSO (2 mL), 90 °C, 8 h, **CA3** (10.3 mol %), [b]isolated yield, [c]aniline (1 mmol), 4-nitroiodobenzene (1 mmol), K_2CO_3 (0.08 g), DMSO (2 mL), 90 °C, 8 h, **CA3** (10.3 mol %), [d]isolated yield

4.4 Conclusion

The first metal free catalyst for Ullmann type coupling for the formation of C-O and C-N coupled derivatives in high yields at relatively mild conditions was introduced. All the reported works were catalyzed by metal salts and ligands at high temperature. Dendritic carboxylic acid functions anchored on mesoporous silica was synthesized and characterized by various physiochemical techniques. Catalytic activity of the samples was tested for C-O and C-N coupling reactions. Three generations such as **CA1**, **CA2** and **CA3** were found to be effective catalysts for both the reactions. In both the reactions, 10.3 mol % of **CA3** gave excellent yield in the presence of DMSO as solvent and K_2CO_3 as base at 90 °C in 8 h. In the case of 2-aminophenol and 4-aminophenol, the catalyst selectively gave C-N coupling product with 79 % and 74 % yield instead of C-O products. It was found that the catalyst could be efficiently recycled and reused for further reactions up to fourth run without loss of efficiency for both the reactions.

Main advantages of the reactions using **CA3** as catalyst are: easy work up procedure, no side products, simple purification procedure, use of metal free catalysts; comparatively low temperature etc. The excellent catalytic performance, thermal stability, and separation of the catalyst by simple filtration make it a good heterogeneous system and useful alternative to other heterogeneous catalysts.

4.5   Experimental

4.5.1 Materials

All reagents were purchased from the local chemical suppliers and were used as received. All the solvents were purified according to the standard procedures.

4.5.2 Synthesis of dendritic carboxylic acid on mesoporous silica

Synthesis of carboxylic acid functionalized dendritic mesoporous silica was discussed in Chapter 2.

4.5.3 General procedure for the C-O and C-N coupling reactions

In a 25 mL round bottomed flask, a mixture of phenol/ amine (1 mmol), 4-nitroiodobenzene (1 mmol), K_2CO_3 (0.08 g) and 2 mL DMSO was taken. To this mixture, 10.3 mol % of **CA3** catalyst was added. The reaction mixture was heated at 90 °C for 8 h. Reaction was monitored by TLC. After completion of the reaction, the catalyst was separated by filtration and washed with DMSO and dichloromethane. The reaction mixture was diluted with water and the product was extracted with dichloromethane. The organic layer was dried over anhydrous sodium sulfate and solvent was removed under reduced pressure to give the pure product.

4.5.4 Reusability studies on C-O and C-N coupling reactions

After the completion of the reaction, the solid catalyst was separated from the reaction mixture by washing the catalyst with DMSO and DCM. The catalyst was acidified with dil. HCl and washed with water to remove any K_2CO_3 on the surface of catalyst. The catalyst was dried under vacuum at 120 °C for 2 h. The dried solid catalyst was weighed and added to a fresh reaction mixture of phenol/amine (1 mmol), 4-nitroiodobenzene (1 mmol), base K_2CO_3 (0.08 g) and 2 mL DMSO. The progress of the reaction was monitored by thin layer chromatography (TLC). The procedure was repeated for four reaction cycles.

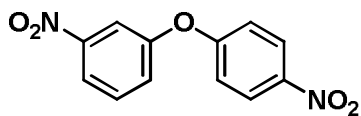### 4.5.5 Characterization of products

4.5.4.1 C-O coupled derivatives (Table 4.7)

4a. 1-Nitro-4-phenoxybenzene
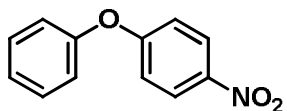
Colorless liquid, LC-MS (M^+) m/z 215; ^{1}H NMR (CDCl$_3$, 400 MHz) δ: 8.19 (d, J = 7.5 Hz, 2H), 7.40-7.46 (m, 2H), 7.25 (t, J = 7.3 Hz, 1H), 7.09 (d, J = 7 .0 Hz, 2H), 7.00 (d, J = 7.5 Hz, 2H); ^{13}C NMR (CDCl$_3$, 100 MHz) δ: 163.3, 154.6, 142.5, 130.3, 125.9, 125.4, 120.5, 117.0.

4b. 1-(3-Nitrophenoxy)-4-nitrobenzene

Yellow solid, m. p. 121°C (120-122 °C)[62], LC-MS (M^+) m/z 260; ^{1}H NMR (CDCl$_3$, 400 MHz) δ: 8.32-8.27 (m, 4H), 7.19-7.15 (m, 4H); ^{13}C NMR (CDCl$_3$, 100 MHz) δ: 160.6, 144.2, 126.2, 119.3.

4c. 1-Methyl-3-(4-nitrophenoxy) benzene
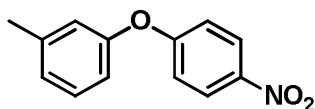
Colorless liquid, LC-MS (M$^+$) m/z 229; ^{1}H NMR (CDCl$_3$, 400 MHz) δ: 8.20-8.22 (m, 2H), 7.25-7.29 (m, 2H), 6.98-7.04 (m, 4H), 2.40 (s, 3H); ^{13}C NMR (CDCl$_3$, 100 MHz) δ: 163.9, 153.4, 142.7, 135.4, 131.6, 126.7, 121.2, 117.5, 21.2.

4.5.4.2 C-N coupled derivatives (Table 4.8)
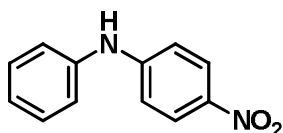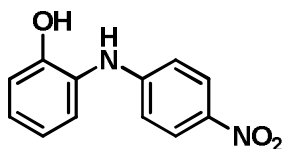
4d. 4-nitro-*N*-phenylaniline

Brown solid, m. p. 132 °C (132-134 °C)[63], LC-MS (M$^+$) m/z 214; ^{1}H NMR (CDCl$_3$, 400 MHz) δ: 8.11(d, *J* = 9.2 Hz, 2H), 7.38 (t, *J* = 8.0 Hz, 2H), 7.20-7.12 (m,3H), 6.93(d, *J* = 7.6 Hz, 2H), 6.34 (s, 1H); ^{13}C NMR (CDCl$_3$, 100 MHz) δ: 150.2, 139.6, 139.4, 129.7, 126.2, 124.6, 121.9, 113.6.

4e. 2-Hydroxy-*N*-(4-nitrophenyl) aniline

Dark brown solid, m. p. 141 °C (140-143 °C)[63], LC-MS (M$^+$) m/z 230; ^{1}H NMR (CDCl$_3$, 400 MHz) δ: 8.40 (d, *J* = 8.3 Hz, 1H), 8.91 (s, 1H), 8.23 (dd, *J* = 9.6 Hz, 1H), 7.45 (m, 1H), 7.37 (d, *J* = 7.6 Hz, 1H), 7.12 (m, 2H), 6.94 (m, 1H), 6.71 (d, *J* = 7.9 Hz, 1H), 5.71 (s, br, 1H); ^{13}C NMR (CDCl$_3$, 100 MHz) δ: 152.7, 143.4, 138.9, 136.2, 128.9, 126.6, 124.7, 121.4, 119.6, 116.1.

4f. 4-Hydroxy-*N*-(4-nitrophenyl) aniline
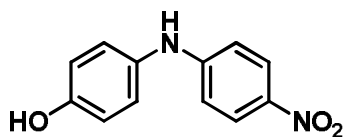
Colorless liquid, LC-MS (M$^+$) m/z 230; ^{1}H NMR (DMSO-d$_6$, 400 MHz) δ: 9.35 (s, br, 1H), 8.37 (s, br, 1H), 7.60 (t, *J* = 2.1 Hz, 1H), 7.51 (d, *J* = 8.0 Hz, 1H), 7.44 (t, *J* = 8.1 Hz, 1H), 7.25 (dd, *J* = 8.0, 1.5 Hz, 1H), 7.07 (d, *J* = 8.7 Hz, 2H), 6.84 (d, *J* = 8.7 Hz, 2H); ^{13}C NMR (CDCl$_3$, 100 MHz) δ: 152.2, 147.9, 145.5, 132.0, 128.4, 123.0, 118.8, 115.0.
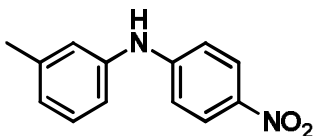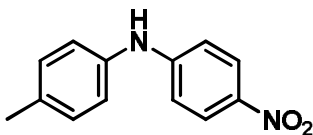
4g. 2-Methyl-*N*-(4-nitrophenyl) aniline
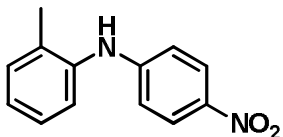
Brown solid, m. p. 132 °C (132-135 °C)[64], LC-MS (M$^+$) m/z 228; ^{1}H NMR (CDCl$_3$, 400 MHz) δ: 8.08 (d, *J* = 10.5 Hz, 2H), 7.18-7.31 (m, 4H), 6.72 (d, *J* = 9.5 Hz, 2H), 6.10 (s, 1H), 2.25 (s, 3H); ^{13}C NMR (CDCl$_3$, 100 MHz) δ: 151.3, 139.1, 137.5, 133.2, 131.4, 127.1, 126.2, 126.1, 124.7, 113.0, 17.8.

4h. 3-Methyl-*N*-(4-nitrophenyl) aniline

Brown solid, m. p. 134 °C (131-134 °C)[64], LC-MS (M$^+$) m/z 228; ^{1}H NMR (CDCl$_3$, 400 MHz) δ: 8.13, 8.10 (m, 2H), 7.25-7.27 (m, 1H), 6.97-7.02 (m, 3H), 6.94, 6.91 (m, 2H), 6.29 (s, br, 1H), 2.37 (s, 3H); ^{13}C NMR (CDCl$_3$, 100 MHz) δ: 150.3, 139.7, 139.6, 139.4, 129.5, 126.2, 125.5, 122.6, 119.0, 113.6, 21.4.

4i. 4-Methyl-*N*-(4-nitrophenyl) aniline

Brown solid, m. p. 132 °C (131-133 °C)[65], LC-MS (M$^+$) m/z 228; ^{1}H NMR (CDCl$_3$, 400 MHz) δ: 8.10, 8.07 (m, 2H), 7.21, 7.18 (m, 2H), 7.12, 7.09 (m, 2H), 6.88, 6.85 (m, 2H), 6.29 (s, br, 1H), 2.36 (s, 3H); ^{13}C NMR (CDCl$_3$, 100 MHz) δ: 150.8, 139.2, 136.6, 134.8, 130.2, 126.2, 122.6, 113.1, 20.9.
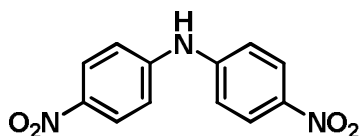
### 4j. 4-Methoxy-*N*-(4-nitrophenyl) aniline
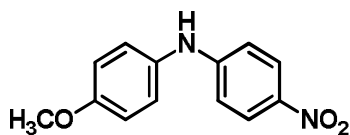
Brown solid, m. p. 150 °C (150-152 °C)[66], LC-MS (M$^+$) m/z 244; ^{1}H NMR (CDCl$_3$, 400 MHz) δ: 8.10, 8.07 (m, 2H), 7.17, 7.14 (m, 2H), 6.95, 6.92 (m, 2H), 6.78, 6.75 (m, 2H), 6.16 (s, 1H), 3.84 (s, 3H); ^{13}C NMR (CDCl$_3$, 100 MHz) δ: 157.4, 151.7, 139.0, 131.9, 126.3, 125.5, 114.9, 112.6, 55.5.

4k. Bis(4-nitrophenyl) amine

Yellow solid, m. p. 145 °C (146-148 °C)[67], LC-MS (M$^+$) m/z 259; ^{1}H NMR (CDCl$_3$, 400 MHz) δ: 8.2 (d, J = 8.8 Hz, 2H), 8.1 (d, J = 8.8 Hz, 1H), 7.21-7.26 (m, 3H), 6.63 (d, J = 8.9 Hz, 2H), 4.36 (s, br, 1H); ^{13}C NMR (CDCl$_3$, 100 MHz) δ: 126.2, 125.9, 117.2, 113.2.

4l. *N*-(4-Nitrophenyl) pyridin-2-amine
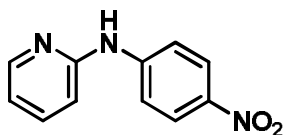
Yellow solid, m. p. 166 °C (166-169 °C)[68], LC-MS (M$^+$) m/z 215; ^{1}H NMR (CDCl$_3$, 400 MHz) δ: 8.34 (d, J = 4.2 Hz, 1H), 8.20 (d, J = 9.3 Hz, 2H), 7.64 (m, 3H), 6.94 (m, 3H); ^{13}C NMR (CDCl$_3$, 100 MHz) δ: 153.9, 148.5, 147.1, 141.4, 138.3, 125.9, 117.6, 116.9, 111.5.

References

[1]   M. B. Smith, *Organic Synthesis*, McGraw Hill, Boston, MA, 2002

[2]   J. Tsuji, *Transition Metal Reagents and Catalysts: Innovations in Organic Synthesis*, Wiley, Chichester, 2000.

[3]   (a) J. Tsuji, *Topics in Organometallic Chemistry: Palladium in Organic Synthesis*, Springer, New York, 2005. (b) A. de Meijere, F. Diederich, *Metal-Catalyzed Cross-Coupling Reactions,* Wiley-VCH, Weinheim, 2004.

[4]   M. Beller, C. Bolm, *Transition Metals for Organic Synthesis,* Wiley-VCH, Weinheim, 2004.

[5]   J. Magano, J. R. Dunetz, *Chem Rev.,* 2011*,* **111,** 2177.

[6]   F. W. Patureau, L. J. Gooben, *Copper-Mediated Cross-Coupling Reactions*, John Wiley & Sons, Hoboken, 2013.

[7]   D. Ma, Q. Cai, H. Zhang, *Org. Lett.*, 2003, **5**, 2453.

[8]   L. Kürti, B. Czako, *Strategic Applications of Named Reactions in Organic Synthesis*, Elsevier: Amsterdam, 2005.

[9]   F. Ullmann, J. Bielecki, *Chem. Ber.*, 1901, **34**, 2174.

[10]   F. Ullmann, J. Bielecki, *Ber Dtsch Chem Ges.*, 1901, **34**, 2174.

[11]   S. Mondal, *Chem. Texts.*, 2016, **2**, 17.

[12]   P. E. Fanta, *Synthesis*, 1974, 9.

[13]   T. Cohen, I. Cristea, *J. Am. Chem. Soc.*, 1976, **98**, 748.

[14]   F. Ullmann, *Chem. Ber.*, 1903, **36**, 2382.

[15]   F. Ullmann, P. Sponagel, *Chem. Ber.*, 1905, **38**, 2211.

[16]   I. Goldberg, *Chem. Ber.*, 1906, **39**, 1691.

[17]   W. R. H. Hurtley, *J. Chem. Soc.*, 1929, 1870.

[18]   J. Lindley, *Tetrahedron*, 1984, **40**, 1433.

[19]   Q. Cai, H. Zhang, B. Zou, X. Xie, W. Zhu, G. He, J. Wang, X. Pan, Y. Chen, Q. Yuan, F. Liu, B. Lu, D. Ma, *Pure Appl. Chem.*, 2009, **81**, 227.

[20]   H. Weingarten, *J. Org. Chem.*, 1964, **29**, 3624.

[21]   A. J. Paine, *J. Am. Chem. Soc.*, 1987, **109**, 1496.

[22]   H. Lin, D. Sun, *Org. Prep. Proced. Int.,* 2013, **45**, 341.

[23]   B. Karimi, F. K. Esfahani, *Chem. Commun.*, 2011, **47**, 10452.

[24]   L. D. Pachon, C. J. Elsevier, G. Rothenberg, *Adv Synth. Catal.*, 2006, **348**, 1705.

[25]   K. Layek, H. Maheswaran, M. L. Kantam, *Catal. Sci. Technol.*, 2013, **3**, 1147.

[26]   V. Calo, A. Nacci, A. Monopoli, P. Cotugno*, Chem. Eur. J.,* 2009, **200**, 1272.

[27]   T. D. Nelson, R. D. Crouch, *Org. React.,* 2004*,* **63**, 265.

[28]   S. K. Movahed, M. Fakharian, M. Dabiri, A. Bazgir, *RSC Adv.*, 2014, **4**, 5243.

[29]   K. Lee, P. H. Lee, *Tetrahedron Lett.*, 2008, **49**, 4302.

[30]   J. Cheng, L. Tang, J. Xu, *Adv. Synth. Catal.*, 2012, **352**, 3275.

[31]   J. Z. Jiang, C. Cai, *Colloids Surf. A: Physicochem. Eng. Aspects,* 2007, **305**, 145.

[32]   R. N. Dhital, C. Kamonsatikul, E. Somsook, H. Sakurai, *Catal. Sci. Technol.*, 2013, **3**, 3030.

[33] R. N. Dhital, C. Kamonsatikul, E. Somsook, K. Bobuatong, M. Ehara, S. Karanjit, H. Sakurai, *J. Am. Chem. Soc.*, 2012, **134**, 20250.

[34] (a) P. N. Craig, *In Comprehensive Medicinal Chemistry*, Drayton, C. J., Pergamon Press, New York, 1991. (b) S. A. Lawrence, *Amines: Synthesis, Properties and Application,* Cambridge University Press, Cambridge, 2004. (c) D. A. Horton, G. T. Bourne, M. L. Smythe, *Chem. Rev.*, 2003, **103**, 893. (d) R. Lygaitis, V. Getautic, J. V. Grazulevicius, *Chem. Soc. Rev.*, 2008, **37**, 770. (e) M. Liang, Chen, *J. Chem. Soc. Rev.,* 2013, **42**, 3453.

[35] W. Zhou, M. Fan, J. Yin, Y. Jiang, D. Ma, *J. Am. Chem. Soc.* 2015, **137**, 11942.

[36] S. Kumari, S. M. Abdul Shakoor, K. Bajaj, S. H. Nanjegowda, P. Mallu, R. Sakhuja, *Tetrahedron Lett.*, 2016, **57**, 2732.

[37] H. Li, J. Oppenheimer, M. R. Smith III, R. E. Maleczka Jr., *Tetrahedron Lett.*, 2016, **57**, 2231.

[38] M. Moorthy, B. Kannan, B. Madheswaran, R. Rangappan, *J. Porous Mater.*, 2016, **23**, 977.

[39] W. Long, W. Qiu, C. Guo, C. Li, L. Song, G. Bai, G. Zhang, H. He, *Molecules*, 2015, **20**, 21178.

[40] Y. Wan, J. Chen, D. Zhang, H. Li, *J. Mol. Cat. A Chem.*, 2006, **258**, 89.

[41] H. Li, J. Chen, Y. Wan, W. Chai, F. Zhang, Y. Lu, *Green Chem.*, 2007, **9**, 273.

[42] H. Li, W. Chai, F. Zhang, J. Chen, *Green Chem.*, 2007, **9**, 1223.

[43] (a) H. Wang, Y. Wan, *J. Mater Sci.*, 2009, **44**, 6553. (b) B. Yuan, Y. Pan, Y. Li, B. Yin, H. Jiang, *Angew Chem. Int. Ed.*, 2010, **49**, 4054.

[44] J. Cheng, G. Zhang, J. Du, L. Tang, J. Xu, J. Li, *J. Mater Chem.*, 2011, **21**, 3485.

[45] A. Kamal, V. Srinivasulu, B. N. Seshadri, N. Markandeya, A. Alarifi, N. Shankaraiah, *Green Chem.*, 2012, **14**, 2513.

[46] A. Monopoli, P. Cotugno, G. Palazzo, N. Ditaranto, B. Mariano, N. Cioffi, F. Ciminale, A. Nacci, *Adv. Synth. Catal.,* 2012, **354**, 2777.

[47] B. Karimi, H. Behzadnia, H. Vali, *Chem. Cat. Chem.*, 2014, **6**, 745.

[48] M. Dabiri, M. Shariatipour, S. K. Movahed, S. Bashiribod, *RSC Adv.*, 2014, **4**, 39428.

[49] X. Wu, L. Tan, D. Chen, X. Meng, F. Tang, *Chem. Commun.*, 2014, **50**, 539.

[50] G. M. Whitesides, W. F. Fisher, J. San Filippo, R.W. Bashe, H. O. House, *J. Am. Chem. Soc.*, 1969, **91**, 4871.

[51] G. M. Whitesides, P. E. Kendall, *J. Org. Chem.*, 1972, **37**, 3718.

[52] C. R. Johnson, G. A. Dutra, *J. Am. Chem. Soc.*, 1973, **95**, 7783.

[53] W. R. Bowman, H. Heaney, P. H. G. Smith, *Tetrahedron Lett.*, 1982, **23**, 5093.

[54] C. L. Jenkins, J. K. Kochi, *J. Am. Chem. Soc.*, 1972, **94**, 856.

[55] R. G. R. Bacon, H. A. O. Hill, *J. Chem. Soc.*, 1964, 1097.

[56] R. G. R. Bacon, H. A. O. Hill, *J. Chem. Soc.*, 1964, 1108.

[57] R. G. R. Bacon, H. A. O. Hill, *J. Chem. Soc.*, 1964, 1112.

[58] R. W. Turner, E. L. Amma, *J. Am. Chem. Soc.*, 1963, **85**, 4046.

[59] B. Nichols, M. C. Whiting, *J. Am. Chem. Soc.*, 1959, 551.

[60] T. K. Dargel, R. H. Hertwig, W. Koch, *Mol. Phys.*, 1999, **96**, 583.

[61] R. T. Stibrany, C. M. Zhang, T. J. Emge, H. J. Schugar, J. A. Potenza, S. Knapp, *Inorg. Chem.*, 2006, **45**, 9713.

[62] S. M. Baghbanian, H. Yadollahy, M. Tajbakhsh, M. Farhang, P. Biparva, *RSC adv.,* 2014, **4**, 62532.

[63] M. S. Wadia, D. V. Patil, *Synth. Commun.*, 2003, **33**, 2725.

[64] X. Tian, R. Wu, G. Liu, Z. Li, H. Wei, H. Yang, D. Shin, L. Wang, H. Zuo, *ARKIVOC,* 2011, **x**, 118.

[65] G. M. K. Hughes, B. C. Saunders, *J. Chem. Soc.,* 1956, **20**, 3814.

[66] J. McNulty, S. Cheekoori, T. P. Bender, J. A. Coggan, *Eur. J. Org. Chem.,* 2007, **9**, 1423.

[67] T. V.Sheremeteva, V. A. Gusinskaya, *Seriya Khimicheskay,* 1966, **4**, 695.

[68] J. Yang, Y. Lin, Y. Lin, F. J. Liao, *Org. Chem.*, 2004, **69**, 3517.

.....ೞೲ.....

DENDRITIC AMINE ON MESOPOROUS SILICA: FIRST ORGANO BASE CATALYST FOR PAAL-KNORR REACTION UNDER SOLVENT FREE CONDITION, A GREEN APPROACH

For the first time, a simple, highly efficient and ecofriendly approach for the preparation of pyrrole derivatives in the presence of dendritic amine on mesoporous silica under solvent free condition is reported. The three generations of dendritic amine on mesoporous silica (G0-G2) was synthesized through a stepwise growth technique and used as catalyst for Paal-Knorr reaction. The maximum yield was observed with third generation (G2) and the catalyst was easily separated from the reaction mixture. Studies showed that dendritic effect of amino groups on the catalyst and hydrogen bond activation was the driving force of the reaction pathway, which has led to the formation of pyrrole derivatives.

5.1 Introduction

Dendrimers are a class of monodisperse macromolecules with regular and highly branched three-dimensional architecture, with high surface functionality and widely used in the fields of medicinal chemistry for drug delivery, biosensors, metal adsorption and catalysis.[1] Recently, dendrimers are becoming increasingly important as an alternative macromolecular architecture to classical polymers in catalytic aplications.[2] 1,3,5-Triazine based dendrimers have received considerable attention due to their ease of synthesis, as well as low cost and chemo-selective reactivity of the starting material. Due to the importance of these compounds, several triazine-based dendrimers have been synthesized during the past decades.[3] The catalytic applications of these dendrimers are limited due to the difficulty in separation from the reaction mixture and recycling. To overcome these difficulties, heterogenizing these dendrimers on solid supports has received increased attention; because of available catalytically active sites, easy catalyst separation, long catalytic life, thermal stability, low hygroscopic properties, easy handling and reusability of catalysts.[4]

Mesoporous organosilica represents an exciting new class of hybrid organic-inorganic materials in different fields such as separation and catalysis. They have excellent properties such as high surface area, regular pore shape, large pore volume, narrow pore size distribution, chemical inertness, good thermal and mechanical stability combined with the properties of the organic moiety.[5] Therefore, these materials have been used for applications in metal cation adsorption, catalyst support, environmental science, and as sensors.[6-10] The high surface area of the

mesoporous silica materials together with strong covalent attachment at the mesopore surface which can make them promising candidates as support in heterogeneous catalysis.[11] So the fixation of active ligands via covalent bonding to a silica surface in order to be used in catalytic processes represents a remarkable aspect of the catalyst heterogenization. Because of these advantages, mesoporous silica was selected as the support for the dendrimeric growth.

Amino groups are important active centers in a base catalyst for many reactions. Primary and secondary amines were used as catalytic centers for organic transformations. First dendritic structure with terminal NH_2 groups synthesized by Tomalia was the PAMAM dendrimer (Figure 5.1(a)).[12] After PAMAM, PPI was synthesized (Figure 5.1(b)).[13] After that, several dendritic amines were synthesized by supported or non-supported way and used them as catalyst for several reactions.[14, 15]
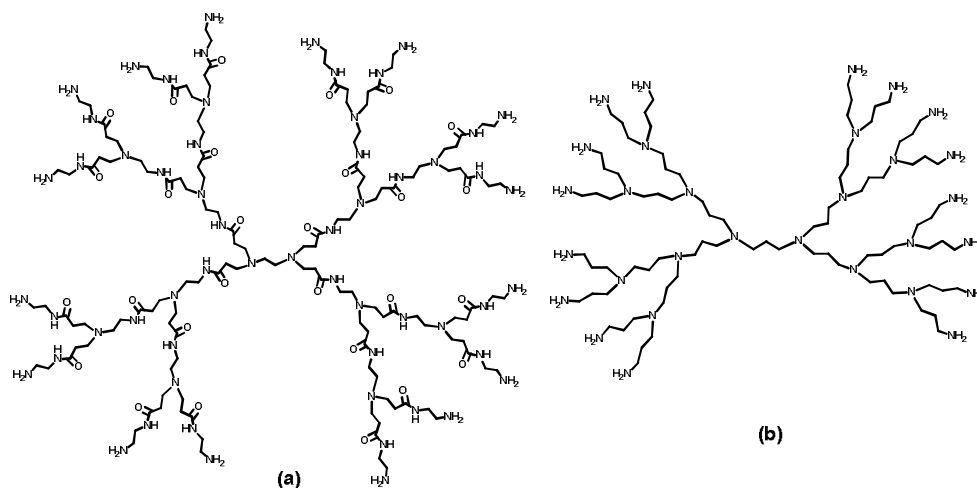

Figure 5.1 Structure of PAMAM (a) and PPI (b) dendrimers

Primary amines, secondary amines and ammonium salts on solid support can act as catalytic center for organic transformations. Figure 5.2 shows the recent amine functionalized catalysts used for different reactions.
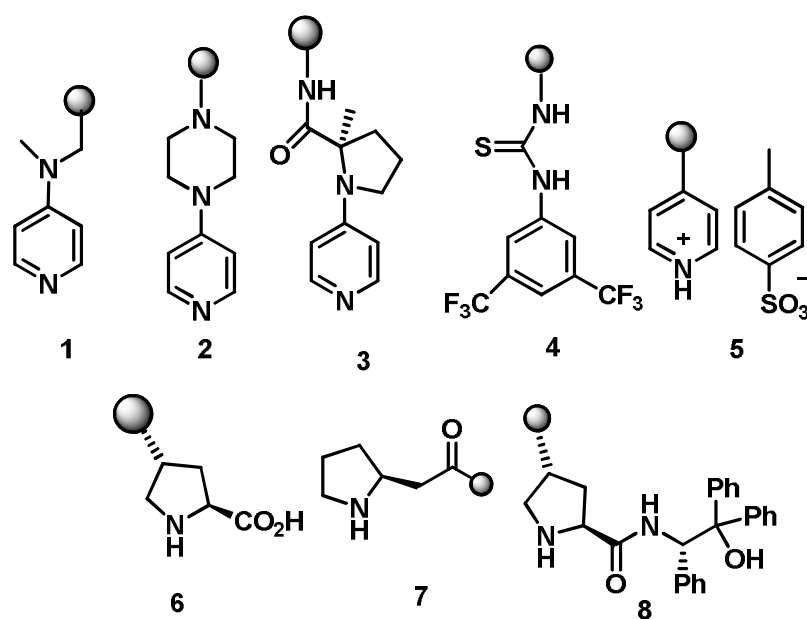

Figure 5.2 Structure of amine active catalyst supported on polymer support[16]

5.1.1 Paal-Knorr reaction

Pyrroles constitute an important class of heterocyclic compounds and numerous biological functions are believed to be mediated through pyrrole formation on macromolecules.[17] Pyrrole adducts on protein and nucleic acid bases have been associated with the active metabolites of several environmental toxicants and found in many bioactive natural molecules such as porphyrins, alkaloids and various drugs including many antiinflammatants, immunosuppressants, COX-2 inhibitors, analgesic,

antitubercular agents as well as the highly successful cholesterol-lowering drug atorvastatin.[18, 19] In addition, they have applications in molecular optics as conducting polymers and in solar cells and batteries, as antioxidant agents and gas sensors.[20] In view of their high significance, many methodologies have been developed for the construction of the pyrrole skeleton. These include the Hantzsch reaction,[21] conjugate addition reaction,[22] annulation reactions,[23, 24] aza-Wittig reaction,[25] Paal-Knorr reaction,[26] transition metal catalyzed cyclizations[27] and other multicomponent reactions.[28, 29] One of the most common approaches to pyrrole synthesis is the Paal-Knorr reaction in which 2,5-dicarbonyl compounds are converted to pyrrole via acid-mediated dehydrative cyclization in the presence of a primary amine (Scheme 5.1).[30] Traditionally, the reaction could effectively proceed in the presence of various acidic reagents such as Brønsted acids (e.g., H_2SO_4, HCl,) and Lewis acids [e.g., $Sc(SO_3CF_3)_3$, $Bi(NO_3)_3 \cdot 5H_2O$, $RuCl_3$, $InCl_3$, $SnCl_2 \cdot 2H_2O$] to promote the condensation.[31, 32] However, there are some limitations with these methodologies such as prolonged reaction times, elevated temperatures, use of hazardous organic solvents, expensive catalysts that are harmful to the environment, use of an additional microwave oven and unsatisfactory yields.[33-35]
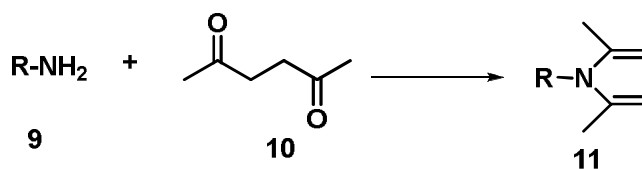
Scheme 5.1 Paal-Knorr reaction

Recently, the Paal-Knorr condensation has been carried out in the presence of a variety of solid acid catalysts such as silica-supported antimony (III) chloride,[36] β-cyclodextrin,[37] gold nanoparticles,[38] polystyrene-supported GaCl$_3$,[39] magnetic nanoparticle-supported glutathione using microwave irradiation technique,[40] nanometer-sized iridium particles[19] and indium-mediated reduction-triggered coupling reaction.[41] In 2015, Cho and coworkers reported the synthesis of pyrroles using aliphatic and aromatic primary amines with diketones excluding both the catalyst and solvent by applying simple stirring at room temperature within 24 h.[42] Microwave irradiation technique was widely reported using Montmorillonite K-10[43-46] with high conversion within short times. Banik, *et al.* reported the synthesis of medically important polyaromatic pyrroles such as N-alkyl(aryl)-2,4-diaryl-1*H*-pyrrol-3-ols[47] and aminomethyl derivatives of furan carboxylic acids[48] using polystyrene sulfonate as catalyst in aqueous medium.[49]

5.2 Objective of the present work

The development of new heterogeneous organocatalysts other than metal-based heterogeneous catalysts has attracted a lot of attention owing to their several advantages including the robustness, low toxicity without metal-leaching problem during the reactions, inertness to moisture and oxygen, and simple handling and storage capability.[50, 51] It was observed that Paal-Knorr reaction would be carried out only in the presence of acidic catalyst and there were no dendrimeric base catalysts developed for this reaction. Most of the reported works focused on the metal catalysed Paal-Knorr reaction. But main drawbacks associated with metal catalyst are toxicity, high cost, need for non commercial ligands and recycling. The

present intension was to develop metal free catalyst for Paal-Knorr reaction as an efficient alternative to the reactions performed by supported or non-supported metal catalyst. Metal free dendritic amine catalysts that are high in activity and reusability have been developed and were applied for Paal-Knorr reaction to meet the related challenges and tried to suggest a new pathway for these reactions.

5.3   Results and discussion

5.3.1 Synthesis of dendritic amine on mesoporous silica

Chlorine functionalized mesoporous silica (**CMS 1**) was synthesized using 3-chloropropyltrimethoxysilane and TEOS by co-condensation method using P123 as surfactant. Dendrimer growth on **CMS 1** was done using bis(3-aminopropyl)amine and cyanuric chloride by step wise growth technique (**G0-G2**). **CMS 1** was reacted with the Schiff's base of BAPA. The Schiff's base was cleaved using 6 N HCl. The sample was denoted as **G0**. The **G0** was reacted with cyanuric chloride in the presence of dry THF at 0 °C (**G0.5**). This was again reacted with Schiff's base of BAPA and cleaved using 6 N HCl (**G1**). Repeating the preceding procedure led to the product **G2**. The structures of **G0**, **G1** and **G2** are shown in the Scheme 5.2. All three generations were successfully characterized by IR spectroscopy, thermogravimetric analysis, low angle XRD, nitrogen adsorption-desorption analysis and solid state ^{13}C NMR spectrum.
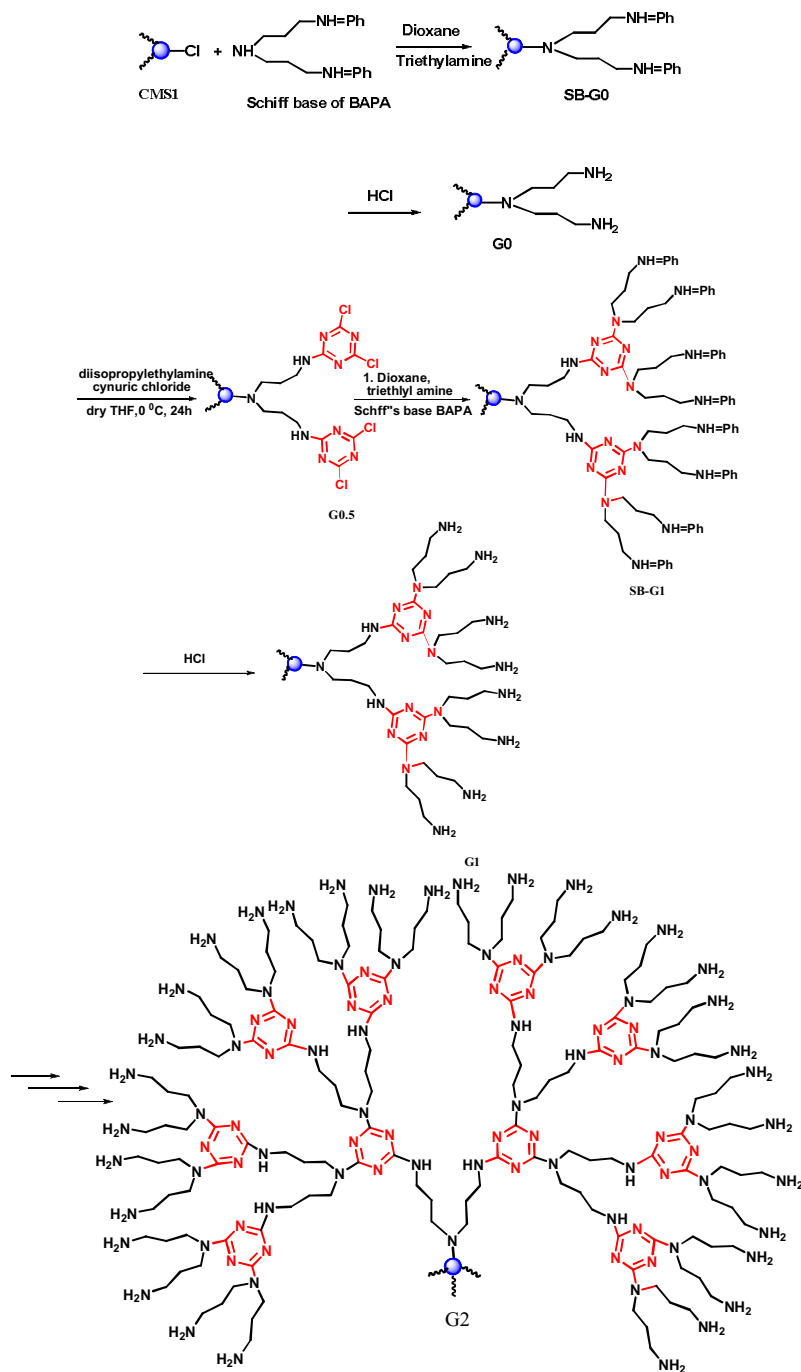
Scheme 5.2 Schematic representation of step-wise growth of the dendritic amine on CMS1 (**G0-G2**)

The amount of amino groups grafted on **G0-G2** dendrimers were quantified by acid–base titration method and the results are summarized in Table 5.1. From the results, the nitrogen content was found to increase upon step-wise growth of amine dendrimer on mesoporous silica, which showed that the grafting, and/or growth of amine dendrimer was successfully done, resulting in increased peripheral amino groups.

Table 5.1 Estimation of amino capacity of **G0-G2**

Sample	Amino capacity (mmol/g)
G0	9.8
G1	12.2
G2	16

5.3.2 Characterization of dendritic amine on mesoporous silica

5.3.2.1 FTIR Studies

The FTIR spectrum of chlorine functionalized silica (**CMS 1**) (Figure 5.3(a)) showed a band at 2951 cm^{-1} indicating the symmetric and asymmetric stretching vibration of CH bond. The band observed at 700 cm^{-1} showed the characteristic vibration of C-Cl bond. The characteristic peaks of silica were observed at 1100-1000 cm^{-1} corresponding to the intense silicon-oxygen covalent bond vibrations and the symmetric stretching vibrations of Si-O-Si appear at 800 cm^{-1}. The bands obtained around 3400-3500 cm^{-1} and 1630 cm^{-1} were associated with stretching vibration of unreacted Si-OH group and adsorbed H$_2$O. In **SB-G0**, a new band at 1677 cm^{-1} gave the proof for the incorporation of Schiff's base of BAPA on silica surface and also disappearance of 700 cm^{-1} was a good sign for the reaction between C-Cl and Schiff's base of BAPA. In **G0**, the absence of the peak at 1677 cm^{-1}

strongly supported the complete cleavage of Schiff's base from BAPA amine grafted on silica. In Figure 5.4(d) in addition to the above mentioned vibrations, new bands at 1570 cm^{-1} (C-N) and 700 cm^{-1} (C-Cl) are good evidences for the presence of triazine fragment on the surface of silica. In **SB-G1**, a new band at 1680 cm^{-1} gave the confirmation for the attachment of Schiff's base of amine on **G0** and disappearance of this peak in **G1** (Figure 5.4(f)) indicated the complete cleavage of Schiff's base from silica.
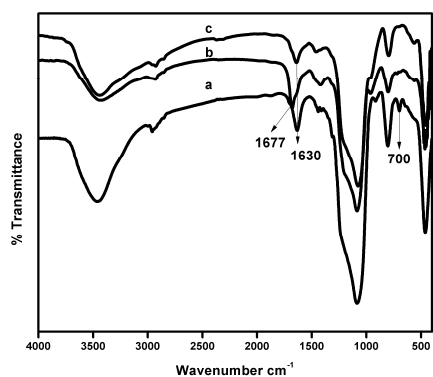

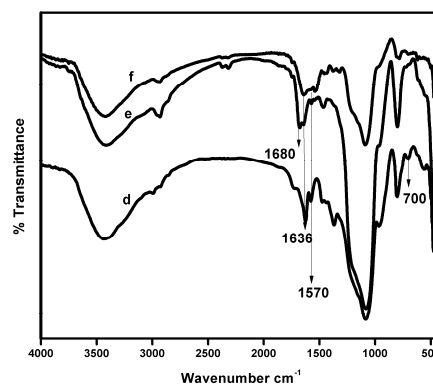**Figure 5.3** IR spectra of (a) **CMS 1** (b) **SB-G0** (c) **G0**

Figure 5.4 IR spectra (d) **G0.5** (e) **SB-G1** (f) **G1**
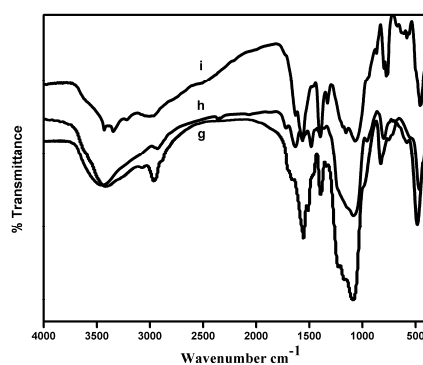

Figure 5.5 IR spectra of (g) **G1.5** (h) **SB-G2** (i) **G2**

In the Figure 5.5, the overall intensities of C-N stretching of triazine, the C-N stretching of BAPA and NH_2 stretching vibrations were increased compared to Figure 5.3 and Figure 5.4. This gives good support for the stepwise growth of dendrimer generation on silica surface.

5.3.2.2 TG-DTG analysis

The thermogravimetric analysis of **G0-G2** was performed under nitrogen atmosphere. For all the samples, a slight weight loss was observed below 100 °C, which is credited to adsorbed water. The decomposition of the **G0-G2** dendrimers starts at 200 °C, exhibited considerable weight loss between 250 °C and 400 °C, that corresponding to the decomposition of the amine component (Figure 5.6 and 5.7). In the case of **G1** and **G2**, one more decomposition was observed above 400 °C. It is connected with the decomposition of the residual alkyl fragments. These results revealed the incorporation and integrity of designed dendritic groups on the surface of silica.
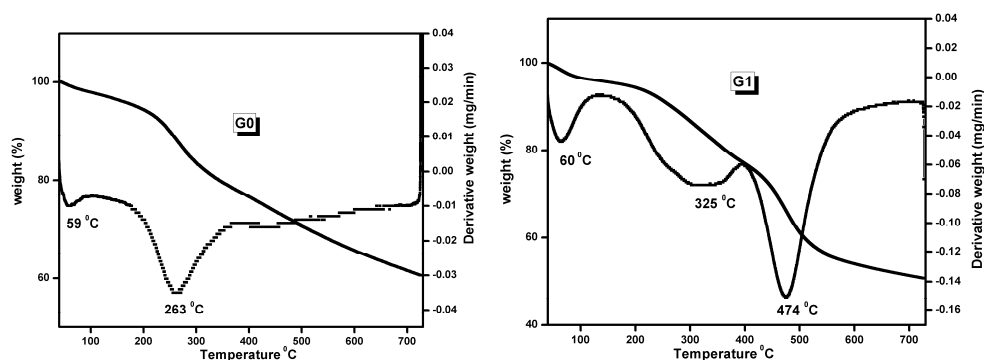

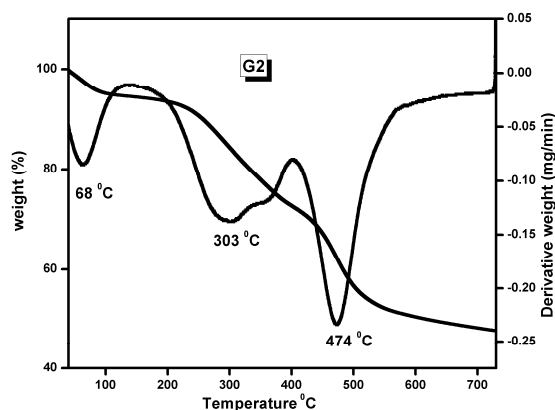**Figure 5.6** TG-DTG analysis of (a) **G0** and (b) **G1**

Figure 5.7 TG-DTG analysis of **G2**

5.3.2.3 XRD analysis

Figure 5.8 shows the powder low angle XRD patterns of **CMS 1** and (**G0-G2**) materials. The **CMS 1** exhibited three well-resolved XRD peaks in the region of $2\theta = 0.5\text{-}2.0°$, which can be indexed to the (100), (110), and (200) diffractions, characteristic of the 2D hexagonal symmetry. The peak positions of **G0** and **G1** samples remained constant after the dendritic growth, suggesting high stability of the mesoporous silica support. However, the incorporation of amino groups causes slight broadness of peaks and a decrease in diffraction peak intensity, indicating a decrease of crystallinity, but not a collapse of the pore structure of mesoporous materials. But in the case of **G2**, the disappearance and/or absence of peaks might be assigned for the destruction of ordered nature of the mesoporous silica through step-wise growth of dendritic amino groups.
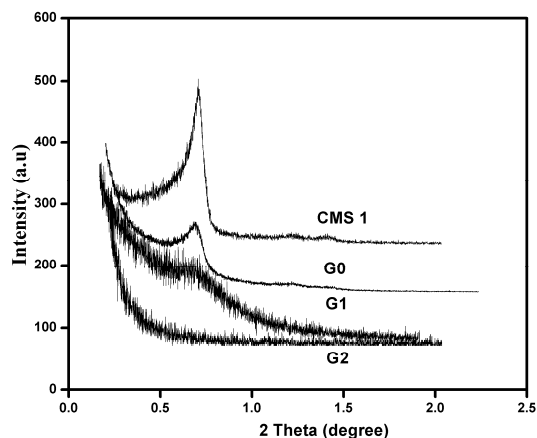
Figure 5.8 Low angle XRD analysis of (a) **CMS 1**
(b) **G0** (c) **G1** (d) **G2**

5.3.2.4 Surface studies using BET method

The surface area of all the three generations (**G0-G2**) was evaluated using BET method, the pore size by BJH method (isotherms with hysteresis).
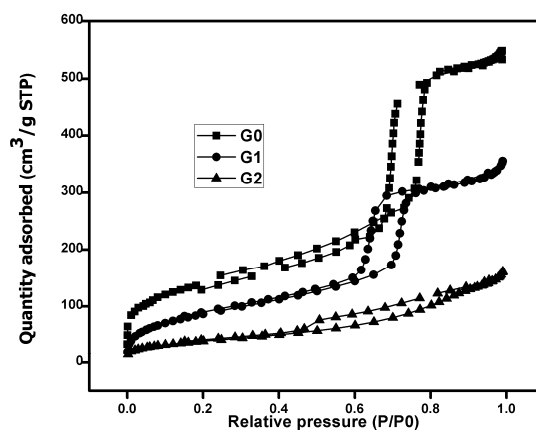

Figure 5.9 N$_2$ adsorption/desorption isotherms of
(a) **G0** (b) **G1** (c) **G2**

The nitrogen adsorption/desorption isotherm of **G0** and **G1** show type IV isotherm with a sharp step up in a narrow range of relative pressure

(P/P$_0$=0.6-0.9) arising from the capillary condensation of nitrogen in the mesopores which proved the mesoporous nature of the synthesized silica support (Figure 5.9). But for **G2**, there was change in the shape of isotherm, which was almost flat. This may be due to the destruction of mesopore of the support with incorporation of dendritic amino groups. Specific surface area, pore volume and pore diameter of **G0-G2** samples was given in the Table 5.2. Such significant decrease of the properties upon grafting is due to pore filling with dendritic amino groups, which was also supported by the XRD and TG results.

Table 5.2 Surface properties of amine functionalized mesoporous silica

Sample	Surface area (m^2/g)	Pore volume (cm^3/g)	Pore diameter (nm)
G0	308	0.54	5.6
G1	193	0.35	3.1
G2	142	0.25	2.9

5.3.2.5 CP-MAS ^{13}C NMR spectrum

^{13}C CP-MAS NMR spectrum is also used to confirm the presence of organic functionalization on the silica surface. Figure 5.10 shows three main peaks below 100 ppm, that is, 45, 20 and 9 ppm corresponding to the carbons attached from the 3-chloropropyltrimethoxysilane. Peak at 63 ppm corresponds to the unreacted methoxy carbon present on silica surface. The other extra resonance peaks at 164, 140, 128 ppm are recognized to different carbon environments in the dendritic amine part, showing the successful growth of dendritic amine on silica surface.
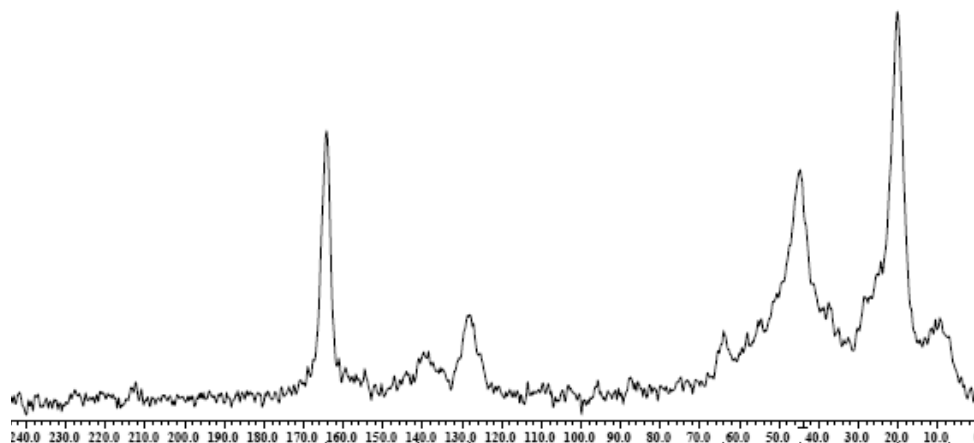
Figure 5.10 Solid state ^{13}C NMR Spectrum of **G2**

5.3.2.6 SEM analysis

SEM images of **CMS 1** and **G2** are shown in the Figure 5.11. When compared with C**MS 1**, the SEM micrographs revealed that the smooth and spherical surface of the **CMS 1** got disrupted and became crushed into irregular clusters after dendritic growth.
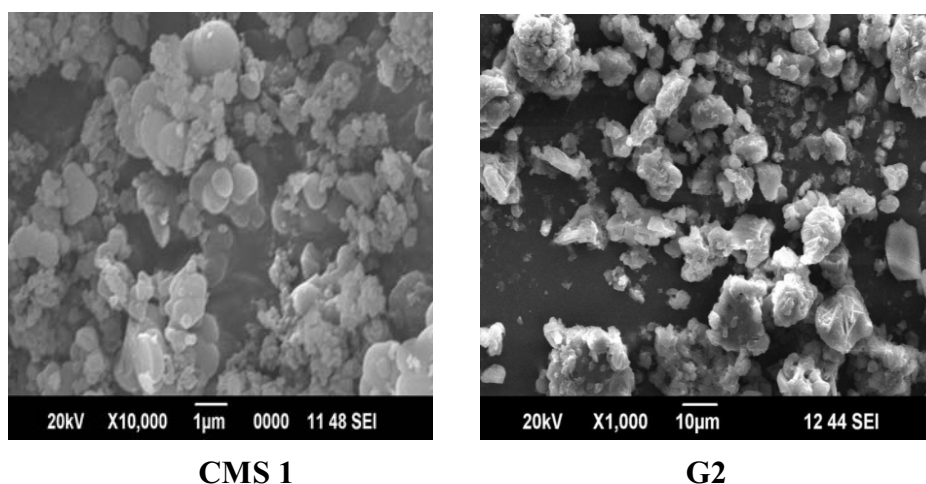

CMS 1   **G2**

Figure 5.11 SEM image of **CMS 1** and **G2**

The results of FTIR, thermogravimetric analysis, low angle XRD, BET isotherm and solid-state ^{13}C NMR spectroscopy, confirmed the incorporation of dendritic amine on mesoporous silica surface.

5.3.3 Catalytic application of dendritic amine on mesoporous silica

The catalytic properties of **G0-G2** materials were investigated using Paal-Knorr reaction as a test reaction (Scheme 5.3). Primarily, the reaction between hexane-2,5-dione and benzyl amine was chosen as a model reaction under solvent free condition to screen for the optimal reaction conditions at room temperature. A preliminary investigation on the reaction between hexane-2,5-dione and benzyl amine was done in the absence of catalyst in which the target product was detected only in trace amounts after 24 h (Table 5.3, entry 1). This result indicated the necessity of a catalyst for this reaction. The reaction was conducted in the presence of 0.003 g of **CMS 1**, but no product was obtained after 2 h. However 30 % yield was observed after 24 h similar to what was obtained in the absence of catalyst (Table 5.3, Entry 2). This means that **CMS 1** is inactive towards this reaction.
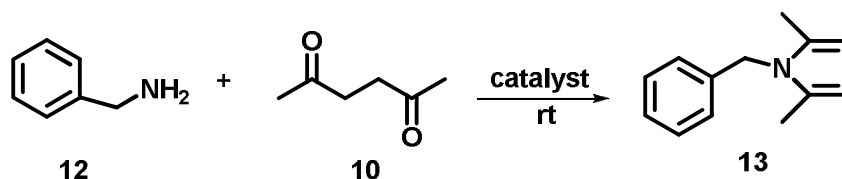
Scheme 5.3 Scheme for Paal-Knorr reaction

The effect of different generation of catalysts **G0**, **G1** and **G2** (4.8 mol % each) on the reaction was examined. The result showed that **G2** was a highly active catalyst achieving very good yield of the pyrroles

within 2 h (Table 5.3, entries 3-5). This result indicated that catalyst with high amino group capacity was needed for achieving high conversion. Encouraged by the aforementioned result, other reaction conditions were investigated. First, the influence of the amount of **G2** on the conversion was examined (Table 5.3 entries 6-9). The best result was obtained in the presence of 4.8 mol % of **G2** with an yield of 92 % and further increase in the amount of catalyst did not increase the yield significantly. As expected, increasing the catalyst concentration led to an enhancement in the yield of the reaction.

Table 5.3 Optimization of reaction conditions

Entry	Name of catalyst	Amount of catalyst (g)	Amount of catalyst (mol %)	Solvent	Yield (%)[a, b]
1	no catalyst	-	-	-	30 (24 h)[c]
2	CMS 1	0.003	-	-	No product[d], 30 (24 h)[c]
3	G0	0.003	4.8	-	73
4	G1	0.003	4.8	-	84
5	**G2**	**0.003**	**4.8**	**-**	**92**
6	G2	0.001	1.6	-	75
7	G2	0.002	3.2	-	82
8	**G2**	**0.003**	**4.8**	**-**	**92**
9	**G2**	**0.004**	**6.4**	**-**	**92**
10	G2	0.003	4.8	Methanol	83
11	G2	0.003	4.8	THF	79
12	G2	0.003	4.8	Toluene	84
13	G2	0.003	4.8	DCM	81
14	G2	0.003	4.8	Acetonitrile	80
15	G2	0.003	4.8	Water	72
16	**G2**	**0.003**	**4.8**	**No solvent**	**92**
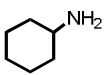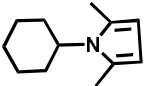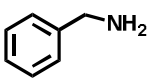
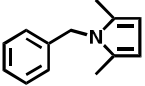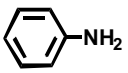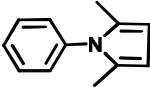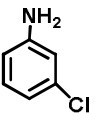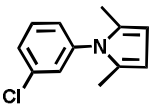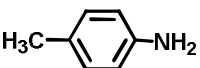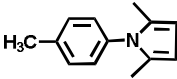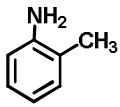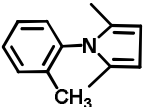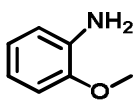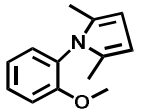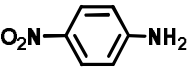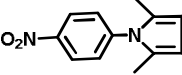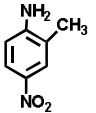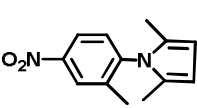[a]benzyl amine (1 mmol), 2,5-hexanedione (1 mmol), room temperature, 2 h, [b]isolated yield. [c]Reaction was monitored for 24 h, [d] no product after 2 h
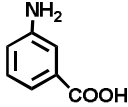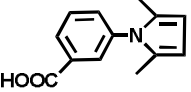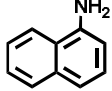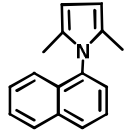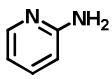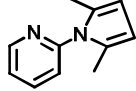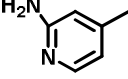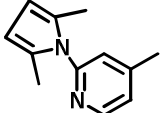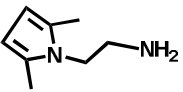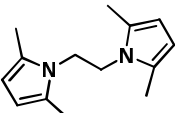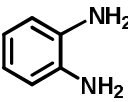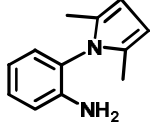
The effect of solvents on the reaction is generally an important variable that must be considered in detail. Solvents such as methanol, THF, toluene, DCM, acetonitrile, and water as well as solvent free condition were used (Table 5.3, entries 10-16). Results showed that solvent free condition was the most effective one for the formation of the desired product in high yield. This is because of the peculiar property of the catalyst that makes easy adsorption of reactants on the surface of the catalyst and high concentration of available catalytically active amino sites for the reactants.

Besides, it was also observed that even at room temperature, reactions provided equally high yields within 2 h. Thus, further reactions were carried out with simple stirring at room temperature. Because of the higher reactivity of amines, molar ratio for both reactants has been taken as 1:1, this makes the reaction selective and quantitative and no further purification of the products was required.

With the optimum conditions in hand, Paal-Knorr reaction of 2,5-hexanedione with several aliphatic primary amines, various aromatic amines, heterocyclic amines and diamines were examined to explore the potential of the present procedure and the results are summarized in Table 5.4. The activity of aliphatic cyclic primary amine such as cyclohexylamine towards Paal-Knorr reaction at room temperature was evaluated (Table 5.4, entry 1). It gave 97 % yield for this reaction. In the case of benzyl amine, it showed 92 % yield (Table 5.4, entry 2).

Table 5.4 Synthesis of N-substituted pyrroles catalyzed by G2

Entry	Primary amine	Product	Yield (%)[a, b, (c)]
1			97 (100)
2			92 (100)
3			89 (100)
4			80 (84)
5			92 (99)
6			90 (80)
7			86 (88)
8			No product
9			No product

10			83 (81)
11			82 (70)
12			90 (100)
13			No product
14			76[d] , 86[e]
15			100[d], no product[e]

[a]amine (1 mmol), 2,5-hexanedione (1 mmol), room temperature, 2 h, 4.8 mol % (**G2**), [b]isolated yield, [c]GC-MS analysis, [d]mono pyrrole product (amine (1 mmol), 2,5-hexanedione (1 mmol)), [e]bispyrrole product (amine (1 mmol), 2,5-hexanedione (2 mmol)).

It was encouraging to work on aromatic amines having electron donating substituent and electron withdrawing substituent (Table 5.4, entries 3-10). Substituted anilines with electron-rich groups enhanced the

percentage conversion when compared to anilines with electron withdrawing substituent. Nitro substituted aniline (Table 5.4, entries 8, 9) did not give the expected pyrrole derivatives. The reaction of 1-aminonaphthalene with diketone also proceeded successfully to give the desired product in good yield (Table 5.4, entry 11). Additionally, the reactivity of heterocyclic amines (Table 5.4, entries 12, 13) was also examined in the presence of **G2**. 2-Aminopyridine, gave 2-(2,5-dimethyl-1*H*-pyrrol-1-yl) pyridine with 100 % conversion, but 2-amino-4-methyl pyridine did not respond to this reaction.

Paal-Knorr reaction of diamines such as ethylene diamine, Benzene-1,2-diamine were also studied (Table 5.4, entries 14, 15). Using a diamino compound as the reactant with 2,5-hexanedione resulted in the formation of multiple products such as mono pyrrole and bispyrrole. It was observed that the reaction between ethylene diamine and 2,5-hexanedione in 1:1 molar ratio resulted in the formation of mono pyrrole as the major product and small amount of bispyrrole was also observed. When shifting the molar ratio of 2,5-hexanedione and ethylene diamine to 2:1, it gave only bispyrrole product in high yield. But in the case of Benzene-1,2-diamine, it gave only mono pyrrole as the major product in both the molar ratios.

There are recent reports of carrying out this reaction in the presence of other catalysts under heterogeneous conditions. The data presented in Table 5.5 show that the present catalyst has great advantage over the reported ones in terms of reaction rate, product yield, amount of catalyst used, reaction condition and catalyst reusability.

Table 5.5 Comparative study of present catalyst with reported catalysts

S.l. No.	Catalyst/Solvent	Temperature/ Time	Catalyst reusability	Yield (%)
1	Vitamin B1(5 mol %)/ Ethanol	rt/ 1 h	-	90[52]
2	[MIMBS]$_3$PW$_{12}$O$_{40}$ (5 mol %)/ CH$_3$CN	80 °C/ 2 h	-	93[53]
3	Aluminum tris (dodecyl sulfate) trihydrate (2.5 mol %) / water	rt/ 3 h	-	96[54]
4	Urea (glycerol)-Choline Chloride	80 °C/ 24 h	-	87[55]
5	(c-Fe$_2$O$_3$@SiO$_2$-OSO$_3$H) (20 mg)	60 °C/ 3 h	5 runs	90[56]
6	MgI$_2$etherate (3 mol %)	70 °C/ 2 h	-	93[57]
7	FePO$_4$ (10 mol %)	rt/ 8 h	-	93[58]
8	Citric acid (1 mol %) / ball mill (30 Hz)	rt/ 30 min	-	71[31]
10	G2 (4.8 mol %)	rt/ 2 h	5 runs	92 (present work)

In order to check whether the silica support has any role in Paal-Knorr reaction, the reaction was conducted in the presence of PEG-NH$_2$.[59] Reaction was carried out at room temperature, using benzylamine and 2,5-hexanedione in the molar ratio of 1:1, in the presence of 4 mol % PEG-NH$_2$ catalyst under solvent free condition. It was found that 95 % yield was obtained for this reaction within 2 h. This is due to the homogeneous nature of PEG-NH$_2$ catalyst. After the reaction, catalyst was removed by washing with water and product was collected in dichloromethane. These results reveal that the amino groups would be the only active sites for this reaction and mesoporous silica support has no role.

5.3.4 Mechanism of the formation of N-substituted pyrroles

The mechanism of the formation of N-substituted pyrroles from cyclocondensation of primary amines with 2,5-dicarbonyl compounds is not well understood. Literature studies showed that different types of mechanisms were reported. Very recently, Abbat *et al*. reported hemiaminal pathway for the Paal-Knorr pyrrole synthesis under proton catalysis conditions.[60] Accordingly, here a plausible mechanism is proposed for the **G2** catalyzed double condensation of hexane-2,5-dione with primary amine and is given in Scheme 5.4.
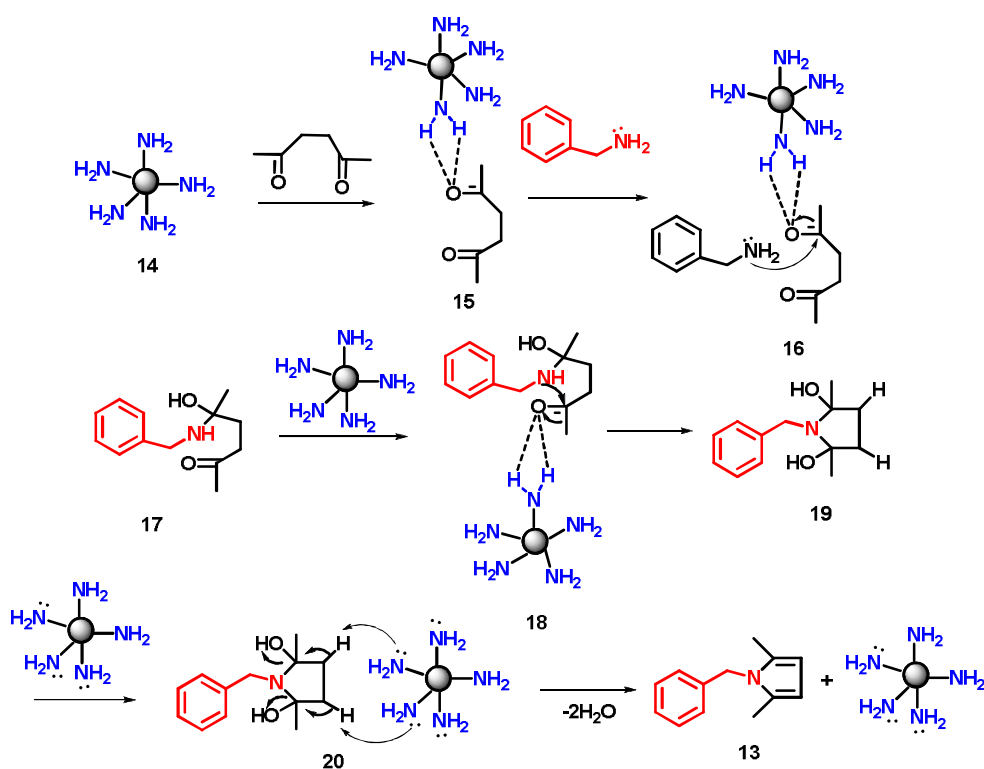
Scheme 5.4 Proposed Mechanism for the formation of N-substituted pyrroles.

Due to the dendritic effect of amino groups present on the catalyst **G2**, it interacts with oxygen atom of carbonyl groups of the dicarbonyl compound to form the hydrogen bonded activated complex **15** and **18**.[61] Amino group of primary amine reacts with these activated carbonyl complex **15** to form the hemiaminal **17**. Nucleophilic attack of the NH group of hemiaminal on the activated carbonyl carbon produces the intermediate 2,5-dihydroxy-2,5-dialkyl-N-alkyl-hydropyrrole **19**. Due to high basicity of **G2**, it abstracts the hydrogens from intermediate **20** followed by the subsequent loss of two molecules of water leading to the formation of the pyrrole **13** and regeneration of catalyst **G2**.

5.3.5 Reusability of the catalyst

Finally, the reusability of the amine catalyst **G2** was studied for this reaction. As shown in Table 5.6, the catalyst was recycled for subsequent runs using the same procedure. It was found that the catalyst was still active even in the fifth run without significant loss of activity. The recovery of the catalyst was very easy. Product was soluble in dichloromethane, while the catalyst remained insoluble. After completion of the reaction, the catalyst was filtered from the reaction mixture, washed with dichloromethane and ethanol, dried at 120 °C for 2 h and reused in subsequent runs.

Table 5.6 Reusability studies

No. of cycles	Yield (%)[a, b]
1	92
2	92
3	90
4	88
5	87

[a]benzylamine (1 mmol), 2,5-hexanedione (1 mmol), room temperature, 2 h, 4.8 mol % (**G2**), [b]Isolated yield.

5.4   Conclusion

In summary, the first dendritic organo base catalyst was introduced for Paal-Knorr reaction for the synthesis of pyrrole derivatives. The presence of high concentration of amino groups on **G2**, makes this powerful base catalyst for the reaction within a short time. Results showed that the main reason for the formation of pyrrole derivatives is the dendritic effect of amino groups present on the catalyst. Pyrroles with different aromatic substitutions, mono pyrrole and bis pyrrole derivatives were obtained in high yield. Reusability of the **G2** catalyst was achieved without significant loss of catalytic activity up to fifth cycle. The catalyst was found to obey the principles of green chemistry. The green aspects of the present method are: use of metal free catalyst, low catalyst loading, shorter reaction time, organic solvents are not needed, facile work-up, purification of the products by non-chromatographic methods, the excellent yield of the products, reaction proceeding at room temperature and the reusability of the catalyst.

5.5   Experimental

5.5.1 Materials

Cyanuric chloride, diisopropylethylamine, 2,5-hexanedione and bis(2-aminopropyl)amine (BAPA) were purchased from Aldrich and used without further purification.

5.5.2 Synthesis of chlorine functionalized mesoporous silica (CMS 1)

Detailed synthetic procedure for the synthesis of **CMS 1** was given in Chapter 2

5.5.3 Step-wise growth of BAPA dendrimer over CMS 1

5.5.3.1 Synthesis of Schiff's base of bis(3-aminopropyl)amine

Schiff's base of bis(3-aminopropyl)amine was prepared by mixing one equivalent of bis(3-aminopropyl)amine (10 mmol) with 2 equivalents of benzaldehyde (20 mmol) at room temperature. Stirring of the mixture was continued until only oil remained and was used for reaction without further purification. Successful completion of the reaction was confirmed by the formation of brown viscous oil.Yield 100 %, brown viscous oil.

5.5.3.2 Incorporation of Schiff's base on CMS 1

To preswollen **CMS 1** (3 g) in 1,4-dioxane (25 mL), suspension of Schiff's base of BAPA (80 mmol, 2.32 mL) was added in the presence of triethylamine (20 mL) and heated at 100 °C for 48 h with occasional stirring. Excess ligand present in the reaction medium acted as acceptor of eliminated HCl resulting in the formation of yellow crystals of ligand HCl complex. The solid materials were filtered off, washed well with water and with dioxane. After solvent extraction with dioxane for 48 h, the silica was collected, washed with ether and dried under vacuum. Yield: 2.8 g, Yellow powder, IR (KBr, cm^{-1}): 1677 (C=N stretching**)**

5.5.3.3 Schiff's base cleavage

The removal of phenyl groups of Schiff's base on silica was achieved by stirring with 6 N HCl at 60 °C for 12 h. Benzaldehyde was liberated as oil during hydrolysis and yellow silica powder formed was filtered off, washed with NaOH solution (5 × 7.5 mL) and with water (5 × 7.5 mL) until the solution was neutral. The silica was washed with methanol, ether, and toluene and dried under vacuum at 80 °C and denoted as **G0**.

Step-wise growth of BAPA dendrimer was carried out over **G0** by similar procedure reported in the literature.[1] Briefly, cyanuric chloride (5.5 g, 30 mmol) and diisopropylethylamine (7.8 mL) in THF (100 mL) was stirred at 0 °C for 2 h. 2.5 g of **G0** was added to the above mixture under stirring and left to react at 0 °C for 20 h. The solid was filtered and washed twice, in series with 20 mL of methanol, 20 mL dichloromethane (DCM) and 20 mL tetrahydrofuran (THF). Subsequently, washed solid was grafted with Schiff's base of BAPA (1 mL, 6.68 mmol) by refluxing in dioxane (25 mL) and triethylamine (25 mL) and heated at 100 °C for 48 h with occasional stirring. The solid materials were filtered off, washed well with water and with dioxane. After solvent extraction with dioxane for 48 h, the silica was collected, washed with ether and dried under vacuum and Schiff's base was cleaved using the same procedure given above. This solid is referred to as **G1**. The yield of **G1** is found to be 2.3 g. Repeating the preceding procedure led to the product **G2** with yield 2.1 g.

G0: Yield 2.7 g, Yellow powder; IR (KBr, cm^{-1}): 3450-3500, 2950, 1100.

G1: Yield 2.3 g, Yellow powder; IR (KBr, cm^{-1}): 3450-3500, 2950, 1570.

G2: Yield 2.1 g, Yellow powder; IR (KBr, cm^{-1}): 3450-3500, 2950, 1570; Solid state ^{13}C NMR (75 MHz) : 164, 140, 128, 63, 45, 20, 9.

5.5.4 Determination of amino capacity

The amino group capacity was determined by acid-base titration method. Typically, 200 mg of the sample (G0-G2) was suspended in 30 mL of 0.1 M HCl solution and stirred at room temperature for 24 h. The filtrate was titrated with NaOH solution (0.1 M).

5.5.5 General procedure for the Paal-Knorr pyrrole synthesis

Primary amine (1 mmol), hexane-2,5-dione (1 mmol) and the catalyst **G2** (0.003 g) were stirred at room temperature for 2 h. The progress of the reaction was monitored by TLC or GC. Upon completion of the reaction, the mixture was filtered off and the solid was dissolved in dichloromethane. The organic layer was evaporated to isolate the pure product.

5.5.6 Reusability studies

The catalyst was simply removed by filtration and washed with DCM and ethanol. The catalyst was dried at 120 °C under vacuum for 2 h. This catalyst was again used for the Paal-Knorr reaction with fresh reactants for five consecutive runs.

5.5.7 Characterization of synthesized compounds (Table 5.4)

1. 1-Cyclohexyl-2,5-dimethyl-1*H*-pyrrole
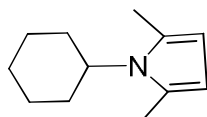
Brown oil, GC-MS (M$^+$) 177; ^{1}H NMR (CDCl$_3$, 400 MHz) δ: 5.65 (s, 2H), 3.85-3.76 (m, 1H), 2.21 (s, 6H), 1.88-1.63 (m, 8H), 1.27-1.09 (m, 2H); ^{13}C NMR (CDCl$_3$, 100 MHz) δ: 127.7, 105.9, 56.3, 32.3, 26.6, 25.6, 14.3.

2. 1-Benzyl-2,5-dimethyl-1*H*-pyrrole
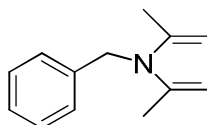
White solid, m. p. 42 °C (40-42 °C)[62], GC-MS (M$^+$) 185; ^{1}H NMR (CDCl$_3$, 400 MHz) δ: 7.22-7.19 (m, 4H), 6.86-6.80 (m, 1H), 5.79 (s, 2H), 4.94 (s, 2H), 2.07 (s, 6H); ^{13}C NMR (CDCl$_3$, 100 MHz) δ: 138.5, 128.7, 128.0, 127, 125.6, 105.3, 46.7, 12.4.

3. 2,5-Dimethyl-1-phenyl-1*H*-pyrrole
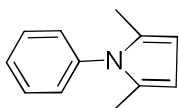
White solid, m. p. 50 °C (50-51 °C)[62], GC-MS (M$^+$) 171; ^{1}H NMR (CDCl$_3$, 400 MHz) δ: 7.57-7.47 (m, 4H), 7.32-7.29 (m, 1H), 6.00 (s, 2H), 2.13 (s, 6H); ^{13}C NMR (CDCl$_3$, 100 MHz) δ: 139.0, 129.1, 128.3,127.7, 13.1.

4. 1-(3-Chlorophenyl)-2,5-dimethyl-1*H*-pyrrole
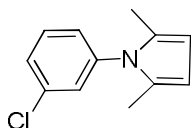
White solid, m. p. 48 °C (48–49 °C)[63], GC-MS (M$^+$) 205; ^{1}H NMR (CDCl$_3$, 400 MHz) δ: 7.40-7.44 (m, 2H), 7.25–7.28 (m, 1H), 7.13-7.16 (m, 1H), 5.93 (s, 2H), 2.07 (s, 6H); ^{13}C NMR (CDCl$_3$, 100 MHz) δ: 143.0, 134.6, 131.4, 128, 124.3, 117.8, 105.0, 12.4.

5. 5-Dimethyl-1-*p*-tolyl-1*H*-pyrrole
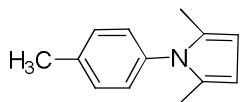
White solid, m. p. 46 °C (44-46 °C)[62], GC-MS (M$^+$) 185; ^{1}H NMR (CDCl$_3$, 400 MHz) δ: 7.32 (d, J = 7.5 Hz, 2H), 7.17 (d, J = 7.8 Hz, 2H), 5.97 (s, 2H), 2.49 (s, 3H), 2.10 (s, 6H); ^{13}C NMR (CDCl$_3$, 100 MHz) δ: 137.5, 136.4, 129.7, 128, 105.5, 21.2, 13.1.

6. 2,5-Dimethyl-1-o-tolyl-1*H*-pyrrole
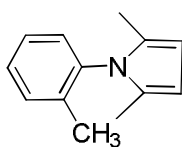
Brown liquid, GC-MS (M$^+$) 185; ^{1}H NMR (CDCl$_3$, 400 MHz) δ: 7.33-7.32 (m, 2H), 7.29-7.27 (m, 1H), 7.16 (d, J = 8.5 Hz, 1H), 5.91 (s, 2H), 1.93 (s, 3H), 1.91 (s, 6H); ^{13}C NMR (CDCl$_3$, 100 MHz) δ: 138.1, 137.1, 130.6, 128.8, 128.3, 128.2, 126.6, 105.2, 17.0, 12.5.

7. 1-(2-Methoxyphenyl)-2,5-dimethyl-1*H*-pyrrole
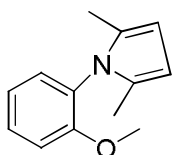
White solid, m. p. 63 °C (62-63 °C)[64], GC-MS (M$^+$) 201; ^{1}H NMR (CDCl$_3$, 400 MHz) δ: 7.40-7.36 (m, 1H), 7.16 (d, *J* = 9.6 Hz, 1H), 7.03-7.01 (m, 2H), 5.91 (s, 2H), 3.77 (s, 3H), 1.97 (s, 6H). ^{13}C NMR (CDCl$_3$, 100 MHz) δ: 155.9, 130.2, 129.3, 129.1, 127.6, 120.6, 111.9, 105.1, 55.6, 12.5.

8. 3-(2,5-Dimethyl-1*H*-pyrrol-1-yl) benzoic acid
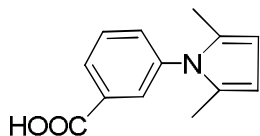
White solid, m. p. 150 °C (148–150 °C)[65], GC-MS (M$^+$) 215; ^{1}H NMR (CDCl$_3$, 400 MHz) δ: 13.17 (s, br, 1H), 8.00 (m, 1H), 7.69 - 7.65 (m, 2H), 7.54 (m, 1H), 5.82 (s, 2H), 1.96 (s, 6H); ^{13}C NMR (CDCl$_3$, 100 MHz) δ: 166.6, 138.5, 132.4, 132.0, 129.7, 128.4, 128.3, 127.5, 106.2, 12.8.

9. 1-(1-Naphthalenyl)-2,5-dimethylpyrrole
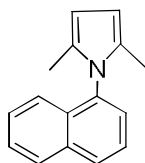
Brown solid, m. p. 116 °C (116-119 °C)[66], GC-MS (M$^+$) 221; ^{1}H NMR (CDCl$_3$, 400 MHz) δ: 7.90-7.92 (d, *J* = 6.5 Hz, 2H), 7.48-7.56 (m, 2H), 7.40-7.44 (d, *J* = 7.0 Hz, 1H), 7.10-7.12 (d, *J* = 7.5 Hz, 1H), 5.98 (s, 2H), 1.87 (s, 6H); ^{13}C NMR (CDCl$_3$, 100 MHz) δ: 135.9, 134.3, 129.9, 128.3, 126.9, 126.3, 123.3, 109.1, 11.5.

10. 2-(2,5-Dimethyl-1*H*-pyrrol-1-yl) pyridine
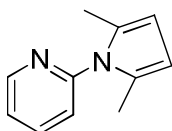
Yellow liquid, GC-MS (M$^+$) 172; ^{1}H NMR (CDCl$_3$, 400 MHz) δ: 8.62-8.64 (m, 1H), 7.82-7.86 (m, 1H), 7.30-7.33 (m, 1H), 7.23-7.28 (m, 1H), 5.93 (s, 2H), 2.15 (s, 6H); ^{13}C NMR (CDCl$_3$, 100 MHz) δ: 158.3, 147.8, 137.3, 124.3, 120.9, 102.7, 12.7.

11. 1,2 Bis(2,5-dimethyl-1*H*-pyrrol-1-yl) ethane
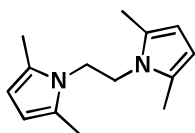
Beige solid, m. p. 135 °C (135-136 °C)[62], GC-MS (M+) 216; ^{1}H NMR (CDCl$_3$, 400 MHz) δ: 5.84 (s, 4H), 4.02(s, 4H) 2.10 (s, 12H); ^{13}C NMR (100 MHz, CDCl$_3$) δ: 127.6, 105.7, 43.9, 11.9.

12. 2-(2,5-Dimethyl-1*H*-pyrrol-1-yl) aniline
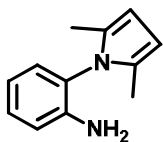
Black needle, m. p. 70 °C (70-73 °C) [42], GC-MS (M+) 186; ^{1}H NMR (CDCl$_3$, 400 MHz) δ: 7.17-7.10 (m, 1H), 7.00 (d, *J* = 7.1 Hz, 1H), 6.74-6.69 (m, 2H), 5.85 (s, 2H), 3.37 (s, br, 2H), 1.90 (s, 6H); ^{13}C NMR (CDCl$_3$, 100 MHz) δ: 144.1, 129.3, 129.3, 128.4, 124.4, 118.2, 115.5, 105.8, 12.3.

References

[1] M. Bhagiyalakshmi, S. D. Park, W. S. Cha, H. T. Jang, *Appl. Surf. Sci.*, 2010, **256**, 6660.

[2] A. S. H. King, L. J. Twyman, *J. Chem. Soc.*, 2002, **1***, 2209.

[3] M. N. Esfahani, I. M. Baltork, A. R. Khosropour, M. Moghadam, V. Mirkhani, S. Tangestaninejad, *J. Mol. Catal. A: Chem.*, 2013, **379**, 243.

[4] K. Aghapoor, L. E. Nia, F. Mohsenzadeh, M. M. Morad, Y. Balavar, H. R. Darabi, *J. Organomet. Chem.*, 2012, **25**, 708.

[5] M. Ferre, R. Pleixats, M. W. Chi Man, X. Cattoen, *Green Chem.*, 2016, **18**, 881.

[6] A. N. Chermahini, M. K. Omran, H. A. Dabbagh, G. Mohammadnezhad, A. Teimouri, *New. J. Chem.,* 2015, **39**, 4814.

[7] L. M. Lang, B. J. Li, W. Liu, L. Jiang, Z. Xu, G. Yin, *Chem. Commun.*, 2010, **46**, 448.

[8]   M. Algarra, M. V. Jimenez, E. Rodriguez-Castellon, A. Jimenez-Lopez, J. Jimenez, *Chemosphere*, 2005, **59**, 779.

[9]   M. Mazloum-Ardakani, M. A. Sheikh-Mohseni, M. Abdollahi-Alibeik, A. Benvidi, *Analyst*, 2012, **137**, 1950.

[10] T. Xie, L. Shi, J. Zhang, D. Zhang, *Chem. Commun.*, 2014, **50**, 7250.

[11] P. S. Sinija, K. Sreekumar, *RSC Adv.*, 2015, **5**, 101176.

[12] D. A. Tomalia, J. R. Dewald, *Dow Chemical Co. US Patent, US 4558120*, 1985.

[13] E. M. M. de Brabander-Van, E. W. M. den Berg, *Angew. Chem. Int. Ed. Engl.,* 1993, **32**, 1306.

[14] G. Rajesh Krishnan, K Sreekumar, Catalysis by Polymer Supported Dendrimers, Their Metal Complexes and Nano Particle Conjugates, Ph. D thesis, 2008, Cochin University of Science and Technology, Cochin, India.

[15] A. Zubia, P. F. Cossio, I. Morao, M. Rieumont, X. Lopez, *J. Am. Chem. Soc.,* 2004, **126**, 5243.

[16] (a) Y. Yang, D. E. Bergbreiter, *Pure Appl. Chem.*, 2013, **85**, 493. (b) D. E. Bergbreiter, J. Tian, C. Hongfa. *Chem. Rev.,* 2009*, **109**, 530. (c) D. E. Bergbreiter, *Chem. Rev.,* 2002*, **102**, 3345.

[17] V. Bhardwaj, D. Gumber, V. Abbot, S. Dhimana, P. Sharmaa, *RSC Adv.*, 2015, **5**, 15233.

[18] A. Kamal, S. Faazil, M. S. Malik, M. Balakrishna, S. Bajee, M. R. H. Siddiqui, A. Alarifi, *Arabian J. Chem.,* 2016*, **9**, 542.

[19] P. Nun, S. Dupuy, S. Gaillard, A. Poater, L. Cavallod, S. P. Nolan, *Catal. Sci. Technol.*, 2011, 1, 58.

[20] D. Forberg, J. Obenauf, M. Friedrich, S. Huhne, W. Mader, G. Motzc, R. Kempe, *Catal. Sci. Technol.*, 2014, **4**, 4188.

[21] (a) F. Palacios, D. Aparico, J. M. Santos, J. M. Vicario, *Tetrahedron*, 2001, **57**, 1961. (b) V. Estevez, M. Villacampa, J. C. Menendez, *Chem. Commun.*, 2013, **49**, 591.

[22] R. K. Dieter, H. Yu, *Org. Lett.*, 2000, **2**, 2283.

[23] A. Arcadi, E. Rossi, *Tetrahedron*, 1998, **54**, 15253.

[24] C. F. Lee, L. M. Yang, T. Y. Hwu, A. S. Feng, J. C. Tseng, T. Y. Luh, *J. Am. Chem. Soc.*, 2000, **122**, 4992.

[25] A. Katritzky, J. Jiang, P. J. Steel, *J. Org. Chem.*, 1994, **59**, 4551.

[26] S. Paul, A. R. Das, *Catal. Sci. Technol.*, 2012, **2**, 1130.

[27] (a) Y. Dong, N. Naranjan, S. L. Ablaza, S. X. Yu, S. Bolvig, D. A. Forsyth, P. W. Le Quesne, *J. Org. Chem.*, 1999, **64**, 2657. (b) C. Haubmann, H. Huebner, P. Gmeiner, *Bioorg. Med. Chem. Lett.*, 1999, **9**, 3143. (c) J. Robertson, R. J. D. Hatley, D. J. Watkin, *J. Chem. Soc.*, *Perkin 1*, 2000, **1**, 3389. (d) N. R. Wurtz, J. M. Turner, E. E. Baird, P. B. Dervan*, Org. Lett.,* 2001, **3**, 1201. (e) J. Chen, M. Liu, X. Yang, J. Ding, H. Wu, *J. Braz. Chem. Soc.*, 2008, **19**, 877.

[28] G. Dou, C. Shi, D. Shi, *J. Comb. Chem.*, 2008, **10**, 810.

[29] A. R. Bharadwaj, K. A. Scheidt, *Org. Lett.*, 2004, **6**, 2465.

[30] G. Minetto, L. F. Raveglia, M. Taddei, *Org. Lett.,* 2004*, **6**, 3.

[31] L. Akelis, J. Rousseau, R. Juskenas, J. Dodonova, C. Rousseau, S. Menuel, D. Prevost, S. Tumkevicius, E. Monflier, F. Hapio*, Eur. J. Org. Chem.*, 2016, **1**, 31.

[32] F. Duan, J. Ding, H. Deng, D. Chen, J. C. M. Liu, H. Wu, *Chin. Chem. Lett.*, 2013, **24**, 793.

[33] N. Neelakandeswari, G. Sangami, P. Emayavaramban, R. Karvembu, N. Dharmaraj, H. Y. Kim, *Tetrahedron Lett.*, 2012, **53**, 2980.

[34] S. Jalal, S. Sarkar, K. Bera, S. Maiti, U. Jana, *Eur. J. Org. Chem.*, 2013, 4823.

[35] N. T. S. Phan, T. T. Nguyen, Q. H. Luu, L. T. L. Nguyen, *J. Mol. Catal. A: Chem.,* 2012, **363**, 178.

[36] H. R. Darabi, M. R. Poorheravi, K. Aghapoor, A. Mirzaee, F. Mohsenzadeh, N. Asadollahnejad, H. Taherzadeh, Y. Balavar, *Environ. Chem. Lett.*, 2012, **10**, 5.

[37] F. J. Duan, J. C. Ding, H. J. Deng, D. B. Chen, J. X. Chen, M. C. Liu, H. Y. Wu, *Chin. Chem. Lett.,* 2014*, **24**, 793.

[38] P. Su, S. Chiu, Y. Lin*, Sens. Actuators, B.,* 2016, **224**, 833.

[39] A. Rahmatpour, *J. Organomet. Chem.*, 2012, **712**, 15.

[40] V. Polshettiwar, B. Baruwati, R. S. Varma, *Chem. Commun.*, 2009, 1837.

[41] B. H. Kim, S. Bae, A. Go, H. Lee, C. Gong, B. M. Lee, *Org. Biomol. Chem.,* 2016*, **14**, 265.

[42] H. Cho, R. Madden, B. Nisanci, B. Torok, *Green Chem.,* 2015*, **17**, 1088.

[43] U. Bora, A. Saikia, R. C. Boruah, *Org. Lett.,* 2003, **5**, 435.

[44] H. Cho, F. Torok, B. Torok, *Green Chem.*, 2014, **16**, 3623.

[45] M. Abid, A. Spaeth, Tcrck, *Adv. Synth. Catal.*, 2006, **348**, 2191.

[46] M. Abid, S. M. Landge, Toriik, *Org. Prep. Proced. Int.*, 2006, **35**, 495.

[47] B. Eftekhari-Sis, A. Akbari, M. Amirabed, *Chem Heterocycl Compd.*, 2011, **46**, 11.

[48] I. M. Lapina, L. M. Pevzner, A. A. Potekhin, *Russ J Gen Chem.,* 2007, **77**, 5.

[49] M. Banik, B. Ramirez, A. Reddy, D. Bandyopadhyay, B. K. Banikl, *Org Med Chem Lett.*, 2012, **2**, 11.

[50] J. Mondal, A. Modak, M. Nandi, H. Uyama, A. Bhaumik, *RSC Adv.,* 2012, **2**, 11306.

[51] L. Tuchman-Shukron, M. Portnoy, *Adv. Synth. Catal.*, 2009, **351**, 541.

[52] H. R. Darabi, K. Aghapoor, A. D. Farahani, F. Mohsenzadeh, *Environ. Chem. Lett.*, 2012, **10**, 369.

[53] L. Gao, L. Bing, Z. Zhang, H. Kecheng, H. Xiaoyun, K. Deng, *J. Organomet. Chem.*, 2013, **735**, 26.

[54] A. A. Jafari, H. Mahmoudi, *Environ. Chem. Lett.*, 2013, **11**, 157.

[55] S. Handy, K. Lavender, *Tetrahedron Lett.*, 2013, **54**, 4377.

[56] S. Cheraghi, D. Saberi, A. Heydari, *Catal. Lett.*, 2014, **144**, 1339.

[57] X. Zhang, G. Weng, Y. Zhang, Y. Li, *Tetrahedron*, 2015, **71**, 2595.

[58] M. Samadi, F. K. Behbahani, *J. Chil. Chem. Soc.,* 2015, 60.

[59] P. B. Sherly, K. Sreekumar, unpublished results.

[60] S. Abbat, D. Dhaked, M. Arfeen, P. V. Bharatam, *RSC Adv.*, 2015, **5**, 88353.

[61] (a) D. Yang, P. Liu, N. Zhang, W. Wei, M. Yue, J. You, H. Wang, *Chem. Cat. Chem.*, 2014, 6, 3434. (b) S. Handy, K. Lavender, *Tetrahedron Lett.,* **2013**, *54*, 4377-4379.

[62] D. Akbaşlar, O. Demirkol, S. Giray, *Synth. Commun.*, 2014, **44**, 1323.

[63] Y. Zhang, G. Weng, J. Chen, D. Ma, X. Zhang, *Main Group Met. Chem.,* 2014, **37**, 131.

[64] H. Lee, B. H. Ki, *Tetrahedron*, 2013, **69**, 6698.

[65] W. Zhu, M. Groh, J. Haupenthal, R.W. Hartmann, *Chem. Eur. J.,* 2013, **19**, 8397.

[66] M. Samadi, F. K. behbahani*, J. Chil. Chem. Soc.*, 2015, 60.

.....ೞ೦ೞ.....

Chapter 6

DENDRITIC AMINE FUNCTIONALIZED MESOPOROUS SILICA: DETAILED STUDY ON HENRY REACTION

In continuation of the present research interest in the development of environmentally benign synthesis using metal free dendritic catalysts supported on mesoporous silica, the rapid synthesis of conjugated nitroalkenes and β-nitro alcohols via Henry reaction in the presence of dendritic amine and proline modified dendritic amine on mesoporous silica catalyst is reported here. The presence of high concentration of amino groups on G2 and GP2 makes the catalysts active enough for this reaction within a short period of time at 50 °C.

6.1 Introduction

Nitroalkenes are significant building blocks in organic synthetic chemistry.[1] The utility of nitroalkenes in organic synthesis is largely due to their ease of conversion into a variety of functionalities such as amines and carbonyl groups.[2] Moreover, nitroalkenes prepared from aromatic aldehydes are especially useful for natural product synthesis, heterocyclic compounds, medicinal field and useful in the area of asymmetric synthesis.[3-7] They are synthetically important products since they have been used as important substrates in a wide variety of transformations including 1,3-dipolar cycloaddition reactions,[8] Friedel–Crafts alkylation,[9] Michael addition,[10] and Diels–Alder reaction.[11] They can react with 1,3-dicarbonyl compounds,[12] organozinc halides,[13] Grignard reagents,[14] organoboranes,[15] dialkyl acetylenedicarboxylates,[16] and organomanganese compounds,[17] to generate structurally diverse products. Besides, nitroalkenes are well known for their biological activity such as antitumor agents, insecticides, fungicides, and in various pharmacologically active substrates.[18-20] Very recently, β-nitrostyrene and its derivatives have also been reported as pro-apoptotic anticancer [21] and antibacterial agents.[22]

Due to the importance of nitrostyrenes in synthetic organic chemistry and pharmaceutical field, several synthetic methods have been developed for the preparation of conjugated nitroolefins.[23-26] Mainly, two strategies for the synthesis of nitrostyrenes have been used. The first method is the direct nitration of aromatic olefins with nitric oxide.[23] The second method involves the Henry condensation of carbonyl compounds with a nitroalkane, followed by antiperiplanar elimination of water from the

resulting nitroaldols (Scheme 6.1).[24-26] The Henry reaction is generally performed under mildly basic conditions with a variety of bases, but the dehydration step requires harsh reaction conditions.
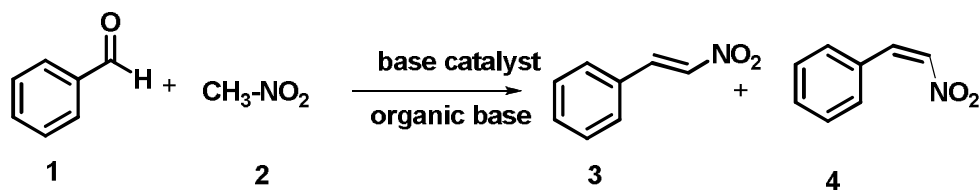
Scheme 6.1 Conventional synthesis of nitroalkenes

The classical methods provide nitroaldols using bicarbonates, alkoxides, alkali metal hydroxides, carbonates, soluble bases, and soluble bases with a surfactant with longer reaction times.[27] Dehydration of nitroalkanols to nitroalkenes was effected by several reagents such as dicyclohexylcarbodiimide,[28] methanesulfonylchloride,[29] pivaloyl chloride[30] and phthalic anhydride.[31]

Only a few one-pot preparations of nitroalkenes have been described, which include the use of microwave and ultrasound techniques in ammonium acetate,[32] amines,[33] ethylenediamine,[34] polymer-supported amines,[35] amphiphilic ionic liquids,[36] ammonium salts[37] and direct nitration of alkenes by using $NaNO_2$ in the presence of various oxidizing agents.[38] However, these one-pot syntheses normally suffer from higher catalyst-loading, poor yields, inconvenient preparation of polymer-supported catalyst, long reaction times, expensive catalysts, large excess of the nitroalkane, severe reaction conditions, difficulty in removal of catalyst from reaction medium and possibility for the formation of many

side products in this reaction (Scheme 6.2). So there is a need to develop a mild and efficient base catalyst for the synthesis of nitroalkenes.
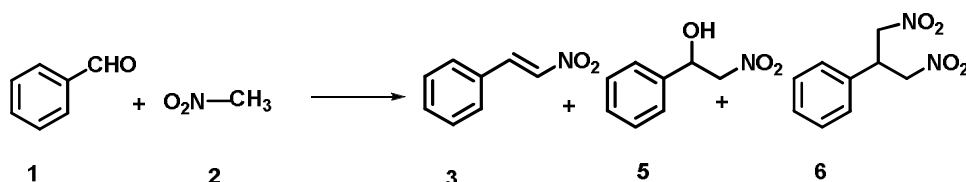
Scheme 6.2 Henry reaction

This encouraged us to reinvestigate the supported amine-catalyzed condensation of nitroalkanes with carbonyl compounds in order to develop a more efficient method for the synthesis of nitroalkenes. There are a few literature reports on supported catalysts towards the Henry reaction which include primary amine immobilized on the silica gel KG-60,[39] silica-alumina-supported amine,[40] polyamine-functionalized mesoporous zirconia[41] and zeolites.[42] Very recently, several acid-base bifunctional catalysts grafted on mesoporous silica nanoparticles have also been utilized to obtain nitrostyrenes starting from benzaldehyde dimethyl acetal.[43, 44]

Although, some of these methods are efficient, many suffer from one or more drawbacks such as the need for expensive and toxic reagents, high temperature, formation of side products, low product yields, complicated reaction assembly, longer reaction time, use of inert reaction conditions, difficulty in purification of products, use of additional bases and large amounts of acid to neutralize the bases etc. Therefore, the development of an efficient, general and environmentally friendly process, which enables rapid and easy access to nitroalkene derivatives, is of great importance,

particularly for the synthesis of complex molecules. In accordance with the principles of green chemistry, the design of catalysts for Henry reaction with easy separation, high catalytic activity, and low cost is currently being pursued.

6.2   Objective of the present work

Literature survey showed that only a few methods are available for the synthesis of conjugated nitroalkenes. Also, there is no supported or non-supported dendritic catalyst developed for this reaction. In continuation of our research interest in the development of environmentally benign synthesis, using metal free dendritic catalysts supported on mesoporous silica, dendritic amine supported on mesoporous silica was synthesized and used as organo base catalyst for this reaction.

6.3   Results and discussion

6.3.1 Synthesis of dendritic amine on mesoporous silica

Synthesis and detailed characterization of dendritic amine functionalized mesoporous silica are given in Chapter 5. Characterization studies strongly support the successful formation of amine dendrimers on mesoporous silica and the mesoporous nature of silica support was maintained after **G2** generation. Structure of **G0**, **G1** and **G2** are given in the Figure 6.1. Due to the presence of high amount of amino groups on the dendrimeric surface, **G0**, **G1** and **G2** dendrimers are used as efficient heterogeneous catalysts for organic transformations.
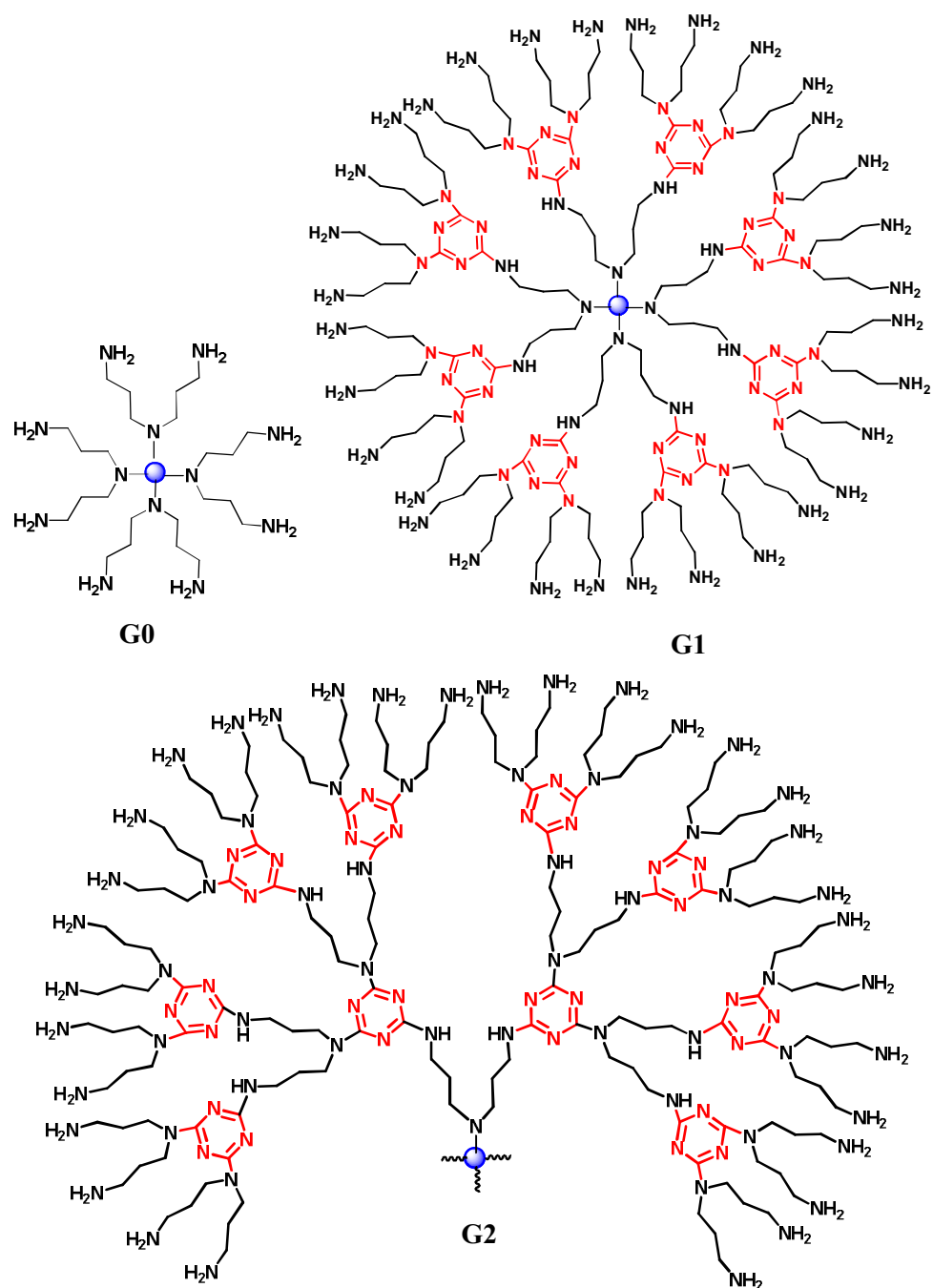
Figure 6.1 Structure of **G0**, **G1** and **G2**

6.3.2 Application as organo base catalyst for aromatic nitroalkene synthesis
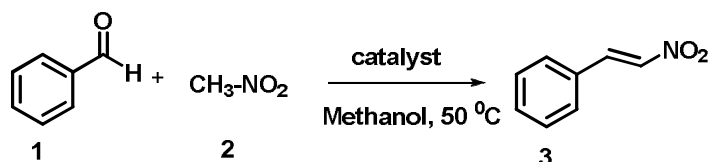
Scheme 6.3 Scheme for the synthesis of nitroalkene

In order to optimize the catalytic performance of the mesoporous silica supported dendritic amine, a model reaction between benzaldehyde and nitromethane was carried out under various reaction conditions (Scheme 6.3). The investigation began with the reaction between benzaldehyde and nitromethane run in the absence of any catalyst at 50 °C in which the target product was detected only in trace amounts (Table 6.1 Entry 1). The yield of the product was enhanced to a great extent when the reaction was conducted in the presence of different generations of catalysts **G0**, **G1** and **G2** (9.6 mol % each) (Table 6.1 Entries 2-3). The reaction proceeded smoothly, and the corresponding nitroalkene was obtained as the product in moderate yield. The results showed that this catalyst was efficient enough to facilitate the Henry reaction to deliver respective nitroalkene product, without using any additional base. Among these catalysts, the highest yield was obtained with **G2** which was selected as the catalyst of choice for further optimization studies (Table 6.1 Entry 4).

Table 6.1 Effect of generation on the synthesis of nitroalkene derivatives

Entry	Catalysts	Yield (%)[a, b]
1	No Catalyst	5 (24h)
2	**G0**	65
3	**G1**	82
4	**G2**	**90**

[a]benzaldehyde (1 mmol), nitromethane (1 mmol), catalyst (9.6 mol %), methanol (2 mL), 50 °C, 3 h, [b]Isolated yield

The above model reaction was performed under different amounts of catalyst **G2**. As can be seen from Table 6.2, catalyst loading of **G2** has a dramatic effect on the above model reaction, high amount of catalyst (0.006 g, 9.6 mol %) was required for affording a high yield of the desired product. When the catalyst loading was increased to more than 0.006 g, there was not much increase in the yield of the product.

Table 6.2 Optimization of amount of catalyst

Amount of catalyst G2 (mg)	Amount of catalyst G2 (mol %)	Yield (%)[a, b]
0.002	3.2	80
0.004	6.4	86
0.006	**9.6**	**90**
0.008	**12.8**	**90**

[a]benzaldehyde (1 mmol), nitromethane (1 mmol) methanol (2 mL), 50 °C, 3 h,
[b]Isolated yield

The effect of temperature on the reaction was studied and the results are given in Table 6.3. First, the reaction was performed at room temperature at 30 °C, but the reaction proceeded slowly and took more than 24 h for 15 % yield. The reaction was performed at 50 °C, yield of the product was increased to 90 % in 3 h. But further increment in temperature did not show remarkable difference in the yield of the product.

Table 6.3 Effect of temperature on the reaction

Entry	Temperature, °C	Yield (%)[a, b]
1	30	15
2	**50**	**90**
3	**60**	**90**
4	**70**	**90**

[a]benzaldehyde (1 mmol), nitromethane (1 mmol), methanol (2 mL), **G2** (9.6 mol %), 3 h, [b]Isolated yield.
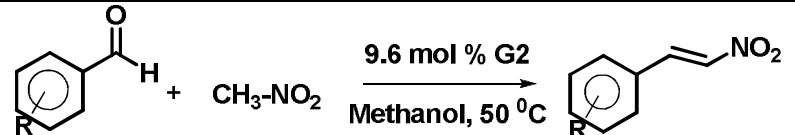
To examine the influence of different solvents, reaction was conducted in protic and aprotic solvents such as methanol, ethanol, ethyl acetate, dichloromethane, acetonitrile and solvent free condition. Results are summarized in the Table 6.4. It was found that methanol was the most effective medium for the generation of the desired products (Table 6.4, Entry 1).
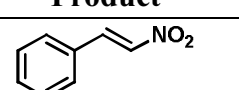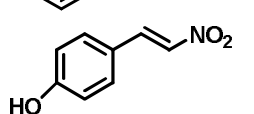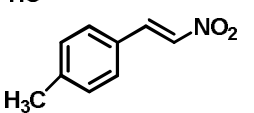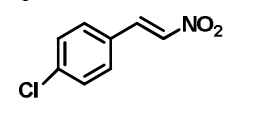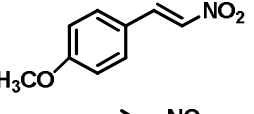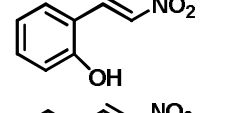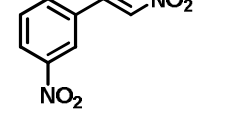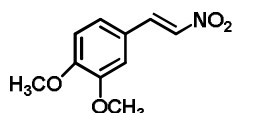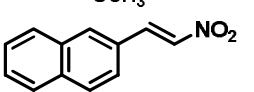
Table 6.4 Optimization of solvent

Entry	Solvent	Yield (%)[a, b]
1	**Methanol**	**90**
2	Ethanol	88
3	Ethyl acetate	79
4	Dichloromethane	75
5	Acetonitrile	72
6	Water	76
7	Solvent free condition	80

[a]benzaldehyde (1 mmol), nitromethane (1 mmol), **G2** (9.6 mol %), 50 °C, 3 h, [b]Isolated yield

With the optimized conditions in hand, Henry reaction was done using various aromatic aldehydes to explore the scope of the present protocol and the results are summarized in Table 6.5. In most cases, it was observed that aromatic aldehydes bearing both electron-donating and electron withdrawing groups readily underwent the transformation, giving good yields of corresponding nitroalkenes.

Table 6.5 Nitroalkene synthesis with diverse aldehydes

Entry	R	Product	Yield (%)[a, b]
1	H		90
2	4-Hydroxy		85
3	4-Methyl		83
4	4-Chloro		92
5	4-Methoxy		90
6	2-Hydroxy		87
7	3-Nitro		89
8	3,4-Dimethoxy		91
9	Naphthaldehyde		84

[a]aldehyde (1 mmol), nitromethane (1 mmol), methanol (2 mL), **G2** (9.6 mol %), 50 °C, 3 h, [b]Isolated yield.

For all the reactions of aryl aldehydes with nitromethane, the more stable *trans*-nitrostyrenes were obtained. The ^{1}H NMR analysis of the crude

product indicated that only the more stable *trans*-nitrostyrene was generated, the less stable *cis*-nitrostyrenes was not detected. The relative E configuration of the double bond was established based on the value of ^{1}H NMR coupling constant between the olefinic protons in the products**.**

6.3.2.1 Mechanism for the formation of (*E*)-nitroalkenes

The reaction pathway can be rationalized by the possible mechanism illustrated in Scheme 6.4.
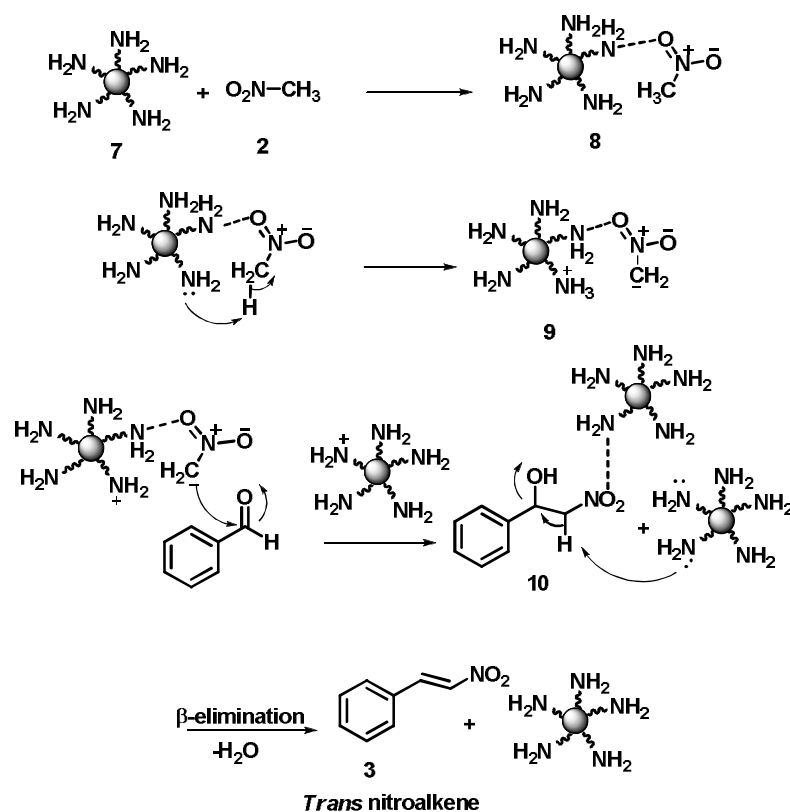
Scheme 6.4 Reaction pathway for the formation of nitroalkene using **G2**

The NH$_2$ group of catalyst **G2** form hydrogen bonded intermediate **8** with nitomethane and other NH$_2$ group abstract proton from methyl group of

nitromethane to form nitromethane carbanion **9**, which acts as the attacking reagent for further steps. It attacks the carbonyl group of benzaldehyde to form a carbinol intermediate **10**. In a subsequent step, **G2** abstracts a proton from intermediate **10** and loses a water molecule to produce the corresponding nitroalkene. The key step in the synthesis of nitroalkenes is the *β*-elimination of H_2O and constitutes an easy and efficient route to (*E*)-nitroalkenes **3**.

6.3.2.2 Reusability of the catalyst G2

After completion of the reaction, the catalyst was filtered from the reaction mixture, washed with dichloromethane, methanol and acetone and dried at 120 °C for 2 h and reused in subsequent runs. The catalyst was reused for subsequent runs using the same procedure. Results are summarized in Table 6.7. The catalyst was still active even in the fifth run with only marginal loss of activity.

Table 6.7 Reusability studies

No. of cycles	Yield (%)[a, b]
1	90
2	88
3	85
4	83
5	82

[a]benzaldehyde (1 mmol), nitromethane (1 mmol), methanol (2 mL), **G2** (9.6 mol %) 50 °C, 3 h, [b]Isolated yield

6.3.3 Synthesis of β-nitroalkanols

It is seen that conjugated nitroalkenes were formed through the intermediate, β-nitroalkanols (Scheme 6.5). In synthetic organic chemistry, β-nitroalcohols are important intermediates, because, they can be easily transformed into synthetically useful intermediates such as carboxylic acids,

aldehydes, α-hydroxy ketones, amino alcohols, azides, sulfides, and other useful compounds by functional group transformation.[45] Amino alcohols obtained by the reduction of β-nitroalcohols have found widespread utility as chiral ligands in asymmetric catalysis, and as important building blocks for natural products as well as pharmaceuticals.[46, 47]
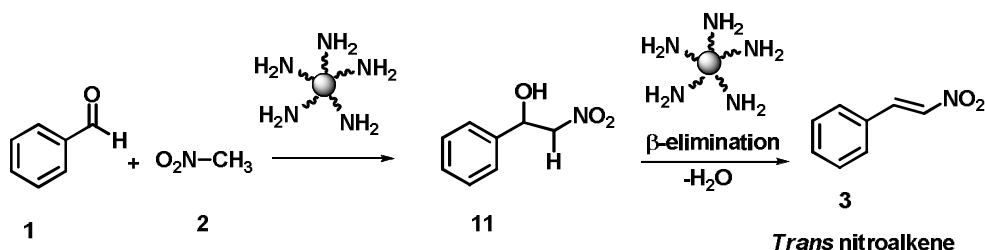
Scheme 6.5 Formation of β-nitroalkanols in the Henry reaction

Due to the importance of chiral nitroalcohols in organic synthesis, considerable efforts have been focused on the development of catalytic enantioselective version of the Henry reaction. Recently reported metal catalysts are Nd/Na,[48] CuCl-chiral camphor Schiff bases,[49] Chiral Ni-Schiff base complexes inside Zeolite,[50] heterobimetallic Cu-Sm-Aminophenol Sulfonamide Complex[51] and nanoporous lanthanide metal–organic frameworks.[52] Some of the reported organocatalysts for this reaction are Urea–pyridine bridged periodic mesoporous organosilica[53] and acid–base bifunctional shell cross-linked micelle nanoreactor.[54]

There are only few reports on the asymmetric Henry reaction in the presence of dendritic catalysts. Dendrimers containing encapsulated tertiary amine were effectively used for the Henry (nitroaldol) reaction by Amber and groups (Scheme 6.6).[55]
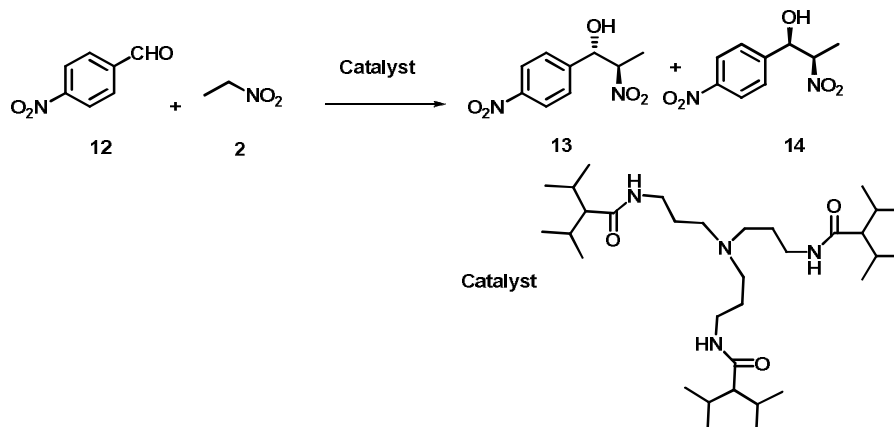
Scheme 6.6 Dendrimer catalyzed Henry reation

Bing, *et al.*[56] reported the focal-functionalized dendritic piperidine catalyzed Henry reaction (Scheme 6.7). They found that G3 (n=2) exhibited moderate to good catalytic activity in the Henry reaction of aromatic and heteroaromatic aldehydes with nitromethane. The catalyst could be readily recovered by the solvent precipitation method, and used up to ten times without a substantial loss of catalytic activity.
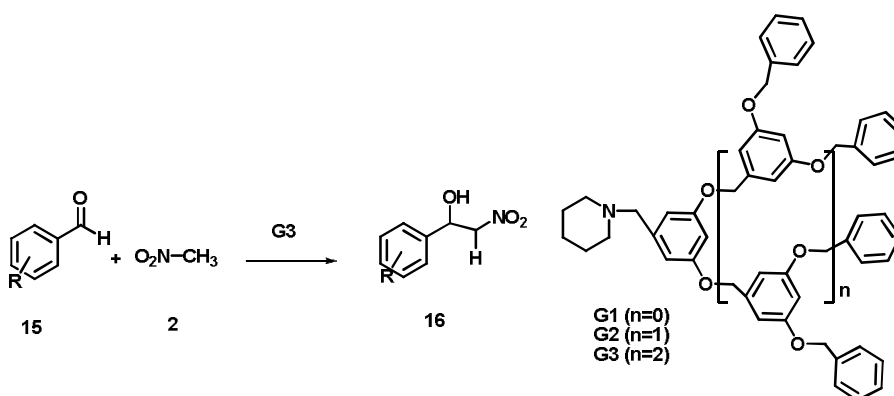
Scheme 6.7 Dendritic piperidine catalyzed Henry reation

Zubia, *et al.*[57] reported the nitroaldol reaction using dendrimers with only one active center at the core (Scheme 6.8). They have prepared three

type of catalysts **MA2**, **DA2** and **TA2** having the activity at core. According to their results, they have obtained a syn:anti ratio of 2:1 in all cases, except when **TA2** was used as catalyst, in which the syn:anti ratio was slightly higher (2.6:1).
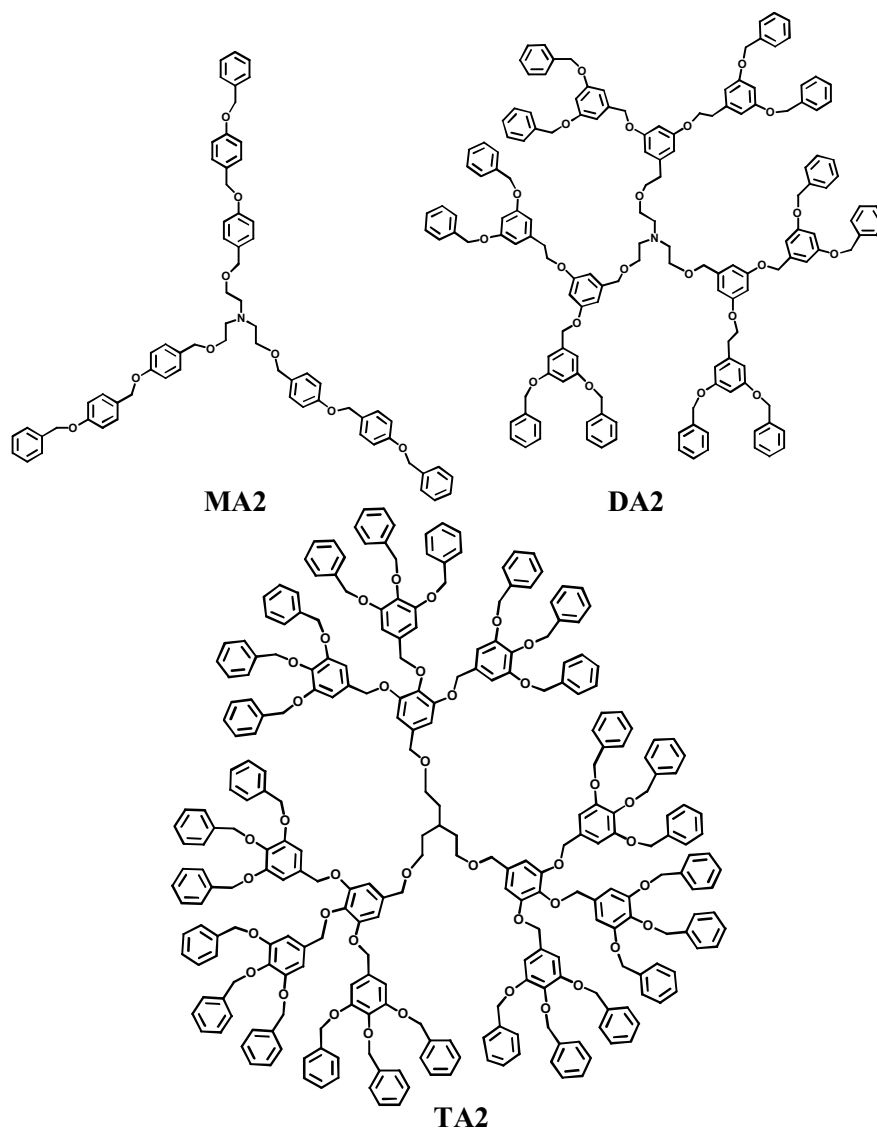
Scheme 6.8 Structures of **MA2**, **DA2** and **TA2**

The mechanism given in the Scheme 6.4 showed that nitroalkene formation happened through the intermediate *β*-nitroalkanols. Due to the application of this intermediate in synthetic organic chemistry, it was decided to collect this intermediate. But *β*-nitroalkanols could not be isolated by changing the reaction conditions like temperature, solvents, amount of catalysts, adding additional base and molar ratio of reactants using **G2** as catalyst. It was decided to modify the catalysts (**G0-G2**) with L-proline and conducted the Henry reaction with these modified catalysts (**GP0-GP2**).

6.3.3.1 Synthesis of dendritic L-proline on mesoporous silica

G0, **G1** and **G2** of dendritic amine on mesoporous silica were modified with Boc-L-Proline in the presence of NMP and DCC and deprotection was done using trifluroacetic acid. Procedure for the synthesis of **GP0**, **GP1** and **GP2** are given in Scheme 6.9, Scheme 6.10 and Scheme 6.11.
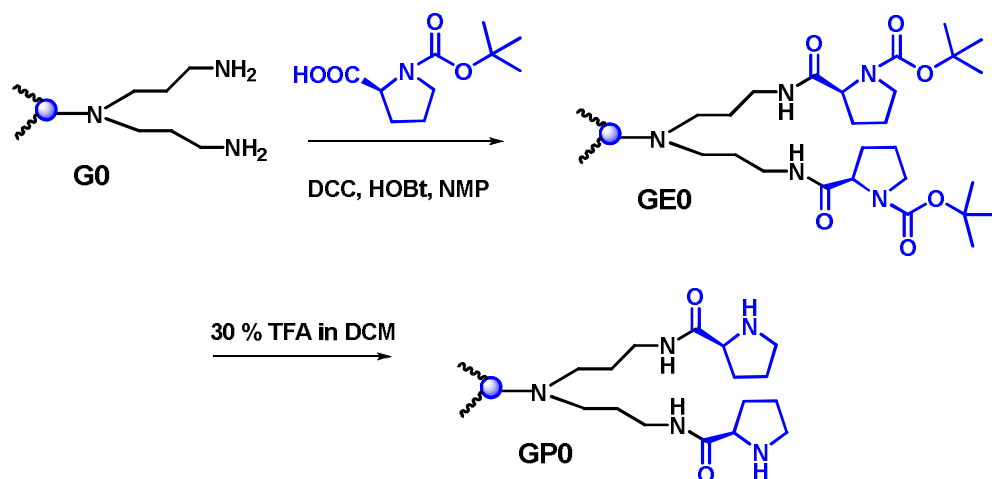
Scheme 6.9 Reaction scheme for the synthesis of **GP0**
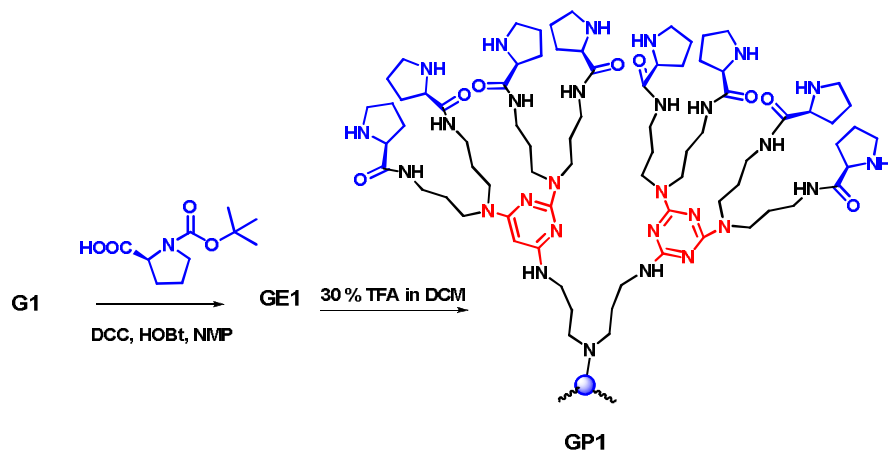
Scheme 6.10 Reaction scheme for the synthesis of **GP1**
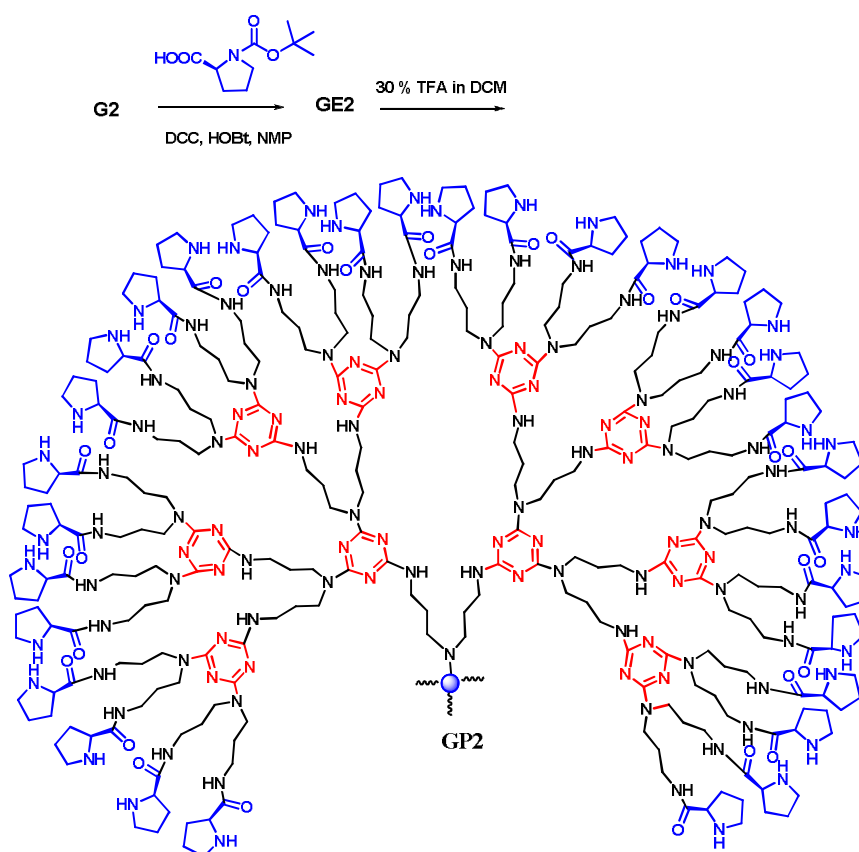
Scheme 6.11 Reaction scheme for the synthesis of **GP2**

6.3.3.2 Characterization of dendritic L-proline on mesoporous silica
6.3.3.2.1 IR spectral studies

Immobilization of Boc-L-proline groups on amine functionalized mesoporous silica frame work was examined by IR spectroscopy in each step. The IR spectra of **GE0** and **GP0** are presented in Figure 6.1. In addition to the normal silica vibrational peaks, a new strong absorption band at 1742 cm^{-1}due to ester carbonyl stretching of Boc carbonyl group was present confirming the effective grafting of Boc-L-proline on silica framework. After deprotection, the peak at 1742 cm^{-1} disappeared and indicated the removal of protecting groups. A sharp peak was observed in **GP** samples due to amide at 1685 cm^{-1}. A band in the region of 1630-1500 cm^{-1} is caused by NH bending vibration of secondary amines and C=N stretching vibration of triazine fragment. In Figure 6.2 and Figure 6.3, the same trend of vibration bands which was shown in Figure 6.1 was observed in **GE1**, **GP1**, **GE2** and **GP2**. Besides, the band intensity of ester and amide region of **GE1**, **GP1**, **GE2** and **GP2** was increased when comparing with Figure 6.1. This is due to the high loading of proline groups on **GP1** and **GP2** generations, which strongly support the successful coupling of amine moiety with chiral amino acid.
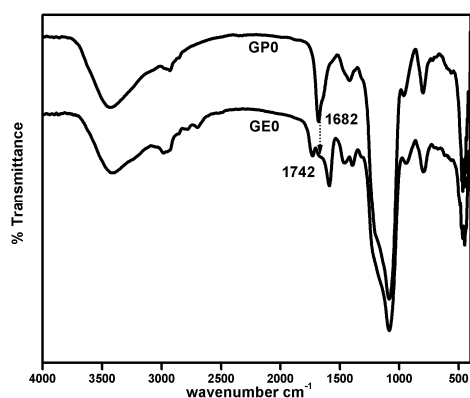
Figure 6.1 IR spectra of **GE0** and **GP0**   **Figure 6.2** IR spectra of **GE1** and **GP1**
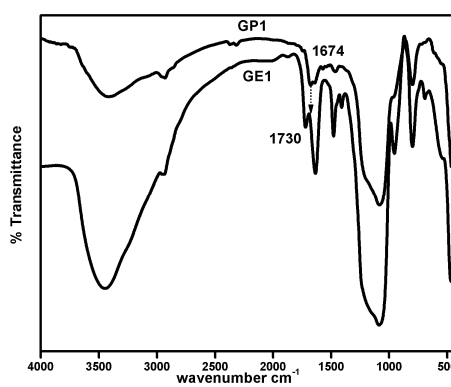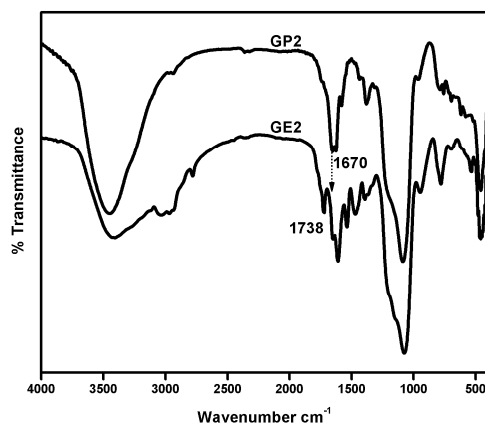
Figure 6.3 IR spectra of **GE2** and **GP2**

6.3.3.2.2 TG-DTG analysis

TG-DTG analysis was performed to determine the thermal stability and degree of organic functionalization on mesoporous silica. The results are summarized in Figure 6.4, Figure 6.5 and Figure 6.6. The TG-DTG curves of **GP0**, **GP1** and **GP2** showed first step degradation below 100 °C corresponding to the removal of moisture. In **GP0**, another weight loss of 15 % occurred at 360 °C which was attributed to the decomposition of chiral amine fragment and further weight loss at 540 °C showed the decomposition of remaining organic fragment. In the case of **GP1**, two weight losses occurred at 424 °C and 554 °C with weight loss of 14 % and 8 % respectively. Apart from this, in **GP2**, a decomposition step with a weight loss of 21 % occurred in the temperature range of 360-420 °C. These results revealed the incorporation and integrity of designed dendritic groups on the surface of silica.
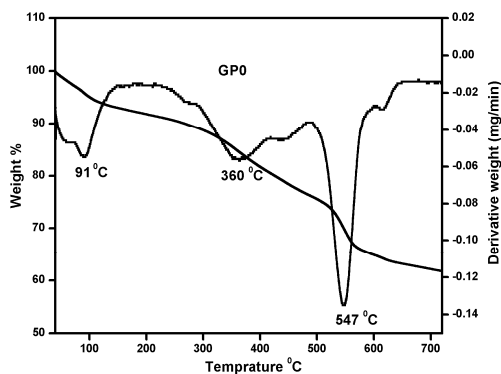
Figure 6.4 TG-DTG plot of **GP0**
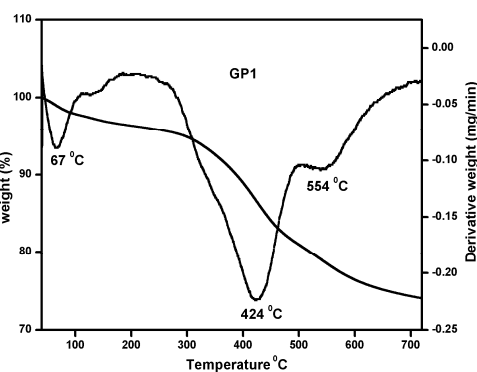
Figure 6.5 TG-DTG plot of **GP1**
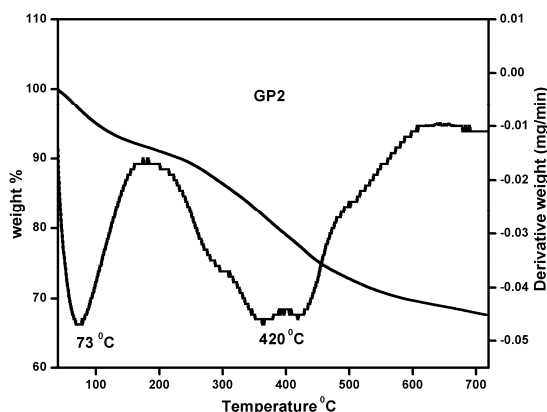
Figure 6.6 TG-DTG plot of **GP2**

6.3.3.2.3 Surface area analysis

The surface area of three generations **GP0-GP2** was evaluated using BET method, the pore size by BJH method (isotherms with hysteresis) and these are given in Figure 6.7. N_2 adsorption isotherms of **GP0** and **GP1** showed type IV adsorption isotherms with H1 hysteresis loop confirming that the mesoporous nature of the materials was retained in each generation. But for GP2, shape of isotherm was almost flat indicated that mesopore structure was destructed.
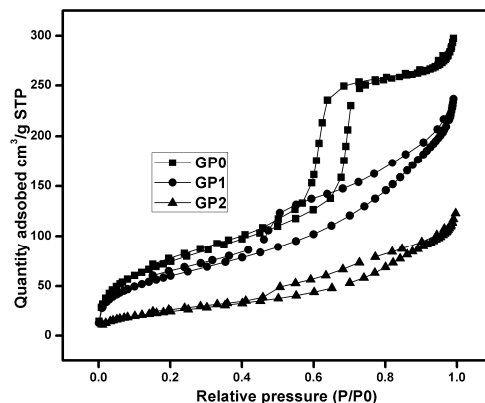
Figure 6.7 N_2 adsorption/desorption isotherms
of **GP0**, **GP1** and **GP2**

This strongly supports the incorporation of high loading of proline groups on the mesoporous silica support. The surface properties of **GP0**, **GP1** and **GP2** are summarized in Table 6.8.

Table 6.8 Surface properties of **GP0**, **GP1** and **GP2**

Sample	S_{BET} (m^2/g)	Pore volume (cm^3/g)	Pore diameter (nm)
GP0	267	0.46	4.1
GP1	213	0.36	2.8
GP2	92	0.19	1.6

6.3.3.2.4 X-ray diffraction studies

The powder X-ray diffraction patterns of the **GP0** and **GP1** are overlayed in Figure 6.8. Silica supported GP0 showed a low angle diffraction d100 peak at 0.8° with low intensity. This is the characteristic peak of mesoporous material which confirmed that the ordered nature of mesoporous silica support was preserved after proline functionalization. But in the case of

GP1 that peak has disappeared indicating the collapse of the ordered nature of mesoporous silica structure.
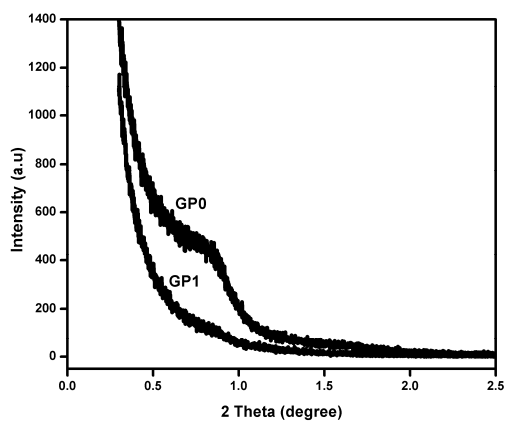
Figure 6.8 Low angle XRD of **GP0** and **GP1**

6.3.3.2.5 SEM Analysis

From the scanning electron micrographs, it was found that, after modification with proline, spherical nature of mesoporous silica disappeared compared with **CMS 1**. This supports the successful modification of **CMS 1** with proline.
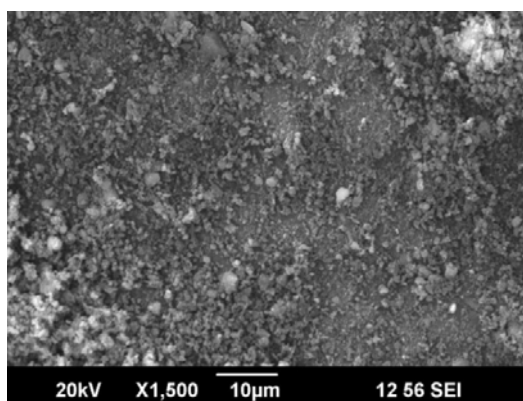
Figure 6.9 SEM image of **GP2**

6.3.4 Asymmetric Henry reaction
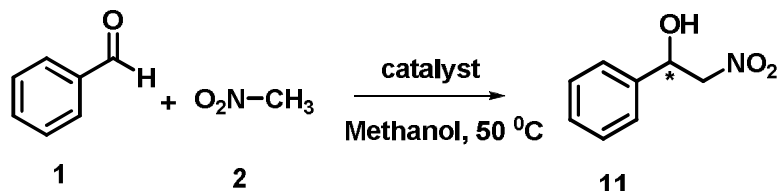
Scheme 6.12 Synthesis of β-nitroalkanol

The present study was initiated with benzaldehyde and nitromethane as model substrates in the presence of 3.1 mol % of **GP2** in methanol as the solvent at reflux temperature for 4 h (Scheme 6.12). It was observed that β-nitroalkanol was obtained as major product in good yield (73 %) after 4 h (Scheme 6.12). The reaction conditions were optimized which include, generation of catalyst, amount of catalyst, reaction temperature and solvent.

The reaction was conducted using different generation of the catalysts such as **GP0**, **GP1** and **GP2**. The reaction was performed in the presence of 3.1 mol % of each catalyst and results are summarized in Table 6.9. It is clear that the best result was obtained by using **GP2** as catalyst, whereas the same reaction could not proceed without any catalyst. So **GP2** was chosen as the catalyst for further optimization studies.

Table 6.9 Effect of catalyst generation

Entry	Catalyst	Yield (%)[a, b]
1	No Catalyst	No product
2	**GP0**	42
3	**GP1**	61
4	**GP2**	73

[a]benzaldehyde (1 mmol), nitromethane (1 mmol), methanol (2 mL), catalyst (3.1 mol %), 50 °C, 4 h, [b]Isolated yield.

The influence of the amount of catalyst **GP2** on the yield of the reaction was studied. When the amount of catalyst was increased from 3.1 to 9.3 mol %, the yield was also increased and the maximum yield was obtained for 9.3 mol % (Table 6.10, entries 1-3). When the amount of catalyst was further increased, there was no change in the product yield (Table 6.10, entry 4).

Table 6.10 Optimization of amount of catalyst

Entry	Amount of catalyst (mg)	Amount of catalyst (mol %)	Yield (%)[a, b]
1	0.002	3.1	73
2	0.004	6.2	86
3	**0.006**	**9.3**	**91**
4	**0.008**	**12.4**	**91**

[a]benzaldehyde (1 mmol), nitromethane (1 mmol), methanol (2 mL), 50 °C, 4 h,
[b]Isolated yield.

Various solvents were studied under optimized reaction conditions and it was interesting to note that maximum yield was obtained in methanol (Table 6.11). This may be because, in highly polar solvents the chances of hydrogen bonding interaction between the catalyst and the substrate would be high and hence increases the reaction yield.

Table 6.11 Optimization of Solvents

Entry	Solvent	Yield (%)[a, b]
1	**Methanol**	**91**
2	Ethanol	88
3	Isopropanol	82
4	Dichloromethane	69
5	Ethyl acetate	81
6	Tetrahydrofuran	84
7	Chloroform	82
8	No solvent	83

[a]benzaldehyde (1 mmol), nitromethane (1 mmol), GP2 (9.3 mol %), 50 °C, 4 h,
[b]Isolated yield.

Furthermore, the optimization was carried out at different temperature conditions. Higher yield was obtained at 50 °C (Table 6.12). After optimizing the reaction conditions, it was observed that after 4 h in the presence of 9.3 mol % of **GP2** the desired product was obtained in good yield without any side product in methanol.

Table 6.12 Effect of temperature

Entry	Temperature, °C	Yield (%)[a, b]
1	30	15
2	**50**	**91**
3	**60**	**91**

[a]benzaldehyde (1 mmol), nitromethane (1 mmol), methanol (2 mL), **GP2** (9.3 mol %), 4 h, [b]Isolated yield.

Based on the optimized results, the scope of Henry reaction for the synthesis of β-nitroalkanols was examined using different aromatic aldehydes. The results are shown in Table 6.13. A wide range of aromatic aldehydes having electron-donating and electron-withdrawing groups at the ortho-, meta-, and para positions was readily tolerated. Notably, the same trend which was seen in the synthesis of nitroalkenes was seen here also. Aromatic aldehydes bearing both electron-donating and electron withdrawing groups readily underwent the transformation, giving good yields and enantioselectivity of corresponding products. In addition, cinnamaldehyde gave good response to this reaction. Besides, the polycyclic aromatic aldehyde 2-naphthaldehyde gave 85 % yield and 80 % enantioselectivity.

Table 6.13 Synthesis of β -nitroalkanols

Entry	R	Product	Yield (%)[a, b]	% ee[c]
1	H		91	86
2	4-Methyl		82	79
3	4-Chloro		93	83
4	4-Methoxy		90	88
5	4-Nitro		96	89
6	4-Bromo		90	84
7	Cinnamaldehyde		84	79
8	Naphthaldehyde		85	80

[a]aldehyde (1 mmol), nitromethane (1 mmol), **GP2** (9.3 mol %), methanol (2 mL), 50 °C, 4 h, [b]Isolated yield, [c]Enantiomeric excess was determined by HPLC on chiral column.

6.3.4.1 Mechanism for the formation of *β* -nitroalkanol

Proposed mechanism for the reaction is given in Scheme 6.13. **GP2** catalyst form the hydrogen bonded intermediate **17** and another NH abstracts the hydrogen from the CH$_3$ group to form the carbanion intermediate **19**. In the next step, **19** undergoes nucleophilic attack on the aldehyde to form the *β*-nitroalkanol **11**.
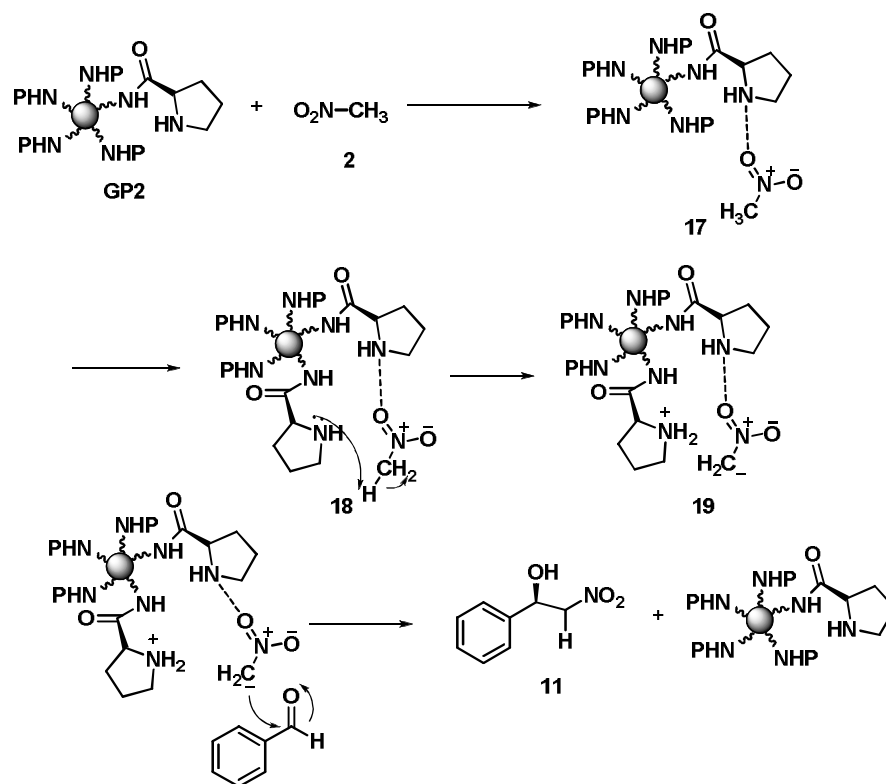
Scheme 6.8 Proposed mechanism for the formation of *β*-nitroalkanol

6.3.4.2 Reusability of the catalyst GP2

After completion of the reaction, the solution was filtered, washed with methanol, acetone and dried under vacuum at 120 °C for about 2 h. The catalyst recovered was reused without loss of significant activity. Details

regarding catalyst reuse with percentage yield are presented in Table 6.14. Successive runs were carried out in order to examine the recyclability of the catalyst. After fifth cycle, catalyst was reused with 86 % yield which indicated that the catalyst was still active for Henry reaction.

Table 6.14 Reusability studies

No. of cycles	Yield (%)[a, b]
1	91
2	90
3	89
4	87
5	86

[a]benzaldehyde (1 mmol), nitromethane (1 mmol), methanol (2 mL), **GP2** (9.3 mol %), 50 °C, 4 h, [b]Isolated yield.

6.4 Conclusion

In conclusion, chemoselective synthesis of conjugated nitroalkene derivatives and β-nitroalkanols were developed by using two different catalysts viz. **G2** and **GP2**. The presence of high concentration of amino groups on **G2** and **GP2** makes the catalysts active enough for this reaction with in short time at 50 °C. The present studies showed that **G2** and **GP2** catalysts can be used as specific catalysts for the synthesis of conjugated nitroalkene derivatives and β–nitroalkanols respectively. The synthesis of nitroalkenes and β-nitroalkanols from aryl aldehydes constitute an advantageous alternative to the methods previously described in the literature due to the following reasons: (a) catalyst was stable under the reaction conditions (b) low catalyst loading (c) this process took place under very mild reaction conditions and no additional basic media was necessary (d) recycling without loss of activity up to fifth run (e) the reaction took

place with total stereoselectivity affording (*E*)-nitroalkenes and *β*-nitroalkanols with high enantioselectivity (*ee*> 79%). All these advantages make **G2** and **GP2** competitive catalysts and thus can be clean and convenient alternatives for other industrially important reactions.

6.5   Experimental

6.5.1 Materials

Boc-L-Proline, DCC, NMP, HOBt, aldehydes, nitromethane and TFA were all purchased from local vendors and used as received. All solvents were purified by standard procedures prior to use.

6.5.2 Synthesis of amine functionalized mesoporous silica (G0, G1 and G2)

Detailed synthetic procedure was given in the Chapter 5

6.5.3 Modification of G0, G1 and G2 with Boc - L-Proline

Active ester of amino acid was prepared by adding HOBt (1.69 g, 2.5 mmol) and DCC (2.58 g, 2.5 mmol) to a solution of Boc-L-Proline (2.69 g) in NMP. This was stirred for 5 min. and the HOBt ester of amino acid was added to 2 g of amine functionalized mesoporous silica (**G0**, **G1** & **G2**). The mixture was shaken for 48 h until the disappearance of blue colour with ninhydrin. DMSO was added to the mixture and shaken for 15 min. At the end of 15 min., DIEA was added. The unreacted reagents and by-products were filtered off. The solid silica product was washed with DCM: MeOH (66:33 v/v), DCM, NMP and dried under vacuum at 50 °C.

GE0: Yield: 1.72 g, Brown powder, IR (KBr, cm^{-1}): 3400-3500, 2934, 1742, 1528, 1412, 1024, 595.

GE1: Yield: 1.70 g, Brown powder, IR (KBr, cm^{-1}): 3400-3500, 2928, 1730, 1538, 1430, 1054, 595.

GE2: Yield: 1.78 g, Brown powder, IR (KBr, cm^{-1}): 3400-3500, 2954, 1738, 1526, 1448, 1095, 595.

6.5.4 Deprotection of Boc from Boc -Proline modified mesoporous silica (GP0, GP1 & GP2)

The Boc-Proline modified mesoporous silica **GE0**, **GE1** & **GE2** (1.5 g) was treated with 30 % TFA in DCM for 5 h. The reaction was monitored using ninhydrin test. The TFA solution was filtered and the resin was washed with DCM. This was treated with 5 % DIEA in DCM (5 min) & 5 % DIEA in NMP: DCM mixture (1:1 v/v) to get the desired product. Finally, product was dried at 50 °C.

GP0: Yield: 1.34 g, Brown powder, Amino capacity: 9.3 mmol/g, IR (KBr, cm^{-1}): 3400- 3500, 2945, 1682, 1518, 1024, 595.

GP1: Yield: 1.28 g, Brown powder, Amino capacity: 11.4 mmol/g, IR (KBr, cm^{-1}): 3400- 3500, 2975, 1674, 1548, 1035, 595.

GP2: Yield: 1.36 g, Brown powder, Amino capacity: 15.4 mmol/g, IR (KBr, cm^{-1}): 3400- 3500, 2915, 1670, 1528, 1045, 595.

6.5.5 General procedure for the synthesis of (*E*)-nitroalkenes

In a typical reaction, aldehyde (1 mmol), nitromethane (1 mmol), methanol (2 mL) and amine functionalized mesoporous silica (**G2**, 9.6 mol %) as catalyst were added to a 100 mL round bottomed flask equipped with a

thermometer and a magnetic stirrer. The mixture was kept in a water bath under stirring at 50 °C for 3 h. The product was analyzed by thin layer chromatography (TLC) and LC-MS. After the reaction, the mixture was cooled to room temperature, ether was added to the mixture which was filtered to remove the catalyst. Upon evaporation of the solvent, crude product was obtained. By adding ethanol to the resulting mixture, yellow to orange solid was obtained and it was recrystallized from ethanol. The product was characterized by ^{1}H NMR and ^{13}C NMR.

6.5.6 Reusability of the catalyst G2

The reusability of the catalyst **G2** for subsequent catalytic cycles was examined using benzaldehyde and nitromethane as the substrates. After the completion of the reaction, the solid catalyst was separated from the reaction mixture by filtration, washed with dichloromethane, methanol and acetone. It was dried in vacuum at 120 °C for about 2 h. The dried solid catalyst was weighed and added to a fresh reaction mixture of benzaldehyde (1 mmol), nitromethane (1 mmol) and methanol (2 mL) at 50 °C for 3 h. The progress of the reaction was monitored by thin layer chromatography (TLC) and LC-MS. The procedure was repeated for five reaction cycles.

6.5.7 General procedure for the synthesis of β-nitroalkanols

In a typical reaction, aldehyde (1 mmol), nitromethane (1 mmol), methanol (2 mL) and proline functionalized mesoporous silica (**GP2**, 9.3 mol %) as catalyst were added successively into a 100 mL round bottom flask equipped with thermometer and magnetic stirrer. The mixture was kept in a water bath under stirring at 50 °C for 4 h. The product was analyzed by thin layer chromatography (TLC) and LC-MS. After the reaction, the mixture was

cooled to room temperature, ether was added to the mixture which was filtered to remove the catalyst. Upon evaporation of the solvent, pure product was obtained. The product was characterized by ^{1}H NMR and ^{13}C NMR. The enantiomeric excess was determined by HPLC, Chiral (OJ-H columns), 270 nm, hexane: isopropyl alcohol 90 : 10, flow rate: 1 mL min^{-1}, was used.

6.5.8 Reusability of the catalyst GP2

The reusability of the catalyst **GP2** for subsequent catalytic cycles was examined using benzaldehyde and nitromethane as the substrates. After the completion of the reaction, the solid catalyst was separated from the reaction mixture by filtration, washed with DCM, methanol and acetone. It was dried under vacuum at 120 °C for about 2 h. The dried solid catalyst was weighed and added to a fresh reaction mixture of benzaldehyde (1 mmol), nitromethane (1 mmol) and methanol (2 mL) at 50 °C for 4 h. The progress of the reaction was monitored by thin layer chromatography (TLC) and LC-MS. The procedure was repeated for five reaction cycles.

6.5.9 Spectral characterization of representative products

6.5.9.1 Characterization of (*E*)-nitroalkenes (Table 6.5)

1) *(E)-(2-Nitrovinyl) benzene*
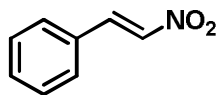
Yellow solid, m. p. 59 °C (58-62 °C)[58], LC-MS (M$^+$) m/z 149; ^{1}H NMR (CDCl$_3$, 400 MHz) δ: 7.80 (d, J = 18 Hz, 1H), 7.48 (d, J = 7.95 Hz, 2H), 7.62-7.65 (m, 3H), 6.40-6.44 (d, J = 18 Hz, 1H); ^{13}C NMR (CDCl$_3$, 100 MHz) δ: 139.1, 137.2, 132.2, 130.2, 130.1, 128.5.

2) (*E*)-1-Hydroxy-4-(2-nitrovinyl) benzene

Yellow crystals, m. p. 166 °C (166-172 °C)[58], LC-MS (M$^+$) m/z 165; ^{1}H NMR (CDCl$_3$, 400 MHz) δ: 10.45 (s, 1H), 8.12 (d, J = 18 Hz, 1 H), 7.28 (d, J = 9.0 Hz, 2 H), 7.76 (d, 2 H, J = 8.5 Hz), 6.58 (d, J = 18 Hz, 1 H); ^{13}C NMR (CDCl$_3$, 100 MHz) δ: 156.8, 139.1, 138.0, 131.0, 123.4, 114.9.

3) (*E*)-1-Methyl-4-(2-nitrovinyl) benzene

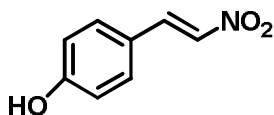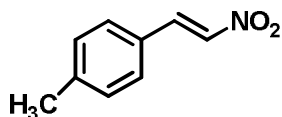Yellow solid, m. p. 102 °C (102 °C)[59], LC-MS (M$^+$) m/z 163; ^{1}H NMR (CDCl$_3$, 400 MHz) δ: 7.98 (d, *J* = 13.6 Hz, 2 H), 7.56 (d, *J* = 13.6 Hz, 2 H), 7.44 (d, *J* = 8.1 Hz, 2 H,), 7.25 (d, *J* = 8 Hz, 1 H), 2.40 (s, 3 H); ^{13}C NMR (CDCl$_3$, 100 MHz) δ: 143.1, 139.1, 136.3, 130.1, 129.1, 127.3, 21.6.

4) (E)-1-Chloro-4-(2-nitrovinyl) benzene
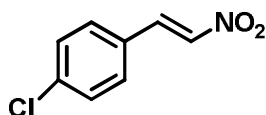
Yellow solid, m. p. 113 °C (113 °C)[60], LC-MS (M$^+$) m/z 183; ^{1}H NMR (CDCl$_3$, 400 MHz) δ: 7.95 (d, *J* = 13.7 Hz, 1H), 7.56 (d, *J* = 13.7 Hz, 1H), 7.46 (dd, *J* = 6.6 Hz, 18.8 Hz, 4 H). ^{13}C NMR (CDCl$_3$, 100 MHz) δ: 128.5, 129.7, 130.2, 137.4, 137.6, 138.3.

5) (*E*)-1-Methoxy-4-(2-nitrovinyl) benzene

Yellow solid, m. p. 86 °C (86 °C)[59], LC-MS (M$^+$) m/z 179; ^{1}H NMR (CDCl$_3$, 400 MHz) δ: 7.97 (d, *J* = 13.6 Hz, 1H), 7.48-7.54 (m, 3H), 6.95 (d, *J* = 8.8 Hz, 2H), 3.86 (s, 3H); ^{13}C NMR (CDCl$_3$, 100 MHz) δ: 162.9, 139.0, 135.0, 131.1, 122.5, 114.9, 55.5.

6) (*E*)-1-Hydroxy-2-(2-nitrovinyl) benzene

Brown yellow solid, m. p. 133 °C (133 °C)[61], LC-MS (M$^+$) m/z 165; ^{1}H NMR (CDCl$_3$, 400 MHz) δ: 8.14 (d, *J* = 13.6 Hz, 1H), 7.97 (d, *J* = 13.6 Hz, 1H), 7.47 (dd, *J* = 1.46 Hz, 1H), 7.33 (t, *J* = 7.6, 9.48 Hz 1H), 7.0 (t, *J* = 7.6, 7.5 Hz, 1H), 6.31 (br, 1H), 6.84 (d, *J* = 11.3 Hz, 1H); ^{13}C NMR (CDCl$_3$, 100 MHz) δ: 156.4, 138.6, 135.9, 133.4, 132.7, 121.6, 117.8, 116.6.

7) (*E*)-1-Nitro-3-(2-nitrovinyl) benzene
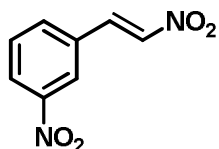
Yellow solid, m. p. 125 °C (125 °C)[62], LC-MS (M$^+$) m/z 194; ^{1}H NMR (CDCl$_3$, 400 MHz) δ: 8.05 (d, *J* = 13.7 Hz, 1H), 7.88 (d, *J* = 7.7 Hz, 1H), 7.66-7.71 (m, 2H); ^{13}C NMR (CDCl$_3$, 100 MHz) δ: 148.9, 139.4, 136.4, 134.6, 132.0, 130.7, 126.3, 123.6.

8) (*E*)-1,2-Dimethoxy-4-(2-nitrovinyl) benzene
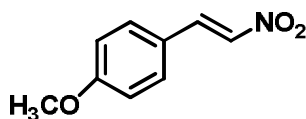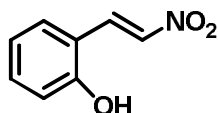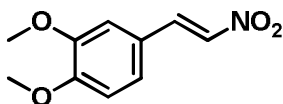
Yellow solid, m. p. 144 °C (144 °C)[63], LC-MS (M$^+$) m/z; ^{1}H NMR (CDCl$_3$, 400 MHz) δ: 7.95 (d, *J* = 13.6 Hz, 1H), 7.52 (d, *J* = 13.6 Hz, 1H), 7.18 (dd, *J* = 1.9 Hz, 1H), 7.0 (d, *J* = 2 Hz, 1H), 6.91 (d, *J* = 8.1 Hz, 1H), 3.94 (s, 3H), 3.92 (s, 3H); ^{13}C NMR (CDCl$_3$, 100 MHz) δ: 152.8, 149.6, 139.3, 135.1, 124.6, 135.2, 127.6, 122.8, 110.2, 56.1, 56.0.

9) (*E*)-2-(2-Nitrovinyl) naphthalene
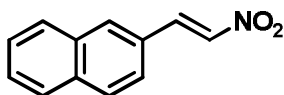
Yellow solid, m. p. 129 °C (129 °C)[64], LC-MS (M$^+$) m/z 199; ^{1}H NMR (CDCl$_3$, 400 MHz) δ: 8.14 (d, *J* = 13.6 Hz, 1H), 8.0 (s, 1H), 7.86-7.89 (m, 3H), 7.68 (d, *J* = 13.6 Hz, 1H), 7.54-7.62 (m, 3H); ^{13}C NMR (CDCl$_3$, 100 MHz) δ: 139.2, 137.1, 134.9, 133.2, 132.3, 129.4, 128.9, 128.4, 128.0, 127.6, 127.3, 123.3.

6.5.9.2 Characterization of *β*-Nitroalkanols (Table 6.13)

1) 2-Nitro-1-phenylethan-1-ol
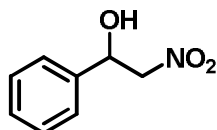
Yellow oil, LC-MS (M$^+$) m/z 167; ^{1}H NMR (CDCl$_3$, 400 MHz) δ: 7.33-7.20 (m, 5H), 5.39 (dd, *J* = 8.3, 5.5 Hz, 1H), 4.58-4.43 (m, 2H), 3.19 (br, 1H); ^{13}C NMR (CDCl$_3$, 100 MHz) δ: 138.1, 129.8, 129.7, 127.9, 77.9, 71.5.

2)   2-Nitro-1-(*p*-tolyl)ethan-1-ol
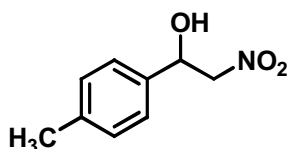
Colourless oil, LC-MS (M$^+$) m/z 181; ^{1}H NMR (CDCl$_3$, 400 MHz) δ: 7.48-7.45 (m, 1H), 7.32-7.28 (m, 1H), 7.28-7.18 (m, 1H), 5.62 (dd, *J* = 9.3, 5.2 Hz, 1H), 4.51-4.36 (m, 2H), 3.04 (br, 1H), 2.36 (s, 3H); ^{13}C NMR (CDCl$_3$, 100 MHz) δ: 136.4, 134.6, 130.9, 129.9,128.2, 125.6, 78.1, 68.2, 21.4.

3) 1-(4-Chlorophenyl)-2-nitroethan-1-ol
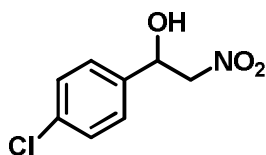
Colourless oil, LC-MS (M$^+$) m/z 201; ^{1}H NMR (CDCl$_3$, 400 MHz) δ: 7.30-7.27 (m, 2H), 7.20-7.17 (m, 2H), 5.40 (dd, *J* = 8.7, 4.2 Hz, 1H), 4.57-4.45 (m, 2H), 3.28 (br, 1H); ^{13}C NMR (CDCl$_3$, 100 MHz) δ: 138.1, 133.2, 129.7, 127.9, 77.9, 70.5.

4) 1-(4-Methoxyphenyl)-2-nitroethan-1-ol
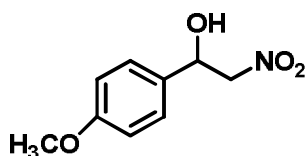
Colourless oil, LC-MS (M$^+$) m/z 197; ^{1}H NMR (CDCl$_3$, 400 MHz) δ: 7.34-7.31 (m, 2H), 6.93-6.87 (m, 2H), 5.40 (dd, J = 9.1, 4.1 Hz, 1H), 4.60 (dd, J = 16.1, 4.3 Hz, 1H), 4.47 (dd, J = 12.3, 8.1 Hz, 1H), 3.76 (s, 3H), 2.90 (br, 1H); ^{13}C NMR (CDCl$_3$, 100 MHz) δ: 159.6, 129.3, 128.3, 114.5, 78.0, 70.7, 55.3.

5) 2-Nitro-1-(4-nitrophenyl)ethan-1-ol
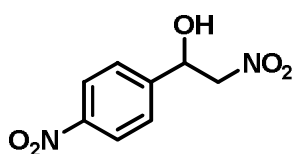
Yellow solid, m. p. 83 °C (82-84 °C)[65]; LC-MS (M$^+$) m/z 212; ^{1}H NMR (CDCl$_3$, 400 MHz) δ: 8.29-8.26 (m, 2H), 7.65-7.62 (m, 2H), 5.62 (dd, J = 8.6, 2.5 Hz, 1H), 4.64-4.55 (m, 2H), 3.12 (br, 1H); ^{13}C NMR (CDCl$_3$, 100 MHz) δ: 147.9, 143.8, 129.4, 124.2, 79.9, 70.7.

6) 1-(4-Bromophenyl)-2-nitroethan-1-ol
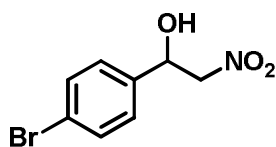
Colourless oil, LC-MS (M$^+$) m/z 244; ^{1}H NMR (CDCl$_3$, 400 MHz) δ: 7.51 (d, J = 4.8 Hz, 2H), 7.27 (d, J = 6.4 Hz, 2H), 5.38 (dd, J = 10.4, 3.6 Hz, 1H), 4.57-4.44 (m, 2H), 3.23 (br, 1H); ^{13}C NMR (CDCl$_3$, 100 MHz) δ: 137.3, 132.2, 127.9, 123.1, 81.9, 70.3.

7) 1-Nitro-4-phenylbut-3-en-2-ol
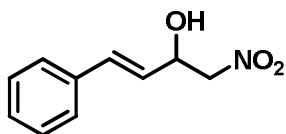
Yellow colour oil, LC-MS (M$^+$) m/z 193; ^{1}H NMR (CDCl$_3$, 400 MHz) δ: 7.39-7.27 (m, 5H), 6.78 (d, J = 9.0 Hz, 1H), 6.13 (dd, J = 19.2, 9.4 Hz, 1H), 5.08-5.05 (m, 1H), 4.51 (d, J = 4.4 Hz, 2H), 2.89 (br, 1H); ^{13}C NMR (CDCl$_3$, 100 MHz) δ: 135.2, 133.4, 128.3, 127.9, 126.0, 125.3, 82.2, 69.4.

8) 1-(Naphthalen-2-yl)-2-nitroethan-1-ol
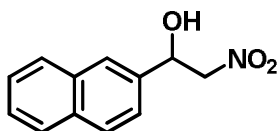
Yellow colour oil, LC-MS (M[+]) m/z 217; ^{1}H NMR (CDCl$_3$, 400 MHz) δ: 7.89-7.83 (m, 4H), 7.54-7.44 (m, 3H), 5.60 (dd, *J* = 18.4, 5.3 Hz, 1H), 4.68 (dd, *J* = 8.2, 2.6 Hz, 1H), 4.62 (dd, *J* = 10.5, 3.7 Hz, 1H), 2.91 (br, 1H); ^{13}C NMR (CDCl$_3$, 100 MHz) δ: 135.8, 133.5, 132.9, 129.0, 128.4, 128.2, 126.2, 125.4, 123.6, 77.8, 71.9.

References

[1] (a) M. P. Sibi, S. Manyem, *Tetrahedron,* 2000, **56**, 8033. (b) N. Ono, in: *The Nitro Group in Organic Synthesis* Wiley-VCH, New York, 2001. (c) A. G. M. Barratt, G. G. Graboski, *Chem. Rev.,* 1986, **86**, 751. (d) A. G. M. Barratt, *Chem. Soc. Rev.,* 1991, **20**, 95.

[2] S. Fioravanti, L. Pellacani, S. Stabile, P. A. Tardella, R. Ballini, *Tetrahedron*, 1998, **54**, 6169.

[3] N. Milhazes, R. Calheiros, M. P. M. Marques, J. Garrido, M. Cordeiro, C. Rodrigues, S. Quinteira, C. Novais, L. Peixe, *Biorg. Med. Chem.,* 2006, **14**, 4078.

[4] W. Y. Wang, P. W. Hsieh, Y. C. Wu, C. C. Wu, *Biochem. Pharmacol.*, 2007, **74**, 601.

[5] (a) F. He, Y. Bo, J. D. Altom, E. J. Corey, *J. Am. Chem. Soc.,*1999, **121**, 6771. (b) L. Novellino, M. d'Ischia, G. Prota, *Synthesis,* 1999, 793.

[6] (a) A. Kamimura, T. Yoshida, H. Uno, *Tetrahedron,* 2008, **64**, 11081. (b) R. Ballini, M. Petrini, *ARKIVOC (Gainesville, FL, U.S.)* 2009, 195.

[7] (a) T. Bui, S. Syed, C. F. Barbas III, *J. Am. Chem. Soc.,* 2009, **131**, 8758. (b) T. Okino, Y. Hoashi, T. Furukawa, X. Xu, Y. Takemoto, *J. Am. Chem. Soc.,* 2005, **127**, 119. (c) A. Cote, V. N. G. Lindsay, A. B. Charette, *Org. Lett.,* 2007, 9. (d) C. Czekelius, E. M. Carreira, *Org. Lett.,* 2004, **6**, 4575. (e) J. Wang, H. Li, L. Zu, W. Wang, *Org. Lett.,* 2006, **8**, 1391.

[8]   M. J. Kurth, M. J. O. Brien, H. Hope, M. Yanuck, *J. Org. Chem.,* 1985, **50**, 2626.

[9]   (a) N. Takenaka, J. Chen, B. Captain, R. S. Sarangthem, A. Chandrakumar, *J. Am. Chem. Soc.,* 2010, **132**, 4536. (b) J. Wu, X. Li, F. Wu, B. Wan, *Org. Lett.,* 2011, **13**, 4834.

[10]   (a) O. M. Berner, L. Enders, D. Tedeschi, *Eur. J. Org. Chem.,* 2002, 1877. (b) T. Okino, Y. Hoashi, Y. Takemoto, *J. Am. Chem. Soc.*, 2003, **125**, 12672.

[11]   (a) N. Ono, *The Nitro Group in Organic Synthesis*, Wiley-VCH: Weinhem, Germany, 2001, Chapter 3, 30. (b) K. Fuji, M. Node, H. Nagasawa, Y. Nanima, S. Terada, *J. Am. Chem. Soc.,*1986, **108**, 3855.

[12]   S. Narayanaperumal, R. C. Silva, K. S. Feu, A. F. Torre, A. G. Corrêa, W. Paixão, *Ultrason. Sonochem.,* 2013, **20**, 793.

[13]   D. Seebach, H. Schafer, B. Schmidt, M. C. Schreiber, *Angew. Chem., Int. Ed. Engl.*, 1992, **31**, 1587.

[14]   (a) C. F. Yao, W. W. Chen, Y. M. Lin, *Tetrahedron Lett.*, 1996, **37**, 6339. (b) J. T. Liu, W. W. Lin, J. J. Jang, J. Y. Liu, M. C. Yan, C. Hung, K. H. Kao, Y. Wang, C. F. Yao, *Tetrahedron*, 1999, **55**, 7115.

[15]   C. F. Yao, C. M. Chu, J. T. Liu, *J. Org. Chem.,*1998, **63**, 719.

[16]   E. Ghabraie, S. Balalaie, M. Bararjanian, H. R. Bijanzadeh, F. Rominger, *Tetrahedron*, 2011, **67**, 5415.

[17]   I. N. Namboothiri, A. J. Hassner, *Organomet. Chem.*, 1996, **518**, 69.

[18]   A. W. A. Brown, D. B. W. Robinson, H. Hurtig, B. J. Wenner, *Canad. J. Res.,* 1948, **26**, 177.

[19]   K. Zee-Cheng, C. Cheng, *J. Med. Chem.*, 1969, **12**, 157.

[20]   (a) O. Dann, E. F. Moller, *Chem. Ber.,* 1949, **82**, 76. (b) O. Schales, H. A. Graefe, *J. Am. Chem. Soc.,*1952, **74**, 4486. (c) A. Plenevaux, S. L. Dewey, J. S. Fowler, M. Guillaume, P. Wolf, *J. Med. Chem.,*1990, **33**, 2015. (d) A. Rosowsky, C. E. Mota, J. E. Wright, J. H. Freisheim, J. J. Heusner, J. J. McCormack, S. F. Queener, *J. Med. Chem.,*1993, **36**, 3103.

[21] R. K. Pettit, G. R. Pettit, E. Hamel, F. Hogan, B. R. Moser, S. Wolf, S. Pon, J. C. Chapuis, J. M. Schmidt, *Bioorg. Med. Chem.,* 2009, **17**, 6606.

[22] S. Kaap, I. Quentin, D. Tamiru, M. Shaheen, K. Eger, H. J. Steinfelder, *Biochem. Pharmacol.,* 2003, **65**, 603.

[23] I. Jovel, S. Prateeptongkum, R. Jackstell, N. Vogl, C. Weckbecker, M. A. Beller, *Adv. Synth. Catal.*, 2008, **350**, 2493.

[24] (a) L. Henry, *Bull. Soc. Chim. France,* 1895, **13**, 999. (b) G. Rosini, R. Ballini, *Synthesis.,* 1988, 833. (c) R. Ballini, G. Bosica, *J. Org. Chem.*, 1997, **62**, 425. (d) P. Kisanga, J. G. Verkade, *J. Org. Chem.*, 1999, **64**, 4298. (e) F. A. Luzzio, *Tetrahedron,* 2001, **57**, 915.

[25] (a) H. B. Hass, E. F. Riley, *Chem. Rev.*, 1943, **32**, 373. (b) R. Ballini, R. Castagnani, M. Petrini, *J. Org. Chem.*, 1992, **57**, 2160. (c) J. M. Concellon, P. L. Bernard, H. Rodriguez-Solla, C. Concellon, *J. Org. Chem.*, 2007, **72**, 5421.

[26] (a) G. Rosini, *in: Comprehensive Organic Synthesis*, C. H. Heathcock, B. M. Trost, I. Fleming), Pergamon Press, Oxford, 1991, 2, chapter 1.10, 321. (b) D. E. Worrall, *Organic Synthesis Coll. Vol. 1*, John Wiley & Sons, Inc., New York, NY, 1941, 413. (c) R. V. Heinzelman, *Org. Synth.,* 1963, **4**, 573. (d) E. McDonald, R. T. Martin, *Tetrahedron Lett.,* 1977, **18**, 1317. (e) N. Ono, H. Kawamura, M. Bougauchi, K. Maruyama, *Tetrahedron,* 1990, **46**, 7483.

[27] R. Ballini, G. Bosica, *J. Org. Chem.,* 1997, **62**, 425.

[28] P. Knochel, D. Seebach, *Synthesis,* 1982, 1017.

[29] J. Melton, J. E. McMurry, *J. Org. Chem.*, 1975, **40**, 2138.

[30] (a) P. Knochel, D. Seebach, *Tetrahedron Lett.,* 1982, **23**, 3897. (b) D. Seebach, P. Knochel, *Helv. Chim. Acta*, 1984, **67**, 261.

[31] (a) G. D. Buckley, C. W. Caife, *J. Chem. Soc.,* 1947, 1471. (b) D. Ranganathan, C. B. Rao, S. Ranganathan, R. Mehrotra, *J. Org. Chem.,* 1980, **45**, 1185.

[32] (a) R. Varma, R. Dahiya, S. Kumar, *Tetrahedron Lett.,* 1997, **38**, 5131. (b) J. McNulty, J. Streere, S. Wolf, *Tetrahedron Lett.,* 1998, **39**, 8013.

[33] (a) H. D. Becker, H. Sorensen, K. Sandros, *J. Org. Chem.*, 1986, **51**, 3223. (b) D. E. Nichols, S. P. Frescas, B. R. Chemel, K. S. Rehder, D. Zhong, A. H. Lewin, *Bioorg. Med. Chem.*, 2008, **16**, 6116. (c) G. J. Kim, H. J. Kim, *Tetrahedron Lett.*, 2010, **51**, 185. (d) B. M. Xi, Z. Z. Jiang, J. W. Zou, P. Z. Ni, W. H. Chen, *Bioorg. Med. Chem.*, 2011, **19**, 783.

[34] J. Yang, J. Dong, X. Lü, Q. Zhang, W. Ding, X. Shi, *Chin. J. Chem.,* 2012, **30**, 2827.

[35] (a) S. Yan, Y. Gao, R. Xing, Y. Shen, Y. Liu, P. Wu, H. Wu, *Tetrahedron,* 2008, **64**, 6294. (b) K. Motokura, M. Tada, Y. Iwasawa, *Angew. Chem.*, *Int. Ed.*, 2008, **47**, 9230. (c) G. Demicheli, R. Maggi, A. Mazzacani, P. Righi, G. Sartori, F. Bigi, *Tetrahedron Lett.*, 2001, **42**, 2401.

[36] A. Alizadeh, M. M. Khodaei, A. Eshghi, *J. Org. Chem.,* 2010, **75**, 8295.

[37] (a) S. Huh, H. T. Chen, J. W. Wiench, M. Pruski, V. S. Y. Lin, *J. Am. Chem. Soc.*, 2004, **126**, 1010. (b) S. L. Poe, M. Kobaslija, D. T. McQuade, *J. Am. Chem. Soc.*, 2006, **128**, 15586.

[38] (a) P. Campos, B. Garcia, M. Rodriguez, *Tetrahedron Lett.,* 2000, **41**, 979. (b) S. Varma, P. Naicker, J. Liesen, *Tetrahedron Lett.,* 1998, **39,** 3977. (c) M. Rao, S. Rao, P. Srinivas, K. S. Babu, *Tetrahedron Lett.,* 2005, **46**, 8141.

[39] L. Soldi, W. Ferstl, S. Loebbecke, R. Maggi, C. Malmassari, G. Sartori, S. J. Yada, *Catal.,* 2008, **258**, 289.

[40] K. Motokura, M. Teda, Y. Iwasawa, *J. Am. Chem. Soc.,* 2007, **129**, 9540.

[41] S. Rana, S. Mallick, K. M. Parida, *Ind. Eng. Chem. Res.,* 2011, **50**, 2055.

[42] R. Ballini, F. Bigi, E. Gogni, R. Maggi, G. Sartoli, *J. Catal.,* 2000*,* **191**, 348.

[43] (a) S. Shylesh, A. Wagener, A. Seifert, S. Ernst, W. R. Thiel, *Chem. Eur. J.*, 2009, **15**, 7052. (b) N. R. Shiju, A. H. Alberts, A. S. Khalid, D. R. Brown, G. Rothenberg, *Angew. Chem., Int. Ed.*, 2011, **50**, 9615. (c) S. Shylesh, A. Wagener, A. Seifert, S. Ernst, W. R. Thiel, *Chem. Cat. Chem.,* 2010, **2**, 1231.

[44] A. Ying, S. Xu, S. Liu, Y. Ni, J. Yang, C. Wu, *Ind. Eng. Chem. Res.,* 2014, **53**, 547.

[45] (a) M. P. Sibi, S. Manyem, J. Zimmerman, *Chem. Rev.,* 2004*,* **104**, 3263. (b) G. Blay, V. Hernández-Olmos, J. R. Pedro, *Tetrahedron: Asymmetry*, 2010, **21**, 578. (c) G. Blay, V. Hernández-Olmos, J. R. Pedro, *Org. Lett.,* 2010*,* **12**, 3058. (d) L. Gu, Y. Zhou, J. Zhang, Y. Gong, *Tetrahedron: Asymmetry,* 2012, **23**, 124.

[46] (a) V. Farina, J. T. Reeves, C. H. Senanayake, J. J. Song, *Chem. Rev.,* 2006*,* **106**, 2734. (b) K. Soai, S. Niwa, *Chem. Rev.*, 1992, **92**, 833. (c) R. Noyori, M. Kitamura, *Angew. Chem. Int. Ed. Engl.,* 1991, **30**, 49. (d) A. Cochi, T. X. Metro, D. Gomez Pardo, J. Cossy, *Org. Lett.*, 2010, **12,** 3693. (e) C. P. Wolf, A. Hawes, *J. Org. Chem.*, 2002, **67**, 2727. (f) P. Merino, T. Tejero, *Angew. Chem. Int. Ed.*, 2004, **43**, 2995. (g) J. L. Vicario, D. Badia, L. Carrillo, E. Reyes, J. Etxebarria, *Curr. Org. Chem.,* 2005*,* **9**, 219. (h) T. X. Metro, A. Cochi, D. Gomez Pardo, J. Cossy, *J. Org. Chem.*, 2011, **76**, 2594. (i) L. Liu, S. L. Zhang, F. Xue, G. S. Lou, H. Y. Zhang, S. C. Ma, W. H. Duan, W. Wang, *Chem. Eur. J.,* 2011, **17**, 7791.

[47] M. Shibasaki, H. Gröer, H. E. N. Jacobsen, A. Pfaltz, H. Yamamoto, *In Comprehensive Asymmetric Catalysis,* 1999, **3**, 1075.

[48] A. Nonoyama, K. Hashimoto, A. Saito, N. Kumagai, M. Shibasaki, *Tetrahedron Lett.*, 2016, **57**, 1815.

[49] T. Jiao, J. Tu, G. Li, F. Xu, *J. Mol. Catal. A: Chem.*, 2016, **416**, 56.

[50] M. Sharma, B. Das, G. V. Karunakar, L. Satyanarayana, K. K. Bania, *J. Phys. Chem.,* 2016, **120**, 13563.

[51] Y. Li, P. Deng, Y. Zeng, Y. Xiong, H. Zhou, *Org. Lett.*, 2016, **18**, 1578.

[52] A. Karmakar, S. Hazra, M. F. C. G. Silva, A. Paul, A. J. L. Pombeiro, *Cryt. Eng. Comm.,* 2016, **18**, 1337.

[53] P. Borah, J. Mondal, Y. Zhao, *J. Cat.*, 2015, **330**, 129.

[54] L. C. Lee, J. Lu, M. Weck, C. W. Jones, *ACS. Catal.,* 2016, **6**, 784.

[55] V. D. Amber, M. Driffield, D. K. Smith, *Org. Lett.*, 2001, **3**, 3075.

[56] Y. Bing, Y. Yin, Z. Yi, W. Zhou, H. Liu, N. Tan, H. Yang, *Tetrahedron Lett.,* 2016, **5**, 2320.

[57] A. Zubia, F. P. Cosso, I. Morao, M. Rieumont, X. Lopez, *J. Am. Chem. Soc.,* 2004, **126**, 5243.

[58] M. S. Kumar, P. Venkanna, S. Ramgopal, K. Ramesh, M. Venkateswarlu, K. C. Rajanna, *Org. Commun.*, 2012, **5:2**, 42.

[59] A. Alizadeh, M. M. Khodaei, A. Eshghi, *J. Org. Chem.,* 2010, **75**, 8295.

[60] M. Yoshida, N. Kitamikado, H. Ikehara, S. Hara, *J. Org. Chem.,* 2011, **76**, 2305.

[61] (a) C. Wang. S. Wan, *Synth. Commun.*, 2002, **32**, 3481.(b) B. C. Das, S. Mohapatra, P. D. Campbell, S. Nayak, S. M. Mahalingam, T. Evans, *Tetrahedron*, 2012, **68**, 1674.

[62] N. Neelakandeswari, G. Sangami, P. Emayavaramban, R. Karvembu, N. Dharmaraj, H. Y. Kim, *Tetrahedron Lett.*, 2012, **53**, 2980.

[63] (a) N. Milhazes, R. Calheiros, M. Paula, M. Marques, J. Garrido, M. Nata´lia, D. S. Cordeiro, C. Rodrigues, S. Quinteira, C. Novais, I. Peixeg, F. Borges, *Bioorg. Med. Chem.*, 2006, **14**, 4078. (b) D. Sawant, R. Kumar, P. R. Maulik, B. Kundu, *Org. Lett.*, 2006, **8**, 8.

[64] (a) M. Luo, B. Yan, *Tetrahedron Lett.*, 2010, **51**, 5577. (b) J. M. Rodríguez, M. D. Pujol, *Tetrahedron Lett.,* 2011, **52**, 2629.

[65] R. Boobalan, G. H. Lee and C. Chen, *Adv. Synth. Catal.*, 2012, **354**, 2511.

.....৪৹ন্ত.....

Chapter 7

SUMMARY AND OUTLOOK

In the past few decades, numerous important ligands, metal salts, and selective reagents have been developed to fulfill synthetic chemists' needs for catalysts for new bond formation, functional group transformation, and the construction of complex organic frameworks. However, the separation, reuse, and recycling of catalysts remained unresolved issues in most cases. Different types of organocatalysts have recently received heightened attention as alternatives to transition-metal catalysts, because, they avoid the use of expensive and sometimes toxic transition metals. However, high mol % loading and their separation, recovery, and reuse are the important problems faced by organocatalysts. To solve these problems, immobilization of organocatalysts on polymer supports which facilitates recovery and reuse of these catalysts is an attractive strategy. Immobilization can more efficiently separate catalysts and can serve as a way to reuse these catalysts. If the number of catalytically active centers on the catalyst surface can be increased, the problem of high mol % loading of the catalyst can be overcome. The synthesis of dendrimers can be thought of in this instance for achieving high loading of functional groups or organically active catalytic centres. In this thesis, the synthesis and characterization of dendritic catalysts on mesoporous silica support have been discussed. These systems were used as organocatalysts for a series of organic reactions.

The thesis contained seven chapters. **Chapter 1** provided a detailed review on the synthesis of dendrimers, their major use as catalysts and need of heterogeneous support for dendrimer catalysis. Major advantages of mesoporous silica as heterogeneous support, its synthesis and functionalization with organic groups were amply highlighted. Besides, some recent examples of supported dendrimer catalysts and mesoporous silica supported dendrimer catalysts for various organic reactions were also included in this chapter.

In **Chapter 2,** synthesis of Brønsted acidic dendrimer on mesoporous silica was discussed. Three generations of dendritic sulfonic acid and carboxylic acid functionalized mesoporous silica were prepared. Both classes of dendrimers were well characterized with different characterization techniques and results strongly supported the formation of desired dendritic structures on mesoporous silica surface. Estimation of acidity showed that third generation of both samples had high acid loading.

In **Chapter 3,** use of dendritic sulfonic acid functionalized mesoporous silica as Brønsted acidic catalyst for two important multicomponent reactions viz. Biginelli reaction and trisubstituted imidazole synthesis were discussed. The experimental parameters were optimized, scope of the substrates and reusability of the catalyst were studied. Results showed that third generation catalysts showed high catalytic activity towards both the reactions. Both the reactions were conducted under solvent free condition and comparatively low temperature. The proposed mechanism was consistent with the observation that high acidity of the catalyst facilitated formation of the pure product without any side products within short reaction time.

Chapter 4 of the thesis has described Ullmann type coupling reaction catalyzed by dendritic carboxylic acid functionalized mesoporous silica. To the best of our knowledge, this is the first metal free catalyst for Ullmann type coupling reaction. Reaction was optimized with various parameters like generation of catalyst, amount of catalyst, temperature, solvent and base. Results showed that reaction carried out with K_2CO_3 as base and DMSO as solvent at 90 °C for 8 h gave good results. Furthermore, product yield obtained under these optimized reaction conditions rivalled those reported for metal salts as catalysts. C-O and C-N coupling reactions were performed with phenol derivatives and amine derivatives respectively. The catalyst showed excellent activity and all substrates gave very good yield within 8 h. A new pathway for the formation of C-O and C-N coupling products was proposed and mechanism was driven by hydrogen bonding capacity of the catalysts. Reusability of the catalyst was also studied, which showed outstanding recyclability with minimal loss of catalytic activity over five consecutive cycles.

Chapter 5 has dealt with the synthesis and characterization of dendritic amine functionalized mesoporous silica and its catalytic application for the synthesis of pyrroles via Paal-Knorr reaction. As with the previous chapter, reaction conditions were optimized and scope of substrates was studied. The third generation catalyst showed high activity towards this reaction. Reactions gave mono pyrroles and bispyrroles selectively. The green aspects of the present method were: use of metal free catalyst, low catalyst loading, shorter reaction times, organic solvents were not needed, facile work-up, purification of the products by non-chromatographic methods, excellent yield of the products, need of only room temperature and the reusability of the

catalyst. A plausible mechanism was proposed highlighting hydrogen bonding capacity of the catalyst as the major contribution for the highly efficient formation of pyrrole derivatives.

In **Chapter 6**, a detailed study of Henry reaction was reported. Dendritic amine on mesoporous silica gave conjugated nitroalkene derivatives in excellent yield under optimized reaction conditions. Dendritic amine on mesoporous silica selectively provided *trans*-nitroalkenes that were formed through the *in situ* dehydration of initially formed nitroalkanols. Due to their importance in synthetic organic chemistry, attempts were made t**o** isolate the nitroalkanol intermediates. The dendritic amine on mesoporous silica was modified with L-proline and three generations of catalysts were synthesized. All of them showed activity towards Henry reaction with the reaction stopping at the intermediate nitroalkanol stage enabling their isolation in high yields. The third generation catalyst showed high activity under optimized reaction conditions. Enantiomeric excess of nitroalkanols determined using chiral HPLC was found to be high. It was attributed to the high hydrogen bonding ability of the catalyst with the substrate as the major driving force for the formation of both the products selectively. The catalysts could be recycled for five consecutive runs without significant loss of activity.

The major achievements of the present work

1) No reports are available on the development of dendritic sulfonic acid and carboxylic acid functionalized mesoporous silica for catalytic application yet. We have, for the first time, developed dendritic sulfonic acid and carboxylic acid functionalized mesoporous silica.

2) Dendritic sulfonic acid functionalized mesoporous silica showed excellent activity and recyclability towards the Biginelli reaction and for the synthesis of trisubstituted imidazoles under solvent free condition.

3) One of the major achievements of the present work is the first report of a metal free catalyst for Ullmann type C-O and C-N coupling reactions under mild reaction conditions. A new pathway for the formation of both type of couplings based on hydrogen bonding ability of the catalyst was proposed. The catalyst showed excellent reusability.

4) Highly loaded amine dendritic structure on mesoporous silica was developed. The catalytic activity of this system was utilized for the synthesis of pyrrole derivatives. To the best our knowledge, this is the first report on organo base catalyzed Paal Knorr reaction.

5) Amine terminated and proline modified dendritic amines were used for chemoselective synthesis of *trans*-nitroalkenes and nitroalkanols under mild reaction conditions respectively. Both the catalysts were reused and showed high activity without significant reduction in activity.

6) In summary, four types of organocatalysts were synthesized and were used efficiently for the above mentioned reactions. Plausible mechanisms based on hydrogen bond activation were proposed for these reactions. The high loading of catalytically active sites and strong mesoporous silica support made them to be suitable for solving the major problems of organocatalysis in the context of green chemistry.

7) After dendrimeric growth on mesoporous silica, surface area and XRD studies revealed that mesopore ordering of support was destructed, especially for the third generation of all the four catalysts. But catalytic studies showed that these catalysts were highly active towards various organic reactions. This is because of the presence of the high capacity of dendrimeric functionality on the surface of mesoporous silica. Reusability studies showed that the structure of dendritic functionalities was preserved on mesoporous silica after the organic reactions. This is because; the formation of dendrimers in the pores and channels of mesoporous silica was retained after each study. So, the four catalytic systems on mesoporous silica were superior in catalytic activity and reusability than the reported amorphous silica supported catalysts.

Future outlook

Due to the interest in the field of metal free catalysts, especially dendritic organocatalysts, attempts will be made to develop catalysts suitable for organic reactions, instead of metal catalysts. Dendritic sulfonic acid functionalized mesoporous silica can be extended to the synthesis of tetrasubstituted imidazoles and other important multicomponent reactions. Dendritic carboxylic acid functionalized mesoporous silica was used as catalyst for C-O and C-N coupling only and can be extended to the C-C and C-S coupling reactions also. In the present investigation, the synthesis of simple pyrrole derivatives was only investigated. Due to the importance of pyrrole derivatives in the biological field, more structurally complex pyrrole derivatives can be synthesized using dendritic amine functionalized mesoporous silica. Dendritic proline modified mesoporous silica can also be utilized for other asymmetric reactions.

.....ೞೞ.....

║║║ **List of Publications** ║║║

Papers published

[1] **K. A. Jisha** and K. Sreekumar, *Dendritic Amine on Mesoporous Silica: First Organo Base Catalyst for Paal-Knorr Reaction under Solvent Free Condition, A Green Approach, Catal. Lett.*, 2017, doi:10.1007/s10562-017-1975-y.

[2] G. Smitha, P. S. Sinija, P. B. Sherlymol, **K. A. Jisha**, K. J. Anjaly, K. Sreekumar, *Heterogeneous Dendronized Polymer with Peripheral Copper Moieties: From Synthesis to Catalysis and Comparison with Dendrigraft Polymer,* Polymer, 2017, **120**, 100.

[3] **K. A. Jisha**, S. Prathapan and K. Sreekumar, *Synthesis of 2,4,5-triaryl-1H-imidazoles in the Presence of Sulfonic Acid Grafted Mesoporous Silica under Solvent Free Condition*, ISBN No: 978-93-80095-738, 277-280, 2016.

[4] **K. A. Jisha**, S. Prathapan and K. Sreekumar, *Base Catalysed Paal-Knorr Reaction for the Synthesis of Pyrrole Derivatives in the Presence of Dendritic Amine Grafted on Mesoporous Silica*, ISBN No: 978-81-930558-1-6, 44-47, 2015.

Papers presented in Conferences

[1] **K. A. Jisha**, S. Prathapan and K. Sreekumar, poster presentation entitled "*First Base Catalyzed Paal-Knorr Reaction using Dendritic Amine Grafted on Mesoporous Silica*" in the 28th Kerala Science Congress held at the University of Calicut, Malappuram during January 2016 (**Best Poster Award**).

[2] **K. A. Jisha**, S. Prathapan and K. Sreekumar, paper presented "*Synthesis of 2,4,5-triaryl-1H-imidazoles in the Presence of Sulfonic Acid Grafted Mesoporous Silica under Solvent Free Condition*" in the International Conference on MATCON 2016 held at CUSAT, Cochin on January 2016.

[3] **K. A. Jisha** and K. Sreekumar, paper presented entitled *"BAPA Dendrimer on Mesoporous Silica: A Highly Effective Reusable Catalyst for One-pot Synthesis of Conjugated Nitroalkenes"* in the International Conference on Advances in Applied Mathematics, Materials Science and Nanotechnology for Engineering and Industrial Applications held at FISAT, Angamaly during January 2016.

[4] **K. A. Jisha**, S. Prathapan and K. Sreekumar, paper presented entitled "*Base Catalyzed Paal Knorr Reaction for the Synthesis of Pyrrole Derivatives in the Presence of Dendritic Amine Grafted on Mesoporous Silica*" in the Prof. K. V. Thomas Endowment National Seminar on Molecular Approach to Current Advances in Chemistry held at S. H. College, Thevara during December 2015.

[5] **K. A. Jisha** and K. Sreekumar paper presented entitled "*Stepwise Growth of Dendritic Bis(3-aminopropyl)amine on Mesoporous Silica as Effective Reusable Catalyst for the Synthesis of Pyrrole Derivatives Via Paal-Knorr Reaction*" in the National Conference on Recent Trends in Bio-inorganic & Organometallic Chemistry (NCBOC- 2015) held at SSIET, Coimbatore during October 2015.

[6] **K. A. Jisha** and K. Sreekumar has participated in the National Seminar on Current trends in Chemistry (CTriC) 2014 held at CUSAT, Cochin during January 2014.

[7] **K. A. Jisha** and K. Sreekumar has participated in the National Seminar on Current trends in Chemistry (CTriC) 2011 held at CUSAT, Cochin during March 2011.

.....ജഞ.....